**ENVIRONMENTAL AND WATER QUALITY
OPERATIONAL STUDIES**

**US Army Corps
of Engineers**

EMPIRICAL METHODS FOR PREDICTING EUTROPHICATION IN IMPOUNDMENTS

Report 3

PHASE II: MODEL REFINEMENTS

by

William W. Walker, Jr.

Environmental Engineer
1127 Lowell Road
Concord, Massachusetts 01742

March 1985
Report 3 of a Series

SECURITY CLASSIFICATION OF THIS PAGE (When Data Entered)

REPORT DOCUMENTATION PAGE

READ INSTRUCTIONS
BEFORE COMPLETING FORM

1. REPORT NUMBER	2. GOVT ACCESSION NO.	3. RECIPIENT'S CATALOG NUMBER
Technical Report E-81-9		

4. TITLE (and Subtitle)	5. TYPE OF REPORT & PERIOD COVERED
EMPIRICAL METHODS FOR PREDICTING EUTROPHICATION IN IMPOUNDMENTS; REPORT 3, PHASE II: MODEL REFINEMENTS	Report 3 of a series
	6. PERFORMING ORG. REPORT NUMBER

7. AUTHOR(s)	8. CONTRACT OR GRANT NUMBER(s)
William W. Walker, Jr.	Contract No. DACW39-78-C-0053-P006

9. PERFORMING ORGANIZATION NAME AND ADDRESS	10. PROGRAM ELEMENT, PROJECT, TASK AREA & WORK UNIT NUMBERS
Dr. William W. Walker, Jr. Environmental Engineer 1127 Lowell Road Concord, Massachusetts 01742	Environmental and Water Quality Operational Studies, Task 1E

11. CONTROLLING OFFICE NAME AND ADDRESS	12. REPORT DATE
DEPARTMENT OF THE ARMY US Army Corps of Engineers Washington, DC 20314-1000	March 1985
	13. NUMBER OF PAGES
	321

14. MONITORING AGENCY NAME & ADDRESS(if different from Controlling Office)	15. SECURITY CLASS. (of this report)
US Army Engineer Waterways Experiment Station Environmental Laboratory PO Box 631, Vicksburg, Mississippi 39180-0631	Unclassified
	15a. DECLASSIFICATION/DOWNGRADING SCHEDULE

16. DISTRIBUTION STATEMENT (of this Report)

Approved for public release; distribution unlimited.

17. DISTRIBUTION STATEMENT (of the abstract entered in Block 20, if different from Report)

19. KEY WORDS (Continue on reverse side if necessary and identify by block number)

Eutrophication   (LC)
Reservoirs (LC)
Reservoir Operation   (WES)
Water Quality--Measurement (LC)
Water Quality Management   (LC)

20. ABSTRACT (Continue on reverse side if necessary and identify by block number)

Empirical eutrophication models are useful tools for some aspects of reservoir water quality assessment and management. This report modifies existing model structures and parameter estimates to improve their generality and permit application under a wider spectrum of reservoir conditions.

A network of models is assembled for predicting reservoir-average concentrations of total phosphorus, total nitrogen, chlorophyll-a, transparency,
(Continued)

DD FORM 1473 EDITION OF 1 NOV 65 IS OBSOLETE
1 JAN 73

Unclassified
SECURITY CLASSIFICATION OF THIS PAGE (When Data Entered)

20. ABSTRACT (Continued).

organic nitrogen, particulate phosphorus, and hypolimnetic oxygen depletion rate (near-dam) as functions of reservoir mean depth, hydraulic residence time, and inflow concentrations of total phosphorus, ortho-phosphorus, total nitrogen, and inorganic nitrogen. Models are tested against several independent lake and reservoir data sets compiled from the literature. An error analysis indicates that the prediction of chlorophyll-a, the most direct measure of eutrophication response, is limited more by variabilities in the biological responses to a given set of nutrient concentrations and other environmental conditions than by uncertainties in predicting pool nutrient levels from external loadings. Inflow available phosphorus concentration and mean depth are shown to explain most of the variance in reservoir trophic state indicators and hypolimnetic oxygen status.

For a given chlorophyll-a concentration and morphometry, hypolimnetic oxygen depletion rates are found to average about 40 percent higher in reservoirs, as compared with northern lakes. The difference may be attributed to effects of oxygen demands exerted by allochthonous organic materials, spatial gradients in chlorophyll, and/or reservoir outlet configuration. Areal depletion rates are shown to be an increasing function of mixed-layer chlorophyll-a concentration, but independent of hypolimnetic temperature and morphometry, for lakes and reservoirs with mean hypolimnetic depths between 2 and 30 m. Because of the general magnitude of the areal depletion rates, all of the thermally stratified reservoirs tested with mean depths less than 10 m reached anoxic conditions (< 2 mg/l dissolved oxygen) at some point during the stratified season. Predicting the hypolimnetic oxygen status in these relatively shallow systems is limited more by ability to predict thermal stratification than by ability to predict depletion rates from trophic status and morphometry. Metalimnetic oxygen depletion is shown to be generally more important than hypolimnetic depletion in deeper reservoirs.

A principal components analysis leads to a two-dimensional classification system for eutrophication-related water quality. The first two components explain 95 percent of the variance in pool nutrient, chlorophyll-a, organic nitrogen, and transparency levels. The first component is interpreted as a quantitative factor which reflects the total nutrient supply. The second is interpreted as a qualitative factor which reflects light-limited primary productivity and the partitioning of nutrients between organic and inorganic forms. Information on both dimensions provides a more complete description of reservoir water quality and its controlling factors than any single variable or index.

Average concentrations inadequately characterize many reservoirs with pronounced spatial gradients in water quality. A computer simulation model is developed and tested for predicting longitudinal gradients in phosphorus and related trophic state indicators. The model accounts for the advection, dispersion, and sedimentation of phosphorus along a given tributary arm. Second-order sedimentation kinetics are shown to be more realistic than first-order kinetics for predicting within-reservoir spatial variations, as well as among-reservoir spatially averaged variations.

Previous reports in this series include: "Report 1, Phase I: Data Base Development" and "Report 2, Phase II: Model Testing."

PREFACE

This report was prepared by Dr. William W. Walker, Jr., Environmental Engineer, Concord, Mass., for the US Army Engineer Waterways Experiment Station (WES) under Contract No. DACW39-78-C-0053-P006, dated 7 June 1978. Previous reports in this series, entitled "Empirical Methods for Predicting Eutrophication in Impoundments," include "Report 1, Phase I: Data Base Development," and "Report 2, Phase II: Model Testing." The study forms part of the Environmental and Water Quality Operational Studies (EWQOS) Work Unit IE, Simplified Techniques for Predicting Reservoir Water Quality and Eutrophication Potential. The EWQOS Program is sponsored by the Office, Chief of Engineers (OCE), US Army, and is assigned to the WES under the purview of the Environmental Laboratory (EL). The OCE Technical Monitors for EWQOS were Dr. John Bushman, Mr. Earl Eiker, and Mr. James L. Gottesman.

The study was conducted under the direct WES supervision of Dr. Robert H. Kennedy and under the general supervision of Mr. Donald L. Robey, Chief, Ecosystem Research and Simulation Division, and Dr. John Harrison, Chief, EL. Dr. J. L. Mahloch was Program Manager of EWQOS.

The Commander and Director of WES during the study was COL Tilford C. Creel, CE. Technical Director was Mr. F. R. Brown.

CONTENTS

CONTENTS (Continued)

LIST OF TABLES

LIST OF FIGURES

7

11

EMPIRICAL METHODS FOR PREDICTING EUTROPHICATION IN IMPOUNDMENTS

PHASE II: MODEL REFINEMENTS

PART I: INTRODUCTION

1. This report describes the development and testing of empirical models for predicting eutrophication and related water quality conditions in impoundments. As Task 1E of the Environmental and Water Quality Operational Studies (EWQOS) Program, the general objective of the research project is to develop simplified water quality assessment procedures which can be applied to Corps of Engineers (CE) reservoirs. The report follows two previous reports in this series: Phase I: Data Base Development (Walker, 1981) and Phase II: Model Testing (Walker, 1982a).

2. Under Phase I, a computerized data base describing morphometric, hydrologic, and water quality characteristics of 299 Corps of Engineer reservoirs was compiled from existing sources. The data were inventoried to assess adequacy for use in model testing. Preliminary statistical analyses were conducted to assess the spatial and temporal variability of water quality conditions and to develop appropriate techniques for data reduction.

3. Under Phase II, data sets required for testing eutrophication models were developed and used in a systematic assessment of existing models. Results of preliminary model testing indicated that certain empirical models could be applied to some reservoirs with expected error magnitudes which were similar to those reported in lake applications. Correlation of errors with region and various reservoir characteristics suggested, however, that model generality was relatively low and that there was room for improvement in certain areas.

4. Most existing models assume that algal growth in impoundments, as measured by chlorophyll-a, is directly related to total phosphorus concentration, which, in turn, is related to external total phosphorus loading, mean depth, and hydraulic residence time. The objective of the research described below is to attempt to improve upon existing models by modifying their structures to account for additional controlling factors which were found to be important in preliminary model testing. Specifically, these additional factors include:

a. Effects of nonlinear retention kinetics on nutrient balances.

b. Effects of inflow nutrient partitioning between dissolved and particulate phases on total nutrient balances and chlorophyll-a production.

c. Effects of seasonal variations in loadings and morphometric characteristics on nutrient balances.

d. Effects of algal growth limitation by light, nitrogen, and flushing rate on chlorophyll-a concentrations.

e. Effects of spatial variations in phosphorus and related trophic state indicators, as controlled by reservoir morphometric, hydrologic, and loading characteristics.

The objective is to improve model generality and reduce error variance by modifying the model structures to account for these additional factors.

5. Limitations in existing data and theoretical understanding partially determine the feasibility of improving upon existing models. Model complexity must be increased in order to account for the additional factors listed above. Choosing model formulations based upon patterns in the data becomes more difficult as the number of factors increases, particularly when the factors are interdependent. As more of the observed variance is explained, an increasing proportion of the unexplained variance (error) is attributed to random errors in the data. The "signal-to-noise" ratio of the error variance decreases as the models become more elaborate and the ability to discriminate among alternative model formulations by examining residuals decreases. The general approach taken below is to base model structures, where possible, upon theoretical considerations. While the theoretical models themselves are simplifications, they tend to have more realism and generality than strictly empirical formulations (e.g., multiple linear regression models). Generality is assessed through systematic analyses of model residuals and tests against independent lake and reservoir data sets compiled from the literature. While the resulting models are more

13

complex mathematically than existing formulations, they are still amenable to hand calculations and data needs have not been substantially increased.

6. Figure 1 maps the locations of impoundments which are used in model development. Details on data reduction and screening procedures have been given previously (Walker, 1982a) and are not repeated here. The general approach is to treat the problem as a series of submodels which are developed and tested independently. Methods for predicting average phosphorus and nitrogen concentrations are treated in Parts II and III, respectively. Part IV develops methods for assessing spatial variations. Part V deals with relationships between hypolimnetic oxygen depletion rate and other trophic state indicators. Part VI develops models which describe nutrient partitioning and which relate reservoir chlorophyll-a and transparency to nutrient concentrations, turbidity, and other controlling factors. A multivariate classification system which is useful for reservoir data summary, interpretation, and ranking is developed in Part VII. Submodels developed in Parts II-VII are summarized and assembled in the form of a model network in Part VIII. Conclusions are listed in Part IX. Appendix A lists and summarizes the data sets used in model development; Appendix B defines the notations used.

7. A final report in this series will consist of a manual to assist field personnel in applying the models developed and tested under the research project. The manual will outline data requirements, application procedures, and limitations. Computer programs to assist in data reduction, model implementation, sensitivity analysis, and error analysis will also be provided.

Figure 1

Regional Distribution of CE Reservoirs Used in Model Development

PART II: PHOSPHORUS RETENTION MODELS

Introduction

8.   Phosphorus retention models link reservoir inflow, pool, and outflow phosphorus levels using mass-balance relationships with empirically estimated phosphorus sedimentation terms. This chapter builds upon the results of preliminary model testing by modifying existing formulations to consider factors which have been found to influence model performance. These factors include:

a. Nonlinear dependence of reservoir phosphorus levels on inflow phosphorus concentration.

b. Effects of inflow phosphorus availability (as measured by the ratio of ortho-P to total P loading).

c. Effects of seasonal variations in volume, outflow, and loadings on growing-season water quality conditions in impoundments which are relatively rapidly flushed.

The investigation focuses on a number of mechanistic and empirical formulations for predicting reservoir outflow and average pool phosphorus concentrations. The initial emphasis is on mechanistic models which are based explicitly upon theoretical representations of reservoir mixing and nutrient dynamics. For example, the simplest mechanistic formulation represents phosphorus sedimentation as a first-order reaction in a completely mixed system. The empirical formulations are derived directly from a statistical analysis of the data and do not rely explicitly upon idealized representations of the system. Models are tested using 14 independent data sets compiled from the literature (Walker, 1982a) and representing conditions and relationships in CE reservoirs, other US reservoirs (US Environmental Protection Agency, National Eutrophication Survey, EPA/NES, 1978), TVA reservoirs (Higgins et al., 1980; Higgins and Kim, 1981), and reservoirs studied under the Organization for Economic Cooperation and Development (OECD) Reservoir and Shallow Lakes Program (Clasen, 1980). The work provides a basis for development of a framework for modeling spatial variations within reservoirs, as described in Part IV.

16

Data Base Refinements

9. The files used in preliminary model testing (Walker,1982a) included data which passed various screening criteria applied to water balances, nutrient balances, and pool monitoring program designs. The input/output data set described hydrology, morphometry; loading, and nutrient outflow in 62 projects during the year of tributary sampling by the EPA National Eutrophication Survey (EPA/NES). The load/response data set described hydrology, morphometry, loading, and pool water quality conditions in 43 projects during the year of pool sampling by the EPA/NES. Based upon additional data review, the following deletions have been made from these data sets:

a. The phosphorus balance of Wister Reservoir (District 25; Reservoir 281) indicates a negative retention coefficient which could be attributed to unrepresentative tributary sampling, since the average flow on the days of sampling the major tributary inflow station on the Poteau River was only 42% of the average flow during the monitoring year. This project was an outlier for most models examined in preliminary testing and has been deleted from both the input/output and load/response data sets.

b. Estimation of inflow concentration for Kanopolis (District 29; Reservoir 106) during the EPA/NES pool monitoring year requires a relatively large extrapolation of flow regimes, from an annual outflow of 194 million cubic meters during the tributary monitoring year to 790 millon cubic meters during the pool monitoring year. This project has been deleted from the load/response data set.

c. Nutrient outflow concentration estimates for Eufaula (District 25; Reservoir 267) are based upon a sampling regime which provided only 6 samples and excluded the April-July period. This project has been deleted from the input/output data set.

Exclusion of these data increases the precision of model parameter and

error statistics for projects with "normal" sampling program designs.

10.   The following refinements have also been made to the load/response data set:

   a. Estimates of summer-average hydrologic and morphometric characteristics have been developed, based upon monthly hydrologic data files.

   b. For projects with annual residence times less than 0.5 year, estimates of summer-average inflow total phosphorus concentrations have been developed, based upon annual-average inflow concentrations, the ratio of summer outflow to annual outflow, and the tributary flow/concentration relationships developed in calculating reservoir nutrient budgets.

   c. Estimates of area-weighted-mean concentrations have been developed for phosphorus and other trophic state indicators, based upon station-mean concentrations and weighting factors estimated from station locations, project morphometry, and maps.

These refinements are discussed in more detail below.

11.   Since the median hydraulic residence time of the projects in the load/response data set is 0.22 year, seasonal variations in hydrology, morphometry, and inflow concentrations are potentially relevant to the prediction of summer-average water quality conditions. The file has been upgraded to include average, May-September, hydrologic and inflow conditions during the EPA/NES pool monitoring period. Corresponding inflow concentrations have been estimated only for projects with annual residence times less than 0.5 year and with significant flow/concentration relationships in the project tributaries. The seasonal inflow concentration estimates are based upon the annual estimates, tributary flow/concentration relationships, and seasonal inflow variations. These estimates are approximate and do not reflect any seasonal variations in inflow concentration which may be independent of flow. In order to reflect the latter, nutrient balances would have to be completely reformulated on a seasonal basis. May-September conditions have been used exclusively in the estimation of mean depths

18

for this data set.

12. The change-in-storage term of the water balance becomes significant in a few projects when summer conditions are considered; a means of incorporating its effect on the flushing rate of the impoundment is required. The generalized nutrient balance equation includes the following terms:

Input = Outflow + Change-In-Storage + Net Sedimentation   (1)

The Change-in-Storage term represents the increase in nutrient mass in the reservoir over the averaging period. The effects of changes in reservoir pool level on the nutrient balance can be partially represented by summing the Change-In-Storage and Outflow terms when computing the effective hydraulic residence time. This is approximate because it accounts for seasonal changes in reservoir volume, but not concentration. The data set is inadequate for direct calculation of the latter. The Change-in-Storage term is neglible for most reservoirs. Complete listings of the input/output and load/response data sets are given in Appendix A.

13. The data set has also been augmented to include information on reservoir outlet operation, described in terms of withdrawal levels (epilimnetic, metalimnetic, hypolimnetic, or combination) during the growing season. The original objective of this data compilation was to provide a means for testing the effects of outlet level on phosphorus retention and other eutrophication response characteristics. The compilation indicates, however, that a major portion of the reservoirs used in model testing have hypolimnetic or mixed discharge levels (see Appendix A). Only one project with an epilimnetic discharge is included in the data set used for testing nutrient retention models. The data set is inadequate to support a statistical analysis of withdrawal level effects on retention model performance, but is used in testing oxygen depletion models (Part V).

Model Development

14. A key assumption of early attempts at phosphorus mass-balance modeling in lakes was that the sedimentation of phosphorus could be represented as a first-order reaction (Vollenweider, 1969) or as a first-order settling process (Chapra, 1975) in a completely mixed system. To account for inadequacies in these assumptions, a number of empirical formulations for describing phosphorus sedimentation were subsequently developed and calibrated to data sets derived primarily from natural lakes. (e.g., Kirchner and Dillon, 1975; Larsen and Mercier, 1976; Vollenweider, 1975, 1976; Jones and Bachman, 1976; Reckhow, 1977; Walker, 1977). While they consider the same basic variables, the empirical models modify the theoretical formulations to account for unexplained variations in the data. For example, the exponent for residence time in the Larsen-Mercier (1976) retention model (.5) differs from the theoretical value (1.0) for a first-order reaction in a mixed system. The empirical functions have lower error variance but still assume that the response of lake (or lake outflow) phosphorus concentration is linear with respect to inflow concentration; i.e., that, for a given residence time and mean depth, lake concentration is proportional to the inflow concentration.

15. Recent models (Canfield and Bachman, 1981; Clasen, 1980; Frisk, 1981) calibrated to large data sets including both reservoirs and natural lakes suggest that the linear response assumption is invalid, or that the phosphorus retention coefficient should not be considered independent of inflow concentration. Higgins and Kim (1981) fit separate retention functions to TVA reservoirs with inflow phosphorus concentrations above and below 25 mg/m^3. Average effective settling velocities were 92 m/yr and 10 m/yr for impoundments with inflow concentrations above and below 25 mg/m^3, respectively. In analyzing the OECD Reservoir and Shallow Lakes data base, Clasen (1980) found that residual variance decreased by about a factor of two when the sedimentation coefficient was allowed to vary (increase) with inflow concentration, using a formulation similar to Canfield and Bachman's.

16. Preliminary testing of these models using the CE reservoir

20

data (Walker, 1982a) generally agrees with the last set of models. Of the published formulations tested without recalibration, the Canfield/Bachman reservoir model provides the best fit of outflow and pool concentration data:*

$$Po \: / \: Pi = 1 - Rp = 1 \: / \: (1 + .11 \: Pi^{.59} \: T^{.41}) \qquad (2)$$

where

Po = reservoir outflow phosphorus concentration (mg/m^3)

Pi = average inflow total phosphorus concentration (mg/m^3)

Rp = total phosphorus retention coefficient (dimensionless)

T = hydraulic residence time (years)

The above equation explains 77% of the variance in the outflow concentration of 60 CE reservoirs with a mean squared error of .035 on a base-10 logarithmic scale.

17. The model and data indicate that for a given residence time, the phosphorus retention coefficient increases with inflow concentration. This response can be considered "nonlinear" in the sense that the effective, first-order sedimentation coefficient is not solely a function of morphometric and hydrologic characteristics, as assumed in earlier models. The nonlinear response is qualitatively consistent with a concept discussed by Harris (1980) and Vollenweider and Kerekes (1979), namely that, compared with eutrophic lakes, oligotrophic lakes tend to recycle nutrients more efficiently within the mixed layer so that a proportionately smaller amount of external nutrient input is lost to the sediments, for a given morphometry and hydrology. The nonlinear response may also be related to complex interactions between dissolved and particulate phosphorus (adsorption/sedimentation processes).

18. Since most of the published empirical models were initially based upon a first-order assumption, a logical approach to refine the models for application to reservoirs would begin by assuming a higher-order reaction. Results presented below demonstrate that if one assumes

* For convenience, symbols and unusual abbreviations are listed and defined in the Notation (Appendix B).

21

a second-order phosphorus sedimentation reaction, the performance of simple, one-parameter, "black-box"[4] models substantially improves. Further refinements are also possible by empirical modification of the second-order formulation to account for effects of inflow phosphorus availability (ortho-P/total P) and overflow rate on the effective second-order decay rate, as described below.

19. Table 1 lists a total of 8 "mechanistic" models calibrated for predicting the annual-average outflow total phosphorus concentrations of 60 CE reservoirs. Each of these models contains only one parameter which describes the sedimentation of phosphorus under the following alternative assumptions:

a. Plug-flow vs. completely mixed system.
b. Decay reaction (volumetric) vs. settling (areal).
c. First-order vs. second-order in impoundment phosphorus concentration.

Error variances for these models range from .030 to .135 on base-10 logarithmic scales. The formulation with the lowest error variance represents phosphorus sedimentation as a second-order, volumetric reaction in a completely mixed system. In this case, the terms of the mass balance equation per unit of reservoir volume and per year are:

$$\text{Inflow} = Pi \text{ / } T \tag{3}$$

$$\text{Outflow} = Po \text{ / } T \tag{4}$$

$$\text{Sedimentation} = K2 \text{ } Po^2 \tag{5}$$

where

$K2$ = effective second-order decay rate (m^3/mg-yr)

The optimal estimate of the decay rate parameter, K2, is .1 m^3/mg-yr. The mean squared error (.030) is somewhat lower than that of the three-parameter, Canfield/Bachman model (.035).

20. In a completely mixed system, the outflow concentration is assumed to equal the average reservoir concentration. Figure 2 compares

Table 1
Formulations and Parameter Estimates of Mechanistic Models
Calibrated for Predicting Outflow Phosphorus Concentrations

Model Formulation	R^2	SE^2
01 Plug-Flow, First-Order, Constant Decay Rate:		
$Po = Pi \exp(-1.663\ T)$	.460	.081
02 Plug-Flow, First-Order, Constant Settling Velocity:		
$Po = Pi \exp(- 8.38\ T / Z)$	.180	.123
03 Mixed, First-Order, Constant Decay Rate:		
$Po = Pi / (1 + 4.09\ T)$	.620	.057
04 Mixed, First-Order, Constant Settling Velocity:		
$Po = Pi / (1 + 32.7\ T / Z)$	.527	.071
05 Plug-Flow, Second-Order, Constant Decay Rate:		
$Po = Pi / (1 + .027\ Pi\ T)$	.660	.051
06 Plug-Flow, Second-Order, Constant Settling Velocity:		
$Po = Pi / (1 + .49\ Pi\ T / Z)$	.100	.135
07 Mixed, Second-Order, Constant Decay Rate:		
$Po = [-1 + (1 + 4\ K2\ Pi\ T)^{.5}] / 2\ K2\ T$	.800	.030
$K2$ = effective decay rate = .10 (m^3/mg-yr)		
08 Mixed, Second-Order, Constant Settling Velocity:		
$Po = [-1 + (1 + 4\ U2\ Pi\ T / Z)^{.5}] / (2\ U2\ T / Z)$	.673	.049
$U2$ = effective settling velocity = .66 (m^4/mg-yr)		

NOTE: parameter estimates and error statistics based upon data
from 60 CE reservoirs, base-10 log scales.

Figure 2

Reservoir Total P vs. Outflow Total P

The figure plots LOG [RESERVOIR TOTAL P, MG/M^3] (y-axis, from 0.8 to 2.6) against LOG [OUTFLOW TOTAL P, MG/M^3] (x-axis, from 0.8 to 2.6). A line of best fit is shown with annotations:

$P = P_o$
$R^2 = .82$
$SE^2 = .030$
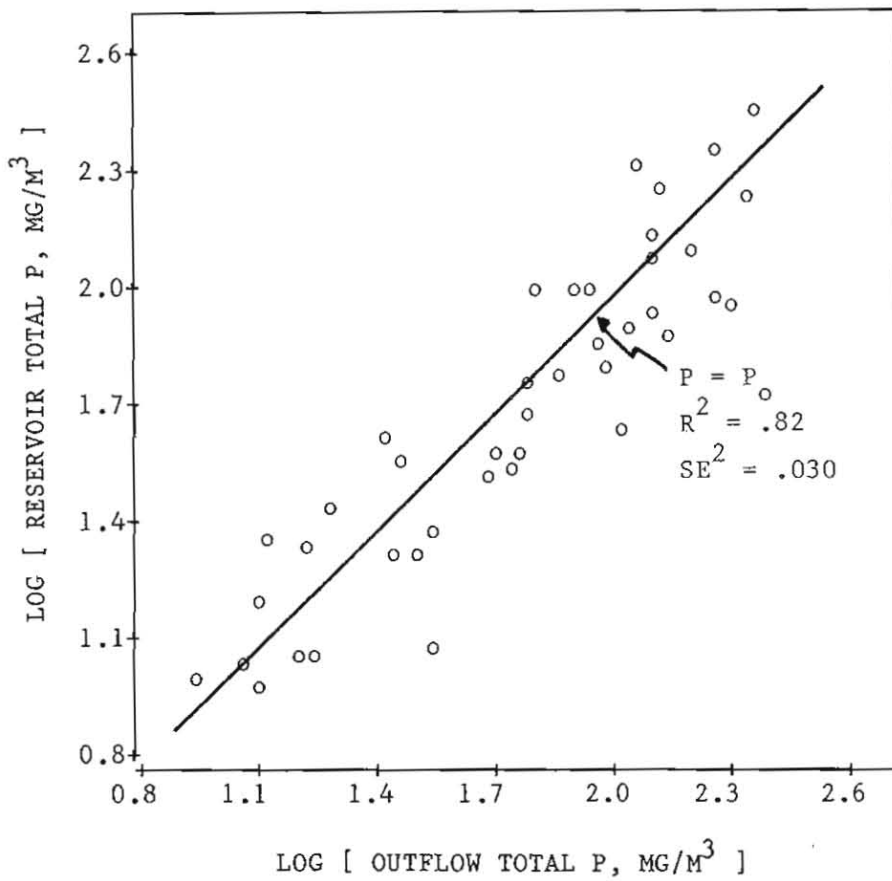
outfl
load/
diffe
relat
seaso
avera
varia
monit
1982
reser
the
conce
than
rese
demo
stro
most
lacu
comp
dire
refl
comp
comp

mass

With
conc
for
from
-.5.

outflow and reservoir-average concentrations derived from the load/response data set. The regression model is not significantly different from a simple equality, $P = P_o$. Variability in this relationship is attributed to random errors in P and P_o estimates, seasonal variations in water quality (growing season P vs. annual-average P_o), possible effects of discharge level on P_o, and year-to-year variations in quality, since the P and P_o estimates derived from EPA/NES monitoring generally correspond to different hydrologic years (Walker, 1982a). Despite the substantial spatial gradients occurring in some reservoirs (Walker, 1980, 1982a), the above model comparisons and the the relationship between reservoir and outflow total phosphorus concentrations indicate that a completely mixed assumption is better than a plug-flow assumption for the purposes of predicting outflow (and reservoir average, see Model Testing) phosphorus concentrations. As demonstrated in Part IV, longitudinal phosphorus gradients are generally strongest in upper-pool areas and weakest in lower-pool areas, where most of the reservoir volume is usually located. In near-dam, lacustrine zones, dispersion usually dominates over advection and the completely mixed assumption is usually not unreasonable (in horizontal directions). Model parameter estimates and error distributions would reflect the net effects of vertical stratification, which would be too complex to model explicitly in this context. Refinements to the completely mixed representation are developed in the Part IV.

21. Under the completely mixed assumption, the solution of the mass-balance equation for outflow phosphorus concentration is given by:

$$P_o = \frac{-1 + (1 + 4\ K2\ T\ P_i)^{.5}}{2\ K2\ T} \tag{6}$$

With this formulation, the sensitivity of the predicted outflow concentration to changes in inflow concentration (percent change in P_o for a 1% change in P_i) ranges from 1 to .5, as residence time ranges from 0 to infinity, while the sensitivity of P_o to T ranges from 0 to -.5. The limiting sensitivity to T (-.5) equals that of the lake

phosphorus retention model developed by Vollenweider (1976) and Larsen and Mercier (1976). Using standard algebraic techniques, it can also be shown that the model generates the reasonable prediction that the inflow and outflow concentrations are equal in the limit of zero residence time (i.e., no reservoir).

22. Table 2 lists and evaluates nine empirical models in relation to the eight mechanistic formulations tested above. Models 09 and 10 are empirical versions of the first-order sedimentation model which assume plug-flow and completely mixed conditions, respectively; these models allow the effective sedimentation coefficient to vary as a power function of residence time, mean depth, and inflow concentration. Each of these models has four parameters which have been optimized for this data set using nonlinear regression. Despite the increased flexibility provided by the four parameters, the mean square error of the best formulation, .027 for model 10, is only marginally better than .030, the value obtained for the one-parameter model 07. Models 11 - 14 in Table 2 are alternative empirical formulations which can be viewed as "special cases" of model 10, with appropriate selection of model coefficients.

23. Model 15 was originally developed by Lappalainen (1975) based upon data from Finnish reservoirs. Several forms of this model were evaluated by Frisk et al. (1981); the one presented in Table 2 worked best for their data set and for the data set evaluated here. It is similar to the plug-flow, second-order model (08 in Table 1), with the exception of the numerator (1 + .0043 Pi T), which places an upper limit on the computed retention coefficient (in this case, .9). The model performs as well as the Canfield and Bachman (1981) reservoir model and recalibration to the CE data set provides no improvement in fit. Lappalainen's second-order kinetic model was later employed by Frisk (1981) in modeling spatial and temporal variations in Finnish reservoirs, as described in Part IV.

24. The above results suggest that the second-order, completely mixed formulation (model 07) compares favorably with the empirical formulations involving more parameters. Refinements (models 16 and 17 in Table 2) are developed below, based upon a systematic analysis of

26

Table 2
Formulations and Parameter Estimates of Empirical Models
for Predicting Outflow Phosphorus Concentrations

Model Formulation	R^2	SE^2
09 Plug-Flow, First-Order, Empirical: $P = Pi \exp (- .805\ T^{.23}\ Z^{.32}\ Pi^{.41})$	.807	.029
10 Mixed, First-Order, Empirical: $P = Pi / (1 + .037\ T^{.42}\ Z^{.45}\ Pi^{.67})$	.820	.027
11 Calibrated to CE Reservoir Pool Concentrations, Walker, 1982: $P = Pi / (1 + .0012\ Pi\ Z)$	.753	.037
12 Vollenweider/Larsen & Mercier Model, 1976: $P = Pi / (1 + T^{.5})$	.413	.088
13 Modified Vollenweider/Larsen & Mercier,1976; Clasen, 1980: $P = Pi / (1 + 2\ T^{.5})$	.633	.055
14 Canfield and Bachman, 1981: $P = Pi / (1 + .11\ Pi^{.59}\ T^{.41})$	.767	.035
15 Lappalainen, 1975; Frisk et al., 1981: $P = Pi (1 + .0043\ Pi\ T) / (1 + .043\ Pi\ T)$	.773	.034
16 This Study, Second-Order, Qs modification: * $K2 = .17\ Qs / (Qs + 13.3)$	.833	.025
17 This Study, Second-Order, Qs and Fot modification: * $K2 = .056\ Qs / ((Qs + 13.3)\ Fot)$ Fot = tributary inflow ortho-P/total-P ratio	.890	.017
18 This Study, Model 14 with Inflow Available P Defined by: $Pia = 1.94\ Pio + .30\ (Pi - Pio)$ Pio = inflow ortho-P (mg/m^3)	.813	.028
19 This Study, Model 16 with Inflow Available P Defined by: $Pia = 2.26\ Pio + .33\ (Pi - Pio)$	.860	.021

* See Model 07, Table 1.

residuals as a function of reservoir morphometric, hydrologic, and inflow characteristics.

25. Figure 3 shows that model 07 tends to underpredict outflow phosphorus concentrations in a few reservoirs with surface overflow rates (or areal water loadings) less than about 10 meters/year. A similar relationship is apparent in other data sets examined below, including EPA/NES reservoirs (Figure 4). One explanation is that reservoirs with low areal water loadings would also tend to have low drainage area to surface area ratios, low areal sediment loadings, and therefore, low sediment accumulation rates. Effects of sediment accumulation rate on phosphorus trapping efficiency have been demonstrated previously (Walker and Kuhner, 1979; Walker, 1982a). One measure of the potential effect of an areal internal phosphorus loading on the water column concentration (mg/m^3) is obtained by dividing the areal loading (mg/m^2-year) by the overflow rate (m/year); the latter is a measure of dilution effect. By this rationale, the potential significance of the internal loading or recycling on water column concentration increases with decreasing overflow rate and may also explain the dependence noted above. The negative residuals in Figure 3 are attributed to differences in response to dissolved vs. particulate loadings, as described in detail below.

26. One way of accounting for the positive residuals in Figures 3 and 4 is to represent the second-order decay rate as a saturation function of overflow rate:

$$K2 = C1 \ Qs \ / \ (Qs + \ C2) \qquad (7)$$

$$Qs = Z \ / \ T \qquad (8)$$

where

   C1, C2 = empirical parameters
   Qs = surface overflow rate (m/yr)
   Z = mean depth (m)

Optimization or parameter estimates yield values of .17 and 13.3 for C1 and C2, respectively, and a residual mean square of .025. This is

28

Figure 3

Model 07 Residuals vs. Surface Overflow Rate
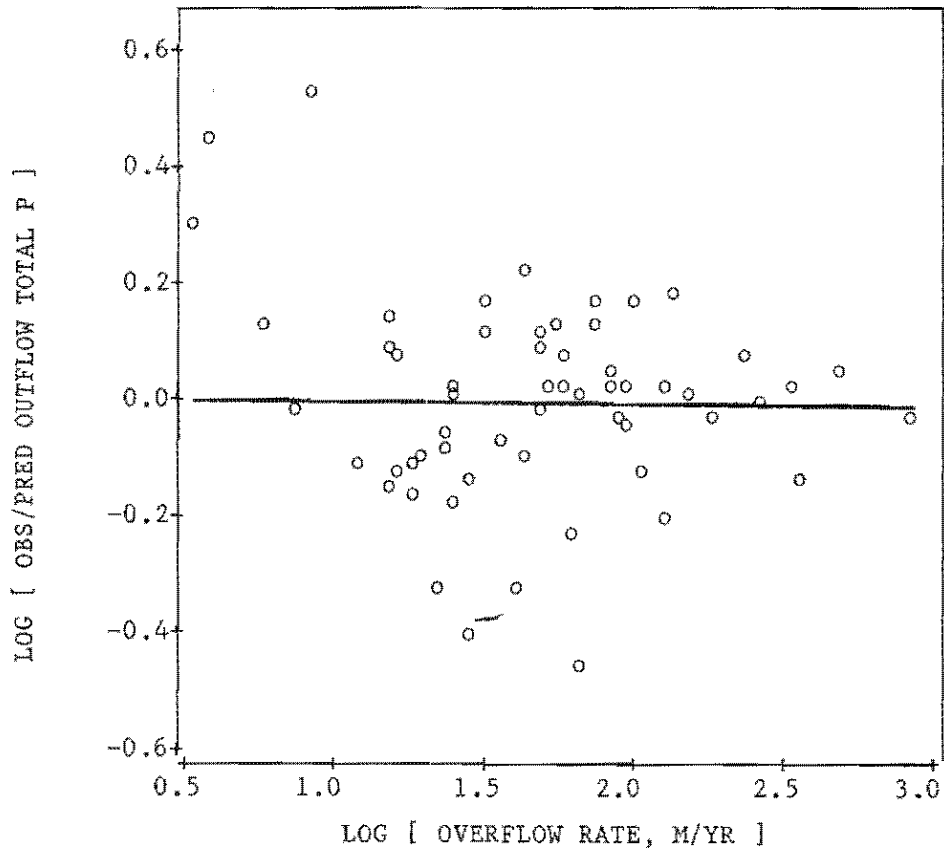
Figure 4

Phosphorus Retention Model Residuals vs. Overflow Rate - EPA/NES Data


```
     1.2 +                             Model 07: Second-Order
         |
         |                                      K2 = .1
     0.9 +                A          B     A
         |                                A
         |              A AA         A
     0.6 +          A          A AA
         |                          A A
         |              A AAAA BB A
         |              A ADAAC   AA
         |              A B  ABAAABA
     0.3 +       AA       ABC A A AAB AA
         |                AABBCCDADCCCCA   AA
         |              A A  AABCACBDCACBEAAA
         |          A       BAACCACGEDD DEAABAAAAAA    A
  R      |
  E 0.0 +----------------A----A-B---DCBBFFEBCBCGEAC-BCD------A
  S      |                A DABEACD A EABCBBAB BBA    A  A
  I      |                B AABABCAC ACABBA DAACA   A
  D      |              B   A  BA A   A    A
  U -0.3 +              A   ABAA AA A
  A      |                  B  A   A       A AAA
  L      |                    A
         |                A           A
    -0.6 +
         ---+---------+---------+---------+---------+---------+------
           -1         0         1         2         3
```

LOG10 [OVERFLOW RATE, M/YR]


```
         |                       Model 16: Second-Order
    0.75 +
         |                      A        K2 = .17 Qs/(Qs + 13.3)
         |                 A
         |               B      A
    0.50 +             A AA A A A
         |          A    A   BB A
         |          A  A  A C  AA
         |              CAA AAAAAAA  A
    0.25 +            ABBABB BCBBCA    A
         |            A  A BADCBCADAAB
  R      |        A    A  CC BCCBBABFCDC BD ABA    A        A
  E      |            A AA BABBCABBEGFACACBBABACBC    A
  S 0.00 +------------------AAACC-AAECBADA-FBBCEC-C--BA------A
  I      |            A AABA  B BC     CBBBCA CBA   A  A
  D      |            A  AAABCBDAD AC AAA AAAAA  A
  U      |              A     C AAA A A  B   AA  A
  A-0.25 +              AA AAA   B A
  L      |       AA AA   A   AAA A
         |              A  AAB   A      A AAA
         |           A   A A
    -0.50 +          A       A       A
         |          B
         |             A
    -0.75 +
         ---+---------+---------+---------+---------+---------+------
           -1         0         1         2         3
```

LOG10 [OVERFLOW RATE, M/YR]

NOTE: symbols denote overlays (A=1 observation, B=2 observations, etc.)
      based upon EPA/NES data from 374 reservoirs
      RESIDUAL = LOG10 [OBSERVED/PREDICTED OUTFLOW P]

referenced as model 16 in Table 2.

27.   With this formulation, the expression for the change in
phosphorus concentration moving through the impoundment becomes:

$$Pi - Po = \frac{Cl\ Qs\ T\ Po^2}{Qs + C2} = \frac{Cl\ Z\ T\ Po^2}{Z + C2\ T} = \frac{Cl\ Z\ Po^2}{Qs + C2} \qquad (9)$$

Of the variables used to represent impoundment morphometry and hydrology
(Qs, T, and Z), only two are statistically independent. The overflow
rate or areal water loading (outflow/area) can be taken as a hydrologic
factor and mean depth (volume/area) as a morphometric factor. Area
appears as a scale factor in each variable. Residence time
(volume/outflow or depth/water loading) is a less fundamental variable
because it is dependent both upon depth and discharge. As overflow rate
approaches infinity (or as residence time approaches zero), Pi-Po
approaches zero. In this situation, flushing rate is controlling, and
inflow quality approaches outflow quality. As overflow rate approaches
zero (or as residence time approaches infinity), Pi-Po is proportional
to depth. The importance of the depth term may reflect influences of
internal recycling or bottom sediment resuspension on the phosphorus
mass balance. These responses seem reasonable in view of the apparent
significance of depth terms in the empirical models calibrated above
(models 09, 10, 11 in Table 2). Most of the other model formulations
presented in Tables 1 and 2 predict zero outflow or reservoir
concentrations in the limit of high residence times, a result which
seems unrealistic in the sense that one would expect to measure finite
phosphorus levels in a lake or reservoir with no outlet.

Inflow Phosphorus Availability

28.   Residuals from phosphorus retention models calibrated to the
CE reservoir data set are positively correlated with the inflow ortho-
P/total P ratio, as shown in Figure 5 for model 16 residuals. This
correlation is qualitatively consistent with differences between
dissolved and particulate phosphorus with respect to bioavailability

Figure 5

Model 16 Residuals vs. Tributary Ortho-P/Total-P Ratio
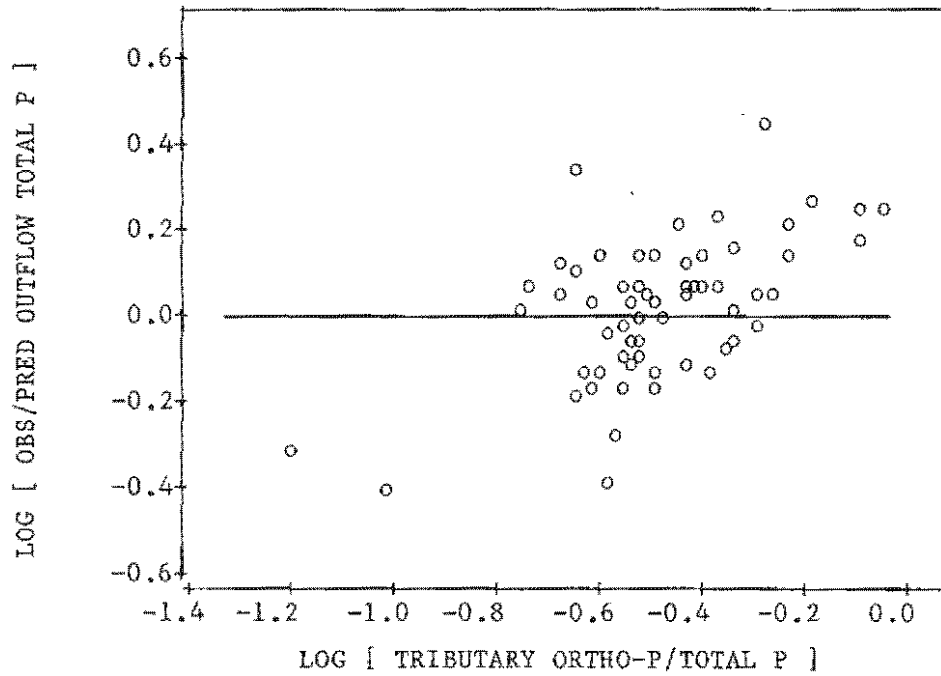
and/or decay rate within impoundments. One means of accounting for inflow phosphorus availability would be to apply weighting factors to the various loading components (Lee et al., 1980; Chapra, 1982; Sonzogni et al., 1982). Alternatively, the effective decay rate could be modeled as a function of inflow characteristics. These approaches are investigated below.

29. Estimates of the "bioavailability" of inflowing particulate phosphorus range from less than 4% to about 50%, depending upon region (within U. S.), sediment characteristics, and assay technique (Li et al., 1974; Porter, 1975; Cowen and Lee, 1976a, 1976b; Armstrong et al., 1977; Logan, 1978; Dorich and Nelson, 1978; Logan et al., 1979). As discussed by Logan et al. (1979), laboratory measurements of sediment phosphorus availability generally reflect equilibrium conditions and assume that availability is not limited by isolation of the sediment from the water column. Because of kinetic limitations, the actual quantities of sediment phosphorus released from particles entering a reservoir may be considerably less than predicted by laboratory bioassays or extraction techniques. Logan et al. (1979) found that rates of sediment phosphorus uptake by algae under laboratory conditions were less than 0.4 percent per day and concluded that the "kinetic rate appears to be more of a limiting factor in the supply of P to algae by sediment than the total available sediment-P." If kinetics are important, then the rates and locations of sediment deposition/resuspension, along with the sediment chemisty, would be critical to determining the ultimate availability and impact. Laboratory studies of phosphorus availability conducted under aerobic conditions may not reflect potential releases under anaerobic conditions, the impacts of which would also depend upon location and mixing characteristics.

30. Chapra (1982) and Sonzogni et al. (1982) defined the term "positional availability" to reflect the net effects of inflow characteristics and sedimentation on lake or reservoir responses to particulate phosphorus loadings in an empirical modeling context. The external phosphorus loading is partitioned into two components with different settling velocities. Because the settling velocity of the

33

particulate fraction is large in relation to that of the dissolved fraction, Chapra (1982) suggested that the resulting mass balance could be formulated as:

$$P = Pi \ (1-fs) \ / \ (1 + U1/ \ Qs) \tag{10}$$

where

P = reservoir total phosphorus concentration (mg/m^3)

Pi = inflow total phosphorus concentration (mg/m^3)

fs = fraction of incoming load immediately settled or positionally unavailable

$U1$ = effective settling velocity (m/yr)

Qs = surface overflow rate (m/yr)

The factor $(1-fs)$ essentially reduces the loading to account for immediate removal of the rapidly settling fraction. In modeling Lake Erie, Chapra assumed an fs factor of .5 for tributary loadings. Chapra subsequently modified the settling velocity formulation to take into account the potential for resuspension in shallow systems using a function of the following form:

$$U1 = Umax \ Z \ / \ (\ Z + \ Zc \ ) \tag{11}$$

where

$Umax$ = maximum settling velocity (m/yr)

Z = mean depth (m)

Zc = depth at which $U1 = .5 \ Umax$ (m)

Optimal parameter estimates based upon data from New York Lakes and Lake Erie were 30.6 m/yr for Umax and 14.3 m for Zc. In shallow systems ($Z \ll Zc$), the predicted settling velocity is proportional to depth; in deep systems ($Z \gg Zc$), it is independent of depth and approaches Umax.

31. Use of this formulation requires calibration of the parameters Umax and Zc and estimation of fs; the latter would presumably vary from one reservoir to another. A weighting scheme similar to that suggested by Lee et al. (1980) could be used to estimate an "effective," or "positionally available" inflow concentration for each reservoir, based upon the estimated partitioning of the inflow between the dissolved and

34

particulate phases. The simplest definition would be:

$$Piav = Pi\ (\ 1 - fs\ ) = \quad Pid \quad + fo\ Pip \qquad (12)$$

where

Piav = inflow available P (mg/m^3)

Pid = inflow dissolved P (mg/m^3)

fo = weighting factor for particulate fraction

Pip = inflow particulate P (mg/m^3)

Based upon phosphorus availability studies, Lee et al. (1980) suggested a nominal value of .2 for fo, with Pid estimated from soluble ortho-phosphorus measurements.

32. The CE data set permits inflow phosphorus partitioning according to the following scheme:
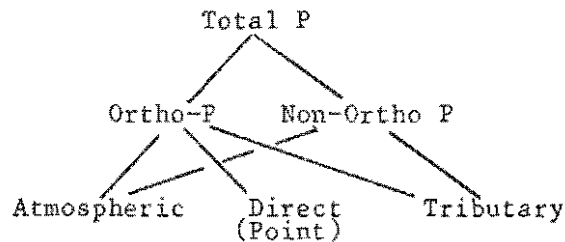
The first partitioning level considers only two components (ortho and non-ortho). The second further distinguishes among atmospheric, direct point-source, tributary ortho, and tributary non-ortho components. In developing the nutrient balances, half of the estimated atmospheric loadings and all of the direct loadings were assumed to be in ortho form (Walker, 1982a). The tributary loading component strongly dominates for most reservoirs and is partitioned based upon direct ortho-P and total P measurements.

33. One problem with implementing the above dissolved/particulate weighting scheme (Equation 12) is the lack of inflow total dissolved phosphorus data. The ortho-phosphorus inflows could be used as surrogates, but the dissolved, non-ortho fractions could be appreciable in some cases. Four weighting schemes have been tested, given the

inflows partitioned as described above:

Scheme 1: Piav = ortho + non-ortho

Scheme 2: Piav = ortho + f1 (non-ortho)

Scheme 3: Piav = f2 (ortho) + f3 (non-ortho)

Scheme 4: Piav = atmos. + f4 (direct) +
f5(tributary ortho) + f6(tributary non-ortho)

where

f1-f6 = empirical weighting factors

The first scheme is a control which treats all inflow fractions equally.
The second provides an empirical weighting factor for the inflow, non-ortho component. The third provides weighting factors for both the ortho and non-ortho components. This assumes that the inflow dissolved phosphorus is proportional to inflow ortho-phosphorus; the two weighting factors also provide a rescaling of the computed retention factor (1-Rp) for use with inflow available P vs. inflow total P. The fourth scheme provides an additional weighting factor to account for possible differences in response to tributary ortho-phosphorus vs. direct point-source loadings. A scaling factor is not provided for the atmospheric component because of its general insignificance in most reservoirs and because estimates of this component are relatively imprecise.

34. Testing of the above schemes involves optimization of the weighting factors to maximize agreement between observed and predicted outflow phosphorus concentrations. Weighting parameters have been estimated for each of four different formulations for the phosphorus retention coefficient, as outlined in Table 3. For each retention model, model mean squared errors are lowest for Scheme 4. Conclusions regarding the relative impacts of the various inflow components are not strongly dependent upon the assumed retention model. Estimates of weighting factors range from .06 - .17 for the tributary, non-ortho component; 1.71 - 2.99 for the tributary, ortho component; and .26 -

36

Table 3
Calibration and Comparison of Inflow Available Phosphorus
Calculation Schemes for Various Retention Models

Loading Component		Retention Model I	II	III	IV
------------------------ Scheme 1 ---------------------------					
Ortho	*	1.00	1.00	1.00	1.00
Non-Ortho	*	1.00	1.00	1.00	1.00
MSE		.055	.035	.025	.100
------------------------ Scheme 2 ---------------------------					
Ortho	*	1.00	1.00	1.00	1.00
Non-Ortho		.71	.74	.91	.36
MSE		.047	.032	.025	.044
------------------------ Scheme 3 ---------------------------					
Ortho		1.81	1.94	2.26	1.29
Non-Ortho		.34	.30	.33	.24
MSE		.041	.028	.020	.043
------------------------ Scheme 4 ---------------------------					
Atmospheric	*	1.00	1.00	1.00	1.00
Direct Point		.46	.21	.35	.26
Trib. Ortho		2.36	2.71	2.99	1.71
Trib. Non-Ortho		.17	.06	.11	.10
MSE		.035	.021	.016	.035

Inflow Available P = Sum (weight x component).
* Weighting factors constrained to 1.0 (others optimized).
MSE = mean squared error, base-10 logarithm.

Model I: Clasen (1980) (Model 13 in Table 2):

$$Po = Pi / (1 + 2 T^{.5})$$

Model II: Canfield and Bachman (1981) (Model 14 in Table 2):

$$Po = Pi / (1 + .11 Pi^{.59} T^{.41})$$

Model III: Second-Order (Model 17 in Table 2):

$$K2 = .17 Qs / (Qs + 13.3)$$

$$Po = (-1 + (1 + 4 K2 Pi T)^{.5}) / 2 K2 T$$

Model IV: Chapra (1982):

$$Po = Pi / (1 + 30.6 T / (14.3 + Z))$$

.46 for the direct, point-source component. Results seem to indicate, therefore, that impoundment responses are related most strongly to variations in tributary, ortho-P loadings and that tributary, non-ortho loadings have relatively low "positional availability" and impact on reservoir outflow concentration. Conclusions are similar when the model coefficients are optimized for predicting reservoir phosphorus (vs. outflow phosphorus) concentrations, as described below.

35. The reasons for the low weights attached to the direct point-source loadings vs. tributary ortho-phosphorus loadings are not immediately obvious but may be related to sediment phosphorus equilibria. While the same conclusion is reached for each retention model, direct point-source phosphorus loadings account for more than 10% of the total phosphorus loadings in only 5 out of the 60 impoundments studied. The estimates of direct point-source loading weights are relatively imprecise and require further study using an expanded data set. The result is not unrealistic, however, when one considers the potential for removal of point-source loadings by adsorption and sedimentation. For example, the exchange of available phosphorus in soil/water suspensions can be approximately represented using a linear adsorption isotherm (Snow and DiGiano, 1976):

$$Y = k \, Pex \qquad (13)$$

$$Ptex = (1 + k \, Cs) \, Pex \qquad (14)$$

where

Y = exchangeable phosphorus adsorbed to solid phase (mg/kg)
k = partition coefficient $(mg/kg)/(mg/m^3)$
Pex = exchangeable phosphorus in solution (mg/m^3)
$Ptex$ = total exchangeable phosphorus in suspension
    = adsorbed phase + dissolved phase (mg/m^3)
Cs = suspended sediment concentration (mg/m^3)

Equilibrations of the above type occur relatively rapidly (Taylor and Kunishi, 1971) and would be expected to be characteristic of impoundment tributaries. The process of sedimentation removes "Cs" from the water

column, but the "equilibrium phosphorus concentration" (Pex) is independent of Cs for a given k value. If a point-source loading in the dissolved phase were added to the inflowing tributary, increasing the total phosphorus concentration by dP mg/m^3, the resulting solution for the equilibrium phosphorus concentration in the dissolved phase is:

$$Ptex' = Ptex + dP = (1 + k\ Cs)\ Pex' \qquad (15)$$

$$Pex' = \frac{Ptex'}{1 + k\ Cs} = Pex + \frac{dP}{1 + k\ Cs} \qquad (16)$$

where

   dP = point-source addition (mg/m^3)

   ' = conditions after equilibration with point-source addition

The marginal effect of dP on Pex' is reduced by the factor $(1 + k\ Cs)$, which accounts for adsorption of the point-source loadings onto the tributary sediments. Subsequent sedimentation within the impoundment would remove some of the point-source loadings in an adsorbed form. Note that a potential still exists for recycling of the adsorbed phosphorus via diffusion from aerobic or anaerobic bottom sediments or by wind-induced resuspension. The above equations demonstrate, however, that adsorption equilibria provide a driving force for removal of point-source phosphorus; this driving force does not exist for tributary, ortho-phosphorus loadings, which have already equilibrated with the suspended sediments prior to entering the impoundment, and may account for some of the differences in the weighting factors found above. According to the above rationale, the effects of direct point-source loadings on the impoundment response would depend upon reservoir-specific factors which are not explicitly considered in the weighting scheme (i.e., k and S).

36. An alternative explanation for the apparently reduced significance of point-source loadings relates to the effects of spatial variations in loading and concentration within the impoundments. Some impoundments with direct point-source loadings would tend to have localized areas of relatively high concentration in the bays or

39

tributary arms where the discharges are located. For example, as a result of upstream point-source discharges, the upper end of the James River arm of the Table Rock Reservoir (District 24; Reservoir 200) has an average phosphorus concentration of about 85 mg/m^3, as compared with an average concentration of about 25 mg/m^3 near the dam. Because of the nonlinear nature of the phosphorus retention function (e.g., second-order in phosphorus concentration), spatial variations can result in significantly higher rates of phosphorus sedimentation, as compared with the completely mixed case. An appropriate analogy is that the "average squared" concentration always exceeds the "squared average" concentration.

37. These explanations, coupled with the fact that reservoirs dominated by direct point-source discharges are only weakly represented in the data set, suggest that it would be imprudent to apply the fourth weighting scheme until it can be further evaluated. The best alternative is to use Scheme 3, which provides weighting factors for the ortho and non-ortho components:

$$Pia = 2.26 \ Pio + .33 \ Pino \tag{17}$$

$$= 2.26 \ (\ Pio + .15 \ Pino \ ) \tag{18}$$

where

   Pia = inflow available P (mg/m^3)
   Pio = inflow ortho-P (mg/m^3)
   Pino = inflow non-ortho-P = Pi - Pio (mg/m^3)

Using this weighting scheme with the second-order decay model reduces model mean squared error from .025 to .020. As Equation 18 more clearly indicates, the coefficient for Pio is interpreted as a calibration factor for the retention model for use with available P vs. total P inflows. The ratio of the Pino coefficient to the Pio coefficient (.15) reflects the relative significance of the two loading components. This ratio varies from .15 to .19 for the four retention models tested in Table 3. Simultaneous optimization of the weighting

40

factors and retention model parameters provides no improvement in the fit.

38. With weighting factors of 2.26 and .33, computed available phosphorus concentrations exceed total phosphorus concentrations for inflow ortho P/total P ratios exceeding .35. While this may be conceptually difficult, it is not a practical problem because the available phosphorus concentration includes a model calibration factor and predictions of outflow or reservoir phosphorus are unbiased.

39. Figure 6 plots approximate 90% confidence ranges for the ortho and non-ortho weighting factors estimated from four data sets. The coefficients have been optimized for predicting outflow and pool phosphorus levels first using all data and subsequently restricting the data to include only projects with one major tributary. Generally, the coefficients are similar for the pool and outflow concentration predictions. The non-ortho-phosphorus weighting factor increases from .33 to about .50 when the data are restricted to projects with one major tributary. While the weighting scheme provides a significant improvement in fit in all cases, the confidence regions for the coefficients are relatively wide and an expanded data set would be required to refine the estimates. One major limitation is that appropriate weighting factors may be site-specific because they would depend upon the composition of the non-ortho-phosphorus loading component, especially particle size distribution, timing, and chemical form (organic vs. inorganic, etc.).

40. An alternative means of accounting for inflow phosphorus availability using the second-order model is to represent the effective decay rate as a power function of tributary inflow ortho/total P ratio:

$$K2 = \frac{C1 \; Qs \; Fot^{C3}}{Qs + C2} \tag{19}$$

where

$K2$ = effective second-order decay rate $(m^3/mg\text{-}yr)$
$C1, C2, C3$ = model parameters

41

Figure 6

90% Confidence Regions for Weighting Factors
Used to Estimate Inflow Available Phosphorus
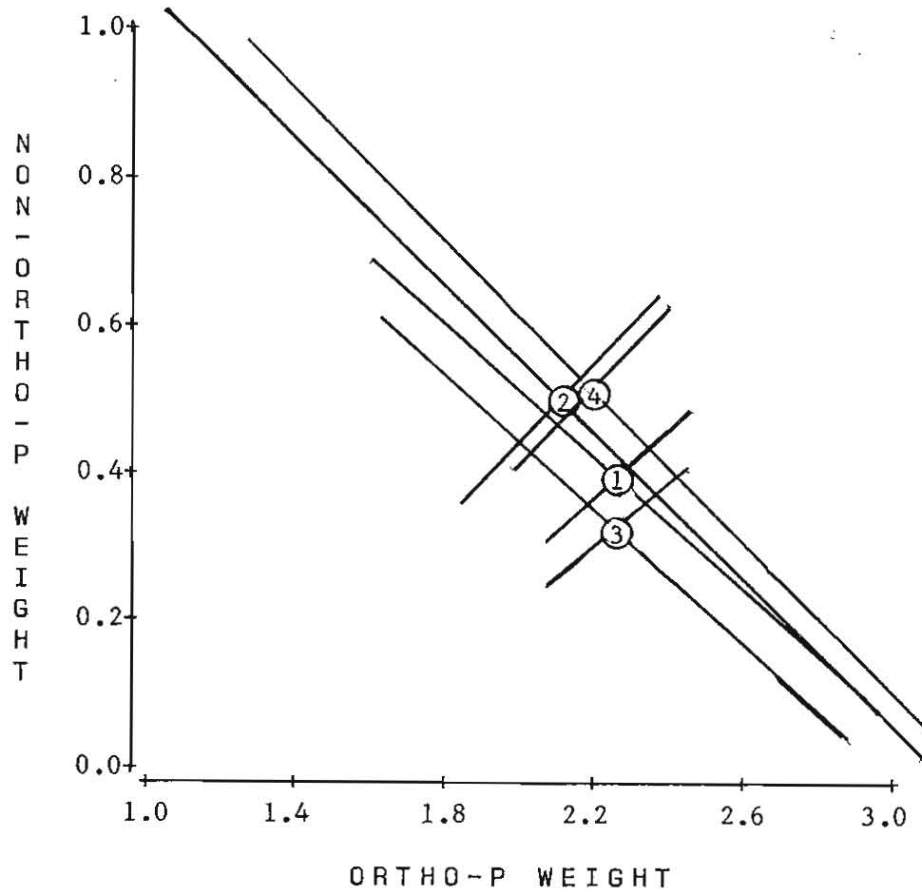
| Symbol | Prediction | Data | N | Optimal Weights* | | |
				Ortho-P	Non-Ortho-P	Ratio
1	Pool P	All	41	2.27	.39	.17
2	Pool P	**1 Major Trib	27	2.11	.50	.24
3	Outflow P	All	60	2.26	.33	.15
4	Outflow P	**1 Major Trib	40	2.19	.51	.23

* Weights defined for Model III, Scheme 3, in Table 3.
** Excluding projects with more than one major tributary.

42

Qs = surface overflow rate (m/yr)

Fot = tributary ortho-P / total P ratio

The tributary ortho-P/total P ratio presumably reflects the distribution of phosphorus between the ortho and non-ortho components which is typical of watershed soils and stream sediments and which would be expected to influence the driving force for phosphorus sedimentation within the impoundment. Note that direct point-source discharges and atmospheric loadings are not considered in the calculation of Fot. Estimation of the parameters of these models yields the following results in comparison with other forms of the second-order decay model:

Model	C1	Parameters C2	C3	SE^2	R^2
07	.10	–	–	.030	.80
16	.17	13.3	–	.025	.85
17	.056	13.3	-1.0	.017	.89

Modification of the basic second-order model to account for effects of overflow rate and inflow phosphorus partitioning decreases the residual mean squared error from .030 to .017. The Fot exponent (-1.0) has a standard error of .24 and is significantly different from zero at $p < .01$.

41. Equation 19 is an alternative to the inflow available phosphorus weighting schemes discussed above. Based upon error magnitudes and residual patterns, it is difficult to distinguish between these two methods of accounting for inflow phosphorus partitioning, given existing data. In most cases, the difference between the predictions of these models is small, especially in relation to model standard errors of .13-.14 log units. As discussed above, the phosphorus loadings of most of the reservoirs in the data base are of non-point origin. Additional data from a wider spectrum of impoundments, including systems influenced by direct point sources, would provide further model discrimination. Time series data from

43

reservoirs undergoing changes in the magnitudes and/or phases (dissolved vs. particulate) of external phosphorus loadings would also permit further model discrimination.

Model Testing

42. Table 4 describes 16 alternative data sets which have been compiled for use in testing the phosphorus retention models developed in the previous section. Observed outflow and pool phosphorus concentrations are compared with the predictions of models 01 - 19, as identified in Tables 1 and 2. The data sets describe conditions in CE reservoirs, other US reservoirs and natural lakes sampled by the EPA National Eutrophication Survey, TVA reservoirs, and reservoirs studied in the OECD Reservoir and Shallow Lakes Project. Data sources and screening criteria are identified in Table 4. To eliminate some impoundments with large errors in nutrient loading estimates and to conform approximately to the limits of the CE data set, impoundments with total phosphorus retention coefficients less than -.1, surface overflow rates less than 0.25 m/yr, and inflow total phosphorus concentrations exceeding 1000 mg/m^3 have been excluded from testing. These are liberal screening criteria which apply to relatively few impoundments.

43. Results are presented in Tables 5 (arranged by data set) and 6 (arranged by model). Mean squared errors are summarized for each data set and model in Table 7. While there is no satisfactory statistical test for comparisons of error variances within each data set, symbols are used in Table 7 to identify variances which are within 20% of the minimum variance found within each data set and model category (mechanistic vs. empirical).

44. Data set A describes input/output relationships in 60 CE reservoirs and was used for model development in the previous section. Data set B is a subset including 40 CE reservoirs with one major tributary arm. This has been analyzed to investigate possible effects of morphometric complexity on model performance. Comparing columns "A" and "B" in Table 7 indicates that all models show reduced mean squared

Table 4
Key to Data Sets Used in Testing Phosphorus Retention Models

Code	Source	Reservoirs	Predicted Variable	n	Notes
A	This Study	CE	Po	60	all reservoirs
B	"	CE	Po	40	1 major tributary
C	"	CE	P	41	annual Pi, T
D	"	CE	P	41	seasonal Pi, T (see text)
E	EPA/NES (1978)	CE	Po	93	NES Compendium
F	"	CE	P	96	"
G	"	US-Res.	Po	294	" excluding CE Reservoirs
H	"	US-Res.	P	275	" excluding CE Reservoirs
I	"	US-Lakes	Po	170	"
J	"	US-Lakes	P	168	"
K	Higgins	TVA	Po	9	Tributary Reservoirs
L	and Kim(1981)	TVA	P	7	Tributary Reservoirs
M	"	TVA	Po	9	Mainstem Reservoirs
N	"	TVA	P	8	Mainstem Reservoirs
O	Clasen(1980)	Global	Po	20	OECD/RSL Reservoirs
P	"	Global	P	19	OECD/RSL Reservoirs

NOTES:
Screening criteria applied to all data sets:
    (1) non-missing values for Pi, T, Z, P (or Po)
    (2) total phosphorus retention coefficient > -.1
    (3) inflow total phosphorus concentration < 1000 mg/m3
    (4) surface overflow rate Z/T > .25 m/yr
    (5) reservoirs with inflow ortho-P estimates and excluding
        artificial pumped storage impoundments (OECD/RSL Study)
n = number of reservoirs

Table 5

Phosphorus Retention Model Error Statistics
Sorted by Data Set

MO DATA	N	MEAN	T	MSE	VAR	MABS	R2
00 A	60	1.696	33.92*	3.025	0.150	1.696	1.000
01 A	60	-0.117	-3.48*	0.081	0.068	0.210	0.460
02 A	60	-0.193	-5.07*	0.123	0.087	0.259	0.180
03 A	60	-0.042	-1.37	0.057	0.056	0.185	0.620
04 A	60	-0.063	-1.26	0.071	0.070	0.191	0.527
05 A	60	0.113	-2.23*	0.051	0.046	0.161	0.660
06 A	60	0.120	2.97*	0.030	0.120	0.251	0.100
07 A	60	-0.013	-0.67	0.030	0.030	0.127	0.800
08 A	60	-0.025	-0.87	0.049	0.049	0.163	0.673
09 A	60	-0.004	-0.18	0.029	0.029	0.133	0.807
10 A	60	-0.005	-0.24	0.027	0.027	0.126	0.820
11 A	60	-0.009	-6.27	0.036	0.036	0.133	0.760
12 A	60	-0.180	-5.89*	0.088	0.056	0.217	0.413
13 A	60	-0.065	-2.21*	0.035	0.052	0.176	0.633
14 A	60	-0.048	-2.05*	0.035	0.033	0.140	0.767
15 A	60	-0.060	-2.64*	0.034	0.031	0.139	0.773
16 A	60	-0.003	-0.14	0.025	0.026	0.123	0.833
17 A	60	0.005	0.30	0.017	0.017	0.105	0.887
18 A	60	-0.005	-0.21	0.029	0.029	0.135	0.811
19 A	60	-0.004	-0.21	0.020	0.021	0.115	0.867

MO DATA	N	MEAN	T	MSE	VAR	MABS	R2
00 B	40	1.752	29.72*	3.205	0.139	1.752	1.000
01 B	40	-0.070	-1.68	0.071	0.071	0.193	0.438
02 B	40	-0.133	-2.92*	0.098	0.083	0.226	0.295
03 B	40	-0.006	-0.16	0.054	0.055	0.177	0.612
04 B	40	0.009	0.23	0.061	0.063	0.176	0.561
05 B	40	-0.017	-0.51	0.043	0.044	0.140	0.691
06 B	40	0.193	3.67*	0.148	0.113	0.246	-0.065
07 B	40	0.027	1.10	0.024	0.024	0.115	0.827
08 B	40	0.028	0.93	0.036	0.035	0.136	0.741
09 B	40	0.035	1.40	0.026	0.025	0.128	0.810
10 B	40	0.033	1.35	0.024	0.024	0.123	0.827
11 B	40	0.033	1.15	0.033	0.033	0.157	0.764
12 B	40	-0.137	-3.91*	0.066	0.049	0.186	0.525
13 B	40	-0.023	-0.74	0.045	0.046	0.172	0.676
14 B	40	-0.003	-0.12	0.023	0.024	0.122	0.835
15 B	40	-0.019	-0.78	0.024	0.024	0.116	0.827
16 B	40	0.035	1.57	0.020	0.020	0.117	0.856
17 B	40	0.009	1.55	0.015	0.014	0.099	0.892
18 B	40	0.034	1.45	0.023	0.022	0.126	0.835
19 B	40	0.026	1.26	0.017	0.017	0.109	0.878

MO DATA	N	MEAN	T	MSE	VAR	MABS	R2
00 C	41	1.669	26.00*	2.950	0.169	1.669	1.000
01 C	41	-0.128	-3.21*	0.093	0.076	0.263	0.450
02 C	41	-0.230	-5.69*	0.118	0.067	0.279	0.302
03 C	41	-0.074	-1.92	0.065	0.061	0.221	0.615
04 C	41	-0.085	-2.04*	0.077	0.071	0.216	0.544
05 C	41	-0.090	-2.44*	0.074	0.066	0.209	0.562
06 C	41	0.086	1.42	0.154	0.152	0.271	0.089
07 C	41	-0.053	-1.72	0.041	0.039	0.145	0.757
08 C	41	-0.064	-1.70	0.061	0.058	0.183	0.639
09 C	41	-0.038	-1.45	0.029	0.028	0.129	0.828
10 C	41	-0.039	-1.47	0.029	0.028	0.133	0.828
11 C	41	-0.040	-1.55	0.029	0.028	0.126	0.828
12 C	41	-0.097	-6.27*	0.089	0.046	0.241	0.473
13 C	41	-0.097	-2.93*	0.053	0.045	0.181	0.686
14 C	41	-0.082	-2.81*	0.041	0.035	0.151	0.757
15 C	41	-0.097	-3.07*	0.050	0.041	0.170	0.704
16 C	41	-0.040	-1.50	0.030	0.029	0.124	0.822
17 C	41	-0.035	-1.58	0.020	0.020	0.111	0.882
18 C	41	-0.043	-1.68	0.028	0.027	0.121	0.834
19 C	41	-0.045	-1.99	0.022	0.021	0.118	0.870

MO DATA	N	MEAN	T	MSE	VAR	MABS	R2
00 D	41	1.669	26.00*	2.950	0.169	1.669	1.000
01 D	41	-0.073	-1.99	0.059	0.055	0.208	0.651
02 D	41	-0.187	-5.15*	0.083	0.054	0.239	0.485
03 D	41	-0.008	-0.25	0.041	0.042	0.168	0.737
04 D	41	-0.015	-0.42	0.052	0.053	0.180	0.692
05 D	41	-0.040	-1.07	0.057	0.057	0.171	0.663
06 D	41	0.180	2.99*	0.177	0.149	0.301	-0.047
07 D	41	-0.002	-0.08	0.028	0.029	0.118	0.834
08 D	41	-0.012	-0.34	0.049	0.051	0.170	0.710
09 D	41	-0.018	-0.52	0.023	0.022	0.114	0.870
10 D	41	-0.006	-0.26	0.021	0.022	0.112	0.876
11 D	41	-0.004	-1.71	0.059	0.037	0.139	0.828
12 D	41	-0.116	-4.04*	0.070	0.035	0.216	0.586
13 D	41	-0.062	-2.22*	0.035	0.028	0.145	0.793
14 D	41	-0.052	-1.99	0.030	0.028	0.128	0.822
15 D	41	-0.043	-1.59	0.032	0.030	0.137	0.811
16 D	41	-0.001	-0.04	0.021	0.021	0.109	0.876
17 D	41	0.004	0.22	0.013	0.013	0.087	0.923
18 D	41	-0.015	-0.65	0.022	0.022	0.119	0.870
19 D	41	-0.007	-0.35	0.015	0.016	0.099	0.911

MO DATA	N	MEAN	T	MSE	VAR	MABS	R2
00 E M	93	1.666	40.79*	2.936	0.159	1.666	1.000
01 E M	93	0.359	3.45*	1.427	1.009	0.510	-4.088
02 E M	93	0.143	1.56	0.795	0.783	0.422	-4.000
03 E M	93	0.182	5.06*	0.160	0.127	0.288	-0.006
04 E M	93	0.185	4.75*	0.174	0.141	0.307	-0.094
05 E M	93	0.135	3.29*	0.133	0.118	0.261	0.151
06 E M	93	0.381	7.60*	0.376	0.234	0.451	-1.365
07 E M	93	0.115	4.57*	0.072	0.059	0.205	0.547
08 E M	93	0.098	3.43*	0.084	0.076	0.225	0.472
09 E M	93	0.068	3.02*	0.051	0.047	0.172	0.679
10 E M	93	0.077	3.43*	0.053	0.047	0.176	0.667
11 E M	93	-0.028	-1.20	0.051	0.051	0.174	0.679
12 E M	93	-0.115	-4.25*	0.080	0.068	0.218	0.497
13 E M	93	0.033	1.20	0.070	0.070	0.216	0.560
14 E M	93	0.024	1.06	0.048	0.048	0.164	0.698
15 E M	93	0.077	3.05*	0.065	0.060	0.196	0.591
16 E M	93	0.060	2.82*	0.046	0.042	0.163	0.711

MO DATA	N	MEAN	T	MSE	VAR	MABS	R2
00 F	95	1.568	43.40*	2.382	0.124	1.568	1.000
01 F	95	0.258	2.46*	1.494	1.041	0.544	-7.839
02 F	95	0.050	0.55	0.771	0.777	0.464	-5.718
03 F	95	0.095	2.31*	0.167	0.160	0.319	-0.347
04 F	95	0.098	2.36*	0.171	0.164	0.313	-0.379
05 F	95	0.036	1.08	0.105	0.105	0.245	-0.153
06 F	95	0.287	6.19*	0.284	0.204	0.395	-1.290
07 F	95	0.071	0.83	0.061	0.061	0.189	0.508
08 F	95	-0.007	0.25	0.072	0.072	0.200	0.439
09 F	95	-0.027	-1.24	0.045	0.045	0.168	0.637
10 F	95	-0.018	-0.80	0.048	0.048	0.171	0.613
11 F	95	-0.123	-5.65*	0.059	0.045	0.198	0.524
12 F	95	-0.205	-6.66*	0.131	0.090	0.287	-0.056
13 F	95	-0.056	-1.77	0.097	0.095	0.246	0.218
14 F	95	-0.068	-2.99*	0.053	0.049	0.175	0.573
15 F	95	-0.019	-0.71	0.064	0.064	0.195	0.484
16 F	95	-0.032	-1.45	0.047	0.046	0.171	0.622

MO DATA	N	MEAN	T	MSE	VAR	MABS	R2
00 G	285	1.728	72.26*	3.147	0.163	1.728	1.000
01 G	285	0.360	4.24*	2.173	2.051	0.523	-12.33
02 G	285	0.510	2.79*	0.510	0.504	0.411	-4.583
03 G	285	0.125	6.14*	0.133	0.118	0.246	0.184
04 G	285	0.135	7.02*	0.162	0.139	0.282	0.006
05 G	285	0.093	4.59*	0.125	0.117	0.224	0.233
06 G	285	0.321	11.11*	0.341	0.238	0.295	-1.092
07 G	285	0.084	5.70*	0.069	0.062	0.182	0.577
08 G	285	0.090	5.41*	0.087	0.079	0.216	0.466
09 G	285	0.065	4.81*	0.056	0.052	0.162	0.656
10 G	285	0.061	4.70*	0.052	0.048	0.160	0.681
11 G	285	-0.003	-0.14	0.056	0.056	0.173	0.656
12 G	285	-0.097	-6.98*	0.071	0.062	0.189	0.564
13 G	285	0.027	1.76	0.063	0.062	0.187	0.613
14 G	285	0.027	2.08*	0.049	0.048	0.162	0.699
15 G	285	0.044	2.96*	0.065	0.063	0.179	0.601
16 G	285	0.042	3.27*	0.049	0.047	0.162	0.699

MO DATA	N	MEAN	T	MSE	VAR	MABS	R2
00 H	278	1.674	70.44*	2.960	0.157	1.674	1.000
01 H	278	0.299	4.13*	1.544	1.460	0.505	-8.834
02 H	278	0.113	2.12	0.949	0.937	0.637	-5.045
03 H	278	0.081	4.41*	0.116	0.108	0.246	0.261
04 H	278	0.115	5.18*	0.149	0.137	0.284	0.051
05 H	278	0.054	2.67*	0.116	0.114	0.229	0.261
06 H	278	0.283	9.61*	0.321	0.241	0.392	-1.045
07 H	278	0.043	2.98*	0.060	0.058	0.176	0.618
08 H	278	0.046	2.75*	0.080	0.078	0.213	0.490
09 H	278	0.022	1.67	0.048	0.048	0.154	0.694
10 H	278	0.018	1.43	0.045	0.044	0.152	0.713
11 H	278	-0.031	-3.89*	0.055	0.053	0.177	0.650
12 H	278	-0.144	-10.06*	0.078	0.057	0.206	0.503
13 H	278	-0.018	-1.26	0.057	0.057	0.182	0.637
14 H	278	-0.018	-1.41	0.046	0.045	0.160	0.707
15 H	278	0.002	0.14	0.059	0.059	0.162	0.624
16 H	278	-0.001	-0.04	0.044	0.044	0.157	0.720

MO DATA	N	MEAN	T	MSE	VAR	MABS	R2
00 I	170	1.653	46.81*	2.947	0.212	1.653	1.000
01 I	170	1.301	5.31*	11.131	9.494	1.367	-51.51
02 I	170	0.955	6.74*	4.363	3.411	1.014	-19.30
03 I	170	0.418	11.89*	0.439	0.218	0.460	-0.811
04 I	170	0.505	15.31*	0.336	0.185	0.522	-1.072
05 I	170	0.315	13.13*	0.312	0.238	0.376	-2.925
06 I	170	0.648	11.96*	0.176	0.082	0.665	-0.340
07 I	170	0.243	10.97*	0.150	0.103	0.276	0.170
08 I	170	0.270	5.15*	0.176	0.194	0.303	-0.057
09 I	170	0.174	3.56*	0.224	0.071	0.247	0.557
10 I	170	0.155	-1.47	0.094	0.057	0.215	0.726
11 I	170	-0.027	1.24	0.058	0.049	0.183	0.769
12 I	170	0.182	9.94*	0.090	-0.053	0.243	0.575
13 I	170	0.132	7.44*	0.070	0.053	0.190	0.670
14 I	170	0.182	9.17*	0.100	0.067	0.237	0.528
15 I	170	0.109	6.78*	0.056	0.044	0.183	0.718

(Continued)

Table 5 (Concluded)

MO DATA	N	MEAN	T	MSE	VAR	MABS	R2
00 J	168	1.541	40.60*	2.617	0.242	1.541	1.000
01 J	168	1.416	5.11*	14.846	12.818	1.519	-60.35
02 J	168	0.964	4.59*	4.590	3.683	1.072	-17.97
03 J	168	0.343	10.91*	0.283	0.166	0.405	-0.169
04 J	168	0.432	13.34*	0.334	0.172	0.462	-0.463
05 J	168	0.237	6.70*	0.265	0.210	0.347	-0.095
06 J	168	0.313	11.56*	0.239	0.413	0.628	-2.054

MO DATA	N	MEAN	T	MSE	VAR	MABS	R2
00 H	9	1.635	28.80*	2.697	0.029	1.635	1.000
01 H	9	0.258	6.69	0.011	0.012	0.082	0.621
02 H	9	0.019	0.52	0.011	0.012	0.083	0.621
03 H	9	0.043	1.16	0.012	0.012	0.087	0.306
04 H	9	0.056	1.53	0.014	0.012	0.092	0.517
05 H	9	0.017	0.47	0.011	0.012	0.083	0.621
06 H	9	0.041	1.08	0.013	0.013	0.094	0.552

MO DATA	N	MEAN	T	MSE	VAR	MABS	R2
00 P	19	1.495	12.16*	2.596	0.287	1.495	1.000
01 P	19	0.022	0.25	0.031	0.075	0.208	0.753
02 P	19	-0.301	-6.91*	0.125	0.036	0.308	0.564
03 P	19	-0.082	1.68	0.049	0.043	0.178	0.829
04 P	19	-0.097	-2.23*	0.064	0.036	0.175	0.847
05 P	19	-0.016	0.32	0.047	0.049	0.181	0.836
06 P	19	0.062	1.03	0.032	0.072	0.222	0.749

Table 5 (Continued)

(Continued)

Table 5 (Concluded)

KEY:

MO	Model Code (OO = Observed Phosphorus)
DATA	Data Set Code
N	Number of Data Points
MEAN	Mean
T	t-test for Bias (|MEAN| > 0)
*	Mean Significantly Different from 0 at p < .05
MSE	Mean Squared Error
VAR	Variance
MABS	Mean Absolute Value
R2	Fraction of Observed Variance Explained

Table 6

Phosphorus Retention Model Error Statistics
Sorted by Model

MO DATA	N	MEAN	T	MSE	VAR	MABS	R2
00 A	60	1.696	33.92*	3.025	0.150	1.696	1.000
00 B	40	1.752	29.72*	3.205	0.139	1.752	1.000
00 C	41	1.669	26.00*	2.950	0.169	1.669	1.000
00 D	41	1.669	26.00*	2.950	0.169	1.669	1.000
00 E	93	1.666	40.29*	2.934	0.159	1.666	1.000
00 F	95	1.568	43.40*	2.582	0.124	1.568	1.000
00 G	285	1.728	72.26*	3.147	0.163	1.728	1.000
00 H	278	1.674	70.44*	2.960	0.157	1.674	1.000
00 I	170	1.653	46.81*	2.943	0.212	1.653	1.000
00 J	168	1.541	40.60*	2.617	0.242	1.541	1.000
00 K	9	1.251	21.32*	1.591	0.031	1.251	1.000
00 L	7	1.279	14.98*	1.680	0.051	1.279	1.000
00 M	9	1.635	28.80*	2.697	0.029	1.635	1.000
00 N	8	1.682	34.51*	2.846	0.019	1.682	1.000
00 O	20	1.515	12.39*	2.579	0.299	1.515	1.000
00 P	19	1.495	12.16*	2.506	0.287	1.495	1.000
01 A	60	-0.117	-3.48*	0.081	0.068	0.210	0.460
01 B	40	-0.070	-1.66	0.074	0.071	0.193	0.468
01 C	41	-0.138	-3.21*	0.093	0.076	0.263	0.450
01 D	41	-0.073	-1.99	0.059	0.055	0.208	0.651
01 E	93	0.359	3.45*	1.127	1.009	0.510	-6.088
01 F	95	0.258	2.46*	1.096	1.041	0.544	-7.839
01 G	285	0.360	4.24*	2.173	2.051	0.523	-12.33
01 H	278	0.299	4.13*	1.544	1.460	0.505	-8.834
01 I	170	1.301	5.51*	11.131	9.494	1.367	-51.51
01 J	168	1.416	5.11*	14.846	12.918	1.519	-60.35
01 K	9	-0.091	-1.05	0.069	0.068	0.220	-1.226
01 L	7	-0.085	-0.81	0.074	0.078	0.228	-0.451
01 M	9	0.022	0.60	0.011	0.012	0.082	0.621
01 N	8	0.059	2.36*	0.008	0.005	0.080	0.579
01 O	20	0.020	0.29	0.088	0.093	0.231	0.706
01 P	19	0.022	0.35	0.071	0.075	0.208	0.753
02 A	60	-0.193	-5.07*	0.123	0.087	0.259	0.180
02 B	40	-0.133	-2.92*	0.098	0.083	0.226	0.295
02 C	41	-0.230	-5.69*	0.118	0.067	0.279	0.302
02 D	41	-0.187	-5.15*	0.087	0.054	0.238	0.485
02 E	93	0.143	1.56	0.795	0.783	0.422	-4.000
02 F	95	0.050	0.55	0.771	0.777	0.464	-5.218
02 G	285	0.156	2.79*	0.910	0.889	0.411	-4.583
02 H	278	0.123	2.12*	0.949	0.937	0.437	-5.045
02 I	170	0.955	6.74*	4.303	3.411	1.014	-19.30
02 J	168	0.964	6.51*	4.550	3.683	1.072	-18.00
02 K	9	-0.281	-3.31*	0.137	0.065	0.316	-3.419
02 L	7	-0.247	-2.74*	0.110	0.057	0.270	-1.157
02 M	9	0.019	0.52	0.011	0.012	0.083	0.621
02 N	8	0.056	2.24	0.008	0.005	0.081	0.579
02 O	20	-0.287	-5.86*	0.128	0.048	0.287	0.572
02 P	19	-0.301	-6.91*	0.125	0.036	0.308	0.564

MO DATA	N	MEAN	T	MSE	VAR	MABS	R2
03 A	60	-0.042	-1.37	0.057	0.056	0.185	0.620
03 B	40	-0.006	-0.16	0.054	0.055	0.177	0.612
03 C	41	-0.074	-1.92	0.065	0.061	0.221	0.615
03 D	41	-0.008	-0.25	0.041	0.042	0.168	0.757
03 E	93	0.187	5.06*	0.160	0.127	0.296	-0.006
03 F	95	0.095	2.31*	0.167	0.160	0.319	-0.347
03 G	285	0.125	6.14*	0.133	0.118	0.246	0.184
03 H	278	0.087	4.41*	0.116	0.108	0.246	0.261
03 I	170	0.418	11.89*	0.384	0.210	0.460	-0.811
03 J	168	0.343	10.91*	0.283	0.166	0.405	-0.169
03 K	9	0.022	0.25	0.061	0.068	0.189	-0.968
03 L	7	0.028	0.26	0.069	0.079	0.235	-0.353
03 M	9	0.043	1.18	0.012	0.012	0.087	0.586
03 N	8	0.080	3.20*	0.011	0.005	0.090	0.421
03 O	20	0.078	1.40	0.065	0.062	0.201	0.783
03 P	19	0.082	1.68	0.049	0.045	0.178	0.829
04 A	60	-0.043	-1.26	0.071	0.070	0.191	0.527
04 B	40	0.009	0.23	0.061	0.063	0.176	0.561
04 C	41	-0.085	-2.04*	0.077	0.071	0.216	0.544
04 D	41	-0.015	-0.42	0.052	0.053	0.180	0.692
04 E	93	0.185	4.75*	0.174	0.141	0.307	-0.094
04 F	95	0.098	2.36*	0.171	0.164	0.313	-0.379
04 G	285	0.155	7.02*	0.162	0.139	0.282	0.006
04 H	278	0.115	5.18*	0.149	0.137	0.284	0.051
04 I	170	0.505	15.31*	0.439	0.185	0.523	-1.071
04 J	168	0.427	13.34*	0.354	0.172	0.462	-0.463
04 K	9	-0.137	-1.45	0.090	0.080	0.269	-1.903
04 L	7	-0.111	-1.01	0.085	0.084	0.257	-0.667
04 M	9	0.056	1.53	0.014	0.012	0.092	0.517
04 N	8	0.092	3.36*	0.013	0.006	0.103	0.316
04 O	20	-0.092	-1.88	0.054	0.048	0.186	0.819
04 P	19	-0.097	-2.23*	0.044	0.036	0.175	0.847
05 A	60	-0.063	-2.23*	0.051	0.048	0.161	0.660
05 B	40	-0.017	-0.51	0.043	0.044	0.140	0.691
05 C	41	-0.098	-2.44*	0.074	0.068	0.209	0.562
05 D	41	-0.040	-1.07	0.057	0.057	0.171	0.663
05 E	93	0.135	3.79*	0.135	0.118	0.261	0.151
05 F	95	0.036	1.08	0.105	0.105	0.245	0.153
05 G	285	0.093	4.59*	0.125	0.117	0.224	0.233
05 H	278	0.054	2.67*	0.116	0.114	0.229	0.261
05 I	170	0.315	8.42*	0.336	0.238	0.376	-0.585
05 J	168	0.237	6.70*	0.265	0.210	0.347	-0.095
05 K	9	-0.210	-3.64*	0.071	0.030	0.231	-1.290
05 L	7	-0.191	-2.78*	0.064	0.033	0.213	-0.255
05 M	9	0.017	0.47	0.011	0.012	0.083	0.621
05 N	8	0.055	2.20	0.008	0.005	0.079	0.579
05 O	20	0.015	0.25	0.069	0.073	0.218	0.769
05 P	19	0.016	0.32	0.047	0.049	0.181	0.836

MO DATA	N	MEAN	T	MSE	VAR	MABS	R2
06 A	60	0.133	2.97*	0.135	0.120	0.251	0.100
06 B	40	0.195	3.67*	0.148	0.113	0.246	-0.065
06 C	41	0.086	1.42	0.154	0.150	0.271	0.089
06 D	41	0.180	2.99*	0.177	0.149	0.301	-0.047
06 E	93	0.381	7.60*	0.376	0.234	0.453	-1.365
06 F	95	0.287	6.19*	0.284	0.204	0.395	-1.290
06 G	285	0.321	11.11*	0.341	0.238	0.295	-1.092
06 H	278	0.283	9.61*	0.321	0.241	0.392	-1.045
06 I	170	0.648	13.13*	0.832	0.414	0.665	-2.925
06 J	168	0.573	11.56*	0.739	0.413	0.626	-2.054
06 K	9	-0.203	-3.08*	0.076	0.039	0.241	-1.452
06 L	7	-0.175	-2.21	0.068	0.044	0.204	-0.333
06 M	9	0.041	1.08	0.013	0.013	0.091	0.552
06 N	8	0.079	2.88*	0.011	0.006	0.096	0.421
06 O	20	0.060	0.87	0.095	0.096	0.252	0.682
06 P	19	0.062	1.01	0.072	0.072	0.222	0.749
07 A	60	-0.015	-0.67	0.030	0.030	0.127	0.800
07 B	40	0.027	1.10	0.024	0.024	0.115	0.827
07 C	41	-0.053	-1.72	0.041	0.039	0.143	0.757
07 D	41	-0.002	-0.08	0.028	0.029	0.118	0.834
07 E	93	0.115	4.57*	0.072	0.059	0.205	0.547
07 F	95	0.021	0.83	0.061	0.061	0.189	0.508
07 G	285	0.084	5.70*	0.069	0.062	0.182	0.577
07 H	278	0.043	2.98*	0.060	0.058	0.176	0.618
07 I	170	0.243	11.06*	0.140	0.082	0.276	0.340
07 J	168	0.154	7.44*	0.095	0.072	0.225	0.607
07 K	9	-0.109	-1.92	0.038	0.029	0.175	-0.226
07 L	7	-0.091	-1.35	0.036	0.032	0.151	0.294
07 M	9	0.043	1.18	0.013	0.012	0.089	0.552
07 N	8	0.082	3.28*	0.011	0.005	0.093	0.421
07 O	20	0.022	0.43	0.050	0.052	0.191	0.833
07 P	19	0.021	0.52	0.030	0.031	0.128	0.895
08 A	60	-0.025	-0.87	0.049	0.049	0.163	0.673
08 B	40	0.028	0.93	0.036	0.036	0.136	0.741
08 C	41	-0.064	-1.70	0.061	0.058	0.183	0.639
08 D	41	-0.012	-0.34	0.049	0.051	0.170	0.710
08 E	93	0.098	3.43*	0.084	0.076	0.225	0.472
08 F	95	0.007	0.25	0.072	0.072	0.200	0.419
08 G	285	0.090	5.41*	0.087	0.079	0.216	0.466
08 H	278	0.046	2.75*	0.080	0.078	0.213	0.490
08 I	170	0.270	10.97*	0.176	0.103	0.303	0.170
08 J	168	0.177	6.92*	0.141	0.110	0.273	0.417
08 K	9	-0.216	-3.12*	0.084	0.043	0.250	-1.710
08 L	7	-0.187	-2.41*	0.070	0.042	0.214	-0.373
08 M	8	0.046	1.26	0.013	0.012	0.092	0.552
08 N	8	0.084	3.07*	0.012	0.006	0.099	0.368
08 O	20	-0.098	-2.00*	0.055	0.048	0.209	0.818
08 P	19	-0.105	-2.64*	0.039	0.030	0.165	0.864

(Continued)

Table 6 (Concluded)

MO DATA	N	MEAN	T	MSE	VAR	MABS	R2
09 A	60	-0.004	-0.18	0.029	0.029	0.133	0.807
09 B	40	0.035	1.60	0.026	0.025	0.129	0.813

MO DATA	N	MEAN	T	MSE	VAR	MABS	R2
12 A	60	-0.180	-5.89*	0.088	0.056	0.217	0.413
12 B	40	-0.137	-3.91*	0.066	0.049	0.186	0.525

MO DATA	N	MEAN	T	MSE	VAR	MABS	R2
15 A	60	-0.060	-2.64*	0.034	0.031	0.139	0.773
15 B	40	-0.019	-0.78	0.024	0.024	0.116	0.827
15 C	41	-0.097	-2.07*	0.050	0.041	0.170	0.704

Table 6 (Continued)

The following three blocks (models 02, 05, 08) appear at the top of the page with their column headers cut off. Columns, reconstructed from context, are: MO DATA | N | MEAN | T | MSE | VAR | MABS | R2

MO DATA	N	MEAN	T	MSE	VAR	MABS	R2
02 I	170	0.955	6.74*	4.303	3.411	1.014	-19.30
02 J	168	0.964	6.51*	4.590	3.683	1.072	-18.00
02 K	9	-0.281	-3.31*	0.137	0.065	0.314	-3.419
02 L	7	-0.247	-2.74*	0.110	0.057	0.270	-1.157
02 M	9	0.019	0.52	0.011	0.011	0.083	0.621
02 N	8	0.056	2.24	0.008	0.005	0.081	0.579
02 O	20	-0.287	-5.86*	0.128	0.048	0.287	0.572
02 P	19	-0.301	-6.91*	0.125	0.036	0.308	0.564

MO DATA	N	MEAN	T	MSE	VAR	MABS	R2
05 I	170	0.315	8.42*	0.336	0.238	0.376	-0.585
05 J	168	0.237	6.70*	0.265	0.210	0.347	-0.095
05 K	9	-0.210	-3.64*	0.071	0.030	0.231	-1.290
05 L	7	-0.191	-2.78*	0.064	0.033	0.213	-0.255
05 M	9	0.017	0.47	0.011	0.012	0.083	0.621
05 N	8	0.055	2.20	0.008	0.005	0.079	0.579
05 O	20	0.015	0.25	0.069	0.073	0.218	0.769
05 P	19	0.016	0.32	0.047	0.049	0.181	0.836

MO DATA	N	MEAN	T	MSE	VAR	MABS	R2
08 I	170	0.220	10.97*	0.176	0.103	0.303	0.170
08 J	168	0.177	6.92*	0.141	0.110	0.273	0.417
08 K	9	-0.216	-3.12*	0.084	0.043	0.250	-1.710
08 L	7	-0.187	-2.41*	0.070	0.042	0.214	-0.373
08 M	9	0.046	1.26	0.013	0.012	0.092	0.552
08 N	8	0.084	3.07*	0.012	0.006	0.099	0.368
08 O	20	-0.098	-2.00*	0.055	0.048	0.209	0.816
08 P	19	-0.105	-2.64*	0.039	0.030	0.165	0.864

(Continued)

Table 6 (Concluded)

MO DATA	N	MEAN	T	MSE	VAR	MABS	R2
09 A	60	-0.004	-0.18	0.029	0.029	0.133	0.807
09 B	40	0.035	1.40	0.026	0.025	0.129	0.813
09 C	41	-0.038	-1.45	0.029	0.028	0.129	0.828
09 D	41	-0.012	-0.52	0.022	0.022	0.114	0.870
09 E	93	0.068	3.02*	0.051	0.047	0.172	0.679
09 F	95	-0.027	-1.24	0.045	0.045	0.168	0.637
09 G	285	0.065	4.81*	0.056	0.052	0.162	0.656
09 H	278	0.022	1.67	0.048	0.048	0.154	0.694
09 I	170	0.174	5.15*	0.224	0.194	0.242	-0.057
09 J	168	0.081	2.55*	0.176	0.170	0.213	0.273
09 K	9	-0.046	-0.89	0.023	0.024	0.140	0.258
09 L	7	-0.024	-0.45	0.018	0.020	0.107	0.647
09 M	9	0.124	3.40*	0.026	0.012	0.136	0.103
09 N	8	0.163	7.29*	0.030	0.004	0.163	-0.579
09 O	20	0.072	1.35	0.060	0.057	0.194	0.799
09 P	19	0.069	1.61	0.038	0.035	0.159	0.868
10 A	60	-0.005	-0.24	0.027	0.027	0.126	0.820
10 B	40	0.033	1.35	0.024	0.024	0.123	0.827
10 C	41	-0.039	-1.47	0.029	0.029	0.133	0.828
10 D	41	-0.006	-0.26	0.021	0.022	0.112	0.876
10 E	93	0.077	3.43*	0.053	0.047	0.176	0.667
10 F	95	-0.018	-0.80	0.048	0.048	0.171	0.613
10 G	285	0.061	4.70*	0.052	0.048	0.160	0.681
10 H	278	0.018	1.43	0.045	0.044	0.152	0.713
10 I	170	0.155	7.58*	0.094	0.071	0.215	0.557
10 J	168	0.060	3.17*	0.063	0.060	0.178	0.740
10 K	9	-0.030	-1.01	0.021	0.020	0.101	0.323
10 L	7	-0.056	-0.56	0.018	0.012	0.115	0.647
10 M	9	0.089	2.44*	0.019	0.004	0.128	0.345
10 N	8	0.128	5.72*	0.020	0.004	0.128	-0.053
10 O	20	0.069	1.28	0.060	0.058	0.200	0.799
10 P	19	0.068	1.56	0.039	0.036	0.156	0.864
11 A	60	-0.009	-0.37	0.036	0.036	0.158	0.760
11 B	40	0.013	1.15	0.033	0.033	0.157	0.763
11 C	41	-0.040	-1.53	0.029	0.027	0.126	0.828
11 D	41	-0.044	-1.71	0.029	0.028	0.130	0.828
11 E	93	-0.028	-1.20	0.051	0.051	0.174	0.679
11 F	95	-0.123	-5.65*	0.059	0.045	0.198	0.524
11 G	285	-0.002	-0.12	0.056	0.056	0.177	0.656
11 H	278	-0.051	-3.69*	0.058	0.057	0.183	0.650
11 I	170	-0.027	-1.47	0.083	0.071	0.228	0.726
11 J	168	-0.134	-6.76*	0.066	0.016	0.112	0.657
11 K	9	-0.066	-1.57	0.019	0.010	0.093	0.387
11 L	7	-0.035	-0.93	0.031	0.010	0.154	0.804
11 M	9	0.136	3.33*	0.037	0.015	0.179	-0.069
11 N	8	0.179	7.16*	0.037	0.005	0.179	-0.947
11 O	20	0.062	0.90	0.093	0.094	0.232	0.689
11 P	19	0.055	0.89	0.071	0.072	0.225	0.753

MO DATA	N	MEAN	T	MSE	VAR	MABS	R2
12 A	60	-0.180	-5.89*	0.088	0.056	0.217	0.413
12 B	40	-0.137	-3.91*	0.066	0.049	0.186	0.525
12 C	41	-0.210	-6.27*	0.089	0.046	0.241	0.473
12 D	41	-0.118	-4.25*	0.070	0.035	0.216	0.586
12 E	93	-0.115	-4.04*	0.080	0.068	0.218	0.497
12 F	95	-0.205	-6.66*	0.131	0.090	0.287	-0.056
12 G	285	-0.097	-6.58*	0.071	0.062	0.189	0.564
12 H	278	-0.144	-10.06*	0.078	0.057	0.206	0.503
12 I	170	0.021	1.24	0.049	0.049	0.160	0.769
12 J	168	-0.078	-4.52*	0.055	0.050	0.175	0.773
12 K	9	-0.162	-2.07	0.075	0.055	0.242	-1.419
12 L	7	-0.135	-1.61	0.060	0.049	0.200	-0.176
12 M	9	0.064	1.75	0.015	0.012	0.098	0.483
12 N	8	0.101	4.04*	0.014	0.005	0.107	0.263
12 O	20	-0.190	-3.73*	0.086	0.052	0.226	0.712
12 P	19	-0.202	-4.40*	0.079	0.040	0.230	0.725
13 A	60	-0.065	-2.21*	0.055	0.052	0.176	0.633
13 B	40	-0.025	-0.74	0.045	0.046	0.159	0.676
13 C	41	-0.097	-2.93*	0.053	0.045	0.181	0.686
13 D	41	-0.062	-2.22*	0.035	0.032	0.145	0.793
13 E	93	0.033	1.20	0.070	0.070	0.216	0.560
13 F	95	-0.056	-1.77	0.097	0.095	0.246	0.218
13 G	285	0.026	1.76	0.063	0.062	0.182	0.613
13 H	278	-0.018	-1.26	0.057	0.057	0.187	0.637
13 I	170	0.182	9.94*	0.090	0.057	0.243	0.575
13 J	168	0.088	5.00*	0.059	0.056	0.193	0.756
13 K	9	-0.028	-0.35	0.051	0.056	0.198	-0.645
13 L	7	-0.005	-0.06	0.046	0.051	0.189	0.098
13 M	9	0.116	3.18*	0.024	0.012	0.123	0.172
13 N	8	0.153	6.84*	0.027	0.004	0.153	-0.421
13 O	20	-0.041	-0.80	0.051	0.052	0.177	0.829
13 P	19	-0.047	-1.04	0.039	0.039	0.167	0.864
14 A	60	-0.048	-2.05*	0.035	0.033	0.140	0.767
14 B	40	-0.003	-0.12	0.033	0.034	0.122	0.835
14 C	41	-0.082	-2.81*	0.041	0.035	0.151	0.757
14 D	41	-0.052	-1.99	0.030	0.028	0.128	0.822
14 E	93	0.024	1.06	0.048	0.048	0.164	0.698
14 F	95	-0.068	-2.99*	0.053	0.049	0.175	0.573
14 G	285	0.027	2.08*	0.049	0.048	0.162	0.699
14 H	278	-0.018	-1.41	0.046	0.045	0.160	0.707
14 I	170	0.132	7.48*	0.070	0.053	0.190	0.670
14 J	168	0.034	1.88	0.056	0.055	0.177	0.769
14 K	9	-0.146	-2.41*	0.051	0.033	0.197	-0.645
14 L	7	-0.119	-1.82	0.040	0.040	0.158	0.216
14 M	9	0.088	2.41*	0.020	0.012	0.113	0.345
14 N	8	0.127	5.08*	0.020	0.005	0.127	-0.053
14 O	20	-0.060	-1.24	0.048	0.047	0.185	0.839
14 P	19	-0.068	-1.74	0.032	0.029	0.146	0.889

MO DATA	N	MEAN	T	MSE	VAR	MABS	R2
15 A	60	-0.060	-2.64*	0.034	0.031	0.139	0.773
15 B	40	-0.019	-0.78	0.024	0.024	0.116	0.827
15 C	41	-0.097	-3.07*	0.050	0.041	0.170	0.704
15 D	41	-0.040	-1.59	0.032	0.030	0.132	0.811
15 E	93	0.077	3.03*	0.065	0.060	0.196	0.591
15 F	95	-0.019	-0.73	0.064	0.064	0.195	0.484
15 G	285	0.044	2.96*	0.065	0.063	0.179	0.601
15 H	278	0.002	0.14	0.059	0.059	0.182	0.624
15 I	170	0.182	9.17*	0.100	0.067	0.237	0.528
15 J	168	0.089	4.46*	0.075	0.067	0.201	0.690
15 K	9	-0.173	-3.10*	0.055	0.028	0.205	-0.774
15 L	7	-0.156	-2.31	0.052	0.032	0.189	-0.020
15 M	9	0.022	0.60	0.011	0.012	0.084	0.621
15 N	8	0.060	2.40*	0.008	0.005	0.081	0.579
15 O	20	-0.002	-0.04	0.056	0.059	0.201	0.813
15 P	19	-0.002	-0.05	0.035	0.037	0.139	0.878
16 A	60	-0.003	-0.14	0.025	0.026	0.125	0.833
16 B	40	0.035	1.57	0.020	0.020	0.117	0.856
16 C	41	-0.040	-1.50	0.030	0.029	0.128	0.822
16 D	41	-0.001	-0.04	0.021	0.021	0.109	0.876
16 E	93	0.060	2.82*	0.046	0.042	0.163	0.711
16 F	95	-0.032	-1.45	0.049	0.046	0.171	0.621
16 G	285	0.042	3.27*	0.049	0.047	0.162	0.699
16 H	278	-0.001	-0.08	0.044	0.044	0.157	0.720
16 I	170	0.109	6.78*	0.056	0.044	0.183	0.736
16 J	168	0.008	0.46	0.050	0.051	0.172	0.793
16 K	9	-0.072	-1.37	0.027	0.025	0.151	0.129
16 L	7	-0.054	-0.87	0.026	0.027	0.120	0.490
16 M	9	0.062	1.70	0.015	0.012	0.097	0.483
16 N	8	0.100	4.00*	0.014	0.005	0.106	0.263
16 O	20	0.038	0.72	0.055	0.056	0.196	0.816
16 P	19	0.038	0.89	0.034	0.035	0.140	0.882
17 A	60	0.005	0.30	0.017	0.017	0.105	0.887
17 B	40	0.029	1.55	0.015	0.014	0.099	0.892
17 C	41	-0.035	-1.58	0.020	0.020	0.111	0.882
17 D	41	0.004	0.22	0.013	0.013	0.087	0.923
17 O	20	0.000	0.00	0.034	0.036	0.154	0.886
17 P	19	-0.002	-0.06	0.019	0.020	0.097	0.934
18 A	60	-0.005	-0.23	0.028	0.029	0.135	0.813
18 B	40	0.034	1.45	0.023	0.022	0.126	0.835
18 C	41	-0.043	-1.68	0.028	0.027	0.131	0.834
18 D	41	-0.015	-0.65	0.022	0.022	0.119	0.870
18 O	20	-0.043	-1.04	0.034	0.036	0.154	0.886
18 P	19	-0.051	-1.70	0.019	0.017	0.115	0.934
19 A	60	-0.004	-0.21	0.020	0.021	0.115	0.867
19 B	40	0.026	1.26	0.017	0.017	0.109	0.878
19 C	41	-0.045	-1.99	0.022	0.021	0.118	0.870
19 D	41	-0.007	-0.35	0.015	0.016	0.099	0.911
19 O	20	0.014	0.32	0.036	0.038	0.160	0.880
19 P	19	0.014	0.45	0.018	0.018	0.094	0.937

Table 7

Summary of Error Mean Squares by Data Set and Model

Data Set

Model	CE				EPA/NES						TVA				OECD	
	A	B	C	D	E	F	G	H	I	J	K	L	M	N	O	P
							Mechanistic Models									
01	81	74	93	59	1127	1096	2698	2148	11131	14846	69	74	11**	8*	88	71
02	123	98	118	87	795	771	1530	1591	4303	4590	137	110	11**	8*	128	125
03	57	54	65	41	160	167	139	121	384	283	61	69	12*	11	65	49
04	71	61	77	52	174	171	173	161	439	354	90	85	14	13	54*	44
05	51	43	74	57	135	105	151	149	336	265	71	74	11**	8*	69	47
06	135	148	154	177	376	284	398	387	832	739	76	68	13*	11	95	72
07	30**	24**	41**	28**	72**	61**	70**	63**	140	95**	38**	36**	13*	11	50**	30**
08	49	36	61	49	84*	72*	91	86	176	141	84	70	13*	12	55*	39
							Empirical Models									
09	29	26	29	22	51*	45**	73	70	224	176	23	18	26	30	60	38
10	27	24	29	21	53*	48*	53*	47**	94	63	21*	18	19	20	60	39
11	36	33	29	29	51*	59	60*	59	58*	83	19**	10**	31	37	93	71
12	88	66	89	70	80	131	89	96	49**	55*	75	60	15	14	86	79
13	55	45	53	35	70	97	73	68	90	59*	51	46	24	27	51	39
14	35	23	41	30	48*	53*	51**	48*	70	56*	51	40	19	20	48	32
15	34	24	50	32	65	64	70	64	100	75	55	52	11**	8**	56	35
16	25	20	30	21	46**	47**	52*	48*	56*	50**	27	26	15	14	55	34
17	17**	15**	20**	13**	–	–	–	–	–	–	–	–	–	–	34**	19*
18	28	22	28	22	–	–	–	–	–	–	–	–	–	–	34**	19*
19	20*	17*	22*	15*	–	–	–	–	–	–	–	–	–	–	36*	18**
Var	150	139	169	169	159	124	166	164	212	242	31	51	29	19	299	287
n	60	40	41	41	93	95	294	275	170	168	9	7	9	8	20	19

NOTES:
Entries = error mean square x 1000, base-10 logarithm
Model codes identified in Tables 1 and 2, data set codes in Table 4
Var = variance of observed outflow P or reservoir P
n = number of reservoirs or reservoir-years
** Lowest mean squared error for given data set and model category
* Mean squared error within 20% of **

50

	OECD	
N	O	P
8*	88	71
8*	128	125
11	65	49
13	54*	44
8*	69	47
11	95	72
11	50**	30**
12	55*	39
30	60	38
20	60	39
37	93	71
14	86	79
27	51	39
20	48	32
8**	56	35
14	55	34
–	34**	19*
~	34**	19*
–	36*	18**
9	299	287
8	20	19

able 4

ory

errors when the data set is restricted to projects with one major tributary arm. This suggests that spatially segmented versions may be appropriate for some reservoirs.

45. Data sets C and D compare model predictions with area-weighted, surface concentrations of total phosphorus measured by the EPA/NES. The former uses annual-average inflow concentrations and hydraulic residence times. The latter uses estimated summer (May-September) inflow concentrations and hydraulic residence times in impoundments conforming to each of the following criteria:

  a. Annual hydraulic residence time < 0.50 year.

  b. Summer phosphorus residence time < 0.25 year.

The rationale for using seasonal averaging schemes is that many of the CE impoundments are rapidly flushed (the median annual residence time is 0.22 year) and summer pool water quality conditions may be related more directly to seasonal inflow and hydrologic conditions than to annual conditions. "Phosphorus residence time" (Omelia, 1972) is defined as the ratio of pool concentration to external loading per unit volume and is a measure of the relative response time of the system to changes in loading conditions:

$$Tp = \frac{T \; P}{Pi} \tag{20}$$

where

  Tp = phosphorus residence time (years)

  T = hydraulic residence time (years)

  Pi = inflow phosphorus concentration (mg/m^3)

Tp estimates have been calculated using summer inflow concentration and residence time estimates for projects with annual residence times less than 0.5 year. Low values of this parameter reflect a high rate of phosphorus turnover in the system and rapid response to seasonal hydrologic variations. The rationale for selecting 0.25 year as a

51

cutoff point is that this would provide at least two phosphorus turnovers during a 6-month growing season, the approximate averaging period for the reservoir water quality conditions. Analysis of residuals for various retention models generally supports this selection. Applying the above criteria to the load/response data set results in use of average-annual inflow conditions for 11 impoundments and summer-average conditions for 30 impoundments. As shown in Table 7 (C vs. D), model error variances are reduced when seasonal variations are considered. Annual inflow and hydraulic conditions have been used exclusively for data sets E - P because estimates of summer conditions are not available.

46. Data sets E - J are derived from the EPA/NES Compendium file, and describe outflow and pool concentrations in CE reservoirs (E and F), other US reservoirs (G and H), and US natural lakes (I and J). Model error variances are similar among the three sets of NES data and are roughly twice those of the CE data sets. The difference partially reflects the more intensive screening and uniform data-reduction procedures used in developing the CE data sets. Another potentially important factor is that the hydraulic residence times, mean depths, and loadings reported in the NES Compendium refer to "long-term-average" conditions, which may deviate significantly from the conditions which were present during the sampling periods.

47. The compilation of data from TVA reservoirs (Higgins and Kim, 1981) has been described previously (Walker, 1982a). These impoundments have been studied in two groups, tributary reservoirs (K and L) and mainstem (Tennessee River) reservoirs (M and N). Model comparisons for these data sets are limited by the small sample size (7 and 9 impoundments, respectively) and relatively low variability of trophic conditions within each group, as indicated by the variances of the observed pool or outflow concentrations. The rapid flushing rates of the mainstem impoundments result in low error variance for all models. At low residence times, outflow concentration approaches inflow concentration and the power to discriminate among alternative retention formulations vanishes. The tributary error variances are more similar

to the other data sets.

48.   The   compilation   of data from the OECD Reservoir and Shallow
Lakes Project (Clasen, 1980) has been described previously (Walker.
1982a).   Data sets N and O have been augmented to include measurements
of outflow total phosphorus and inflow ortho-phosphorus concentrations.
Maximum discrimination among the models is afforded by restricting the
OECD data set to 20 reservoir-years (2 years of data for each of 10
different reservoirs) with inflow ortho-P estimates.

49. Major conclusions derived from Table 7 are as follows:

a. Within the mechanistic model category, model 07 has the lowest
   mean squared error for each data set, with the exception of the
   TVA mainstem impoundments (M and N). As discussed above, all
   error variances are low for the latter group and model
   discrimination is hindered by sample size, low residence time,
   and limited range of phosphorus concentrations.   These results
   suggest that the representation of phosphorus sedimentation as a
   second-order reaction in a mixed system is the most general of
   the one-parameter mechanistic models tested.

b. For the EPA/NES data sets (E − J), the mean squared errors of
   models 10, 14, and 16 are lowest within the empirical model
   category. When applied to predict outflow concentrations of
   natural lakes (I), model 16 has a significant positive bias (.11
   log units or 29%), as do most of the other reservoir models.
   The Vollenweider/Larsen-Mercier model (12) works slightly better
   than model 16 for predicting lake outflow concentration (Data
   Set I, MSE = .049 vs. .056), but the reverse is true for pool
   concentration (Data Set J, MSE = .055 vs. .050). Compilation of
   ortho-phosphorus loading data for natural lakes would   be
   required to further assess lake/reservoir differences with
   respect to choice of model.

c. For the TVA tributary reservoirs (K and L), model 11 has the
   lowest mean squared error for predictions of outflow and pool
   phosphorus concentrations. Errors for models 10, 14, and 16 are
   similar to those found in the CE data sets. Model testing for

53

the TVA reservoirs would be enhanced by compilation of inflow ortho-phosphorus concentrations and seasonal hydrologic conditions.

d. Within the empirical model group, the models accounting for inflow phosphorus availablility (17 - 19) have the lowest mean squared errors for each data set providing inflow ortho-P data (A-D, O-P). Modification of the second-order decay model to account for effects of overflow rate and inflow phosphorus availability reduces mean squared errors by 37 - 58%. Generally, it is difficult to distinguish among models 17, 18, and 19 on the basis of model error. The models explain between 88 and 94% of the variance in the independent OECD/RSL data sets (O and P).

Results of these studies indicate that between-reservoir variations in outflow and pool total phosphorus concentrations can be successfully modeled using a mechanistic formulation which assumes that the sedimentation of phosphorus is a second-order reaction. Improvements in fit are achieved by empirical adjustment of the effective decay coefficient to account for effects of overflow rate. Effects of inflow phosphorus availability can be accounted for by adjusting the decay rate (model 17) or effective inflow concentration (model 19). The Canfield/Bachman model modified for the effects of phosphorus availablility (model 18) also works well and should be considered as an alternative. In the absence of ortho-phosphorus loading data, models 14 or 16 generally appear to be the most accurate for use in reservoirs.

50. Observed and predicted outflow and pool phosphorus concentrations are shown in Figures 7 and 8, respectively, for the CE data set and model 17. Observed and predicted outlet and pool phosphorus concentrations for the OECD/RSL data set and model 17 are shown in Figures 9 and 10, respectively. Residuals for the CE and OECD data sets combined are plotted against various reservoir characteristics in Figure 11. Residual histograms are presented in Figure 12, using symbols to differentiate CE Districts, as identified in Appendix A. Most of the residuals lie in the -.2 to .2 range, which corresponds to

54

Figure 7

Observed and Predicted Outflow Phosphorus Concentrations
Using Model 17
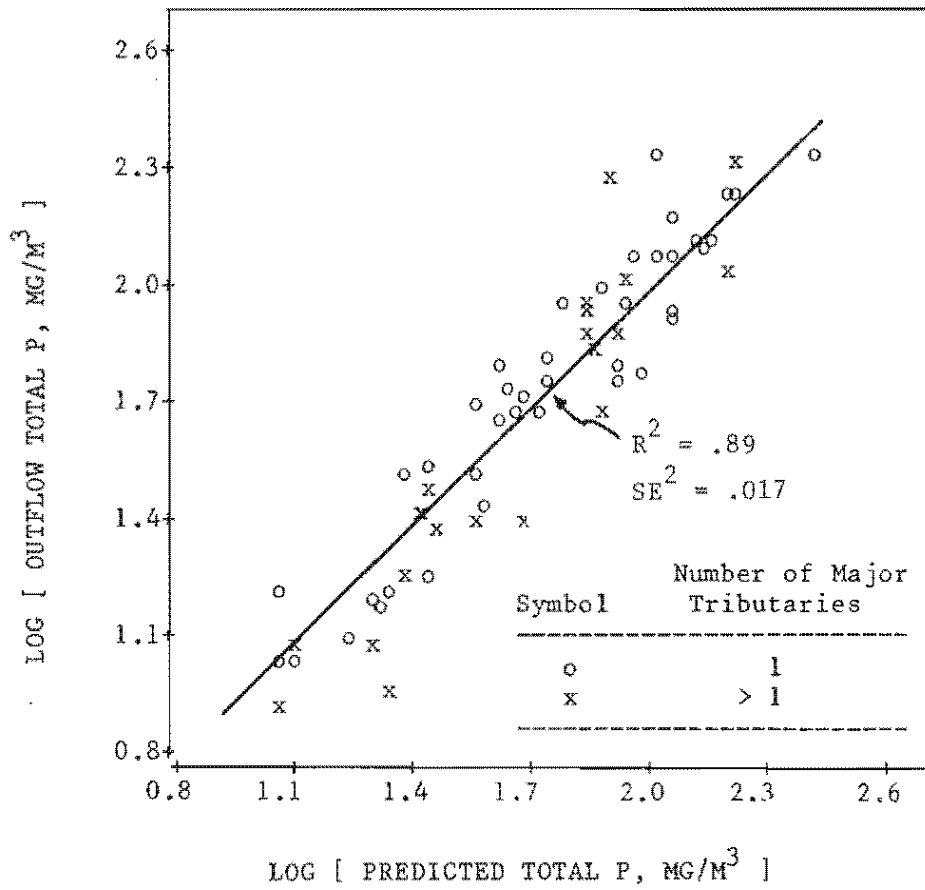
Model:

$$Po = [-1 + (1 + 4\ K2\ Pi\ T)^{.5}] / (2\ K2\ T)$$

$$K2 = .056\ Qs\ /\ [\ Fot\ (Qs + 13.3)\ ]$$

Figure 8

Observed and Predicted Pool Phosphorus Concentrations
Using Model 17
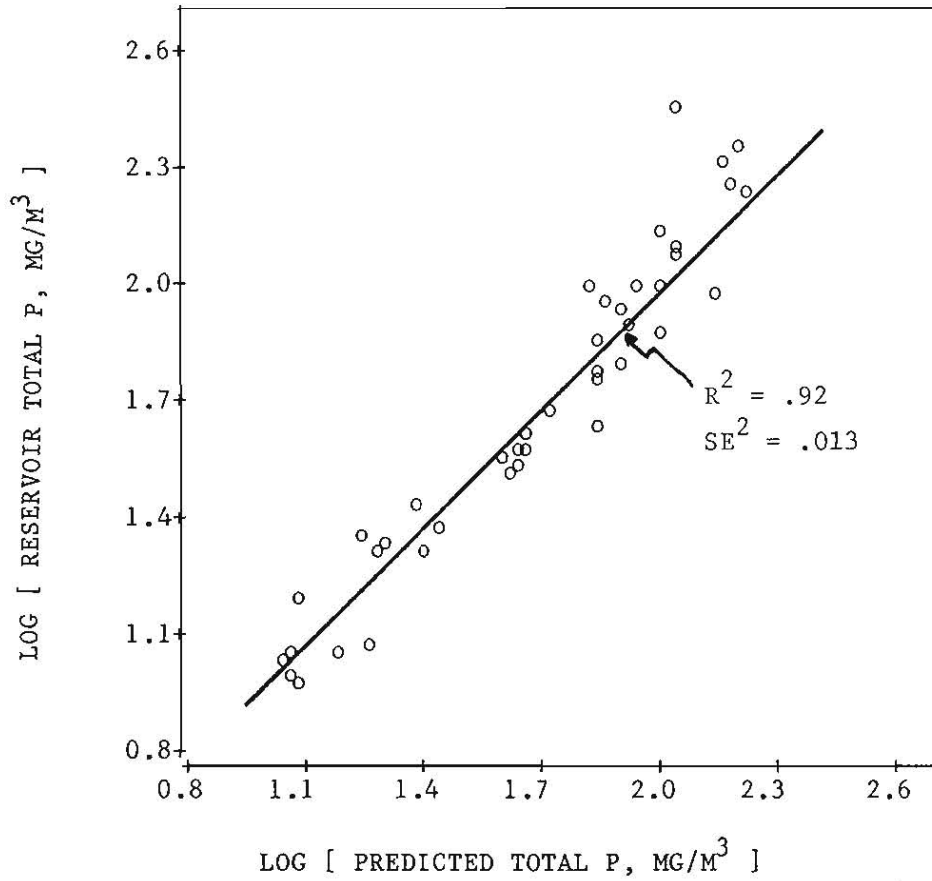
Model:

$$P = [-1 + (1 + 4 K2 Pi T)^{.5}] / (2 K2 T)$$

$$K2 = .056 Qs / [Fot (Qs + 13.3)]$$

Figure 9

Observed and Predicted Outflow Phosphorus Concentrations
Using Model 17 and the OECD/RSL Data Set
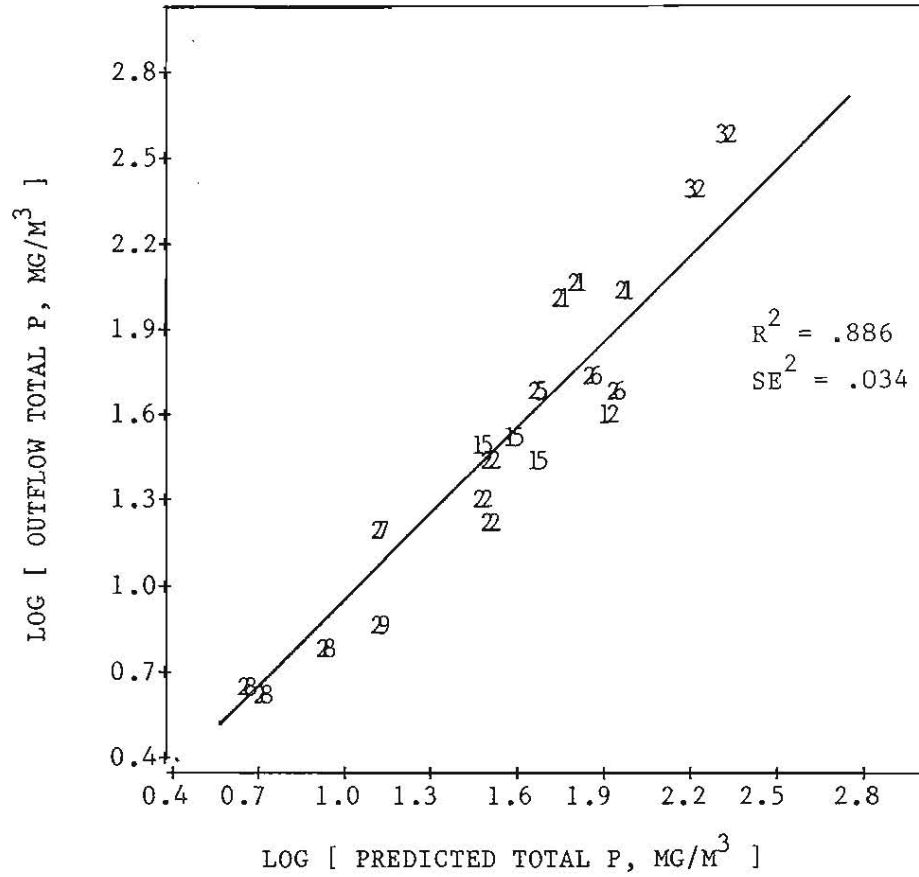
Symbol	Reservoir	Location
12	Nisramont	Belgium
15	El Burguillo	Spain
21	Mt. Bold	Australia
22	Wahnbach	Germany
25	Sorpe	Germany
26	Mohne	Germany
27	Verse	Germany
28	Sose	Germany
32	Enneppe	Germany

Figure 10

Observed and Predicted Pool Phosphorus Concentrations
Using Model 17 and the OECD/RSL Data Set
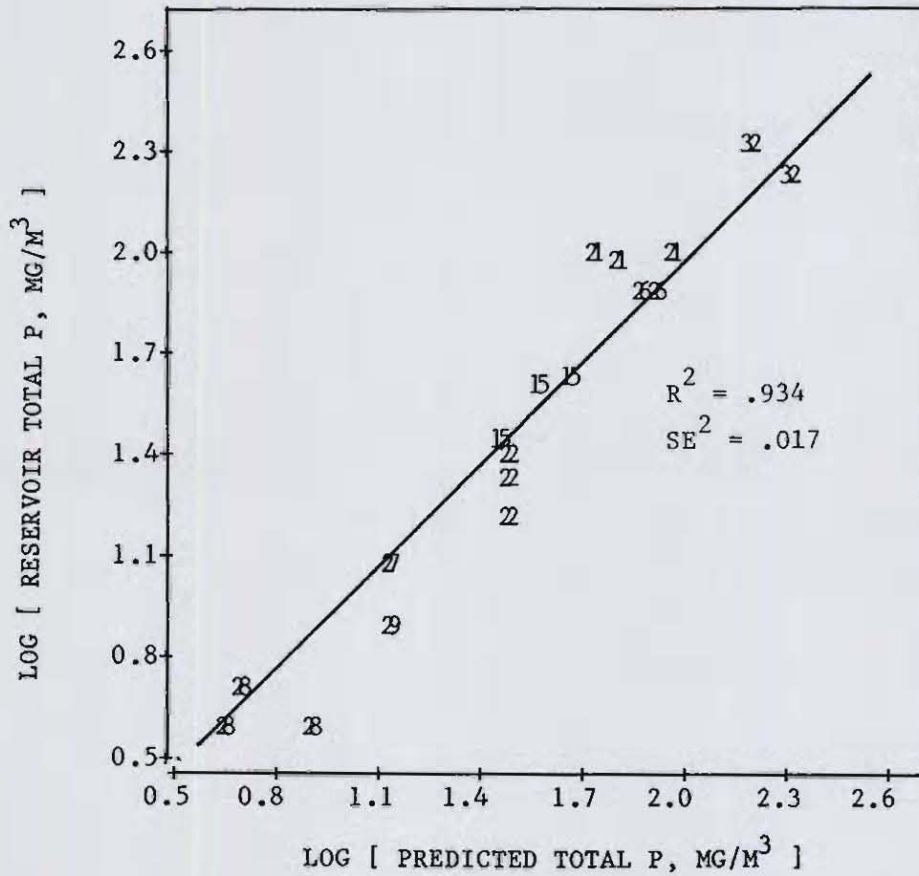
Symbol	Reservoir	Location
15	El Burguillo	Spain
21	Mt. Bold	Australia
22	Wahnbach	Germany
25	Sorpe	Germany
26	Mohne	Germany
27	Verse	Germany
28	Sose	Germany
29	Furwigge	Germany
32	Enneppe	Germany

Figure 11

Model 17 Residuals vs. Reservoir Characteristics
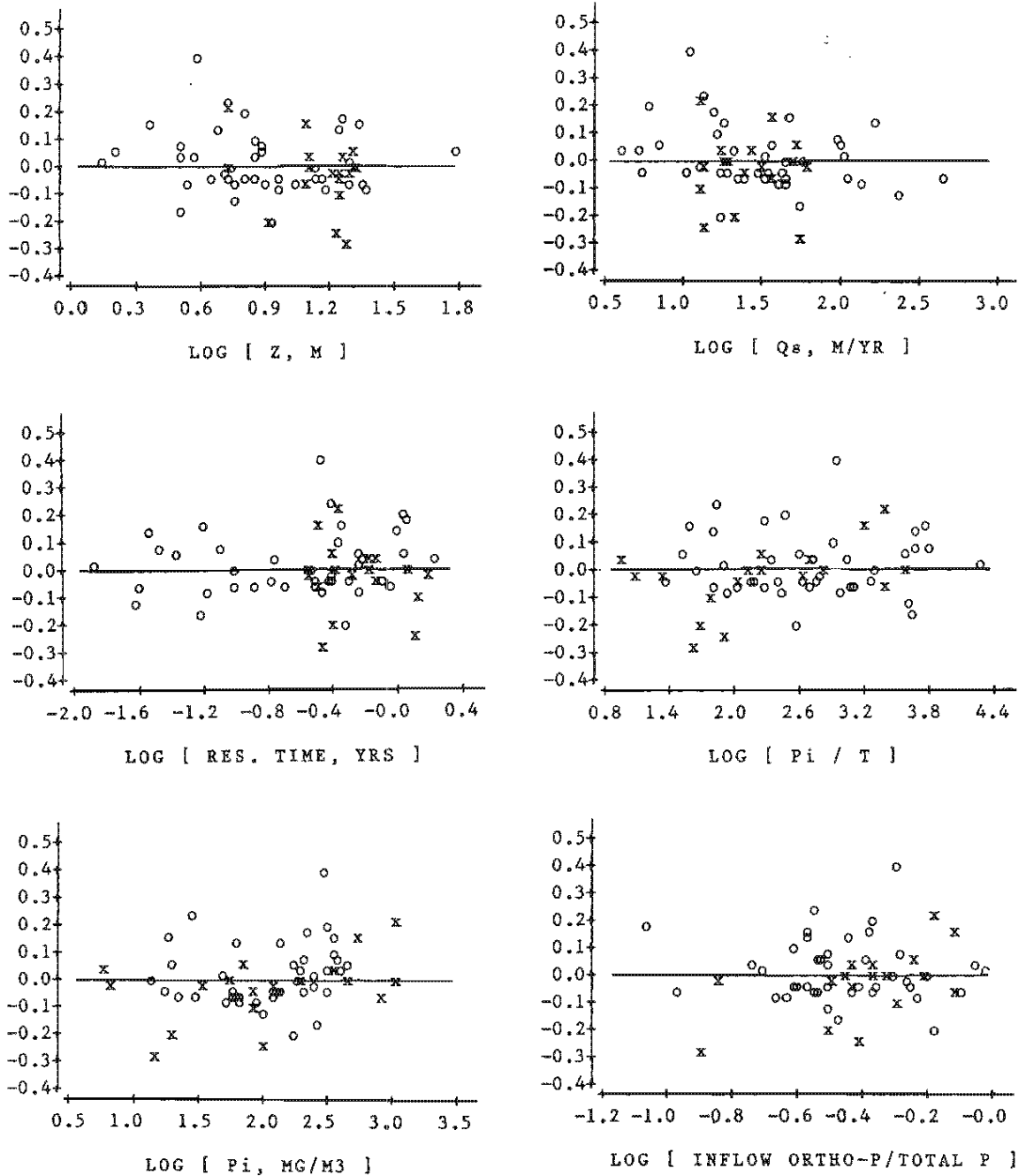
Symbols: o = CE Reservoir,   x = OECD Reservoir
Y Axis: log(Observed / Predicted Reservoir p)

Figure 12
Histograms of Model 17 Residuals*

```
                    Outflow P              Outflow P         Reservoir P
                    One Major Trib.      > One Major Trib.

        .40 |                            |                  |15  (15-237, Ashtabula)
        .35 |15  (15-237, Ashtabula)     |                  |
        .30 |                            |                  |
        .25 |                            |                  |
        .20 |                            |                  |
        .15 |10 19 19 25 31 35           |                  |25 25 26
        .10 |17 17 20 33                 |17 20 20 25       |18 19 24 25
        .05 |10 17 19 26                 |16 18 26          |17 17 29
        .00 |03 17 18 19 25 25 29 29     |16 24 30          |03 04 17 20 20 24 29 30 31
       -.05 |10 17 25 26 29              |08 10             |06 17 19 20 24 29
       -.10 |14 22 24 26 29              |                  |10 10 16 16 16 17 17 18 19 25
       -.15 |04 10 16 17 17 18           |10 19 24 25       |17 18
       -.20 |29                          |17 26             |17 19 19
       -.25 |                            |                  |
       -.30 |                            |06 = (06-372, Kerr) |
       -.35 |                            |                  |
       -.40 |                            |                  |
       -.45 |                            |08 = (08-330, Hartwell)
```

LOG10(Residual), minimum of interval

Model:

$$P = [-1 + (1 + 4 \ K2 \ Pi \ T)^{.5}] / (2 \ K2 \ T)$$

$$K2 = .056 \ Qs / [\ Fot \ (Qs + 13.3) \ ]$$

---

* Reservoir codes are defined in Appendix A (Tables A1 and A2).

an erro
performa
Ashtabul
51.
loading
water q
above,
concentr
nonlinea
segmenta
52.
coeffici
the mod
m/yr) an
contribu
phosphor
and in
(Omernik
in the
relative
contribu
bottom s
bottom
intermit
lakes a
Ashtabul
set (28
systemat
not appa

53.
phosphor
residual

60

an error margin of plus or minus 58%. Regional biases in model performance are not evident. Outliers are apparent in the cases of Ashtabula (Code 15-237), Kerr (Code 06-372), and Hartwell (Code 08-330).

51. Kerr and Hartwell have relatively complex morphometry and loading distributions which create marked spatial variations in surface water quality, both among and within tributary arms. As discussed above, the model would be expected to overpredict outflow concentrations in such a case because the retention function is nonlinear with respect to concentration. More elaborate spatial segmentation schemes would be appropriate for these types of reservoirs.

52. Ashtabula (Code 15-237) has a total phosphorus retention coefficient of essentially zero and is a positive outlier for most of the models examined. The reservoir has both a low overflow rate (7.8 m/yr) and high tributary ortho-P/total P ratio (.51) which would contribute to a low effective decay rate. The average inflow dissolved phosphorus concentration of 144 mg/m^3 is primarily of non-point origin and indicative of phosphorus-rich soils in eastern North Dakota (Omernik, 1977). Ashtabula is included on the list of "problem" lakes in the United States compiled by Katelle and Uttormark (1971). The relatively shallow mean depth of the reservoir (3.8 meters) may contribute to internal recycling of phosphorus via resuspension of bottom sediments and/or high rates of phosphorus release from anoxic bottom sediments during winter ice-cover and during periods of intermittent summer stratification, which are typical of shallow prairie lakes and reservoirs (Papst et al., 1980; Mathias and Barica, 1980). Ashtabula also has the highest alkalinity of the reservoirs in the data set (288 g/m^3); while this may reflect sediment phosphorus chemistry, a systematic relationship between retention model errors and alkalinity is not apparent for other reservoirs in the data set.

Error Analysis

53. A first-order error analysis has been applied to the phosphorus retention model calibrated above in order to partition residual variance into the following components:

61

<u>a</u>. Error variance in inflow concentration estimates.

<u>b</u>. Error variance in observed outlet or reservoir concentrations.

<u>c</u>. Error variance in effective decay rate.

The first two represent the data error component of the total residual variance; these variance terms have been estimated in the data reduction procedure (Walker, 1982a). The model error component is expressed as a error variance in the second-order decay rate, estimated from Equation 19. This has been estimated by difference from the total observed residual variance and the data error components.

54. The equations used in formulating the error analysis are given in Table 8. Model error, component <u>c</u> above, vanishes as the outflow concentration approaches the inflow concentration in the limit of low hydraulic residence times. Prediction error variance increases with hydraulic residence time because the sedimentation term of the mass balance becomes increasingly important (relative to the inflow term) in determining the predicted reservoir or outflow concentration.

55. Pooled error variance terms are given in Table 9, based upon outflow and reservoir phosphorus predictions. The calibrated error variance for the effective decay rate, .023 on log10 scales, corresponds approximately to a 95% confidence (2 standard error) factor of 2.0. This means that effective decay rates estimated from Equation 19 are generally accurate to within a factor of 2. Because of the structure of the model, the sensitivity (log-scale first-derivative) of the predicted reservoir or outlet phosphorus concentration to the estimated decay rate ranges from 0.0 at low residence times to .5 at high residence times. Combined with the decay rate variance estimate, corresponding model error factors range from 1.0 at zero residence time to 1.42 at high residence times. The estimated decay rate variance is conservative (high) because additional data error components attributed to overflow rate and tributary ortho-P/total P ratio have not been considered, although these terms are likely to be small in relation to the other data and model error components. The error balance equations can be used to construct prediction confidence limits, given error estimates for inflow concentration and decay rate.

Table 8
Error Balance Equations for Second-Order Decay Model

Model:

$$Pe = (-1 + X) / 2\ K2\ T$$

$$X = (1 + 4\ K2\ Pi\ T)^{.5}$$

$$K2 = .056\ Qs/ ((Qs + 13.3)\ Fot)$$

Error Balance Equation for Total Residual Variance:

$$Var(log(P/Pe)) = Var(log(P)) + SPi^2\ Var(log(Pi)) + SK2^2\ Var(log(K2))$$

$$SPi = \quad Pi\ /\ X\ Pe$$

$$SK2 = \quad (4\ Pi\ K2\ T\ /\ X + 2 - 2\ X)\ /\ 4\ K2\ T\ Pe$$

where

    Pe = estimated reservoir or outlet P (mg/m^3)

    P = observed reservoir (or outlet) P (mg/m^3)

    T = residence time (years)

    $K2$ = effective second-order decay rate $(m^3/mg\text{-}yr)$

    Pi = inflow total P concentration (mg/m^3)

    Fot = tributary ortho-P / total P ratio

    Qs = surface overflow rate (m/yr)

    SPi = first derivative of $log(Pe)$ with respect to $log(Pi)$

    $SK2$ = first derivative of $log(Pe)$ with respect to $log(K2)$

    Var = variance operator

    X = dummy variable

Table 9
Error Balance Terms for Phosphorus Retention Model

Source	Mean Sensitivity	Source Variance	Product
----- Outlet P, 1 major tributary, n=40 ------			
Inflow P	.483	.0055*	.0027
Decay Rate	.108	.0230**	.0025
Outflow P	1.000	.0089*	.0089
Total Estimated Residual Variance			.0140
Observed Residual Variance			.0146
-------------- Reservoir P, n=41 -----------------			
Inflow P	.443	.0055*	.0024
Decay Rate	.123	.0230**	.0028
Reservoir P	1.000	.0071*	.0071
Total Estimated Residual Variance			.0123
Observed Residual Variance			.0128

NOTES:
   Equations given in Table 8
   Variance terms on log10 scales
   Sensitivity = squared first derivative
* Error variance estimated from input data
** Decay rate variance (model error) estimated by difference

PART III: NITROGEN RETENTION MODELS

56. Nitrogen limitation of algal growth is important in some reservoirs, particularly those in the West and others which are heavily impacted by point sources, which tend to be rich in phosphorus relative to algal growth requirements. As discussed by Bachman (1980), the nitrogen cycle in lakes and reservoirs includes atmospheric exchanges (nitrogen fixation and denitrification) which are not found in the phosphorus cycle and which may limit the applicability of a mass-balance modeling approach. Despite this potential limitation, the models developed and tested in the following section have lower error variances than their phosphorus counterparts. The approach parallels that used for phosphorus, but is less intensive. Data sets used in model development and testing are listed in Appendix A.

57. Figure 13 shows the relationship between pool (area-weighted, surface-layer, growing-season) and outflow (annual, flow-weighted-average) total nitrogen concentrations in 41 CE reservoirs. Pool nitrogen concentrations average 67% of the outflow values (vs. 100% in the case of phosphorus). Under "plug-flow" conditions, average pool concentrations would be expected to exceed those in the outflow. The differences are most likely attributed to the effects of seasonal variations, since pool concentrations reflect growing-season conditions and the outflow concentrations are annual, flow-weighted values. In most areas of the country, calculations of the latter place heavy weights on spring measurements, which would tend to be higher because of greater runoff, lower temperature, and lower biological uptake within the reservoir. Year-to-year variations in hydrologic conditions might also be reflected in Figure 13, because the outflow and pool concentrations were generally measured by the EPA National Eutrophication Survey in different hydrologic years. Because of the apparent differences between pool and outflow nitrogen levels, predictive models are developed separately below.

58. Outflow and pool N/P ratios are plotted against inflow N/P ratios in Figures 14 and 15, respectively. Figure 14 indicates that, on

Figure 13

Reservoir Total N vs. Outflow Total N
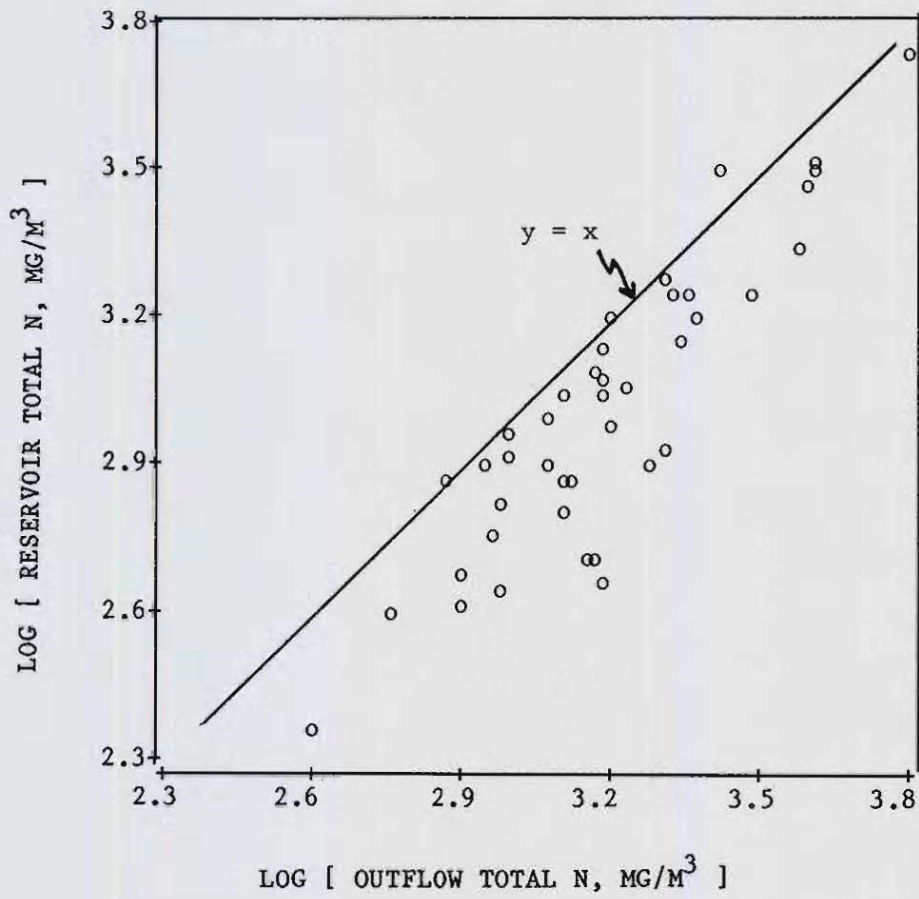
Figure 14

Outflow Total N/P vs. Inflow Total N/P
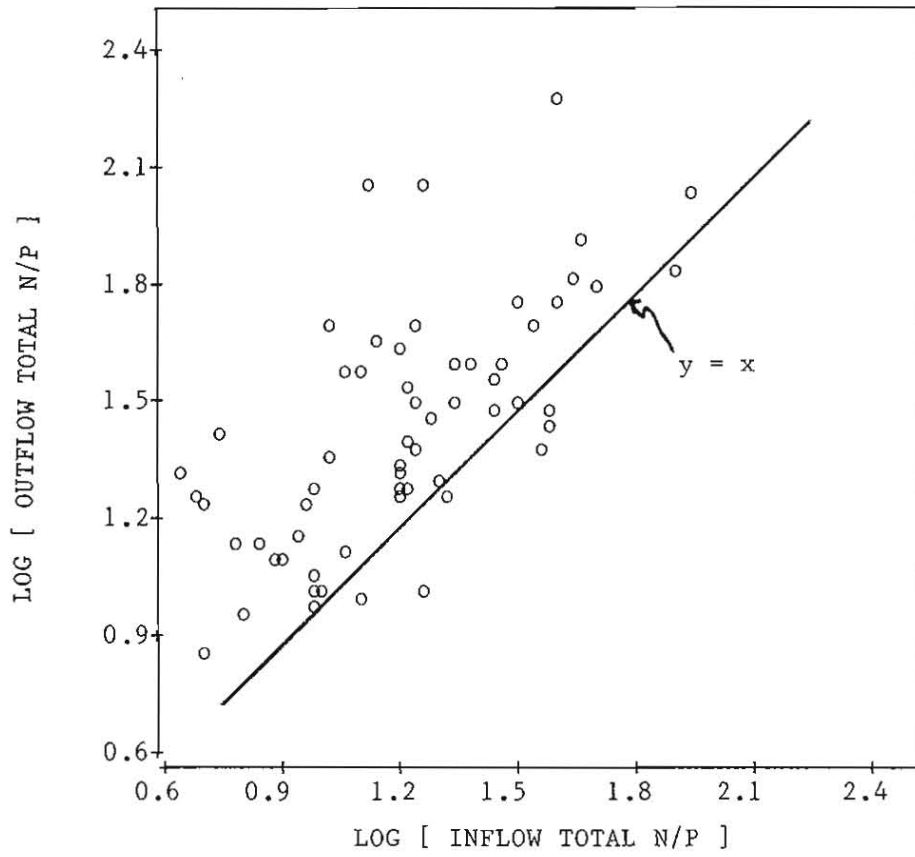
Figure 15

Reservoir Total N/P vs. Inflow Total N/P
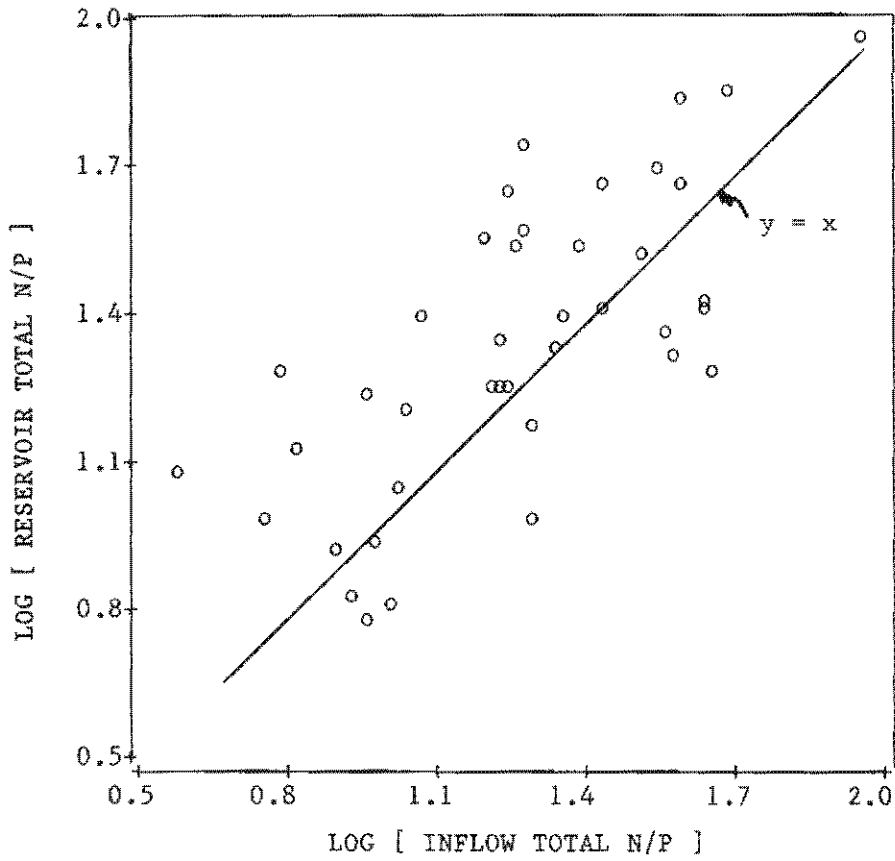
the basis of annual mass balances, the N/P ratio increases moving through most impoundments; this suggests a higher trapping efficiency for phosphorus and a greater potential for phosphorus limitation than indicated by inflow N/P ratio, particularly for reservoirs with inflow N/P less than 10. The enrichment of nitrogen may reflect a greater affinity of sediments for phosphorus and nitrogen fixation. The nitrogen enrichment is less strong in the case of pool N/P ratio (Figure 15).

59. Outflow and pool nitrogen concentrations are plotted against inflow concentrations in Figures 16 and 17, respectively. Figure 16 shows that several reservoirs in the low inflow concentration range have negative retention coefficients. These reflect random errors in the inflow and outflow estimates as well as nitrogen sources which are not accounted for in the nutrient balances (e.g., nitrogen fixation). The lower analytical detection limit for Kjeldahl nitrogen (200 mg/m^3) in the EPA National Eutrophication Survey pool samples may also be a factor in some cases. Only two projects have negative retention coefficients based upon pool nitrogen concentrations.

60. Model formulations, parameter estimates, and error statistics for predicting outflow and pool nitrogen concentrations are presented in Tables 10 and 11, respectively. In predicting pool concentrations, May-September inflow concentrations and hydraulic residence times have been used for most projects, according to the criteria used in testing phosphorus models (annual hydraulic residence less than 0.5 year and summer nitrogen residence time less than 0.25 year). Estimates of summer inflow nitrogen concentrations are approximate because they are based upon flow/concentration relationships in project tributaries and do not reflect seasonal variations in concentrations which are independent of flow. Conclusions regarding choice of model are similar when annual conditions are used, although the error magnitudes are slightly higher.

61. Because of possible biases in the mean values related to the EPA/NES TKN detection limit of 200 mg/m^3, the data sets used in model testing exclude projects with total nitrogen (inflow, pool, or outflow)

Figure 16

Outflow Total N vs. Inflow Total N
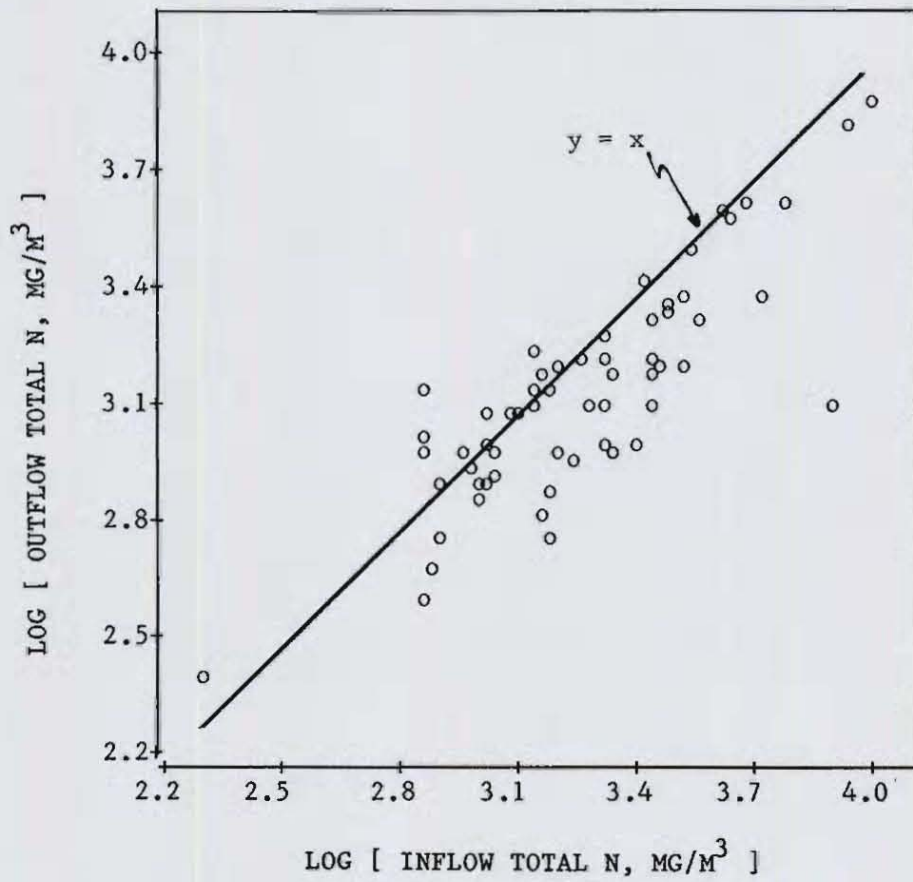
Figure 17

Reservoir Total N vs. Inflow Total N
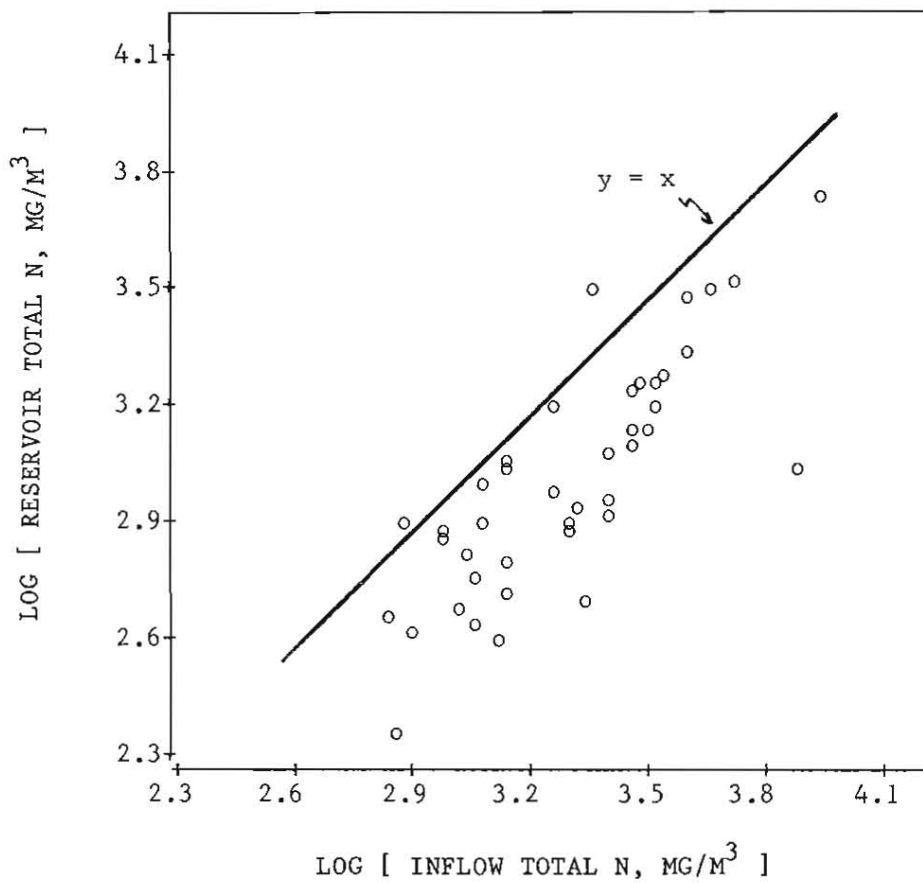
Table 10
Models for Predicting Outflow Nitrogen Concentrations

	R^2	SE^2

Model 01: Bachman (1980) — Volumetric Loading:

$$No = Ni \,/\, (\, 1 + .0159\, Ni^{.59}\, T^{.41}\,) \qquad .75 \quad .018$$

Model 02: Bachman (1980) — Areal Loading:

$$No = Ni \,/\, (\, 1 + .00162\, Ni^{.71}\, Z^{.71}\, T^{.29}\,) \qquad .49 \quad .037$$

Model 03: Bachman (1980) — Flushing Rate:

$$No = Ni \,/\, (\, 1 + .693\, T^{.45}\,) \qquad .77 \quad .017$$

Model 04: Generalized:

$$No = Ni \,/\, (\, 1 + .011\, Ni^{.63}\, Z^{-.09}\, T^{.66}\,) \qquad .86 \quad .010$$

Model 05: Second-Order, Mixed:

$$No = (\, -1 + (1 + 4\, K2\, Ni\, T\,)^{.5}\,) \,/\, (2\, K2\, T) \qquad .85 \quad .011$$

$$K2 = .00123\ m^3/mg\text{-}yr$$

Model 06: Modified Second-Order:

$$K2 = .000694\, Qs\, Fin^{-.62} \,/\, (\, Qs + 2.2\,) \qquad .87 \quad .009$$

Fin = inflow inorganic N / inflow total N

Model 07: Modified Second-Order — Available N:

$$K2 = .00123\ \ m^3/mg\text{-}yr \qquad .87 \quad .010$$

Nia = 1.22 Nin + .76 (Ni − Nin)

Nia = inflow available nitrogen (mg/m^3)

NOTE: based upon data from 53 CE reservoirs.

Table 11
Models for Predicting Pool Nitrogen Concentrations
Using Seasonal-Average Inflow Conditions

	R^2	SE^2

Model 01: Bachman (1980) - volumetric loading:

$$N = N_i / (1 + .0159\ N_i^{.59}\ T^{.41}) \qquad\qquad .84 \quad .012$$

Model 02: Bachman (1980) - areal loading:

$$N = N_i / (1 + .00162\ N_i^{.71}\ Z^{.71}\ T^{.29}) \qquad .83 \quad .013$$

Model 03: Bachman (1980) - flushing rate:

$$N = N_i / (1 + .693\ T^{.45}) \qquad\qquad\qquad .48 \quad .038$$

Model 08: Generalized:

$$N = N_i / (1 + .0081\ N_i^{.62}\ Z^{.30}\ T^{.47}) \qquad .88 \quad .009$$

Model 09: Second-Order, Mixed:

$$N = (-1 + (1 + 4\ K_2\ N_i\ T)^{.5}) / (2\ K_2\ T) \qquad .84 \quad .011$$

$$K_2 = .00315\ m^3/mg\text{-}yr$$

Model 10: Modified Second-Order:

$$K_2 = .0035\ Q_s\ Fin^{-.59} / (Q_s + 17.3) \qquad\qquad .90 \quad .008$$

$$Fin = \text{tributary inorganic N / inflow total N}$$

Model 11: Modified Second-Order - Available N:

$$Nia = 1.05\ Nin + .43\ (N_i - Nin) \qquad\qquad\qquad .91 \quad .007$$

$$K_2 = .00157\ Q_s / (Q_s + 2.8)$$

$$Nia = \text{inflow available nitrogen } (mg/m^3)$$

NOTE: based upon data from 39 CE reservoirs.

concentrations less than 300 mg/m^3. A review of NES data listings indicates that projects in this category generally have a high percentage of pool TKN values reported as less than 200 mg/m^3. As a partial screen against unsampled nitrogen sources and other random errors, projects with total nitrogen retention coefficient less than -0.1 have also been excluded from model testing. The data sets used in model testing include 53 and 39 projects for the outflow and pool models, respectively.

62. The first three models in Tables 10 and 11 were developed by Bachman (1980), based upon EPA National Eutrophication Survey data from 479 lakes and reservoirs. The models are similar in structure to the phosphorus models developed by Canfield and Bachman (1981) and tested in the previous section. They relate the effective first-order sedimentation coefficient to volumetric loading (model 01), areal loading (model 02), and flushing rate (model 03). Bachman's models were originally calibrated for predicting median, pool total nitrogen concentrations. Models 01 and 02 explain 82-80% of the variance in the pool concentrations with mean squared errors of .013-.015.

63. Models 04 and 08 are generalized versions of Bachman's models which permit the sedimentation coefficient to vary as a power function of mean depth. inflow concentration, and residence time. Parameter optimization for each data set reduces mean squared errors to .009 (pool N) and .010 (outflow N) and provides slight improvements over Bachman's original parameter estimates. The parameter estimates reflect a strong dependence of the sedimentation coefficient on inflow concentration (exponents of .57 to .63). As in the case of phosphorus, this suggests a nonlinear loading response.

64. The remaining models are analogous to the second-order kinetic formulations developed for phosphorus. Calibration of the one-parameter decay models (05 and 09) indicates effective decay rates of .0012 m^3/mg-yr for predicting outflow nitrogen, vs. .0032 m^3/mg-yr for predicting pool nitrogen based upon seasonal inflow conditions. Differences in these parameter estimates reflect differences between outflow and pool concentrations, as discussed above. Modifications of the second-order

74

model to account for effects of overflow rate and inflow nitrogen availability have greater effects on the pool nitrogen models than on the outflow models.

65. Weighting schemes to account for inflow nitrogen availability are presented for various nitrogen retention models in Table 12. The nutrient balances developed previously permit partitioning of the inflow total nitrogen concentrations into organic and inorganic components. Weight ratios (organic/inorganic) range from .54 to .62 for three outflow nitrogen models and from .36 to .43 for three pool nitrogen models. Thus, inflow nitrogen availability seems to be somewhat more important for predicting pool nitrogen concentrations than for predicting outflow nitrogen concentrations and conclusions are relatively independent of the particular retention model employed. While optimization of the weighting factors provides significant reductions in residual error, inflow nitrogen partitioning appears to be less important than inflow phosphorus partitioning, for which the optimal relative weights (non-ortho/ortho) range from .15 to .19 (see Part II). This may reflect a greater association of inflow phosphorus with sediments and the presence of dissolved organic nitrogen compounds which are not readily removed by sedimentation.

66. Table 13 describes eight data sets which have been compiled for use in testing the nitrogen models presented in Tables 10 and 11. Error statistics are summarized for outflow nitrogen models in Table 14 and for pool nitrogen models in Table 15. Based upon a comparison of error statistics across data sets, models 03 and 06 appear to have the most generality for predicting outflow concentrations, although the comparison is hindered by lack of inflow inorganic nitrogen data from the EPA/NES Compendium data bases. Model 06 has an average bias of .11 log units when applied to the OECD/RSL outflow data. Models 01, 10, or 11 appear to work best for predicting pool nitrogen levels, except all are biased by .21-.27 log units when applied to the OECD/RSL pool data.

67. Observed and predicted pool nitrogen concentrations for the OECD/RSL data set using models 03 and 10 are shown in Figures 18 and 19, respectively. While model 03 fits best in its original form, it tends

Table 12
Inflow Available Nitrogen Weighting Schemes Calibrated for Use
with Various Nitrogen Retention Models

Model	Inflow Weights * Inorganic Win	Organic Worg	Ratio	RSS	R^2

------------------------ Outflow Nitrogen Models (n=53) ----------------------

Bachman (1980):

$$No = Ni / (1 + .0159 Ni^{.59} T^{.41}) *$$

	Win	Worg	Ratio	RSS	R^2
*	1.00	1.00	1.00	.954	.75
*	1.71	.92	.54	.518	.87

$$No = Ni / (1 + .643 T^{.45})$$

| 1.00 | 1.00 | 1.00 | .878 | .77 |
| 1.22 | .70 | .57 | .705 | .82 |

This Study, Second-Order Model:

$$K2 = .00123 \ (m^3/mg\text{-}yr)$$

| 1.00 | 1.00 | 1.00 | .568 | .85 |
| 1.22 | .76 | .62 | .507 | .87 |

------------------------ Pool Nitrogen Models (n=39) ----------------------

Bachman (1980):

$$N = Ni / (1 + .0159 Ni^{.59} T^{.41})$$

| 1.00 | 1.00 | 1.00 | .463 | .84 |
| 1.38 | .49 | .36 | .271 | .91 |

$$N = Ni / (1 + .693 T^{.45})$$

| 1.00 | 1.00 | 1.00 | 1.473 | .49 |
| 1.02 | .44 | .43 | .445 | .85 |

This Study, Second-Order Model:

	Win	Worg	Ratio	RSS	R^2
$K2 = .0045 \ Qs/(Qs + 7.2)$	1.00	1.00	1.00	.413	.86
$K2 = .00157 \ Qs/(Qs + 2.8)$	1.00	1.00	1.00	.846	.71
$K2 = .00157 \ Qs/(Qs + 2.8)$ **	1.05	.43	.41	.259	.91

Nia = Inflow Available Nitrogen (mg/m^3) calculated from:
      Nia =   Win Niin   + Worg Niorg
Niin = inflow inorganic nitrogen (mg/m^3) Ratio = Worg/Win
Niorg = inflow organic nitrogen (mg/m^3) RSS = residual sum of squares
Win = inflow inorganic nitrogen weight
Worg = inflow organic nitrogen weight

* For each model, first row gives statistics for unweighted case
   (Win=Worg=1.0); second row gives statistics for optimal weights.
** Parameters of decay rate formulation (.00157, 2.8) optimized
   simultaneously with inflow weighting factors;
   (.0045,7.2) are optimal for weighting factors = 1.0.

Table 13
Key to Data Sets Used in Testing Nitrogen Retention Models

Code	Source	Reservoirs	Predicted Variable	n	Notes
A	This Study	CE	No	53	all reservoirs
B	"	CE	N	39	seasonal Ni, T (see text)
C*	EPA/NES (1978)	CE	No	88	NES Compendium
D*	"	CE	N	96	"
E*	"	US-Res.	No	265	" excluding CE Reservoirs
F*	"	US-Res.	N	242	" excluding CE Reservoirs
G	Clasen(1980)	Global	No	14	OECD/RSL Reservoir-Years
H	"	Global	N	13	OECD/RSL Reservoir-Years

screening criteria applied to all data sets:
- (1) non-missing values for N_i, T, Z, N (or No)
- (2) total nitrogen retention coefficient > -.1
- (3) inflow total nitrogen concentration < 10000 mg/m^3
- (4) N_i, N, and No > 300 mg/m^3
- (5) surface overflow rate Z/T > .25 m/yr
- (6) reservoirs with inflow inorganic N estimates and excluding artificial pumped storage impoundments (OECD/RSL Study)

* Inflow inorganic nitrogen concentrations not available for EPA/NES data sets; estimated at 42% of inflow total nitrogen concentration (average of CE data).

Table 14
Error Statistics for Outflow Nitrogen Models

D MODEL	N	MEAN	T	MSE	VAR	MABS	R2
---------------- CE Data Set -----------------							
A 00	53	3.130	83.77*	9.869	0.074	3.130	1.000
A 01	53	0.083	5.76*	0.018	0.011	0.116	0.757
A 02	53	0.131	6.74*	0.037	0.020	0.157	0.500
A 03	53	-0.030	-1.73	0.017	0.016	0.094	0.770
A 04	53	-0.002	-0.15	0.010	0.010	0.081	0.865
A 05	53	-0.007	-0.49	0.011	0.011	0.080	0.851
A 06	53	-0.009	-0.69	0.009	0.009	0.074	0.878
A 07	53	0.003	0.22	0.010	0.010	0.079	0.865
--------------- EPA/NES/CE Reservoirs ----------------							
C 00	88	3.092	116.49*	9.619	0.062	3.092	1.000
C 01	88	0.146	13.06*	0.032	0.011	0.155	0.484
C 02	88	0.167	11.08*	0.048	0.020	0.180	0.226
C 03	88	0.022	1.74	0.014	0.014	0.098	0.774
C 04	88	0.086	7.08*	0.021	0.013	0.117	0.661
C 05	88	0.082	6.75*	0.020	0.013	0.116	0.677
C 06	88	0.048	4.29*	0.013	0.011	0.094	0.790
C 07	88	0.098	8.06*	0.023	0.013	0.123	0.629
-------------- EPA/NES/NON-CE Reservoirs --------------							
E 00	265	3.088	194.21*	9.600	0.067	3.088	1.000
E 01	265	0.125	14.76*	0.034	0.019	0.146	0.493
E 02	265	0.143	13.01*	0.052	0.032	0.175	0.224
E 03	265	0.010	1.12	0.021	0.021	0.105	0.687
E 04	265	0.072	7.90*	0.027	0.022	0.118	0.597
E 05	265	0.064	6.87*	0.027	0.023	0.117	0.597
E 06	265	0.032	3.78*	0.020	0.019	0.102	0.701
E 07	265	0.081	8.89*	0.029	0.022	0.123	0.567
----------------- OECD/RSL Study -----------------							
G 00	14	3.311	47.51*	11.023	0.068	3.311	1.000
G 01	14	0.218	6.26*	0.064	0.017	0.229	0.059
G 02	14	0.372	7.78*	0.168	0.032	0.376	-1.471
G 03	14	0.023	0.54	0.024	0.025	0.116	0.647
G 04	14	0.121	3.28*	0.033	0.019	0.156	0.515
G 05	14	0.135	3.49*	0.038	0.021	0.167	0.441
G 06	14	0.085	2.31*	0.025	0.019	0.137	0.632
G 07	14	0.122	3.23*	0.034	0.020	0.160	0.500

Key:
D   Data Set Code (see Table 13)
MODEL   Model Code (00 = observed nitrogen, see Table 10)
N   Number of Reservoirs
MEAN   Mean Residual
T   T-test for |MEAN| > 0
* |T| > 0 at p < .05
MSE   Mean Square
VAR   Variance
MABS   Mean Absolute Value

78

Table 15
Error Statistics for Pool Nitrogen Models

D MODEL	N	MEAN	T	MSE	VAR	MABS	R2
------------------ CE Data Set ------------------							
B 00	39	3.003	68.94*	9.089	0.074	3.003	1.000
B 01	39	−0.025	−1.37	0.012	0.013	0.096	0.835
B 02	39	0.025	1.32	0.013	0.014	0.094	0.828
B 03	39	−0.142	−6.43*	0.038	0.019	0.162	0.484
B 08	39	−0.003	−0.18	0.009	0.010	0.084	0.851
B 09	39	−0.010	−0.57	0.011	0.012	0.095	0.838
B 10	39	−0.008	−0.53	0.008	0.008	0.079	0.900
B 11	39	0.006	0.37	0.007	0.007	0.079	0.910
------------------ EPA/NES/CE Reservoirs ------------------							
D 00	96	2.914	113.75*	8.555	0.063	2.914	1.000
D 01	96	−0.015	−1.10	0.018	0.018	0.105	0.714
D 02	96	0.002	0.13	0.021	0.022	0.118	0.667
D 03	96	−0.131	−8.12*	0.042	0.025	0.165	0.333
D 08	96	0.026	1.68	0.024	0.023	0.123	0.619
D 09	96	0.032	1.91	0.028	0.027	0.133	0.556
D 10	96	−0.015	−1.04	0.020	0.020	0.110	0.683
D 11	96	0.017	1.18	0.020	0.020	0.109	0.683
------------------ EPA/NES/NON−CE Reservoirs ------------------							
F 00	242	2.928	160.04*	8.655	0.081	2.928	1.000
F 01	242	−0.025	−2.46*	0.025	0.025	0.124	0.691
F 02	242	−0.010	−0.86	0.033	0.033	0.138	0.593
F 03	242	−0.149	−12.76*	0.055	0.033	0.177	0.321
F 08	242	0.015	1.35	0.030	0.030	0.133	0.630
F 09	242	0.020	1.71	0.033	0.033	0.141	0.593
F 10	242	−0.039	−3.50*	0.031	0.030	0.138	0.617
F 11	242	−0.007	−0.64	0.029	0.029	0.134	0.642
------------------ OECD/RSL Study ------------------							
H 00	13	3.291	46.19*	10.894	0.066	3.291	1.000
H 01	13	0.211	9.82*	0.050	0.006	0.211	0.242
H 02	13	0.363	10.69*	0.146	0.015	0.363	−1.212
H 03	13	0.019	0.60	0.012	0.013	0.090	0.818
H 08	13	0.283	9.31*	0.092	0.012	0.283	−0.394
H 09	13	0.267	9.18*	0.081	0.011	0.267	−0.227
H 10	13	0.240	11.17*	0.063	0.006	0.240	0.045
H 11	13	0.268	11.55*	0.078	0.007	0.268	−0.182

Key:
D   Data Set Code (see Table 13)
MODEL   Model Code (00 = observed nitrogen, see Table 11)
N   Number of Reservoirs
MEAN   Mean Residual
T   T-test for |MEAN| > 0
* |T| > 0 at p < .05
MSE   Mean Square
VAR   Variance
MABS   Mean Absolute Value

79

Figure 18

Observed and Predicted Pool Nitrogen Concentrations
Using Model 03 and the OECD/RSL Data Set
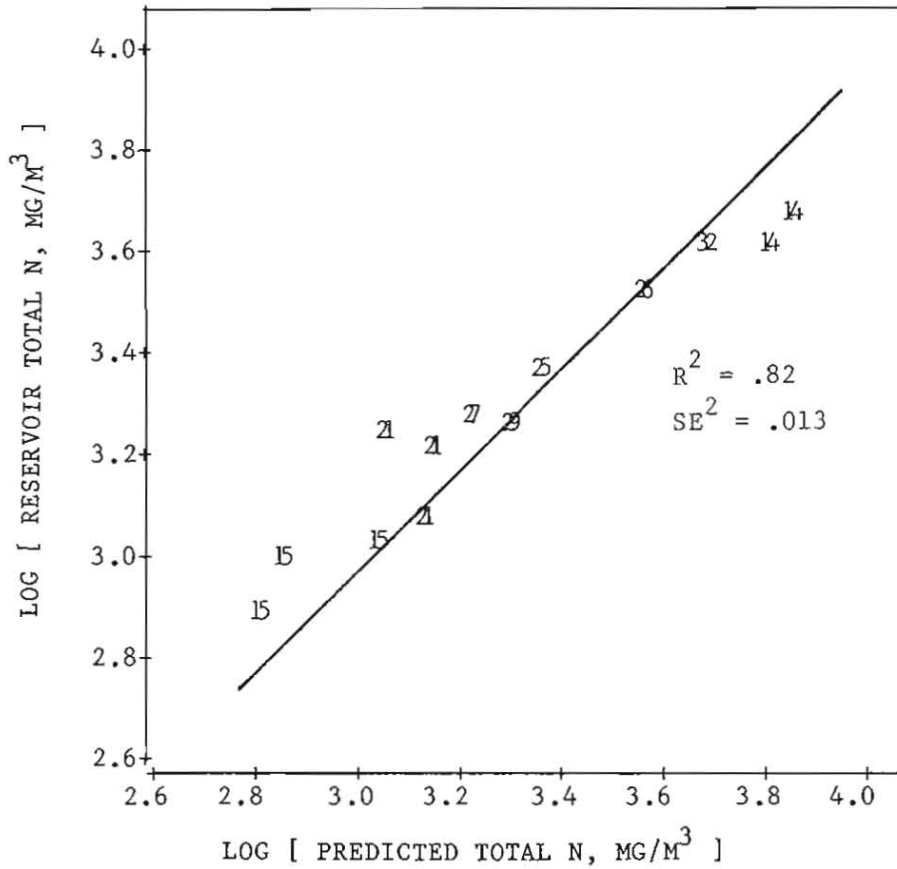
Symbol	Reservoir	Location
14	Brielse Meer	Netherlands
15	El Burguillo	Spain
21	Mt. Bold	Australia
25	Sorpe	Germany
26	Mohne	Germany
27	Verse	Germany
29	Furwigge	Germany
32	Enneppe	Germany

Model:

$$N = Ni / (1 + .693 \, T^{.45})$$

Figure 19

Observed and Predicted Pool Nitrogen Concentrations
Using Model 10 and the OECD/RSL Data Set
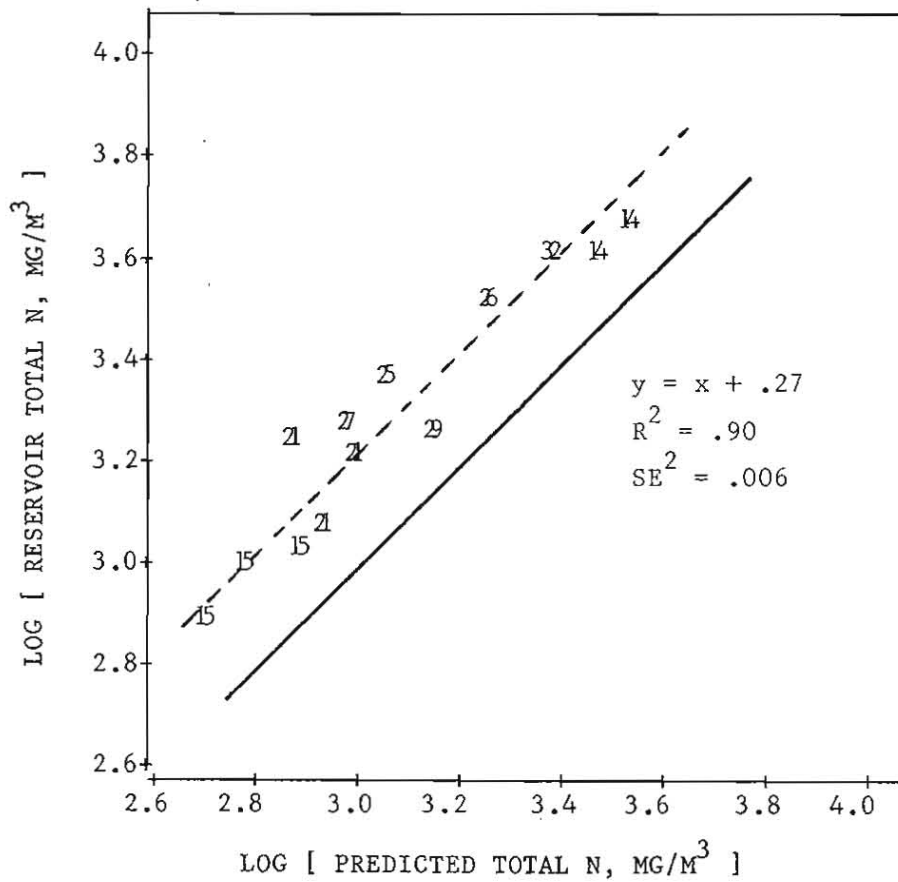
$$y = x + .27$$
$$R^2 = .90$$
$$SE^2 = .006$$

Symbol	Reservoir	Location
14	Brielse Meer	Netherlands
15	El Burguillo	Spain
21	Mt. Bold	Australia
25	Sorpe	Germany
26	Mohne	Germany
27	Verse	Germany
29	Furwigge	Germany
32	Enneppe	Germany

Model:

$$N = [-1 + (1 + 4\ K2\ Ni\ T)^{.5}] / (2\ K2\ T)$$

$$K2 = .0035\ Qs\ Fin^{-.59} / (Qs + 17.3)$$

to underpredict nitrogen levels in the low concentration range and overpredict in the high range. This probably reflects the first-order assumption which is inherent in the formulation and which is contra-indicated by the EPA/NES data and other versions of Bachman's models. When corrected for a consistent bias of .27 log units, model 10 is a reasonable predictor of pool nitrogen concentrations for the OECD/RSL data set (Figure 18). Reasons for the apparent differences between the (primarily European) OECD and the EPA/NES data sets with respect to nitrogen dynamics (or data) are unclear and require additional study. The comparison is based upon a relatively small sample of OECD reservoirs with nitrogen loading data (14 reservoir-years, 8 different reservoirs).

68. Outflow and pool nitrogen predictions for the CE data set are shown in Figures 20 and 21 using models 06 and 10, respectively. These models explain 88% and 90% of the variance in the observed concentrations with mean square errors of .009 and .008 log units, respectively. Results indicate that despite the open-ended and complex nature of the nitrogen cycle, most of the among-reservoir variance in pool and outflow nitrogen concentrations can be predicted from external nitrogen loadings, reservoir morphometry, and reservoir hydrology. Average effects of nitrogen fixation or denitrification are inherent in the model parameter estimates and residuals are independent of inflow and pool N/P ratios. In reservoirs with relatively high concentrations of nitrogen-fixing blue-greens, however, it is possible that pool and outflow nitrogen levels may be underpredicted by models of the above sort. Refined data sets are needed to support analyses of nitrogen fixation effects and further assessment of the negative biases observed for the OECD/RSL data set.

Figure 20

Observed and Predicted Outflow Nitrogen Concentrations
Using Model 06 and CE Data Set
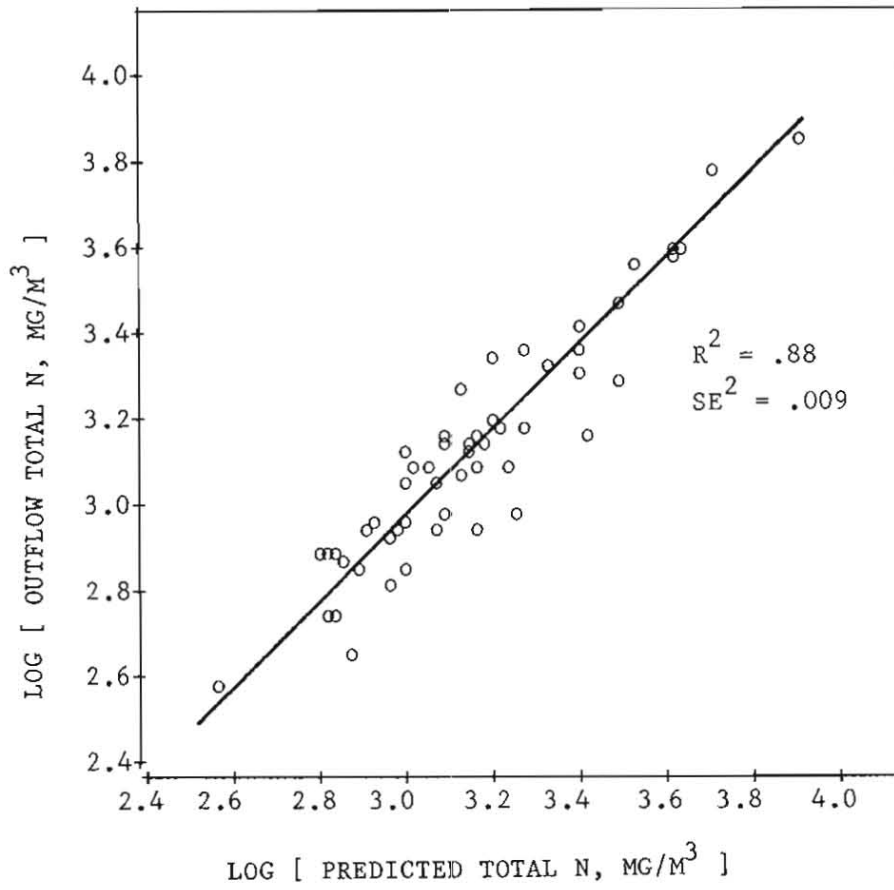
Model:

$$N_o = [-1 + (1 + 4 K2 \ Ni \ T)^{.5}] / (2 K2 \ T)$$

$$K2 = .000694 \ Qs \ Fin^{-.62} / (Qs + 2.2)$$

83

Figure 21

Observed and Predicted Pool Nitrogen Concentrations
Using Model 10 and CE Data Set
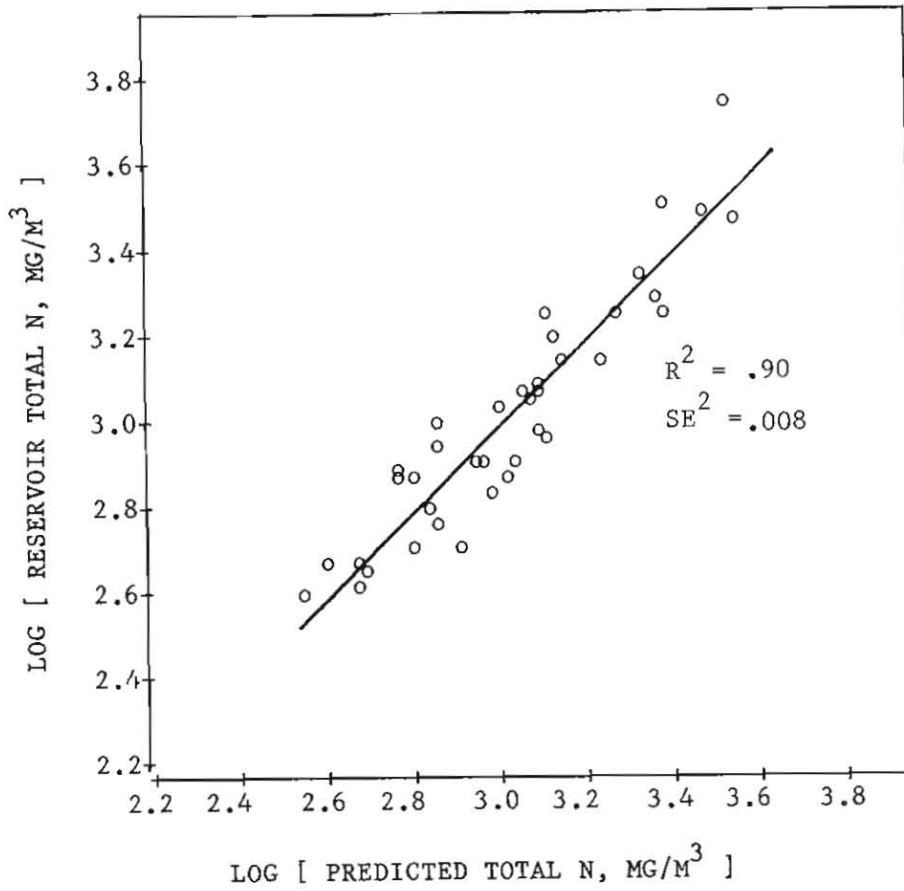
Model:
$$N = [-1 + (1 + 4 \text{ K2 Ni T})^{.5}] / (2 \text{ K2 T})$$

$$\text{K2} = .0035 \text{ Qs Fin}^{-.59} / (\text{Qs} + 17.3)$$

PART IV: PHOSPHORUS GRADIENT MODELS

Introduction

69. Results described in previous chapters indicate that between-reservoir variations in average outflow and pool nutrient concentrations can be effectively simulated by assuming second-order decay kinetics. In many reservoirs, however, estimates of average, mixed-layer nutrient concentrations are incomplete descriptors of trophic status because of spatial variations, which can occur in three general categories:

a. Variations in average water quality among tributary arms.

b. Variations between embayments and open waters within a given tributary arm.

c. Longitudinal variations along the main channel within a given tributary arm.

Variations of the first type reflect differences in morphometry, hydrology, and nutrient inflow among major tributary arms, which could be modeled separately using the methods developed in previous chapters. Variations of the second type are similar to the first, but on a smaller scale and probably beyond the scope of a simplified analysis because of the detailed information required for representation of spatial variations in morphometry, loading, and mixing. Variations of the third type reflect the cumulative effects of nutrient sedimentation and transport along a major tributary arm moving downstream toward the dam.

70. This chapter develops methods for modeling variations of the third type by assuming that longitudinal gradients reflect the net effects of three fundamental processes: advection, dispersion, and sedimentation. Other hydrodynamic factors, such as underflows or interflows, would also be expected to influence longitudinal gradient potential. Explicit modeling of these phenomena is beyond the scope of a simplified analysis, although their importance and effects would be reflected in parameter estimates and error distributions.

85

71. The simulation of advection and dispersion essentially involves a transformation of spatial and temporal scales and provides additional tests for the phosphorus sedimentation models developed in Part II. Through a velocity transformation, spatial variance observed along the length of a reservoir could be interpreted as temporal variance occurring within a given water mass, provided that local inflows and mixing are represented. Thus, simulation of spatial gradients presents a test for empirical mass balance models which is more severe, and possibly more useful, than tests based upon cross-sectional (i.e., reservoir-to-reservoir or lake-to-lake) variations in spatially averaged conditions (Reckhow and Chapra, 1983). The types of variations considered below are perhaps closer to the intended uses of empirical models in a management context, given the lack of time-series data to permit model testing in a dynamic mode (i.e., predicting responses of individual reservoirs to changes in average nutrient loading regime).

72. Two approaches are considered. A simplified method relates phosphorus gradient potential (as measured by the ratio of maximum to minimum, station-mean concentrations) to impoundment morphometric, hydrologic, and inflow characteristics. This method can be implemented with a calculator and/or graph. A more complex approach predicts phosphorus variations as a continuous profile from the inflow to the dam and requires a computer program for implementation. The development and testing of these methods are discussed below, based upon data from impoundments in which one major tributary accounts for more than two-thirds of the total nutrient and water inflow. Extension to more complex morphometries would involve separate treatment of major tributary arms and modifications to account for spatial variations in nutrient and water inflow along the length of a given tributary arm.

Simplified Gradient Analysis

73. This section develops a screening tool which can be used to distinguish reservoir arms with significant phosphorus gradient potential from those in which the predictions of a relatively simple, completely mixed model would be adequate. The method employs

dimensionless variables used in chemical reactor design (Levenspiel, 1972). The establishment of spatial gradients within a given reservoir arm can be related to two primary factors:

a. The opportunity for phosphorus retention within the impoundment, as determined by residence time, depth. inflow phosphorus concentration, and inflow phosphorus availability.

b. The relative importance of advection and dispersion as longitudinal transport processes.

The spatial distributions of inflow and loading are also potentially important, especially in reservoirs with more than one major tributary arm. The analysis below is confined to reservoirs dominated by one major tributary, although the concepts could be extended and applied piecemeal to reservoirs with more complex morphometries.

74. Maximum gradient development would occur under plug-flow conditions (no longitudinal dispersion) and high potential for phosphorus sedimentation (as controlled by inflow concentration and residence time). The following equations describe the dynamics of a second-order reaction under two idealized mixing scenarios:

$$Nr = K2 \ Pi \ T \tag{21}$$

$$\text{Plug Flow:} \quad Po/Pi = 1 \ / \ (1 + Nr) \tag{22}$$

$$\text{Mixed:} \quad Po/Pi = [-1 + (1 + 4 \ Nr)^{.5}] \ / \ (2 \ Nr) \tag{23}$$

where

Nr = dimensionless reaction rate group

$K2$ = effective second-order decay rate $(m^3/mg\text{-}yr)$

Pi = inflow phosphorus concentration (mg/m^3)

T = hydraulic residence time (years)

Po = outflow phosphorus concentration (mg/m^3)

As demonstrated in Part II, the effective decay rate is related to surface overflow rate and tributary ortho-P/total P ratio. It was also demonstrated that the completely mixed equation is a better predictor of

outflow concentration than the plug-flow equation, a result which seems contraintuitive. Regardless of mixing scenario, the solution for the Po/Pi ratio can be expressed in terms of the dimensionless reaction parameter, Nr. Figure 22 plots the Po/Pi ratio against Nr for projects with one major tributary arm. The solid line (A) depicts the solution of the completely mixed equation using the calibrated decay rate function (Equation 19). The dashed lines depict solutions of the plug-flow (B) and completely mixed (C) equations with a two-fold downward adjustment in the calibrated decay rate. Differences among the curves are indistinguishable in relation to random variations in the data for dimensionless reaction rates less than about 3, which includes more than half of the reservoirs. At higher Nr values, the curves diverge and outflow concentrations are lower for the plug-flow solution. The dashed lines envelope the observed data at higher Nr values. It seems reasonable that differences in mixing characteristics could partially account for observed Po/Pi variations between curves B and C at a given Nr value. Thus, the model calibration for the completely mixed case could be interpreted as a "compromise" between the plug-flow and completely mixed cases with an appropriate adjustment in the effective decay rate. It can also be shown that the solution for average reservoir phosphorus concentration under plug-flow conditions, derived from integrating the plug-flow equation from 0 to T and dividing by T, is indistinguishable from the solution for the completely mixed case at reasonable values of Nr. Thus, the completely mixed model for predicting reservoir-average conditions is not inconsistent with observed spatial gradients and plug-flow behavior.

75. For a given effective decay rate (typically .1 m^3/mg-yr), end-to-end variations in phosphorus concentration would be limited by the solution of the plug-flow equation and would thus depend upon the product of the effective decay rate, inflow phosphorus concentration, and residence time. Reservoirs with relatively small values of this product would have limited potential for phosphorus retention and gradient establishment, regardless of the extent of longitudinal mixing.

76. Based upon chemical reactor theory (Levenspiel, 1972), the

Figure 22

Effect of Mixing Regime on Phosphorus Outflow Predictions
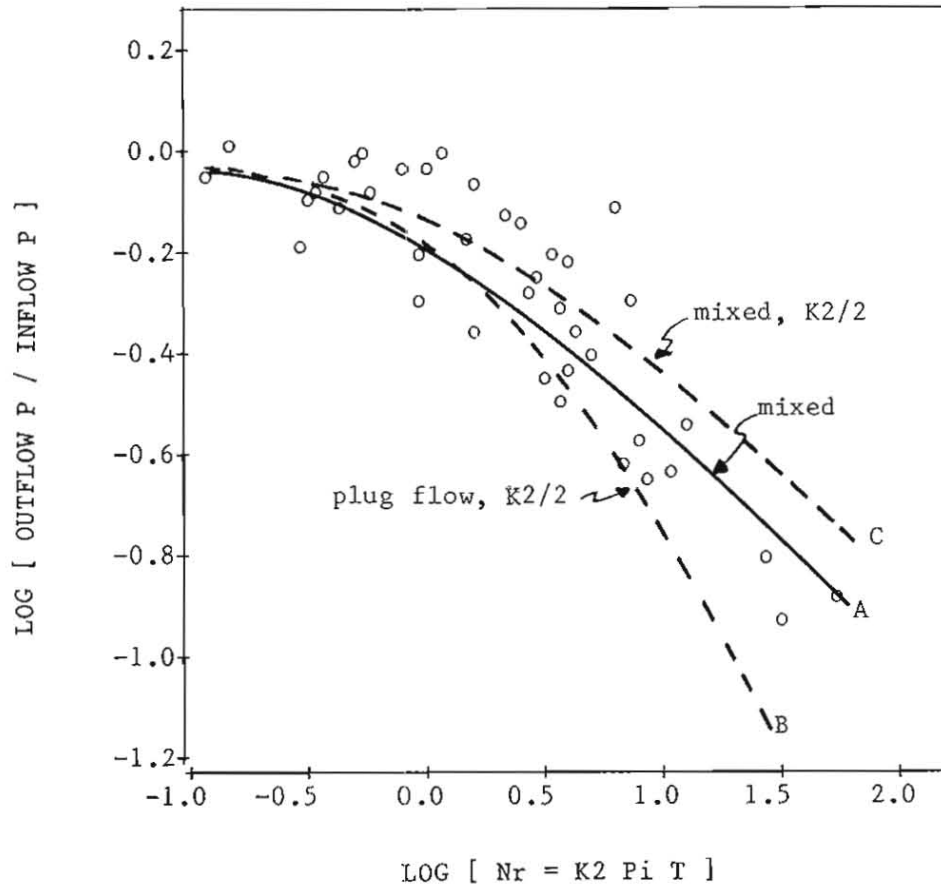
relative importance of advection vs. dispersion can be assessed using
the following dimensionless parameter:

$$Nd = D \: / \: U \: L \qquad\qquad (24)$$

$$U = L \: / \: T \qquad\qquad (25)$$

where

        Nd = dimensionless dispersion rate

        D = longitudinal dispersion coefficient (km^2/yr)

        U = nominal advective velocity (km/yr)

        L = reservoir length (km)

        T = mean hydraulic residence time (years)

At high values of Nd, dispersion dominates over advection and the system
approaches a completely mixed condition. The advective velocity
calculated above represents an idealized average; velocity would be
constant only for a uniform, completely mixed channel. To provide some
scale perspective, values of Nd less than about .1 are very close to the
plug-flow condition, while values exceeding 20 are close to the
completely mixed condition.

     77. Levenspiel (1972) presents a graphical method for assessing
the effects of back-mixing (dispersion) on the performance of chemical
reactors, assuming a second-order decay reaction and a constant cross-
sectional area. In terms of the above equations, performance is related
to the dimensionless parameters Nr and Nd. By analogy, these parameters
should also be of use for predicting reservoir phosphorus gradients.

     78. The scheme is tested below using data from 24 CE reservoirs
with one major tributary arm and EPA/NES sampling program designs which
are judged adequate for detection of longitudinal gradients, based upon
review of station maps. Ratios of station-mean phosphorus
concentrations have been calculated to reflect end-to-end variability
within each reservoir (pool stations only). Morphometric, hydrologic,
and nutrient inflow data correspond to the years of EPA/NES pool
sampling; May-September inflow concentrations and hydraulic residence
times have been used for most impoundments, according to the criteria

developed in Part II. The data set is listed in Appendix A.

79. An effective decay rate has been computed for each impoundment using the model calibrated in Part II:

$$K2 = \frac{.056 \ Qs}{Fot \ (Qs + 13.3)} \tag{26}$$

where

$K2$ = effective second-order decay rate (m^3/mg-yr)

Qs = surface overflow rate (m/yr)

Fot = tributary ortho-P/total P ratio

The remaining problem is the estimation of longitudinal dispersion coefficients. Literature reviews indicate a range of 32-3200 km^2/yr reported for horizontal eddy diffusivities in lakes by Lam and Jacquet (1976), 934-28,000 km^2/yr for longitudinal dispersion in estuaries reported by Hydroscience (1971), and 100-47,250 km^2/year for longitudinal dispersion in nontidal rivers by Fischer (1973). There are no "typical" values or established methods for predicting longitudinal dispersion coefficients in reservoirs. Chapra and Reckhow (1983) suggest use of conservative tracers to quantify dispersion coefficients for individual reservoirs, but this type of data is generally unavailable for the reservoirs studied here. Two estimation schemes are tested below. One assumes a constant coefficient for all reservoirs of 2000 km^2/year, a "reasonable" value based upon calibrations of the simulation model developed in the next section and literature ranges. Results below are independent of the particular value assumed, however, because it is removed as a scale factor in the parameter estimation process. The second approach employs a model presented by Fischer et al. (1979) for predicting longitudinal dispersion coefficients in rivers:

$$D = 11 \ U^2 W^2 / (Z \ Us) \tag{27}$$

91

$$Us = 3122 \; (S \; Z)^{.5} \qquad\qquad (28)$$

$$Se = 1.23 \times 10^{-9} \; U^2 \; Z^{-1.32} \qquad\qquad (29)$$

where

D = longitudinal dispersion coefficient (km2/yr)

W = mean width (km)

Z = mean depth (m)

Us = shear velocity (km/yr)

Se = slope of energy grade (m/km)

To estimate shear velocity and slope, Manning's equation is used with an "n" (roughness factor) value of .04. Calculated shear velocities average about 10% of the respective mean advective velocities. Fischer et al. (1979) note that this method generally gives predictions which agree with field measurements to within a factor of four and that the field measurements themselves are subject to considerable error. The above equations can be solved for the dispersion coefficient:

$$D = 100 \; U \; W^2 \; Z^{-.84} \qquad\qquad (30)$$

80.   Because it is based upon data from rivers, the applicability of Fischer's method to reservoirs is uncertain. Phosphorus profile simulations are generally more sensitive to dispersion and advection in the upper ends of reservoir pools than in the near-dam, more lacustrine areas, where the assumptions and conditions of the model are more likely to be violated. Effects of wind mixing and vertical stratification are possibly important in reservoirs, but are not explicitly accounted for in the model. Despite these potential problems, results presented below indicate that use of Fischer's method is preferable to assuming a constant dispersion rate. For the present purposes, this method appears to be generally satisfactory because of the relatively low sensitivity of the predicted phosphorus gradients to assumed dispersion coefficients in most situations. The parameter estimation procedure would also

92

adjust for any consistent bias in the model formulation.

81. When the above equations are combined, the resulting expression for dimensionless dispersion rate is:

$$Nd = D / U L = 100 \ W^2 \ Z^{-.84} \ L^{-1} \qquad (31)$$

where

Nd = dimensionless dispersion rate

L = pool length (km)

Note that the result is independent of velocity or flow. Nd is exclusively a function of morphometry and mean width is the most important determining factor. The result is consistent with the intuitive concept that the length to width ratio (L/W) should be an important factor determining the relative importance of longitudinal mixing. The importance of width may also implicitly account for average effects of wind fetch on mixing induced by surface currents. Figure 23 presents dimensionless dispersion rates for three reservoirs, ranging from an approximate plug-flow condition (Beaver. $Nd=.071$) to a completely mixed condition (Cherry Creek, $Nd=23.7$).

82. The relationship between gradient potential and the dimensionless rate groups can be represented using a model of the following form:

$$Pmax/Pmin = 1 + Nr / (1 + B1 \ Nr^{B2} \ Nd^{B3}) \qquad (32)$$

where

$Pmax$ = mean total P at upper end of reservoir pool (mg/m^3)

$Pmin$ = mean total P at lower end of reservoir pool (mg/m^3)

$B1,B2,B3$ = empirical parameters

For plug-flow conditions ($Nd = 0$), the predicted gradient equals the plug-flow solution ($1 + Nr$). As dispersion rate increases, the gradient vanishes and $Pmax/Pmin$ approaches 1.0. The interaction between Nr and Nd is consistent with a formulation presented by Levenspiel

93

Figure 23

Dimensionless Dispersion Rates
for Three CE Reservoirs

1 km

Cherry Creek
Nd = 23.7

5 km

Mosquito Creek
Nd = .36

10 km

Beaver
Nd = .071
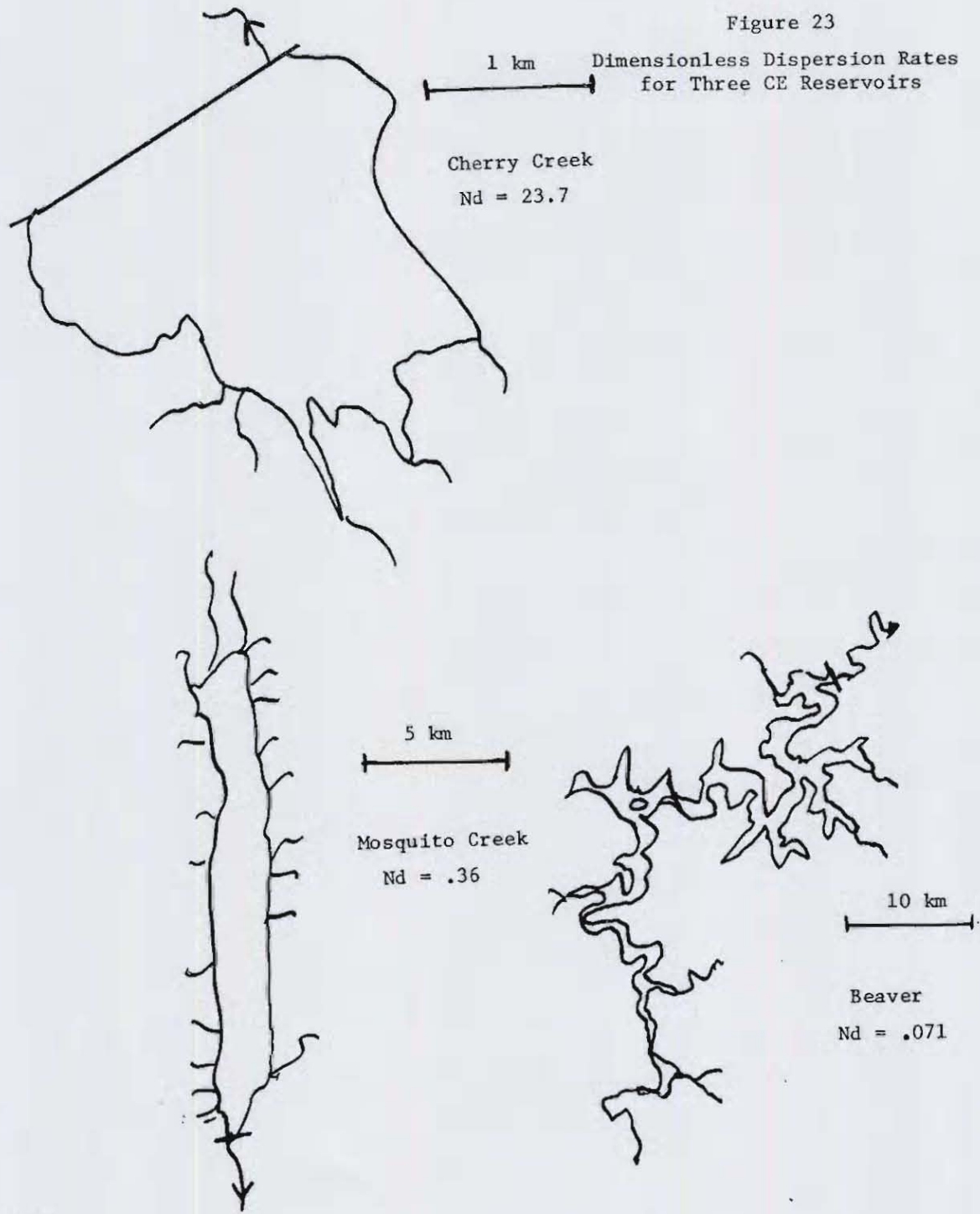
(1972) for small deviations from plug-flow and is responsible for both Nr and Nd occurring in the denominator of the above equation. Optimal parameter estimates for each dispersion assumption are listed in Table 16. The mean squared error is lower for Fischer's dispersion formulation (.012), as compared with the constant dispersion assumption (.015). Because the parameter estimates B1 and B2 are not significantly different, the best model can be expressed as:

$$Pmax/Pmin = 1 + Nr / (1 + 1.5 Nr^{.29} Nd^{.29}) \qquad (33)$$
$$(R^2 = .85, SE^2 = .012)$$

The calculated dimensionless groups used in model calibration are listed in Table 17. Observed and predicted gradients are presented in Figure 24. The parameters and error statistics exclude data from Lake Ashtabula (Code 15-237). As discussed in the previous chapter, this reservoir has essentially zero phosphorus retention capacity, possibly as a result of significant internal loading, and is not typical of other reservoirs in the data set; accordingly, the model overpredicts the gradient in this case.

83. Figure 25 is a graphical solution of the above equation depicting contours of constant gradient potential as a function of dimensionless reaction and dispersion rate groups. Maximum gradient potential exists in the upper, left-hand portion of the plot (high Nr, low Nd); minimum potential, in the lower, right-hand portion (low Nr, high Nd). The contour lines are more nearly horizontal than vertical and reflect a relative insensitivity to Nd, as compared with Nr. The locations of reservoirs used in developing the model are also indicated in Figure 25 and should be used as a guide for assessing model applicability to other reservoirs.

84. The above analysis demonstrates that phosphorus gradients can be predicted in reservoirs with relatively simple morphometry, based upon dimensionless parameters calculated from inflow phosphorus concentration, length, residence time, and surface area. The method assumes representative distribution of sampling stations and that most

Table 16

Parameter Estimates and Error Statistics of Models for Predicting
Longitudinal Phosphorus Gradients

Parameter Estimates

Dispersion Formulation	B1	B2	B3	SE^2	R^2
$D = 2000 \text{ km}^2/\text{yr}$	1.12	.45	.22	.015	.82
Fischer, et al. (1979)	1.63	.26	.32	.013	.85
Fischer, et al. (1979)	1.50	.29	.29	.012	.85

Model:

$$Pmax/Pmin = 1 + Nr / (1 + B1 \ Nr^{B2} \ Nd^{B3})$$

Pmax = maximum, station-mean phosphorus concentration (mg/m^3)

Pmin = minimum, station-mean phosphorus concentration (mg/m^3)

Nr = dimensionless reaction rate

Nd = dimensionless dispersion rate

Notes:
Based upon data from 23 reservoirs
Mean squared erors on Log_{10} scales

96

Table 17

Listing of Dimensionless Dispersion Rates, Reaction Rates,
and Phosphorus Gradients

Project*	Nd	Nr	Pmax/Pmin
03307	0.326	0.353	1.072
10003	0.091	0.143	1.202
10411	0.013	0.975	1.514
15237	0.206	5.195	1.202
16243	0.194	10.480	5.370
17241	0.453	7.007	3.162
17245	0.555	1.032	1.514
17248	0.400	1.960	1.660
17249	0.230	0.646	1.778
17256	0.350	0.823	1.349
18092	0.107	7.089	2.754
18120	0.249	0.906	2.291
19119	0.195	0.578	1.738
19122	0.080	5.614	2.630
19340	0.173	4.124	2.951
20081	5.932	3.851	1.380
20087	1.485	4.376	2.754
24011	0.071	7.493	5.248
24013	0.111	0.897	1.862
25105	3.545	3.357	2.570
25278	0.225	2.401	1.862
29108	9.213	24.323	2.754
30235	0.858	126.763	25.119
31077	0.023	1.402	1.288

* First 2 digits = CE district code
  Last 3 digits = CE reservoir code (see Appendix A)
Nd = dimensionless dispersion rate = D / U L
      using Fisher et al. (1979) dispersion model
Nr = dimensionless reaction rate = K2 Pi T
Pmax/Pmin = dimensionless phosphorus gradient
            = maximum/minimum station-mean total P

Figure 24

Observed and Predicted Phosphorus Gradients
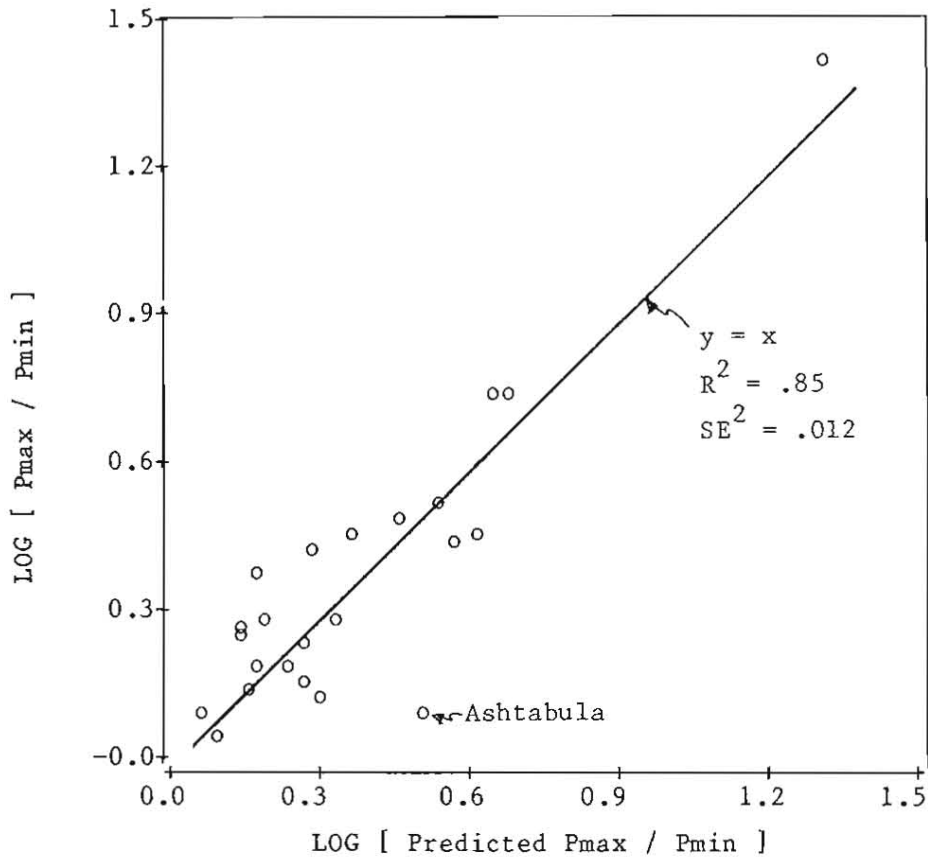
Model:

$$\log(P_{max}/P_{min}) = 1 + Nr / (1 + 1.5 \, Nr^{.29} \, Nd^{.29})$$

Nr = dimensionless reaction rate

Nd = dimensionless dispersion rate

Figure 25

Phosphorus Gradient Contours as a Function of Dimensionless
Dispersion and Reaction Rate Groups
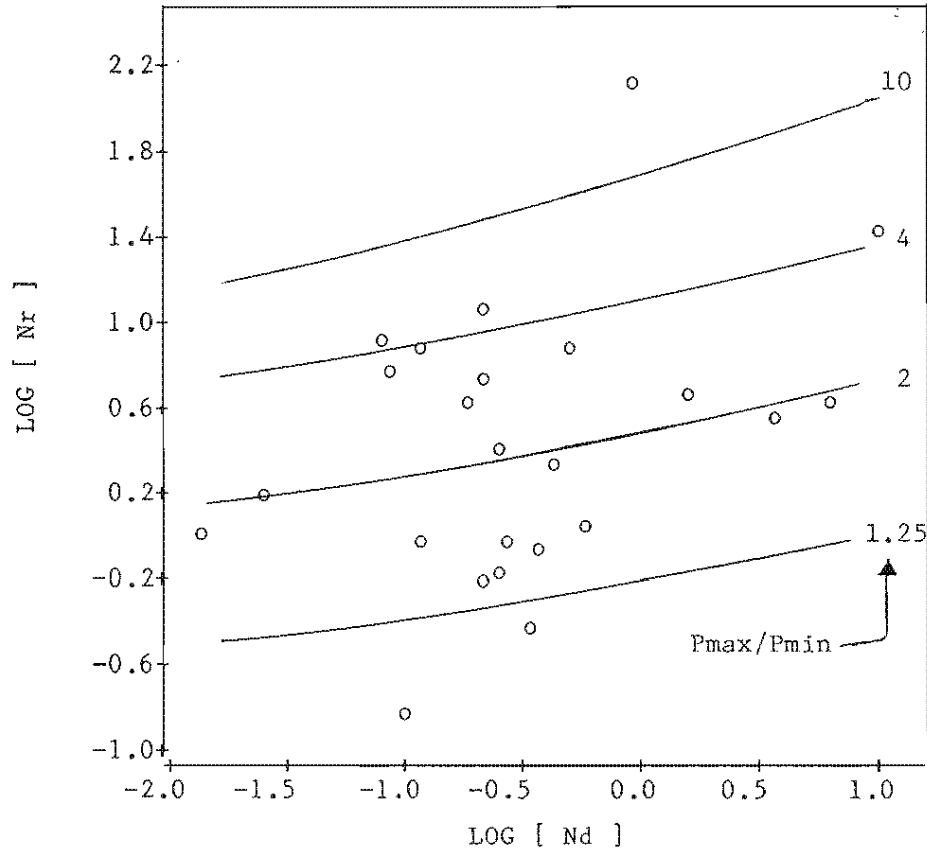
X Axis:

    Nd = dimensionless dispersion rate

$$= 100 \ W^2 \ Z^{-.84} \ L^{-1}$$

Y Axis:

    Nr = dimensionless reaction rate

      = K2 Pi T

    K2 = .056 Qs / [(Qs + 13.3) Fot]

(at least two-thirds) of the inflow and phosphorus loading occurs at the reservoir headwaters. The formulation is consistent with a basic model accounting for advection, dispersion, and second-order decay. Estimates of the ranges of surface, growing-season phosphorus concentrations likely to be encountered can be calculated for projects conforming to morphometric constraints. The ratio of maximum to minimum phosphorus concentration is less than 2 in about half of the projects studied; in these cases, simplified analyses using a completely mixed phosphorus retention model formulation would perhaps be adequate. The simulation model developed in the next section can provide more detailed indications of spatial variations, while accounting for the morphometry, inflow distribution, and loading distribution characteristic of each impoundment.

Phosphorus Gradient Simulation

85. One method of simulating spatial gradients is to divide the reservoir into a series of segments which are assumed to be completely mixed and apply a phosphorus retention model separately to each segment. Some basis for defining the segments is required, however, because of the highly nonlinear nature of many of the retention functions. For example as shown previously (Walker, 1982a), if the Vollenweider/Larsen-Mercier expression is used for each segment:

$$Ps/Psi = 1 / (1 + Tss^{.5}) \tag{34}$$

where

Ps = segment outflow phosphorus concentration (mg/m^3)

Psi = segment inflow phosphorus concentration (mg/m^3)

Tss = segment residence time (years)

the predicted reservoir outflow concentration is very sensitive to the assumed number of segments, for a given total volume and residence time, as shown in the following table of predicted reservoir outflow P to inflow P ratios:

100

Total Residence	Number of Segments of Equal Residence Time				
Time, years	1	2	3	4	5
.2	.69	.58	.50	.45	.40
.4	.61	.48	.39	.33	.29
.6	.56	.42	.33	.27	.23
.8	.53	.38	.29	.23	.19

Some a-priori basis for estimating model segmentation would be required for successful application of this approach. Appropriate segment boundaries are not always immediately obvious from a reservoir map. Another drawback is that the predicted phosphorus profile would consist of a series of step-changes in concentration which would be inconsistent with the continuous gradients typically observed. Sensitivity to assumed segmentation would be even greater for the second-order decay rate formulation developed previously.

86. Carlson et al. (1979) used a segmented model to simulate phosphorus gradients in Lake Memphremagog, a long (40-km) and narrow (mean width = 2.4 km) lake on the Quebec-Vermont border. Average observed total phosphorus concentrations range from 48 mg/m^3 at the southern inflow station to 9.2 mg/m^3 in the most northern basin. The lake was divided into a series of four completely mixed basins. Water, phosphorus, nitrogen, and chloride balances were formulated separately on each basin. Only advective transport between the basins was considered. Phosphorus sedimentation within each basin was represented as a first-order reaction. Effective sedimentation rates (1/yr), estimated from observed phosphorus concentrations, varied with basin and month over a 15-month period. Calibrated phosphorus sedimentation coefficients were much lower in the less-productive northern basins; this is qualitatively consistent with the nonlinear sedimentation kinetics described previously.

87. Another method for modeling spatial gradients suggested by Higgins and Kim (1981) employs a plug-flow hydraulic representation and

a first-order settling velocity for phosphorus:

$$Pt/Pi = \exp(-K1\ t) \qquad (35)$$

$$K1 = U1\ /\ Z \qquad (36)$$

where

Pt = P concentration at time of travel t (mg/m^3)

t = time of travel from upper end of pool (years)

$K1$ = effective, first-order sedimentation coefficient (1/yr)

Z = mean depth (m)

$U1$ = effective settling velocity = 61 m/yr (calibrated value)

This model eliminates the choice of model segments, but fails to account for effects of any back-mixing (dispersion) which may occur, particularly in near-dam areas. Based upon review of spatial variance plots for CE reservoirs, phosphorus gradients tend to be most pronounced at the upper ends of many reservoirs and to diminish as the dam is approached. Since widths, depths, and cross sections also usually increase moving downstream, advective velocities decrease moving downstream and the Higgins-Kim model would tend to overpredict spatial gradients near the dam.

88. As presented in Part II, calibration of the above model to predict outflow concentrations in CE reservoirs yields an optimal settling velocity of 8 m/yr (in place of 61 m/yr suggested by Higgins and Kim) and a mean squared error of .12 (base-10 logarithm), compared with mean squared errors of .03 for the second-order formulation with a constant decay rate and .017 for the second-order formulation with decay rate estimated as a function of overflow rate and tributary ortho-P/total P ratio. The settling velocity model does not generalize very well across reservoirs.

89. In applying the model to Cherokee Reservoir, Higgins and Kim also assumed simple rectangular morphometry (constant cross-sectional area along the length of the impoundment). This representation is unrealistic for most reservoirs. Analytical solution of the model as a function of distance becomes difficult for more realistic morphometries.

102

90. Frisk (1981) developed a simulation model for predicting longitudinal phosphorus gradients in Finnish lakes and reservoirs. The model divides the water body into a series of Continuous Stirred Tank Reactors (CSTR's) and constructs water and phosphorus balances separately on each element. Based upon work by Lappalainen (1975) and Frisk et al. (1980), the sedimentation of phosphorus within each CSTR is represented as a second-order reaction. Phosphorus variations from 30 to 10 mg/m^3 along the major axis of Lake Paijanne were simulated by dividing the water body into a series of 34 CSTR's with an effective second-order decay rate of .044 $m^3/mg-yr$ (Figure 26). Applications to other lakes employed decay rates ranging from .088 to .29 $m^3/mg-yr$. A similar kinetic scheme was also used to simulate temporal variations in phosphorus.

91. Frisk's approach accounts for longitudinal variations in morphometric and hydrologic characteristics and employs a second-order kinetic scheme which is consistent with results found above. Because of the nonlinear kinetics and effects of numeric dispersion (Fischer et al., 1979), however, predicted profiles would be sensitive to assumed segmentation and the model does not explicity account for longitudinal dispersion.

92. The gradient model described below has been developed independently of Frisk's work, but employs a similar hydraulic and kinetic scheme. The major distinctions are the explicit accounting for longitudinal dispersion and approximate control over numeric dispersion in the hydraulic network. Water and phosphorus balances are formulated for each element to account for advection, dispersion, and decay. Fine grid sizes (short segment lengths) can be selected, so that simulations provide a continuous profile which is essentially independent of assumed segmentation.

93. A Fortran computer program, Reservoir Phosphorus Gradient Model (RPGM), has been written to perform these calculations. Applications of the existing program are limited to reservoirs with one major tributary which accounts for at least two-thirds of the inflow and phosphorus loading. With additional programming effort, the code could

103

Figure 26

Simulated Phosphorus Profiles in Lake Paijanne
(Frisk, 1981)
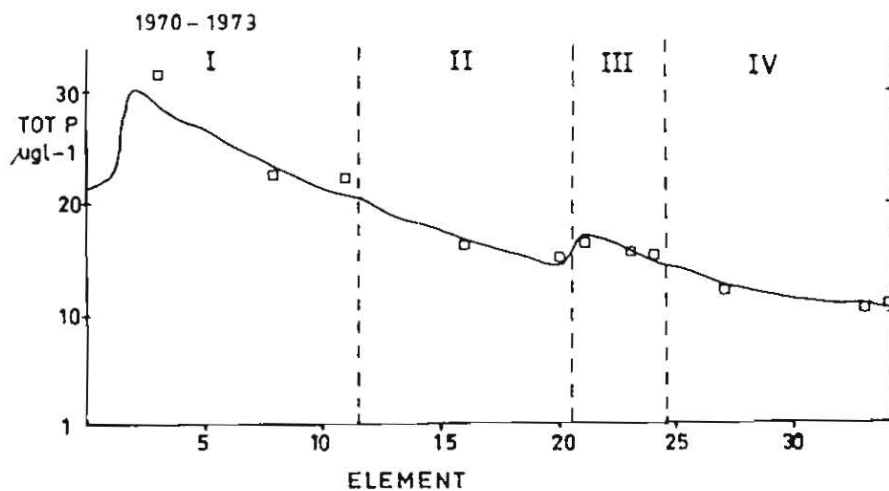
a. Calibration, average values of the years 1970–1973.
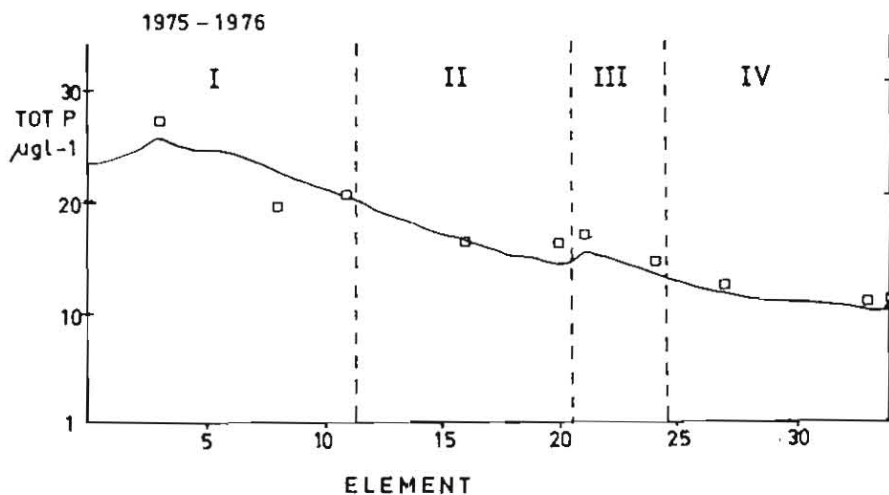
b. Verification, average values of the years 1975–1976.

Application of the steady-state total phosphorus model
to Lake Paijanne, which was divided into four subbasins
and 34 computational elements from the north to the south.
NOTE: □ = observed values, ── = calculated values.

be modified to permit simulation of more complex morphometries and/or loading distributions using the same basic modeling approach. Program structure and applications are described below. The code and a user's manual will be presented in a future report (Walker, in preparation).

94. The reservoir is divided into a series of equal-length segments (computational elements). Morphometric data are input in the form of maximum depths and top widths at specific stations, indexed by river kilometer, which increases from zero moving down the pool. The program estimates segment hydraulic cross sections, segment areas, and volumes by interpolating between the morphometric stations. After a first iteration, the input maximum depths and top widths are rescaled so that the calculated total reservoir volume and surface area match their respective input values. Because of the rescaling, the input station depths and widths can be _relative_ values (convenient for estimation from maps). This calculation scheme was designed for use with available data, including maximum station depths and relative widths estimated from EPA/NES maps. The program could be easily modified to permit direct input of cross sections in cases where this information is available.

95. Hydraulic cross sections are represented as a single-term power function in total depth:

$$A_c = W_s H / (b + 1)$$

(37)

where

A_c = hydraulic cross section (m^2)

W_s = station top width (m)

H = station maximum depth (m)

b = reservoir-specific morphometric factor

The b parameter determines the average shape of the cross section (e.g., 1 = triangular, .5 = parabolic, 0 = rectangular). The program interpolates the input widths and depths at segment boundaries and subsequently calculates segment cross sections, surface areas, and

105

volumes. After a first iteration, scaling factors for the input station widths and maximum depths are calculated from the following:

$$F_w = A_{r*} / A_r \qquad (38)$$

$$F_z = (V_{r*} / V_r) / F_w \qquad (39)$$

where

F_w = width scaling factor

A_{r*} = input total surface area of reservoir (km^2)

A_r = calculated total surface area of reservoir (km^2)

F_z = depth scaling factor

V_{r*} = input total volume of reservoir $(hm^3$ or 10^6 m3$)$

V_r = calculated total volume of reservoir (hm^3)

Before the second iteration, the program multiplies the input widths and depths by the respective scale factors, and then recalculates the segment morphometries. Because of the rescaling, final results are independent of the input parameter b.

96. Water and nutrient balances are specified by the following input variables:

QT = total outflow (million m^3/yr)
PI = inflow total P concentration (mg/m^3)
GQ = fraction of inflow volume input at upper end of pool
GW = fraction of phosphorus loading input at upper end of pool

Inflow phosphorus concentrations are corrected for evaporation, i.e., calculated as total loading divided by reservoir outflow. Specified fractions of the inflow volume and phosphorus loading are input to the first (most upstream) segment. The remainders of the inflow and loading are distributed uniformly along the length of the reservoir. Because of these distributions, applications of the existing code are limited to

106

reservoirs in which most (roughly two-thirds) of the inflow and loading occur at the upper end. Nonuniform loading and inflow distributions could be simulated with appropriate modifications in the code.

97. The program formulates water and phosphorus balances around each computational element, as outlined in Figure 27. The system consists of two sets of simultaneous equations, one for flow and one for concentration. The flow balance is solved directly. The concentration equations are in the form of a tridiagonal matrix. Because of the nonlinear term attributed to the second-order decay reaction, the equations must be solved iteratively. An initial concentration vector is guessed and the equations are solved repeatedly until a neglible change in concentration is observed from one iteration to the next. The solution of the tridiagonal matrix at each iteration is derived using the back-substitution algorithm implemented in the QUAL-II model (Roesner et al., 1977).

98. The effective second-order sedimentation coefficient is constant across segments and can be estimated as a function of overflow rate and inflow ortho-P/total P ratio using Equation 26. The error analysis conducted in Part II indicates that estimates from this equation are accurate roughly to within a factor of two, based upon predictions of outflow and reservoir-mean phosphorus concentration. In some cases, the parameter can be tuned to match observed phosphorus profiles, although Equation 26 estimates have been used exclusively in the applications discussed below.

99. Longitudinal dispersion coefficients are estimated as a function of width, depth, and velocity using a power function of the form:

$$D = C1 \; W^{C2} \; Z^{C3} \; U^{C4} \tag{40}$$

where

C1, C2, C3, C4 = input parameters

The above equation is applied to estimate a dispersion coefficient for

107

each segment. Fischer's equation (C1 = 100, C2 = 2, C3 = −.84, C4 = 1, see Equation 30) has been used exclusively in the applications discussed above. The above function provides flexibility for using alternative dispersion estimation methods and/or parameter values. To prevent use of values which are unreasonably high in relation to those found in the literature (see above), computed dispersion coefficients are restricted to a maximum value of 100,000 km^2/yr. As outlined in Figure 27, a numeric dispersion coefficient is also estimated for each model segment and subtracted from the specified longitudinal dispersion coefficient, if the latter is larger. This provides an approximate means of adjusting for the effects of numeric dispersion on the simulated profiles.

100. Once the solution to the phosphorus balance is reached, concentrations of chlorophyll, inverse transparency, and organic nitrogen are estimated using empirical relationships of the following form:

$$\log(Y_i) = A1 + A2 \log(C_i) \tag{41}$$

where

C_i = predicted total phosphorus in segment i (mg/m^3)

Y_i = predicted Chl-a, Organic n, or 1/Secchi in segment i

A1, A2 = input parameters for each component

Nominal input values for the parameters are based upon regressions of phosphorus-limited, CE reservoir data (Walker, 1982a):

Predicted Variable	Intercepts A1	Slopes A2
Chlorophyll-a	−.60	.98
1/Secchi Depth	−1.18	.66
Organic N	1.80	.52

Figure 27
RPGM Mass Balance Equations

WATER BALANCE:
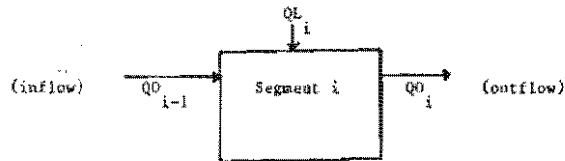
PHOSPHORUS BALANCE:
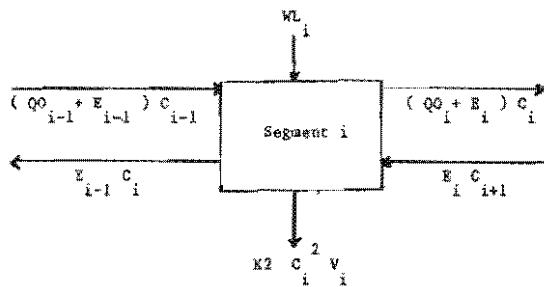
DISPERSION CALCULATIONS:

$$U_i = QO_i / AC_i \quad , \quad Z_i = V_i / AS_i \quad , \quad W_i = AC_i / Z_i$$

$$DF_i = 100 \ U_i \ W_i^2 \ Z_i^{-.84} \quad , \quad DN_i = LS \ U_i / 2$$

$$D_i = DF_i \quad \text{if} \ DF_i > DN_i \quad , \quad D_i = 0 \quad \text{if} \ DF_i <= DN_i$$

BOUNDARY CONDITIONS:

segment definitions: 0 = inflow, n = outflow

$$E_0 = E_n = 0$$

$$E_i = D_i \ AC_i / LS \qquad , \quad \text{if} \ i > 0 \ \text{and} \ i < n$$

$$C_0 = GW \ QT \ PI / QO_0 \qquad , \quad QO_0 = QT \ GQ$$

$$WL_i = QT \ PI \ (1 - GW) / n \quad , \quad QL_i = QT \ (1 - GQ) / n$$

SYMBOL DEFINITIONS:

C_i = total P concentration in segment i (mg/m^3)

E_i = eddy diffusive flow between segments i and $i+1$ (hm^3/yr)

D_i = longitudinal dispersion coefficient for segment i (km^2/yr)

DN_i = numerical dispersion coefficient for segment i (km^2/yr)

DF_i = Fischer longitudinal dispersion coefficient for segment i (km^2/yr)

QO_i = advective flow from segment i to segment $i+1$ (hm^3/yr)

QL_i = local inflow to segment i (hm^3/yr)

WL_i = local phosphorus loading to segment i (kg/yr)

U_i = net advective velocity in segment i (km/yr)

AC_i = hydraulic cross section of segment i ($m^2 \times 10^3$)

AS_i = surface area of segment i (km^2)

W_i = mean width of segment i (km)

V_i = volume of segment i (hm^3)

QT = total inflow (hm^3/yr)

$K2$ = second-order decay rate ($m^3/mg-yr$)

PI = inflow total phosphorus concentration (mg/m^3)

GQ = fraction of inflow volume entering at upper end of pool

GW = fraction of phosphorus loading entering upper end of pool

LS = segment length (km)

n = total number of segments

Z_i = mean depth of segment i (m)

In the applications discussed below, adjustments in the intercept parameters (A1) are used to calibrate the model to observed profiles. The slope parameters (A2) are held fixed at the above values. All response parameters are fixed for a given reservoir. Adjustments of the intercepts from one reservoir to another reflect variations in the biological response to total phosphorus, which would depend upon such factors as algal species, turbidity, temperature, flushing rate, etc. (see Part VI). Responses will generally be overpredicted in cases of nitrogen limitation.

101. In a final step, the program plots observed and predicted profiles of total phosphorus and the other response measurements. Observed values are provided at the end of the input file, indexed by a sampling station identifier, sample date (month), and river kilometer. Different plot symbols are used to identify sample dates or station codes. An option for linear or logarithmic scale plots is also provided.

102. Table 18 summarizes input information for five reservoirs and one natural lake which have been used to demonstrate the model. Basic morphometric characteristics and sampling station locations are shown in Figure 28. Ranges of size, trophic status, and location are represented. The group includes four CE reservoirs (Beaver, Berlin, Sakakawea, and Cumberland (alias Wolf Creek)), one TVA reservoir (Cherokee; Higgins and Kim, 1981), and Lake Memphremagog, a long, narrow natural lake on the Vermont/Quebec border which has been studied extensively (Carlson et al., 1979). End-to-end variations in surface mean total phosphorus concentrations in these impoundments range from approximately 4-fold (Cumberland) to 18-fold (Sakakawea).

103. Observed and predicted total phosphorus profiles are shown on linear scales in Figure 29. Figures 30-35 present log-scale plots and sensitivity analyses for each variable. Sensitivities to the effective sedimentation and dispersion rates are shown in the latter using the symbols defined as follows:

Table 18

Summary of Lake and Reservoir Data Used in
Phosphorus Gradient Simulations

Lake/Reservoir:	Beaver	Berlin	Sakaka-wea	Cumber-land	Cherokee	Memphre-magog
CE Project Code	24-011	16-243	30-235	19-122	TVA	Nat.Lake
Location	Arkansas	Ohio	N.Dakota	Kentucky	Tennessee	Vt/Quebec
References	A	A	A	A	B,C	D,E
Input Data:						
Length (km)	120	26	270	155	82	39
Area (km2)	119	12.3	1393	205	78	83
Volume (hm3)	2110	65.2	25062	4767	1084	1639
Outflow (hm3/yr)	2100	163.6	21854	8369	3735	880
Inflow P (mg/m3)	63	251	219	50	120	33
Inflow Ortho-P/TP	.27	.27	.07	.22	.41	.30
Headwater Flow Frac.	.72	.60	.95	.82	.90	.65
Headwater Load Frac.	.80	.75	.95	.84	.90	.84
Segment Length (km)	2	.1	3	2	1	.3
Computed Variables:						
Res. Time (yr)	1.01	.40	1.15	.57	.29	1.86
Mean Depth (m)	17.7	5.3	18.0	23.3	13.9	19.8
Calibrated Response Intercepts:						
Chl-a	-.70	-.60	-.90	-.60	-.60	-.30
Secchi	-1.20	-1.00	-1.20	-1.05	-1.18	-1.30
Organic N	1.80	1.97	1.84	1.84	1.84	-
Dimensionless Variables:						
Reaction Rate	7.5	10.5	127	5.45	3.72	5.09
Dispersion Rate	.072	.198	.870	.08	.121	.945

References: A - This Study, Walker,1982a   B - Higgins and Kim,1981
            C - USEPA,1975   D - Carlson et al.,1979
            E - Peters, 1979

Figure 28

Maps of Impoundments Used in Phosphorus Gradient Simulations

20 km

SAKAKAWEA

3 km

MEMPHREMAGOG

5 km

BEAVER

2 km

BERLIN

5 km

CHEROKEE

10 km

CUMBERLAND
(WOLF CREEK)

● Sampling Station

112
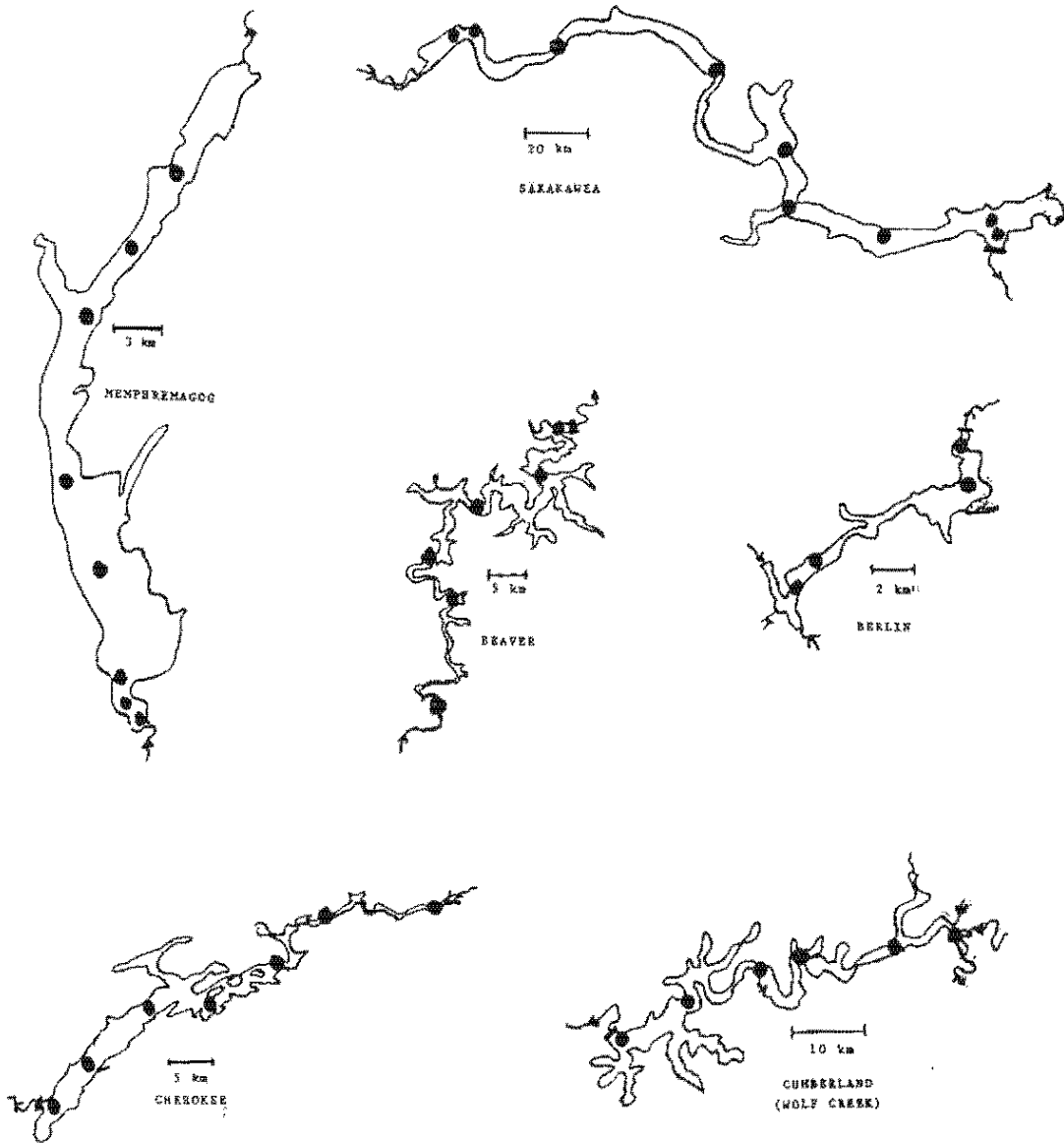
Figure 29
Observed and Predicted Longitudinal Phosphorus Profiles
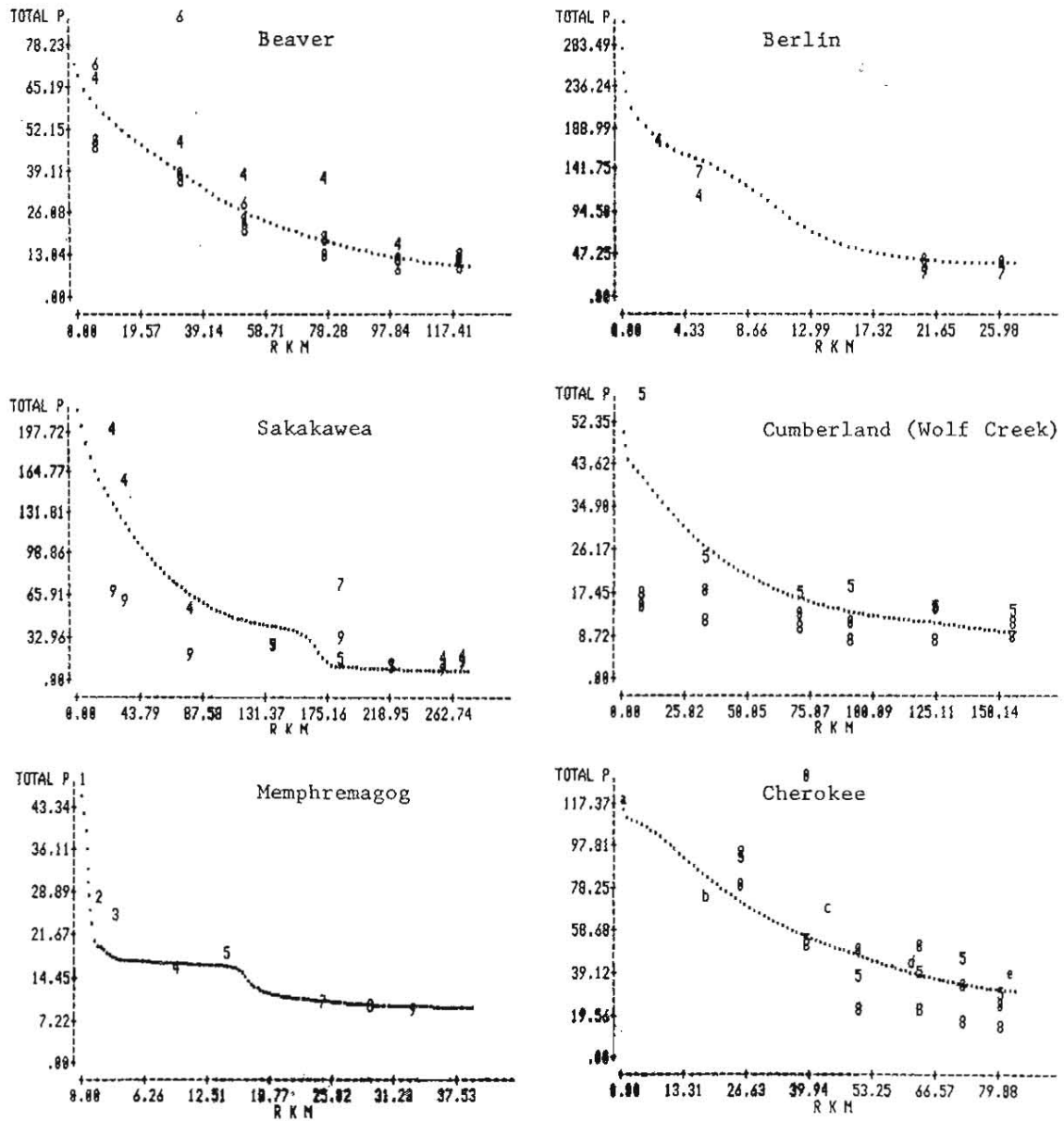
Dotted Line = Predicted Total Phosphorus Profile (mg/m^3)
Symbol = Observed Value, Last Digit of Sample Month
      = Station Mean (Memphremagog)
      = TVA Station Mean (Letters, Cherokee)

113

Figure 30

RPGM Simulations for Beaver Reservoir
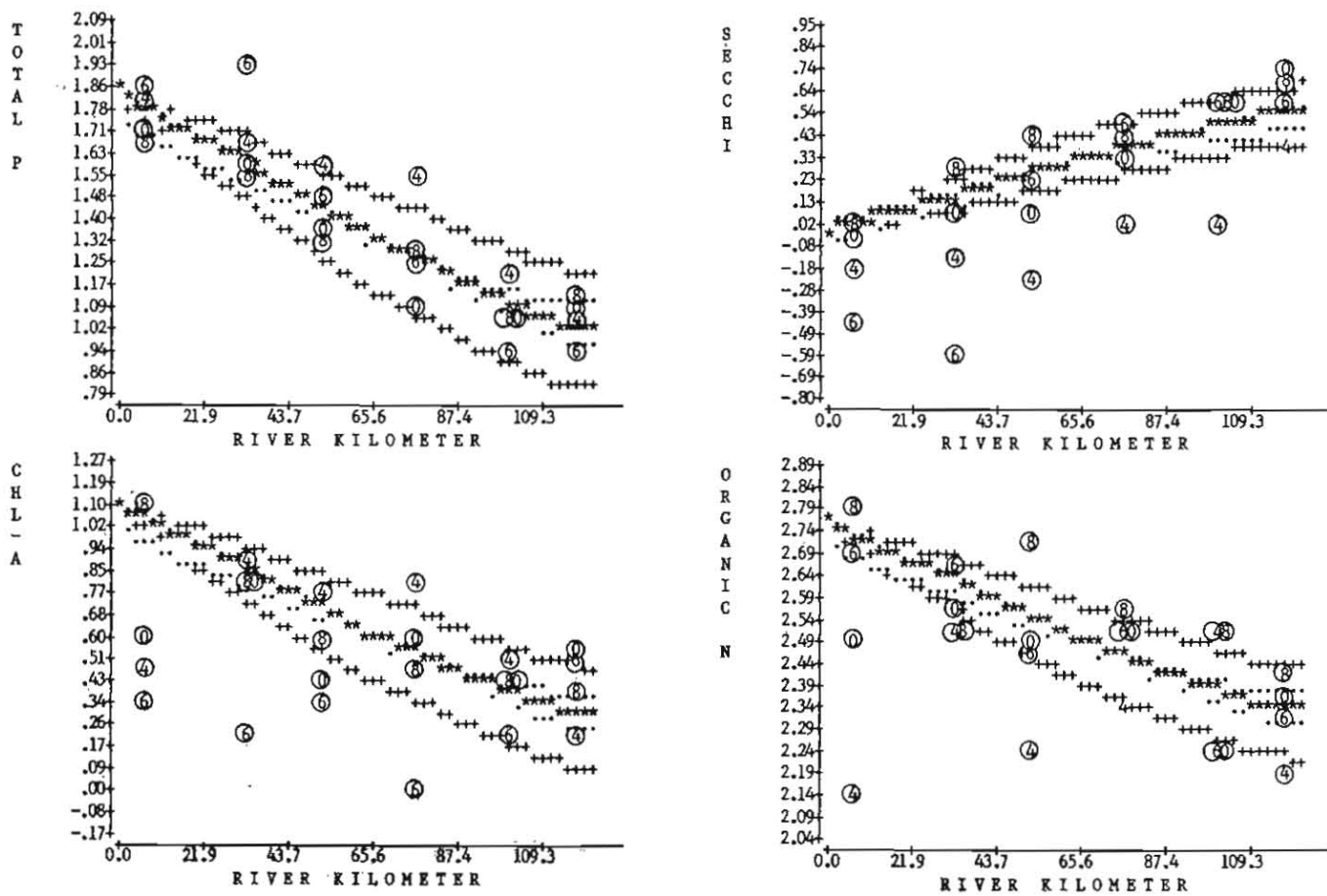
log10 scales, total p, chlorophyll-a, organic n (mg/m^3), Secchi (m)
(n)   observed station-mean concentration for sample month n (e.g., 4 = April, 0 = October)
**   simulated profile; ++ 2-fold variations in K2; ... 4-fold variations in D

114

Figure 31

RPGM Simulations for Berlin Reservoir
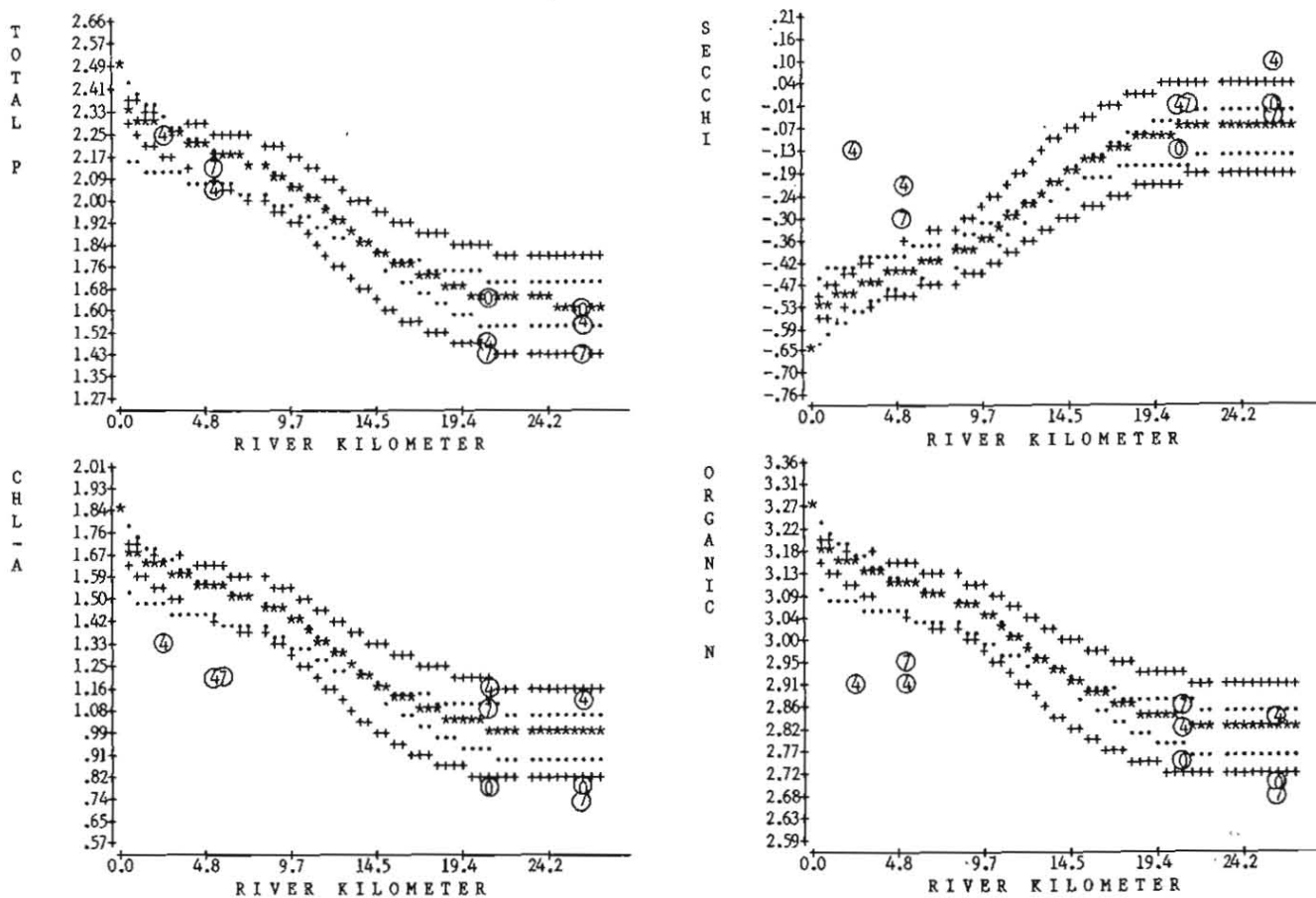
115

log10 scales, total p, chlorophyll-a, organic n (mg/m^3), Secchi (m)
ⓝ   observed station-mean concentration for sample month n (e.g., 4 = April, 0 = October)
** simulated profile; ++ 2-fold variations in K2; ... 4-fold variations in D

Figure 32

RPGM Simulations for Lake Sakakawea
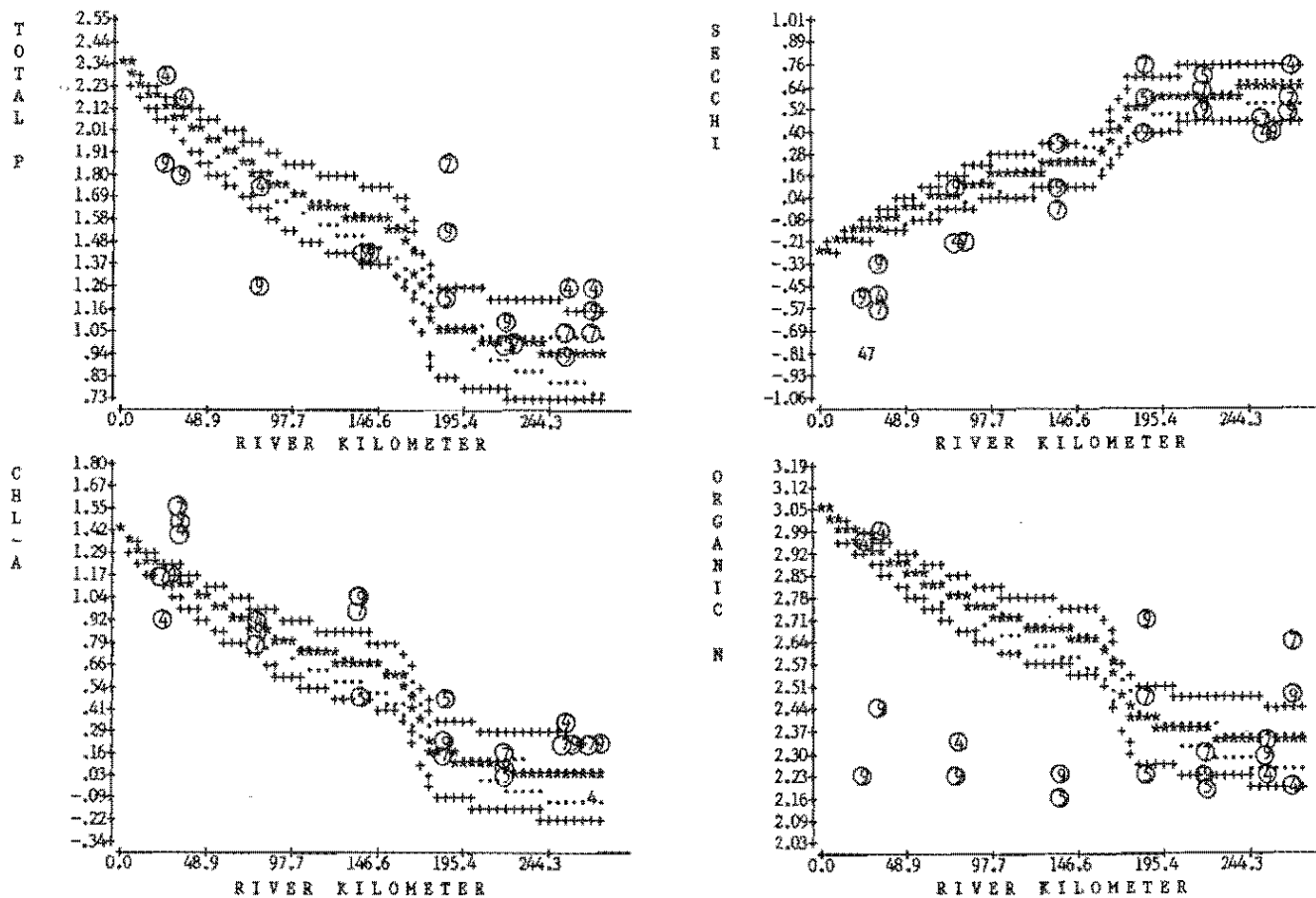
log10 scales, total p, chlorophyll-a, organic n (mg/m³), Secchi (m)
(n) observed station-mean concentration for sample month n (e.g., 4 = April, 0 = October)
** simulated profile; ++ 2-fold variations in K2; ... 4-fold variations in D

Figure 33

RPGM Simulations for Lake Cumberland (Wolf Creek)
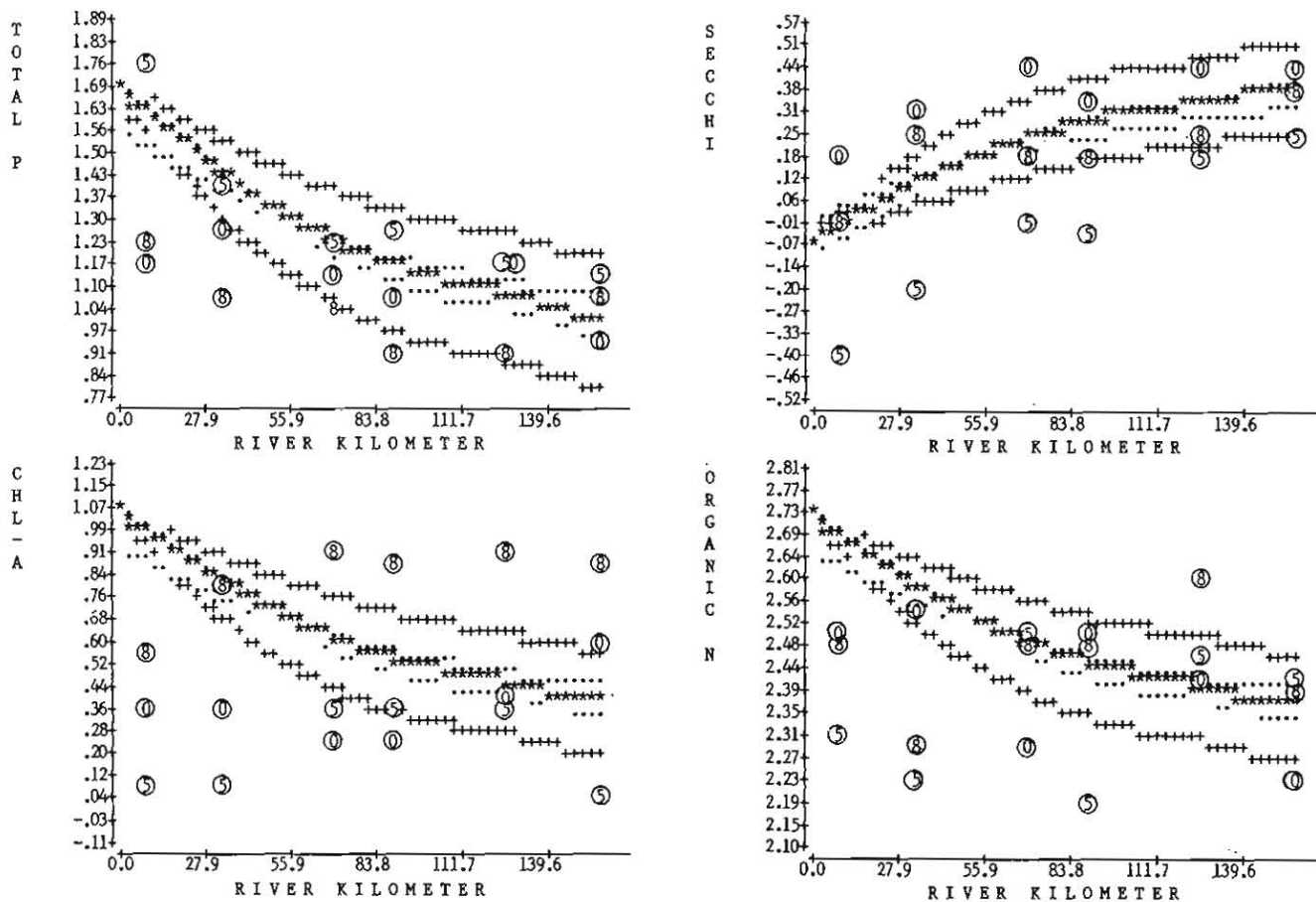
log10 scales, total p, chlorophyll-a, organic n (mg/m³), Secchi (m)
ⓝ   observed station-mean concentration for sample month n (e.g., 4 = April, 0 = October)
**   simulated profile; ++ 2-fold variations in K2; ... 4-fold variations in D

117

Figure 34

RPGM Simulations for Cherokee Reservoir

log10 scales, total p, chlorophyll-a, organic n (mg/m^3), Secchi (m)

(n)   observed station-mean concentration for sample month n (EPA/NES data) (a)   observed station-mean phosphorus, TVA data (Higgins and Kim, 1981)

**   simulated profile; ++   2-fold variations in K2; ... 4-fold variations in D
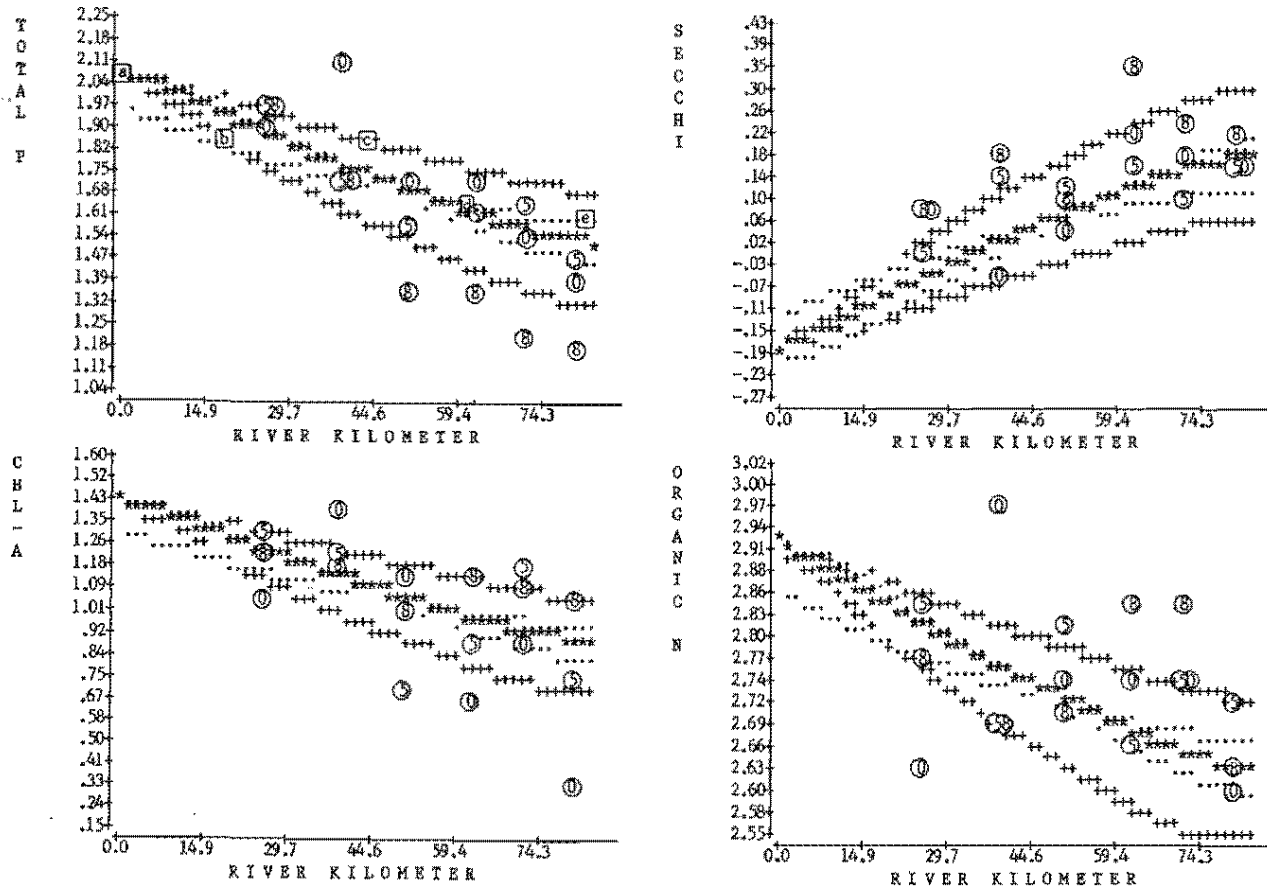
118

log10 scales, total p, chlorophyll-a, organic n (mg/m³), Secchi (m)
ⓝ   observed station-mean concentration for sample month n (EPA/NES data) ⓐ   observed station-
     mean phosphorus, TVA data (Higgins and Kim, 1981)
**   simulated profile; ++   2-fold variations in K2; ... 4-fold variations in D

Figure 35

RPGM Simulations for Lake Memphremagog

119
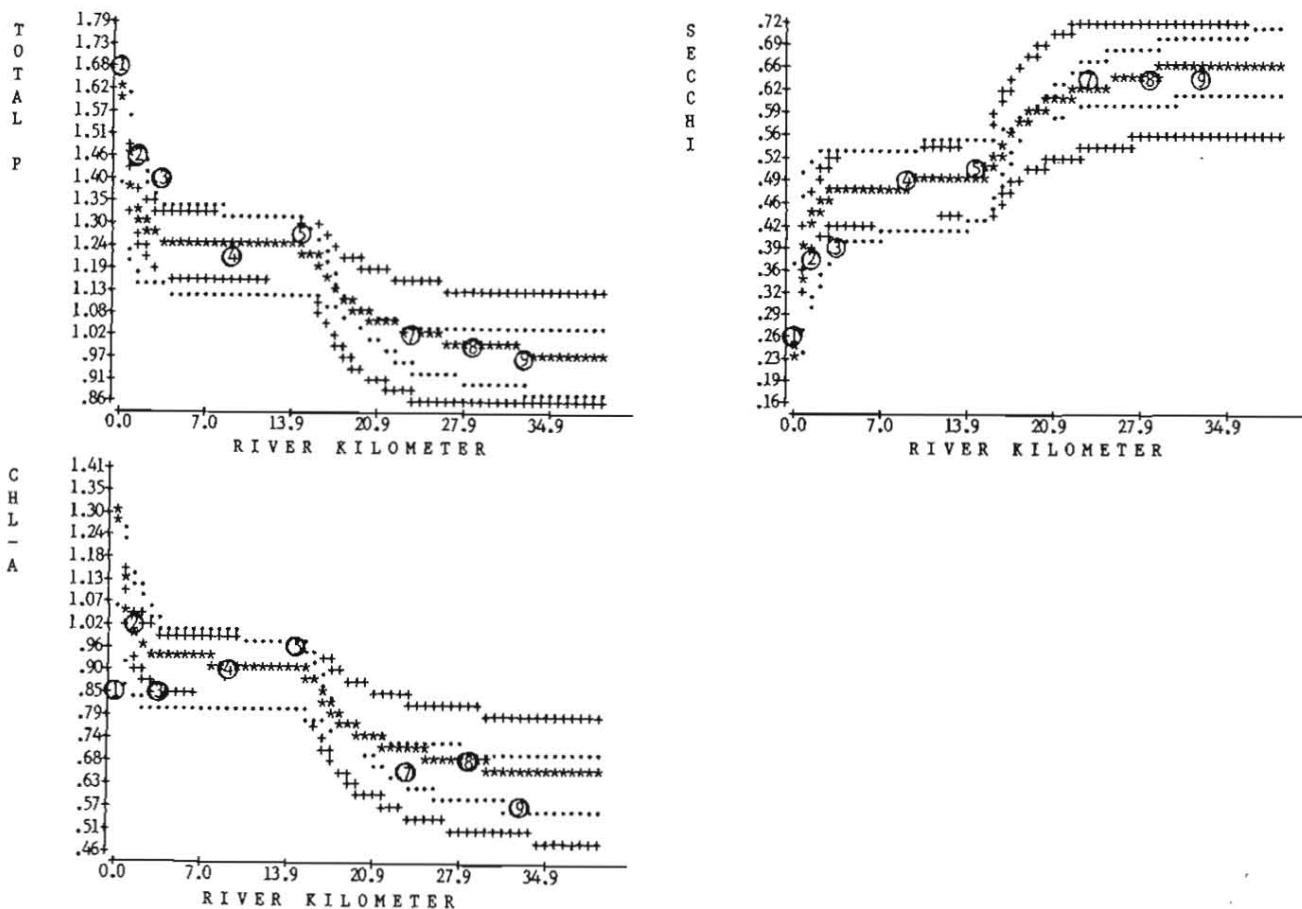
log10 scales, total p, chlorophyll-a, (mg/m³), Secchi (m)
ⓐ   observed station-mean concentration (Carlson et al., 1979)
**   simulated profile; ++   2-fold variations in K2; ... 4-fold variations in D

Symbol	Meaning
*	nominal K2 and D estimates (Equations 26 and 30)
+	effects of 2-fold variations in K2
.	effects of 4-fold variations in D

The 2-fold variations in K2 reflect the approximate confidence limits for predictions of Equation 26. The 4-fold variations in D reflect the approximate confidence limits for predictions of Equation 30, as applied to river data (Fischer et al., 1979). As discussed above, the actual confidence limits for applications of Equation 30 to reservoirs are unknown. The 4-fold variations are used primarily to indicate relative sensitivities.

104. The simulations indicate that profiles are generally more sensitive to the decay rate than to dispersion and that Equation 26 provides a reasonable estimate of the effective decay rate. Models of this type are designed to predict seasonally averaged conditions. Most of the observed data points in Figures 29-35 are individual measurements and considerable scatter is expected. Some of the scatter is associated with sample date and reflects different hydrologic regimes; for example, the observed phosphorus profile in Cumberland was consistently higher during the May sampling round. The predicted profiles do not reflect the effects of temporal variations in inflow volume and phosphorus concentration, which would be considerable in some cases.

105. Variability in phosphorus and other trophic indicators tends to be greater at the upper ends of the reservoirs in many cases; this partially reflects greater sensitivity to hydrologic variations. The applicability of the response regression equations in upper pool areas is limited because of this variability and low residence time, which imposes kinetic limitations on algal response to phosphorus. Chlorophyll and/or organic nitrogen values are overpredicted at the most upstream station in Beaver, Berlin, Cumberland, Sakakawea, and Memphremagog. Cumulative times of travel at these stations are less than .01 year. Modifications of the response equations to account for kinetic limitations might improve model simulations in these areas.

Overprediction of transparency in upper pool areas in some cases might
be partially attributed to incoming sediment loads.

106. The model overestimates the gradients in phosphorus and
other trophic indicators in Lake Cumberland (Figure 33) during the
August and October sampling rounds. A review of the data from this
reservoir indicates substantial vertical gradients in total phosphorus
during these periods. Since the August round was conducted before the
onset of anoxic conditions in the hypolimnion, higher phosphorus
concentrations in the bottom waters are probably not associated with
releases from bottom sediments. It seems likely that the vertical
gradients reflect transport of most of the inflowing phosphorus loading
as an underflow or interflow, below the averaging depth of the
observations shown in Figure 33 (0-4.5 meters). Because of this
behavior, a model of this type would tend to overpredict spatial
variations in surface water quality. The model provides a reasonable
prediction of average conditions in the lower-pool areas, however.

107. The insensitivity of the predicted phosphorus profiles to
longitudinal dispersion suggests that relatively large errors in the
dispersion coefficient estimates can be tolerated in model applications.
It does not mean, however, that the dispersion process can be ignored.
Figure 36 shows observed and predicted phosphorus profiles for Lake
Memphremagog for two cases: one using Fischer's dispersion formula, the
the other assuming zero dispersion. Some finite dispersion remains in
the latter case because of the effects of numeric dispersion associated
with model segmentation. Because of the reduction in longitudinal
mixing, lowering the dispersion coefficient generally causes an increase
in the simulated profile in the upper pool areas and a decrease in the
lower pool areas. Including dispersion obviously provides a better
simulation of the observed station means in Lake Memphremagog. In most
applications, dispersion sensitivity tends to be greatest in upper pool
areas, where conditions tend to be more variable because of the factors
discussed above. Despite the fact that Fischer's dispersion equation is
not based upon reservoir data, simulations indicate that it provides a
reasonable predictive tool for this application. Direct verification

121

Figure 36

Sensitivity of Lake Memphremagog Phosphorus Simulation
to Longitudinal Dispersion
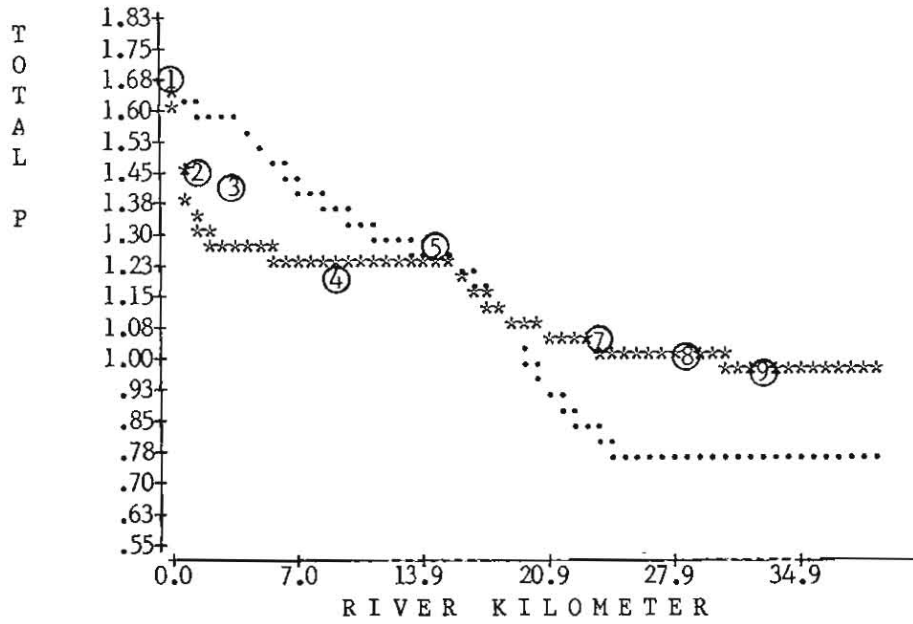
log10 scales, total p in mg/m^3
ⓝ observed station-mean concentration (Carlson et al., 1979)
*** dispersion coefficient estimated from Fischer's equation
... no longitudinal dispersion

122

based upon conservative tracer data would provide additional insights.

108. In summary, RPGM is a potentially useful tool for estimating the levels and gradients in phosphorus and related trophic state indicators in reservoirs. The model is obviously an incomplete representation of reservoir hydrodynamics, since it does not directly account for vertical stratification, underflows, interflows, etc. Much more elaborate models and more exhaustive data bases would be required for direct simulation of these processes and their influences on phosphorus dynamics.

109. Simulations tend to be weakest at stations nearest the reservoir inflow, where sensitivity to hydrologic variations, hydrodynamic factors, longitudinal dispersion, and potential kinetic limitations on algal growth tend to be most important. Potential errors and variability in the inflow volumes and concentrations limit testing and applications of the model. A major advantage of the model is that it can be applied with relatively limited data and could be of use in sampling program design. The relationships developed above provide reasonably reliable, a-priori estimates for the decay and dispersion rate parameters. These estimates can be refined by direct tuning to field data. If extensive tuning is required, a need for separate calibration and testing data sets arises. The fact that spatial gradients can be simulated using the formulation and parameter estimates derived from the cross-sectional analysis of phosphorus retention models (Part II) is additional support for the validity of the phosphorus sedimentation model. The possiblity of using inflow "available phosphorus" concentrations (model 19 in Table 2) in gradient simulations should be explored.

110. While somewhat more complex than traditional empirical modeling schemes, RPGM should still be considered a "black-box" approach, although the term "black-channel" is perhaps more descriptive. A key aspect of the model is the representation of phosphorus dynamics using three fundamental mechanisms: advection, dispersion, and second-order decay. With these assumptions, the model could be upgraded to permit simulation of more complex morphometries, including multiple arms

123

and embayments and arbitrary spatial distributions of inflow and loading. The possibility of adapting this type of model for time-variable simulations (Frisk, 1981) should also be considered, but would require additional data and testing.

PART V: HYPOLIMNETIC OXYGEN DEPLETION

Introduction

111. This section describes the development and analysis of a data set relating hypolimnetic oxygen depletion (HOD) rate to other measures of reservoir trophic status and morphometry. Uniform data screening criteria and reduction procedures are employed to develop a data set for assessing near-dam oxygen depletion rates in 37 CE reservoirs. Within-reservoir variations in oxygen depletion rates are also studied using data from 46 stations located in 12 reservoirs. Relatively intensive data from two reservoirs (Eau Galle and De Gray) studied under the Environmental and Water Quality Operational Studies (EWQOS) program are used for for independent model testing. The applicabilities of the models to estimating oxygen depletion rates in reservoir discharges are assessed using an independent data base from TVA reservoirs provided by Higgins (1982).

112. Results indicate that the areal HOD rate is correlated with epilimnetic chlorophyll-a concentrations and other surface-water measures of trophic status, including total phosphorus, transparency, and organic nitrogen. Over the range of conditions examined, no temperature or morphometric dependence of the areal depletion rate is indicated, contrary to previous studies of data from natural lakes (Cornett and Rigler, 1979; Walker, 1979; Charlton, 1980). Since areal HOD rates are apparently independent of morphometry, volumetric HOD rates (of more direct concern to water quality management) are inversely related to mean hypolimnetic depth.

113. Comparisons with lake data derived from the literature indicate that at a given chlorophyll-a level, reservoir oxygen depletion rates average 41% higher than lake depletion rates. Possible reasons for this difference are discussed in relation to effects of spatial variations in chlorophyll-a concentrations within reservoirs and regional factors responsible for differences in allochthonous oxygen demands. About half of the difference between the average lake and

reservoir responses can be explained if near-dam oxygen depletion rates are related to area-weighted, reservoir-mean chlorophyll, rather than near-dam, station-mean values. Another half can explained by possible effects of outlet level in reservoirs, for a given chlorophyll-a concentration and hypolimnetic depth. oxygen depletion rates in reservoirs with exclusively hypolimnetic discharges average about 20% higher than depletion rates in reservoirs with other modes of discharge, although the difference is barely statistically significant. The average chlorophyll/areal HOD relationship in reservoirs with surface or mixed outlet modes is apparently similar to that found in natural lakes.

114. Reservoir metalimnetic oxygen depletion rates are calculated and related to hypolimnetic depletion rates and morphometry. Results indicate that the ratio of metalimnetic to hypolimnetic depletion rate increases with mean hypolimnetic depth. Within-reservoir variations in volumetric HOD rates are shown to be significant in many reservoirs, but generally less strong than variations predicted using models calibrated for predicting between-reservoir, near-dam variations. This lower sensitivity may be attributed to effects of longitudinal mixing within reservoir hypolimnia.

Data Set Development

115. Compared with the simple averaging schemes used for chlorophyll and other trophic state indicators, the calculation of hypolimnetic oxygen depletion (HOD) rates is a relatively complex procedure involving the following steps:

a. Selection and screening of oxygen and temperature profile data.

b. Estimation of thermocline level.

c. Specification of elevation/area/capacity relationships.

d. Volume-weighting of oxygen concentrations below the thermocline on each sampling date.

e. Calculation of depletion rates.

126

The reliability of a calculated HOD value for a given reservoir reflects the accuracy of the monitoring and morphometric information as well as the validity and consistency of the calculation procedure, as described below.

116. A staged screening procedure has been employed to extract oxygen and temperature profile from the CE water quality data base. The first stage involved creation of a subfile containing oxygen and temperature measurements from pool monitoring stations located in reservoirs for which surface total phosphorus data were also available. For a given station and year, the adequacy of data for HOD calculations has been assessed based upon the availability of at least two vertical profiles with the following attributes:

a. Reasonable top-to-bottom distribution of samples.

b. Vertical stratification, defined as a top-to-bottom temperature difference of at least 4 degrees C.

c. Mean hypolimnetic oxygen concentrations in excess of 2 mg/liter.

The first constraint provides adequate data for spatial weighting within the hypolimnion on each sampling date. The second is based upon the concept that HOD is valid as a measure of productivity only in waterbodies which are vertically stratified. The third is designed to minimize the negative bias which would be introduced into calculated HOD rates under oxygen-limited conditions.

117. Displays of oxygen and temperature vs. elevation for each station-year have been used as aids in data screening and estimation of thermocline levels. For each date, sample elevations have been estimated from reported depths and reservoir surface elevations interpolated from month-end values in the hydrologic data file. Thermocline levels have been defined based upon the criteria suggested by Cornett and Rigler (1979). As shown in Figure 37, the upper extent of the hypolimnion has been defined at the intersection of one line tangent to the region of maximum temperature gradient (thermocline) and another line tangent to the bottom of profile. A corresponding

127

Figure 37

Thermocline Definitions
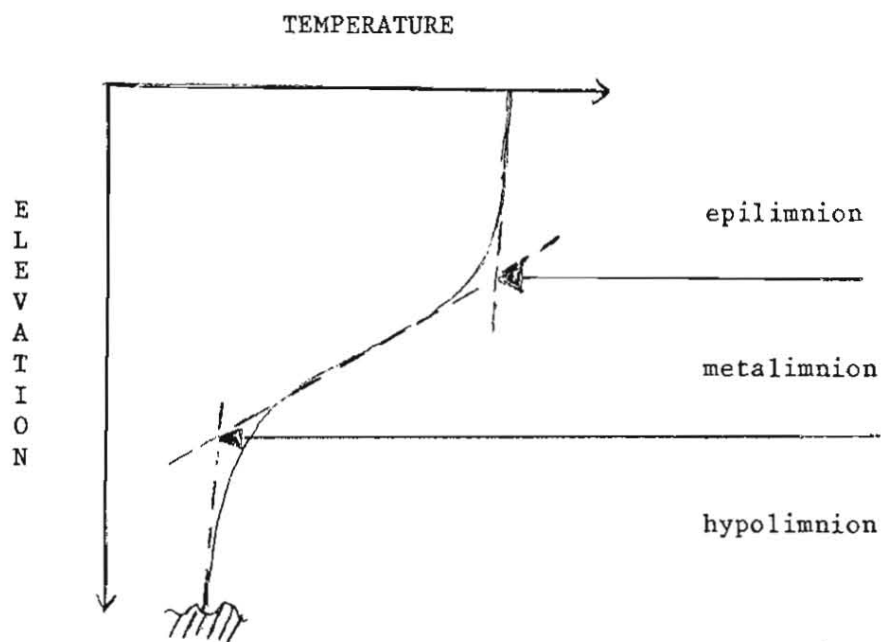
procedure has been used to define the upper extent of the metalimnion, the site of significant oxygen depletion in some reservoirs. Fixed hypolimnetic and metalimnetic elevations have been estimated for each station-year based upon the last vertical profile used in HOD calculations. The possibility of modifying the calculation procedure to account for thermocline migration is suggested as a topic for future research. While some subjectivity still remains in the estimation procedure, the sensitivities of calculated HOD values to assumed thermocline levels are generally small in relation to other sources of error introduced in model testing, including sampling variability in mean chlorophyll estimates and inherent model error.

118. The following procedure has been used to estimate the volume-averaged concentration of oxygen in the hypolimnion on each sampling date:

a. Interpolate the observed oxygen profile at a uniform depth interval from the bottom of the reservoir to the top of the hypolimnion, with the depth interval selected to give about 25 interpolated values.

b. Calculate the surface area of the reservoir at each interpolated elevation using the morphometric polynomials developed previously (Walker, 1982a).

c. Calculate the hypolimnetic-average concentration as the area-weighted average at the interpolated elevations.

Between any two sample dates, oxygen depletion rates have been calculated from:

$$HOD_v = (O_1 - O_2)/(t_2 - t_1) \tag{42}$$

$$HOD_a = HOD_v Z_h \tag{43}$$

$$Z_h = V_h / A_h \tag{44}$$

where

HOD_v = volumetric hypolimnetic oxygen depletion rate (mg/m^3-day)

HOD_a = areal hypolimnetic oxygen depletion rate (mg-/m^2-day)

O_i = average oxygen concentration on day t_i (mg/m^3)

Z_h = mean depth below elevation E_h (m)

E_h = elevation at upper boundary of hypolimnion (m)

V_h = volume below elevation E_h (hm^3)

A_h = surface area at elevation E_h (km^2)

For station-years with more than two profiles conforming to the above screening criteria, average depletion rates have been calculated using the first and last sample dates.

119. The above procedure has been repeated for each of two upper boundaries: HOD rates are calculated to the upper boundary of the hypolimnion and total oxygen depletion (TOD) rates are calculated to the upper boundary of the metalimnion. Estimates of average metalimnetic oxygen depletion (MOD) rates are derived by difference:

$$V_m = V_t - V_h \tag{45}$$

$$MOD_v = (TOD_a A_t - HOD_a A_h) / V_m \tag{46}$$

where

V_m = metalimnetic volume (hm^3)

V_t = volume below elevation E_t (hm^3)

E_t = elevation of upper boundary of metalimnion (m)

MOD_v = volumetric metalimnetic oxygen depletion rate (mg/m^3-day)

130

$$TOD_a = \text{areal depletion rate below elevation } E_t \quad (\text{mg/m}^2\text{-day})$$

$$A_t = \text{surface area at elevation } E_t \quad (\text{km}^2)$$

Average hypolimnetic temperatures have been estimated using the above interpolation and area-weighting procedure. To characterize vertical stratification, maximum temperature gradients (deg C/m) and total top-to-bottom temperature differences have been derived from interpolated temperature profiles.

120. In reservoirs with relatively high transparencies, photosynthesis in or below the thermocline can bias calculated oxygen depletion rates. A local maximum in the oxygen profile is indicative of this phenomenon, particularly in the metalimnion. It is relatively rare in these reservoirs, based upon the fact that a metalimnetic maximum was observed in only 1 out of 37 cases. This reservoir (Dale Hollow, Code 19-343) has the highest transparency (6.4 meters) in the data set. In this case, the total depletion rate has been calculated using oxygen concentrations which are restricted to values less than saturation.

121. Because of the availability of chlorophyll and nutrient loading estimates, development of an HOD data set has focused initially on projects sampled by the EPA National Eutrophication Survey (EPA/NES). The bimonthly sampling design employed by the EPA/NES was inadequate as a basis for HOD calculations in some projects because sample rounds were spaced too far apart to provide at least two profiles under both stratified and oxic conditions, except in relatively unproductive and/or deep reservoirs. Data from other agencies have been used to supplement the EPA/NES profiles and to improve the representation of eutrophic impoundments in the model testing data set.

122. The data set used for HOD model testing is listed in Appendix A. Corresponding water quality, morphometirc, and hydrologic information have been derived from previous data summaries (Walker, 1981, 1982a). Water quality data summaries include both near-dam, station-mean and area-weighted, reservoir-mean values. The development of a data set for testing within-reservoir variations in oxygen depletion is discussed separately below.

131

123. To provide a basis for lake/reservoir comparisons, HOD data from 34 natural lakes have been compiled from previous studies (Walker, 1979, 1982c; Norvell and Frink, 1975; Lasenby, 1975; Rast, 1978). The original oxygen and temperature profile data used in calculating lake HOD rates were available for 10 Vermont lakes (Walker, 1982c) and 7 Connecticut lakes (Norvell and Frink, 1975). These cases have been reviewed to ensure that they are consistent with the screening criteria and calculation procedures used in developing the reservoir data set. Screening of the other lake data has not been possible because raw data were not readily available.

124. To permit use of all lake data in residuals analysis, missing values for hypolimnetic temperature and mean hypolimnetic depth have been estimated from the following regression equations derived from the remaining natural lakes:

$$T_h = 11.9 + .40 \ Z - .34 \ Z_x \qquad (R^2 = .70, \ SE^2 = 1.8) \qquad (47)$$

$$Z_h = -4.0 + .31 \ Z + .33 \ Z_x \qquad (R^2 = .87, \ SE^2 = .87) \qquad (48)$$

where

T_h = mean hypolimnetic temperature (deg C)

Z = mean lake depth (m)

Z_x = maximum lake depth (m)

Temperatures estimated from the above equation have been restricted to values greater than 4 degrees C. The range of latitudes in the lake data set (approximately 41-46 degrees N) is insufficient to identify regional effects on hypolimnetic temperatures. Table 19 presents a statistical summary of the lake and reservoir data analyzed below.

Chlorophyll/Areal HOD Relationship

125. Areal HOD rate was originally proposed as a measure of lake primary productivity by Hutchinson (1938). Of the surface water quality

132

Table 19

Statistical Summary of Lake and Reservoir Data Used in Oxygen Depletion Studies

Variable	Mean	Std. Dev.	Minimum	Maximum
------------------ Natural Lakes (n = 34) * ----------------------				
Mean Depth (m)	12.2	6.8	4.6	33.0
Maximum Depth (m)	30.0	18.3	11.3	76.0
Hypol. Mean Depth (m)	9.7	8.1	2.0	29.6
Hypol. Temperature (deg-C)	7.6	2.6	4.0	12.0
Chlorophyll-a (mg/m^3)	5.3	6.9	0.8	31.0
Areal HOD Rate (mg/m^2-day)	434	267	130	1280
------------------ CE Reservoirs (n = 37) ----------------------				
Mean Depth (m)	13.4	6.3	3.4	35.0
Maximum Depth (m)	41.2	20.1	10.7	101.2
Summer Hyd. Res. Time (yrs)	0.8	0.8	0.1	3.8
Max. Temp. Difference (deg-C)	13.5	3.4	5.0	18.0
Max. Temp. Gradient (deg-C/m)	1.2	0.6	0.3	2.3
Hypol. Temperature (deg-C)	11.9	2.1	7.0	15.0
Chlorophyll-a (mg/m^3)	4.9	3.2	1.4	15.3
Hypol. Max. Depth (m)	25.0	15.4	5.5	82.3
Hypol. Mean Depth (m)	8.2	5.3	2.9	30.4
Hypol. Surface Area (km^2)	36.5	91.6	1.2	553
Areal HOD Rate (mg/m^2-day)	625	219	265	1267
Metal. Max. Depth (m)	33.7	18.1	8.5	94.5
Metal. Mean Depth (m)	11.1	6.0	4.0	34.8
Metal. Surface Area (km^2)	65.9	158	2.3	964
Areal TOD Rate (mg/m^2-day)	783	278	334	1397
Vol. MOD Rate (mg/m^3-day)	86	61	21	286

* Excludes 4 lakes with mean hypolimnetic depths less than
  2 meters not used in regressions.

133

data available for characterizing trophic status (chlorophyll-a, total phosphorus, organic nitrogen, and transparency), chlorophyll-a is the most direct measure of algal standing crop and productivity. Figure 38 shows the relationship of areal HOD rate and chlorophyll-a on logarithmic scales, using different symbols to distinguish natural lakes from reservoirs. In order to conform to the morphometric limits of the reservoir data set and thus permit comparisons of lake and reservoir responses, data from four lakes with mean hypolimnetic depths less than 2 meters have been excluded; conditions in these lakes are examined separately below. The relationships in Figure 38 are represented by the following regression equation:

$$\log(\text{HODa}) = 2.34 + .45 \log(\text{Bs}) + .15 \text{ type} \qquad (49)$$
$$(R^2 = .73, \ SE^2 = .013)$$

where

Bs = station-mean chlorophyll-a (mg/m^3)

type = 0 for lakes, 1 for reservoirs

The above model is essentially an analysis of covariance which indicates that, at a given chlorophyll-a level, reservoir HOD rates average .15 log units (41%) higher than lake HOD rates. Both the chlorophyll and type terms are significant at the 95% confidence level. An interaction term (type x chlorophyll-a) has also been investigated but found insignificant; this indicates that there is no apparent effect of impoundment type on the HOD/chlorophyll slope. Additional terms, including mean depth, mean hypolimnetic depth, hypolimnetic temperature, and their respective interactions with impoundment type, have also been tested but found insignificant. The above equation is consistent with Hutchinson's original model and is the best summary of the combined lake and reservoir data set. Interpretation of the apparent lake-reservoir differences is difficult, however, because of the complicating factors discussed below.

126. Figure 39 plots the residuals from the above model as a function of mean hypolimnetic depth, identifying the four excluded lakes

Figure 38

Areal HOD Rate vs. Chlorophyll-a

reservoirs
$y_2 = 2.49 + .45 x$
$R^2 = .65$, $SE^2 = .0076$

lakes
$y_2 = 2.34 + .45 x$
$R^2 = .66$, $SE^2 = .020$

LOG [HODa, MG/M^2-DAY]

LOG [CHLOROPHYLL-A, MG/M^3]
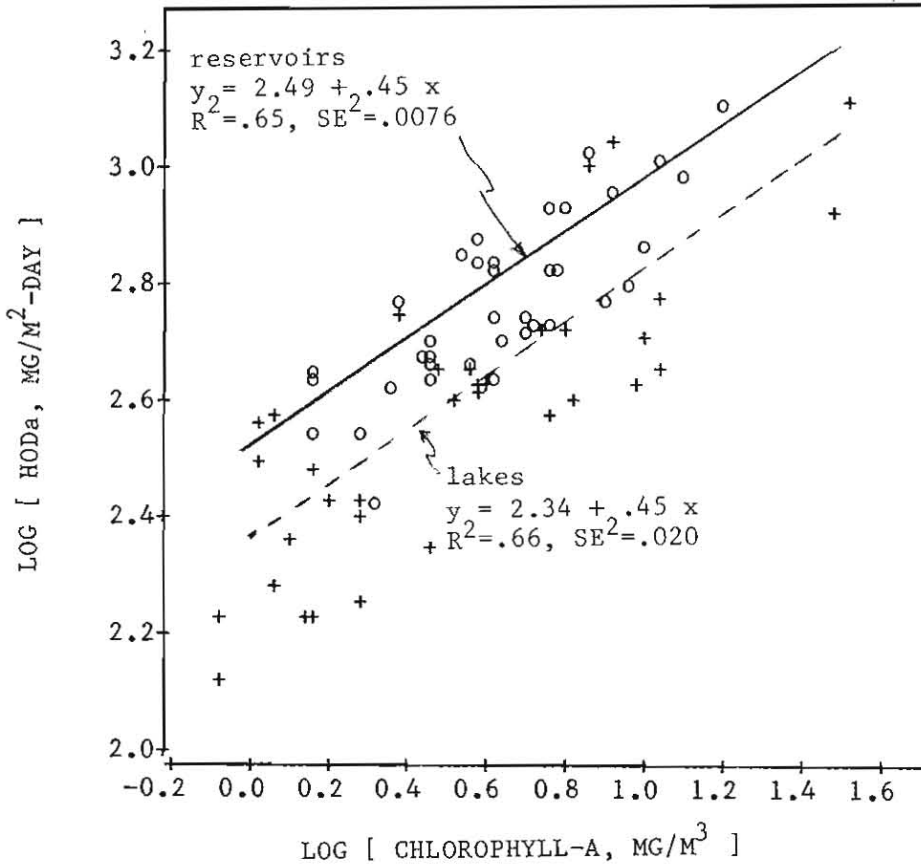
Symbols:

o = CE Reservoir
+ = Natural Lake, Zh > 2 m

Figure 39

HOD Model Residuals vs. Mean Hypolimnetic Depth
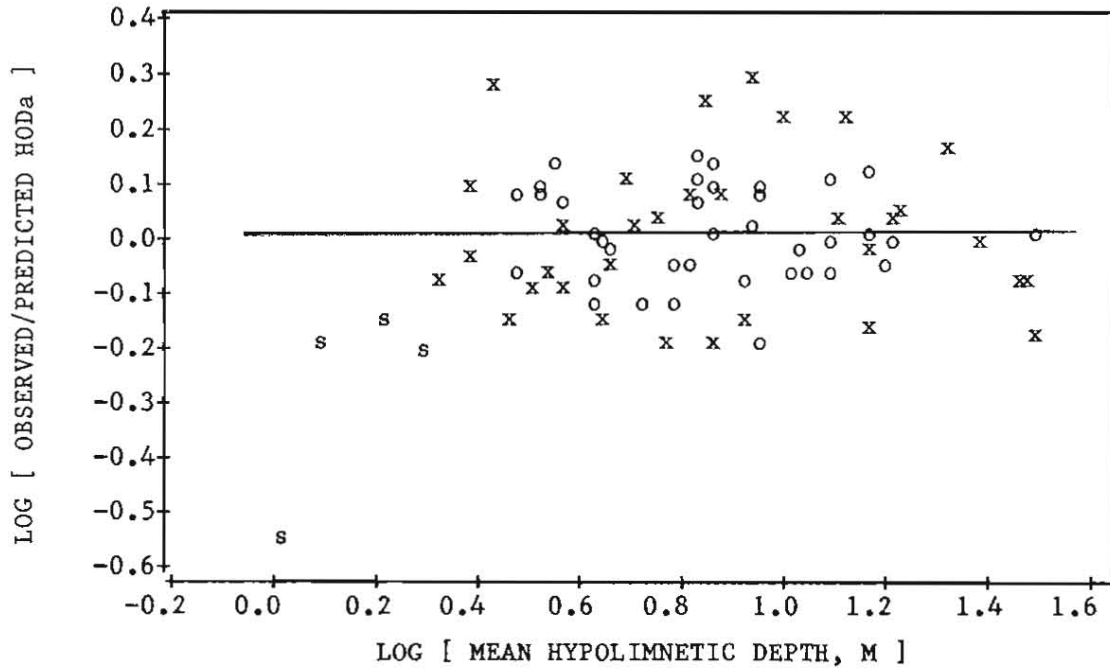
Symbols:
    o = CE Reservoir
    x = Natural Lake, Zh > 2 m
    s = Natural Lake, Zh < 2 m

with Zh values less than 2 meters discussed above. For these lakes, residuals range from -.15 to -.56. Thus, the model tends to over-predict HODa values in lakes with relatively shallow hypolimnetic depths. No morphometric dependence is apparent, however, for the reservoirs, which have Zh values ranging from 2.9 to 30 meters, or for the lakes with Zh values in excess of 2 meters.

127. When applied to predicting volumetric HOD rates, the above model takes the following form:

$$\log(\text{HODv}) = 2.34 + .45 \log(\text{Bs}) - \log(\text{Zh}) + .15 \text{ type} \tag{50}$$
$$(R^2 = .93, SE^2 = .013)$$

where

Zh = mean hypolimnetic depth (m)

Volumetric HOD rates are more important than areal HOD rates from a water quality management prespective because they directly determine the decline in average hypolimnetic oxygen concentrations during the stratified period. Coefficients of the above model reflect the relative importance of chlorophyll-a level (.45) vs. hypolimnetic depth (1.0) as factors controlling volumetric HOD rates. As shown in Figure 40, the model explains 93% of the variance in the observed reservoir HODv rates with a mean squared error of .0076. Corresponding lake statistics are 92% and .020, respectively.

128. Other studies of natural lake data (Cornett and Rigler, 1979, 1980; Walker, 1979; Charlton, 1980) have indicated that relationships between chlorophyll-a and areal HOD rate are not independent of morphometry and/or hypolimnetic temperature. These alternative models are described in Table 20 and tested against the reservoir and lake data sets in Table 21. When applied to the reservoir data set with original coefficients, the lake models underpredict HOD rates by averages ranging from .063 to .186 log units, or 16% to 53%. This is consistent with the effects of impoundment type noted above. Adjustments in slope and/or intercept are required to fit these models to the reservoir data set and results are generally inferior to the simple HODa/chlorophyll/type regression described above and represented as

137

Figure 40

Volumetric HOD Rate vs. Chlorophyll-a and Mean Hypolimnetic Depth

reservoirs
$y_2 = 2.49 + x_2$
$R^2 = .93$, $SE^2 = .0076$

lakes
$y_2 = 2.34 + x$
$R^2 = .92$, $SE^2 = .020$

Symbols:
  o = CE Reservoir
  + = Natural Lake, Zh > 2 m

138
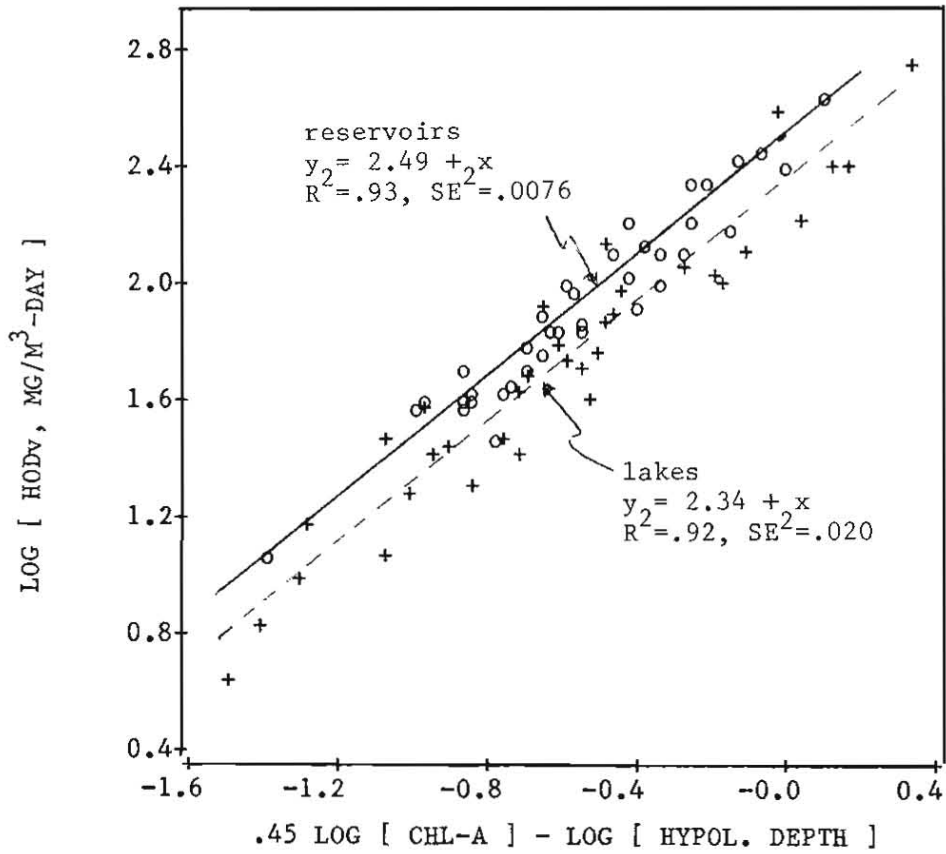
Table 20

Models Relating Areal Oxygen
Depletion Rate to Chlorophyll and Morphometry

Symbols:

$HODa$ = areal oxygen depletion rate (mg/m^2-day)
Z = mean depth (m)
Zh = mean hypolimnetic depth (m)
Th = mean hypolimnetic temperature (deg-C)
B = mean chlorophyll-a (mg/m^3)
I = trophic state index (dimensionless)
$F(Z)$ = mean depth morphometric term (dimensionless)
$F(Zh)$ = mean hypolimnetic depth morphometric term (dimensionless)
$F(B)$ = chlorophyll productivity function (dimensionless)
$F(Th)$ = temperature effect term (dimensionless)

Model A: Walker(1979), 30 natural lakes, excluding morphometric term

$$I = 20 + 33.2 \log(B)$$

$$\log(HODa) = 1.94 + .016 \ I = 2.26 + .53 \log(B)$$

Model B: Walker(1979), 30 natural lakes, including morphometric term

$$I = 20 + 33.2 \log(B)$$

$$F(Z) = -.58 + 4.55 \log(Z) - 2.04 \ [\log(Z)]^2$$

$$\log(HODa) = F(Z) + .0204 \ I = F(Z) + .41 + .68 \log(B)$$

Model C: Charlton(1980), 6 Great Lakes

$$F(B) = 1.15 \ B^{1.33} \ / \ (9 + 1.15 \ B^{1.33})$$

$$F(Th) = 2 \ [(Th - 4)/10]$$

$$F(Zh) = Zh \ / \ (50 + Zh)$$

$$HODa = 70 + 4090 \ F(B) \ F(Th) \ F(Z)$$

Model D: Charlton(1980), 6 Great Lakes + 20 small lakes

$$HODa = 120 + 3800 \ F(B) \ F(Th) \ F(Z)$$

Model E: This Study, logarithmic model, 37 CE Reservoirs

$$\log(HODa) = 2.49 + .45 \log(B), \quad (R^2 = .66, \ SE^2 = .0076)$$

139

Table 21
Error Statistics for
Models Relating Chlorophyll-a to Areal Oxygen Depletion Rate

MODEL	Residuals Using - Original Coefficients -						Observed vs. Predicted --------- Regression ---------			
	MEAN	MSR	VAR	R^2-a	R^2-b	R^2-c	INT	SLOPE	SB	MSE-R
-----	-----	-----	Reservoirs (n=37)		Observed Variance = .0215					-----
A	.186*	.0421	.0078	−.96	.64	.65	.565	.853	.104	.0076
B	.063*	.0260	.0227	−.21	−.06	.26	1.476	.478	.129	.0159
C	.131*	.0503	.0342	−1.33	−.59	.11	1.978	.300	.130	.0192
D	.104*	.0398	.0298	−.85	−.39	.10	1.878	.335	.146	.0193
E	.000	.0072	.0074	.67	.66	.65	.000	1.000	.055	.0076
-----	-----	-----	Lakes (n=34)		Observed Variance = .0579					-----
A	.044	.0216	.0202	.63	.65	.66	.373	.870	.109	.0199
B	−.041	.0233	.0223	.60	.61	.69	.628	.743	.086	.0180
C	.125*	.0595	.0454	−.03	.22	.31	1.024	.632	.160	.0401
D	.066	.0449	.0417	.22	.28	.30	.722	.738	.190	.0406
E	−.146*	.0402	.0193	.31	.67	.66	.150	1.009	.058	.0199

Models defined in Table 20

Residual Statistics:
    MEAN = mean residual = log(observed HODa) − log(predicted HODa)
    MSR = mean squared residual
    VAR = residual variance
    R^2-a = r-squared, using original model coefficients
    R^2-b = r-squared, adjusting intercept
    R^2-c = r-squared, adjusting slope and intercept

Regression Statistics (observed vs. predicted log(HODa)):
    INT = regression intercept
    SLOPE = regression slope
    SB = standard error of regression slope
    MSE = mean squared error

* Mean residual significantly different from zero at $p < .05$.

"Model E" in Tables 20 and 21. When slopes and intercepts are adjusted, Models A and E perform identically; this results from the fact that they are linear transformations of each other, as shown in Table 20. Models B-D include morphometric terms and perform relatively poorly on the reservoir data set, even after recalibration (R^2=.10 to .26).

129. Additional graphic and statistical analyses of the reservoir data set indicate that residuals from the above regression model are independent of the morphometric, hydraulic, and thermal stratification characteristics listed in Table 19. The ranges over which these tests have been conducted are important, however. Mean hypolimnetic depths ranged from 2.9 to 30.3 meters; unidentified morphometric effects may exist outside this range. In particular, incomplete oxidation of organic matter (Charlton, 1980) and/or increased importance of oxygen transfer into the hypolimnion may result in overprediction of areal HOD rates in reservoirs with shallower hypolimnetic depths; this appears to be the case in lakes with mean hypolimnetic depths less than 2 meters, although the validity of the HOD calculations in these shallow lakes has not been checked.

130. The availability of adequate data from calculating HOD rates in shallow reservoirs is severely limited by sampling frequency. For example, at an average chlorophyll-a level of 4 mg/m^3, the above model predicts an areal depletion rate of 585 mg/m^2-day, which corresponds to a volumetric depletion rate of 585 mg/m^3-day or 18 g/m^3-month in a reservoir with a mean hypolimnetic depth of 1 meter. The above rate of oxygen loss is high in relation to the typical monthly or bimonthly sampling frequency; monitoring programs would have to be designed to provide a high-frequency sampling just after the onset of stratification in order to provide adequate data for estimation of HOD rates in this type of reservoir. Use of monthly data in such a case would most likely result in underestimation of the HOD rate, because the first sampling date used in calculations would tend to precede stratification and/or the second would tend to follow the loss of hypolimnetic oxygen. Sampling frequency and timing are especially critical in shallow lakes or reservoirs. It is possible that some of the apparent morphometric

dependencies of areal HOD rate reported in the literature could have resulted from use of inadequate data from shallow lakes.

131. The concept that hypolimnetic temperature is an important controlling factor for lake HOD rates has been discussed by Cornett and Rigler (1979) and Charlton (1980). It should be noted, however, that neither of these studies demonstrated the statistical significance of a temperature correction term. No temperature dependence is indicated for the reservoir and lake data sets examined above. Effects of impoundment type are partially confounded with those of temperature, since mean Th values are 11.9 and 7.8 degrees C for the reservoir and lake data sets, respectively. Charlton (1980) assumed that HOD rates doubled with each increase of 10 degrees C, which corresponds to a log(HOD) vs. Th slope of .03. At this rate, the 4.1 deg C difference in mean temperature could account for an average difference of .12 log units in areal HOD, compared with the difference of .15 noted above. The temperature term in Equation 49 is insignificant. however, when both temperature and impoundment type are included as independent variables or when the lake and reservoir data sets are tested separately. While the data sets seem to suggest a causal factor related to impoundment type, the possiblity of an underlying temperature influence should be noted.

132. The lack of dependence of HOD rate on temperature is not unreasonable from a theoretical perspective. The basic assumption underlying areal HOD as a measure of productivity is that the controlling factor is the rate of input of organic materials into the hypolimnion, not the rate at which those organic materials are oxidized. This point is illustrated with the following mass balance calculation on a unit volume of hypolimnion under quasi-steady-state conditions:

$$Wbod = Kd\ Cbod + Ka\ Cbod \qquad (51)$$

$$Cbod = Wbod\ /\ (Kd + Ka) \qquad (52)$$

$$HODv = Kd\ Cbod = Wbod\ Kd\ /\ (Ka + Kd) \qquad (53)$$

where

Wbod = organic matter (BOD) input to hypolimnion $(mg/m^3\text{-day})$

Cbod = mean hypolimnetic BOD concentration (mg/m^3)

Kd = BOD oxidation rate (1/day)

Ka = BOD accumulation rate, (1/day)

have

tant

and

that

of a

i for

dment

an Th

sets,

each

slope

ature

. HOD,

term

re and

lake

s seem

iblity

s not

mption

the

ito the

dized.

:ion on

(51)

(52)

(53)

-day)

Organic matter (BOD) entering the hypolimnion is assumed to be oxidized at a rate Kd (1/day) or accumulate at a rate Ka (1/day). The locations of oxidation and accumulation could include the water column and/or bottom sediment. The temperature-dependence of the oxidation rate, Kd, is consistent with the effects of temperature on microbial activity. The solution of the equation indicates that for Kd >> Ka (i.e., most of the entering organic matter is oxidized rather than accumulated), HODv is independent of the rate parameters and therefore independent of temperature. If the oxidation and accumulation rate parameters have the same temperature dependence, then HODv will be independent of temperature for all values of Ka and Kd. Hypolimnetic temperatures seem more likely to influence the standing crop of organic matter in the water column and sediment (Cbod) than the HOD rate. For a given organic loading and mean hypolimnetic depth. a reservoir with a relatively cold hypolimnion would tend to have higher concentrations of organic matter in the hypolimnion and bottom sediment but the same HOD rate, as compared with a reservoir with a relatively warm hypolimnion.

133. A number of factors may contribute to the apparent effects of impoundment type on HOD rate. These effects should be interpreted cautiously because they are confounded with temperature and possible effects of differences in data-reduction procedures. Since the reservoir model is based upon near-dam stations, the effects of spatial variations in chlorophyll at upstream stations may also be important. If the HOD rate measured near the dam reflects the cumulative effects of productivity throughout the reservoir, then higher chlorophyll levels at upstream stations could influence the chlorophyll/HOD relationship measured at the dam. Estimates of spatially weighted mean chlorophyll concentrations were available for 30 of the reservoirs with HOD data. The spatially weighted chlorophyll-a values average .155 log units (standard error = .025) above the near-dam values. Applied to the chlorophyll slope in Equation 49, this would explain .070 or 47% of the apparent effects of impoundment type, assuming that the HOD effect is spatially cumulative and that upstream/downstream variations in

143

chlorophyll are not important in lakes. Effects of different chlorophyll averaging procedures are examined further below. Another possibly contributing factor is that the reservoir chlorophyll estimates are based primarily upon EPA/NES data from April-October inclusive, while the lake chlorophyll numbers are generally summer averages. Analyses of variance using reservoir data indicate, however, that fixed seasonal effects on chlorophyll are minimal when the averaging period is restricted to April through October (Walker, 1981). A mechanistic interpretation of the apparent effects of impoundment type on the chlorophyll/HOD rate relationship is that allochthonous demands are more important in reservoirs because of regional factors, generally higher flushing rates, and/or higher benthic demands attributed to organic matter in flooded soils.

Alternative Oxygen Depletion Models

134. Relationships between areal HODa rate and four surface-water measures of trophic state (chlorophyll, total phosphorus, transparency, and organic nitrogen) are summarized in Table 22, based upon reservoir data. To explore the effects of different averaging procedures, both station-mean and area-weighted, reservoir-mean conditions have been tested as independent variables. Estimates of the latter are available for 30 out of the 37 reservoirs with HODa data. Both linear and logarithmic formulations have been tested. Significant positive correlations are apparent in all cases. For a given independent variable, it is difficult to distinguish among alternative averaging procedures and model formulations in a statistical sense. The linear models employing reservoir-average water quality conditions generally tend to have higher correlation coefficients, although diagnostic plots indicate that the variance of the residuals of the linear models increases with estimated depletion rate. Use of reservoir-mean chlorophyll values decreases the intercept of the logarithmic model by .07 and thus explains about half of the apparent lake/reservoir differences, as discussed above.

135. The linear formulations essentially partition the areal HOD

144

rent
ther
ates
ive,
ges.
fixed
od is
istic
the
more
igher
ganic

-water
rency,
ervoir
both
e been
ilable
ar and
sitive
endent
eraging
linear
nerally
c plots
models
ir-mean
del by
servoir

al HOD

Table 22

Summary of Regression Models Relating Areal Hypolimnetic Oxygen
Depletion Rate to Other Measures of Reservoir Trophic State

Independent Variable (x)	Averaging	(a) Intercept	(b) Slope	Standard Error of Estimate	Correlation Coefficient
---------------- linear models: HODa = a + b x ----------------------					
Chlorophyll-a	S	343	57	126	.823
Total P	S	427	11.0	169	.617
Organic N	S	324	.84	188	.553
1/Secchi	S	348	589	166	.664
Chlorophyll-a	R	283	49	117	.864
Total P	R	388	10.4	158	.713
Organic N	R	164	1.21	161	.733
1/Secchi	R	340	571	170	.685
----------- logarithmic models: log(HODa) = a + b log(x) ------------					
Chlorophyll-a	S	2.49	.45	.087	.810
Total P	S	2.38	.34	.110	.572
Organic N	S	1.72	.42	.132	.478
1/Secchi	S	2.93	.40	.115	.634
Chlorophyll-a	R	2.41	.46	.096	.781
Total P	R	2.36	.32	.107	.628
Organic N	R	.86	.75	.110	.705
1/Secchi	R	2.94	.47	.114	.668

NOTES:
Units: HODa (based upon near-dam station) mg/m^2-day
        Chl-a, Total P, Organic N mg/m^3
        1/Secchi   1/m
Averaging of water quality data: S = near-dam, station mean
                                 R = area-weighted, reservoir mean
Number of Observations = 37 for "S" regressions
                       = 30 for "R" regressions
Phosphorus regressions exclude data from two nitrogen-limited
         reservoirs (32-204, Kookanusa and 35-029, Mendocino).
All correlations significant at $p < .01$.

rate into two components, one related to trophic status and the other unrelated. These relationships are depicted graphically in Figure 41, using reservoir-mean water quality conditions as independent variables. The strongest correlation is based upon chlorophyll-a:

$$HODa = 283 + 49\ Bm \qquad (r=.86,\ SE=117,\ linear\ scale) \qquad (54)$$

where

$$Bm = area\text{-}weighted,\ reservoir\text{-}mean\ chlorophyll\text{-}a\ (mg/m^3)$$

The residual variance of this and the other linear models increases somewhat with estimated depletion rate. This increasing variance is expected because sampling errors in the mean chlorophyll and other water quality variables are stable only on a logarithmic scale.

136. The intercept ($283\ mg/m^2$-day) in Equation 54 presumably represents the average allochthonous component of HODa. The second term represents a eutrophication-related component. At a typical algal chlorophyll-a content of 1% and algal respiration equivalent of 2 mg oxygen per mg algae, the slope of the chlorophyll-a term suggests an average algal settling velocity of .25 m/day, which is within the range of values reported in the literature (Zison et al., 1978). According to this model, HOD rates are controlled primarily by the allochthonous organic demands in the low chlorophyll range. Residuals reflect the combined effects of reservoir-to-reservoir variations in intercept (reflecting allochthonous demands), the chlorophyll-a slope (reflecting algal species and settling velocities), and random data errors.

137. The higher HODa correlations with the reservoir-mean vs. station-mean condition may reflect the cumulative loading effects discussed above and/or the larger sample size and greater precision of the reservoir-mean concentration estimates. When both reservoir-mean and station-mean chlorophyll-a values are used as HODa predictors, the following model results:

$$HODa = 284 + 27\ Bm + 29\ Bs \qquad (R=.88,\ SE=111,\ linear\ scale) \qquad (55)$$

146

(54)

Figure 41

Linear Models Relating Areal HOD Rate to Reservoir-Mean
Trophic State Indicators

reases

e is

water

umably

d term

algal

f 2 mg

ts an

range

ling to

thonous

ect the

tercept

lecting

an vs.

effects

sion of

ir-mean

s, the

) (55)

147
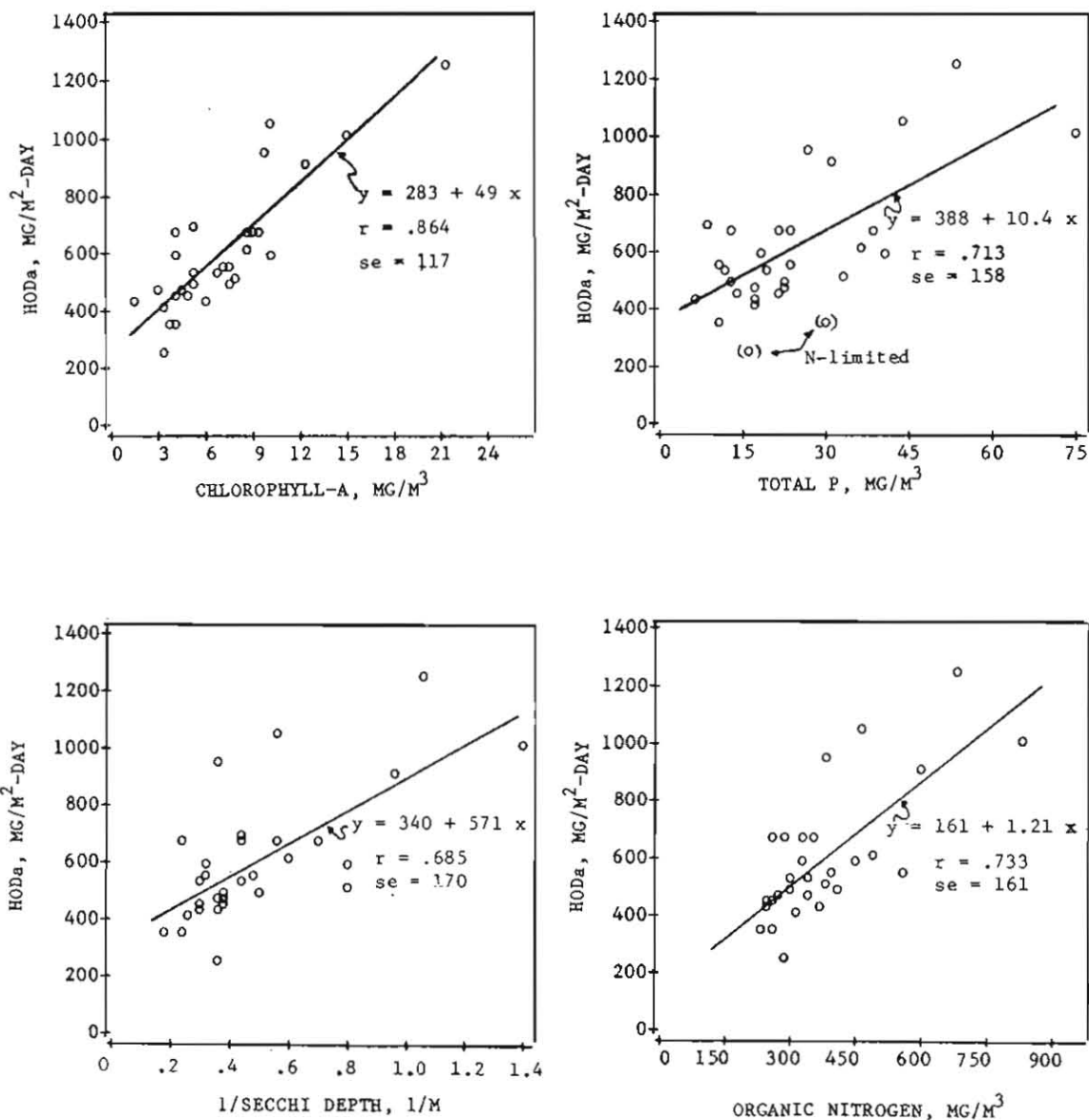
where

B_m = area-weighted, reservoir-mean chlorophyll-a (mg/m^3)

B_s = mean chlorophyll-a at near-dam station (mg/m^3)

In this formulation, both the B_m and B_s are significant and contribute about equally to the predicted HODa value. This suggests that near-dam depletion rates reflect a combination of upstream and near-dam surface water quality conditions; perhaps a weighted-average of chlorophyll concentrations at stratified stations would be the best predictor. Other factors, such as differences in the precision of the B_m and B_s estimates, could also influence the relative values of the above coefficients. Since the reduction in standard error relative to Equation 54 is minimal (117 vs. 111), models based upon reservoir-average conditions seem adequate.

138. As shown in Figure 41, areal HOD rate is also correlated with total phosphorus (r=.68), inverse Secchi depth (r=.69), and organic nitrogen (r=.73). Unlike the other relationships, the intercept in the HODa/organic nitrogen relationship is not significantly different from zero. An average HODa/organic N ratio of 1.67 is indicated. The low intercept may reflect an allochthonous component of organic nitrogen (or organic carbon, which would be correlated with organic nitrogen) which contributes to oxygen depletion. Another factor of possible importance is the relatively low precision of the organic nitrogen data in the low concentration range. The EPA National Eutrophication Survey reported total Kjeldahl nitrogen values down to a minimum of 200 mg/m^3; concentrations reported as less than this value have been included as 200 mg/m^3 in averaging procedures. Effects of inorganic particulates would also be expected to contribute to errors in the HODa/Total P and HODa/Secchi depth relationships. Observed and predicted volumetric HOD rates based upon the linear models are shown in Figure 42.

139. The above correlations suggest that HODa and HODv rates can successfully be incorporated into an empirical model network (see Part VIII). As discussed above, it is difficult to distinguish the linear from the logarithmic formulations in a statistical sense. The logarithmic models have more stable error distributions and are therefore preferred for use in a predictive mode. The logarithmic
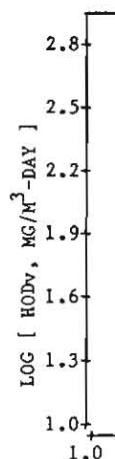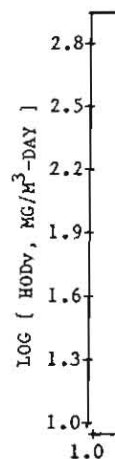
148

Figure 42

Linear Models Relating Volumetric HOD Rate to Reservoir-Mean
Trophic State Indicators and Mean Hypolimnetic Depth
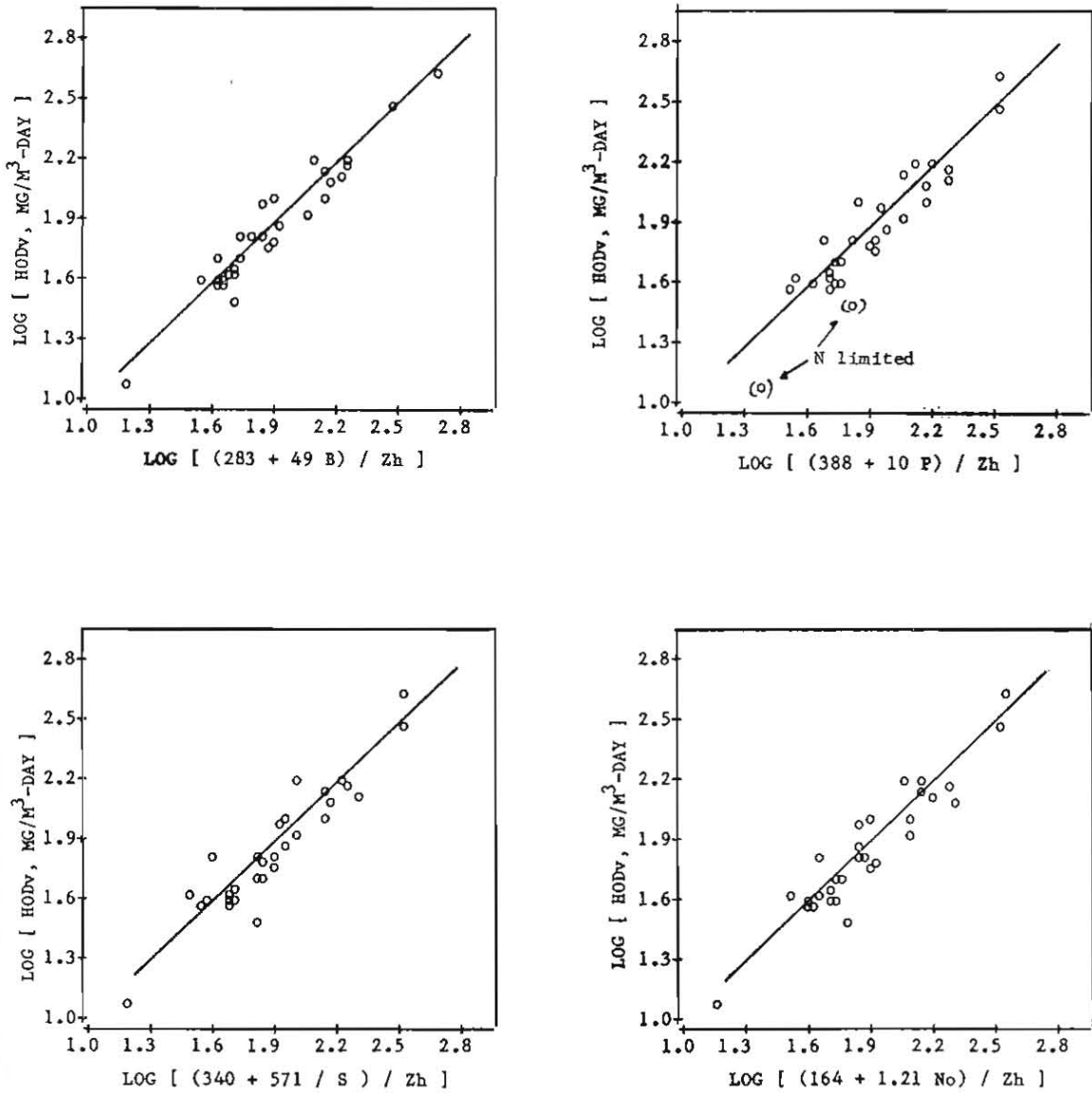
formulations also suggest a normalization scheme which would be useful for data interpretation and prediction. These models can be expressed in the following general form:

$$\log(HODv) = a0 + a1 \log(Chlorophyll\text{-}a) + a2 \log(Depth) \qquad (56)$$

where

a0,a1,a2 = empirical parameters

The chlorophyll-a term can represent reservoir-mean or station-mean concentrations. The models tested above employ mean hypolimnetic depth as a measure of morphometry (depth). In some situations, such as in the analysis of spatial variations discussed below and/or when thermocline levels are unknown, it is useful to employ other measures of morphometry, including maximum hypolimnetic depth and maximum reservoir depth. In these cases, the alternative depth terms act as surrogates for mean hypolimnetic depth. Testing of the six alternative formulations of the above model (using each of the two chlorophyll averaging procedures and each of the three measures of depth) indicates that the chlorophyll slope is not significantly different from .5 and the depth slope is not significantly different from -1. in each case. These results suggest the following normalization procedure for HODv data:

$$a0 = \log (HODv\ Depth / Chlorophyll\text{-}a^{.5}) \qquad (57)$$

Expressions of the above form can be considered "normalized oxygen depletion rates." Distributions are summarized in Table 23 for the various measures of chorophyll-a and hypolimnetic morphometry. The variance of each expression reflects inherent model and data errors. Generally, expressions using mean hypolimnetic depth have significantly lower variance than those employing maximum hypolimnetic depth or maximum total depth. Thus, mean hypolimnetic depth should be used as a predictor when possible. In situations where hypolimnetic and/or thermocline levels are unknown, the following regression models can be

Model

1
2
3

4
5
6

NOTES:
HO:

Zh
Zx
Zx
Bd
Bm
R2

150

:ful
;sed

(56)

nean

epth

the

line

of

voir

ates

tive

hyll

.ates

and

:ase.

HODv

(57)

xygen

the

The

rors.

antly

h or

as a

nd/or

an be

Table 23

Distributions of Normalized Volumetric HOD Rates

Formulation: $\log (HODv * Depth / \sqrt{Chlorophyll-a})$

Model	Depth Term	Chl-a Term	n	Mean	Variance	R^2	Min.	Percentiles 25%	50%	75%	Max.
1	Zh	Bd	37	2.47	.0075	.931	2.27	2.40	2.46	2.54	2.61
2	Zxh	Bd	37	2.94	.0140	.872	2.66	2.87	2.95	3.05	3.18
3	Zx	Bd	37	3.19	.0151	.862	2.82	3.10	3.21	3.26	3.40
4	Zh	Bm	30	2.38	.0090	.920	2.18	2.31	2.36	2.45	2.60
5	Zxh	Bm	30	2.85	.0128	.883	2.57	2.79	2.83	2.94	3.06
6	Zx	Bm	30	3.09	.0154	.860	2.73	3.02	3.09	3.16	3.30

NOTES:

HODv = volumetric oxygen depletion rate in hypolimnion,
        measured at near-dam station (mg/m^3-day)
Zh = mean hypolimnetic depth (m)
Zxh = maximum hypolimnetic depth (m)
Zx = maximum total depth (m)
Bd = near-dam, station-mean chlorophyll-a (mg/m^3)
Bm = area-weighted, reservoir-mean chlorophyll-a (mg/m^3)
R2 = percent of HODv variance explained by model =
        1 - statistic variance / HODv variance

used to estimate mean hypolimnetic depth:

$$\log(Zh) = -.58 + .57 \log(Zx) + .50 \log(Z) \tag{58}$$
$$(R^2 = .85, SE^2 = .0076)$$

$$\log(Zx - Zxh) = -.064 + .80 \log(Zx) \tag{59}$$
$$(R^2 = .79, SE^2 = .0067)$$

where

Zx = maximum total depth (m)

Z = mean total depth (m)

Zxh = maximum depth of hypolimnion (m)

Zh = mean hypolimnetic depth (m)

These regressions are based upon the model development data set and are applicable to reservoirs with mean hypolimnetic depths between 3 and 16 meters and maximum total depths between 20 and 70 meters. Equation 18 estimates the distance from the surface of the reservoir to the upper boundary of the hypolimnion.

140. Table 24 summarizes HOD data compiled independently for two CE reservoirs intensively monitored under the EWQOS Field Studies Program, Eau Galle and De Gray. The distributions of normalized oxygen depletion rates for these reservoirs are compared with the data set analyzed above in Figures 43-45. As shown in Figure 43, the observed volumetric depletion rate for Eau Galle is about .5 log units, or a factor of 3, higher than the maximum HODv in the model development data set. This reflects both a relatively high mean chlorophyll (51 vs. 16 mg/m^3) and low mean hypolimnetic depth (1.2 vs. 2.8 m). Thus, data from Eau Galle lie considerably outside of the range of the model development data set and present a relatively severe test of the models. The near-dam depletion rates in De Gray lie near the low end of the observed HODv values; this reflects a relatively low mean chlorophyll-a concentration (1.9 mg/m^3) and high mean hypolimnetic depth (12.4 m). EPA/NES data from De Gray are also included in the model development data set; the EWQOS data are considerably more intensive, however, and from a different year (1981 vs. 1974).

Table 24

Independent Data from EWQOS Field Studies Used for HOD Model Testing

Reservoir	Eau Galle	-----	De Gray	-----	
Station	20	01	04	10	12
Chlorophyll-a (mg/m^3)					
Station-Mean	51	1.9*	1.9	3.2	5.1
Reservoir-Mean	51	2.7	–	–	–
Maximum Depth (m)	9	57	46	26	16
Maximum Hypol. Depth (m)	1.52	40	29	8.5	4.9
Mean Hypol. Depth (m)	1.26	12.4	–	–	–
Volumetric HOD (mg/m^3-day)	1335	30(32)**	40	97	149
Areal HOD (mg/m^2-day)	1682	372	–	–	–

NOTES:
  HOD calculation dates: 81/04/28 - 81/05/05 for Eau Galle
                              81/03/17 - 81/04/28 for De Gray
  Chlorophyll-a values refer to April-October 1981 means,
          depths less than 15 feet.
  * Station 01 chlorophyll-a for De Gray (near dam) assumed
          equal to Station 04 value.
** HODv = 30 mg/m^3-day calculated using areal weights derived from
          reservoir hypsiograph.
      = 32 mg/m^3-day calculated using areal weights derived from
          station width vs. elevation power function.

3)

9)

l are
3 and
ion 18
upper

or two
tudies
oxygen
a set
served
or a
t data
l vs.
data
devel-
. The
served
concen-
EPA/NES
a set;
from a

Figure 43

Distributions of Volumetric HOD Rates

```
log (HODv)
mean = 1.93, var = .109          EWQOS Field Studies

(minimum of interval)
3.20|
3.10|                                      o Eau Galle
3.00|
2.90|
2.80|
2.70|
2.60|16
2.50|
2.40|18 18 18
2.30|18 18
2.20|19 29
2.10|18 18 18 29
2.00|06 18 26
1.90|02 26 26
1.80|03 18 24 25 26
1.70|16 19 19
1.60|16 17 22 24 24 24 24
1.50|17 30
1.40|35                                    o De Gray
1.30|
1.20|
1.10|
1.00|32
```

NOTE: Histogram symbols denote CE district code.

Figure 44
Distributions of Normalized Volumetric Depletion Rates for
Models Using Near-Dam Chlorophyll-a Values

$$\log (HOD\dot{v} \ Zh \ / \ Bd^{.5})$$
mean = 2.46, var = .0075   EWQOS Field Studies

```
2.60|19
2.55|02 16 18 18 24 30
2.50|16 18 18 18 18 25
2.45|16 17 18 24 24 26 29 32
2.40|17 18 19 24 26          o De Gray
2.35|03 18 18 19 22 24       o Eau Galle
2.30|06 26 29
2.25|35
```

$$\log (HODv \ Zxh \ / \ Bd^{.5})$$
mean = 2.94, var = .0140   EWQOS Field Studies

```
3.15|18
3.10|18 18
3.05|18 18 19 26 29
3.00|18 24 30
2.95|16 17 19 24 24 24 25    o De Gray
2.90|02 16 18 22 24 32
2.85|17 18 19 26 26
2.80|06 18
2.75|03 16 29
2.70|
2.65|18 35
2.60|
2.55|
2.50|
2.45|                        o Eau Galle
```

$$\log (HODv \ Zx \ / \ Bd^{.5})$$
mean = 3.19, var = .0151   EWQOS Field Studies

```
3.40|18
3.35|18 18
3.30|18 29
3.25|18 19 24 26 26 26
3.20|16 18 18 18 19 24 25 30  o Eau Galle
3.15|02 16 17 24 26
3.10|19 24 24 29              o De Gray
3.05|03 06 16 18 22
3.00|17 32
2.95|18
2.90|
2.85|
2.80|35
```

155

Figure 45
Distributions of Normalized Volumetric HOD Rates for
Models Using Area-Weighted Mean Chlorophyll Concentrations

```
                     .5
log ( HODv Zh / Bm  )
mean = 2.38, var = .00898          EWQOS Field Studies

2.55|16
2.50|02 19 26
2.45|24 24 26
2.40|16 18 18
2.35|03 19 24 24 24 25 29         oo Eau Galle / De Gray
2.30|17 17 22 26 29 30
2.25|06 16 18 19 26 32
2.20|
2.15|35


                     .5
log ( HODv Zxh / Bm  )
mean = 2.85, var = .0128           EWQOS Field Studies

3.05|26 26
3.00|19 24
2.95|16 18 29
2.90|24 24 24
2.85|17 22 24                      o De Gray
2.80|02 03 17 18 19 19 25 26 29
2.75|06 26 30
2.70|16 16 18 32
2.65|
2.60|
2.55|35
2.50|
2.45|                             o Eau Galle


                    .5
log ( HODv Zx / Bm  )
mean = 3.09, var = .0154           EWQOS Field Studies

3.25|16 26 26
3.20|18 29                         o Eau Galle
3.15|18 24 24 24 29
3.10|19 19 26
3.05|02 03 17 19 24 24 25 26
3.00|06 16 22                      o De Gray
2.95|16 17 18 30
2.90|
2.85|
2.80|32
2.75|
2.70|35
```

141. Distributions of normalized depletion rates are summarized in Figures 44 and 45, using near-dam and reservoir-mean chlorophyll-a values, respectively, and each of the three alternative morphometric terms. Generally, agreement between the EWQOS and model development data sets is best for models using mean hypolimnetic depth. Eau Galle deviates significantly from the other reservoirs when maximum hypolimnetic depth is used as a measure of morphometry. This reflects the unusual hypolimnetic morphometry of this reservoir, which has a volume development ratio (maximum depth/mean depth) of only 1.2 in the hypolimnion, as compared with an average of about 3 for the other reservoirs. Thus, Eau Galle apparently has a relatively broad and flat bottom topography. Combined with the error distributions of the normalized depletion rate statistics, results for Eau Galle indicate that information on hypolimnetic morphometry should be incorporated into the interpretation of HOD data when possible.

142. Figure 46 tests for effects of summer withdrawal levels on normalized volumetric HOD rates computed using mean hypolimnetic depth as a measure of morphometry. A total of five outlet operation categories have been defined to reflect the principal levels of water withdrawal during the late spring and early summer months, the period which generally corresponds to the HOD rate calculations. A total of 19 out of the 29 projects with withdrawal level information had exclusively hypolimnetic discharges. The remaining discharged various mixtures of hypolimnetic, metalimnetic, and epilimnetic waters. While the size of the data set does not permit a distinction among members of the latter group, there is a slight, though statistically significant difference between the hypolimnetic group and the other projects combined. Normalized depletion rates averaged about .07 log units (17%) higher for the hypolimnetic group. Based upon a t-test for comparing means of two groups with unequal sizes and unequal variances (Snedecor and Cochran, 1972), the difference between the two groups of reservoirs is significant at the 10% and 5% levels for normalized depletion rates calculated using station-mean and reservoir-mean chlorophyll-a values, respectively.

Figure 46
Distributions of Normalized
Volumetric Depletion Rates Grouped by Outlet Level

$\log (\text{HODv Zh} / \text{Bd}^{.5})$ (using station-mean chlorophyll-a)

Summer Outlet Level

```
           H              H/M        E/M/H      E/M        E      No Data
        ----------------------------------------------------------------
2.625 |
2.600 | 19
2.575 | 24 30                                               02 18
2.550 | 16 18 26                                            18 18
2.525 |                                                     25
2.500 | 16 18          18
2.475 |                            16 32
2.450 | 24 24 26                              29             17 18
2.425 | 24 26
2.400 | 18 19 24                                            17
2.375 | 19             18 18 22
2.350 |                                  03
2.325 | 06             26
2.300 |                            29
2.275 |
2.250 | 35
        ----------------------------------------------------------------

        n:     19                    10
     mean:  2.471                  2.411    t = 2.07, prob(>t) < .10
  std dev:   .090                   .067
```

$\log (\text{HODv Zh} / \text{Bm}^{.5})$ (using reservoir-mean chlorophyll)

Summer Outlet Level

```
           H              H/M        E/M/H      E/M        E      No Data
        ----------------------------------------------------------------
2.600 | 16
2.575 |
2.550 |
2.525 | 19 26
2.500 | 24                                                 02
2.475 | 24
2.450 | 26
2.425 | 16 18
2.400 |                18
2.375 |                                  03
2.350 | 19 24 24 24                                29       17 25
2.325 | 30             22          29                       17
2.300 | 19 26                      32
2.275 | 06             18          16
2.250 |                26
2.225 |
2.200 |
2.175 | 35
        ----------------------------------------------------------------

        n:     17                     9
     mean:  2.405                  2.330    t = 2.36, prob(>t) < .05
  std dev:   .107                   .055
```

Outlet Levels: E = Epilimnetic, M = Metalimnetic, H = Hypolimnetic

143. Analyses of larger data sets are needed to develop firm conclusions on the effects of outlet level. It is worth noting, however, that these effects may explain some of the differences between lake and reservoir responses to chlorophyll-a noted above. Using reservoir-mean chlorophyll-a values, average normalized depletion rates are 2.41 for reservoirs with hypolimnetic outlets, 2.33 for reservoirs with other operation modes, and 2.32 for lakes. Thus, essentially all of the apparent effects of impoundment type can be explained by effects of outlet level and spatial chlorophyll-a variations in reservoirs. The relationship between chlorophyll-a and areal HOD rate in reservoirs with surface or mixed outlet configurations is apparently similar to the relationship found in natural lakes.

144. Oxygen depletion data compiled for TVA reservoirs by Higgins (1982) provides an independent basis for testing one of the normalized depletion rate statistics described above using outflow oxygen depletion data. Volumetric HOD rates have been computed based upon time series of average, weekly oxygen concentrations in reservoir discharges between 1974 and 1976. Oxygen measurements were taken prior to aeration by reservoir outlet structures. Higgins has estimated a "maximum" and "mean" depletion rate for each reservoir; the former corresponds to the steepest point in the oxygen vs. date curve (generally in April or May) and the latter has been estimated from the dates and levels of yearly maximum and yearly minimum dissolved oxygen concentrations. Because of the possible effects of outlet level and reservoir hydrodynamics, there is no guarantee that outflow oxygen depletion rates calculated in the above way would equal values calculated based upon vertical profile data and the standard area-weighting procedures described above. Because oxygen concentrations in some of the reservoir discharges drop below 2 mg/liter and yearly maximum oxygen concentrations generally occur prior to the onset of stratification, the "maximum" depletion rates probably correspond more closely than the "mean" rates to those which would be calculated from vertical profile data. While Higgins has also estimated mean hypolimnetic depths for these reservoirs assuming a fixed thermocline level of 6 meters, the latter assumption is unreliable when

159

tested against data from CE reservoirs, with thermocline levels ranging from 5 to 33 meters. In the absence of vertical profile data to assess thermocline levels in these reservoirs, maximum and mean normalized depletion rates have been computed using maximum total depth as a measure of morphometry. The compilation of water quality, morphometric, and hydrologic data for TVA reservoirs for model testing has been described previously (Walker, 1982a) and is summarized in Appendix A. Figure 47 compares the distributions of normalized depletion rates for CE reservoirs, TVA mainstem, and TVA tributary reservoirs.

145. As a group, the mainstem reservoirs deviate significantly from the CE and TVA tributary reservoirs. The mainstem impoundments are distinguished by relatively low hydraulic residence times (.007 - .038 year) and shallow mean depths (4.2-12.3 meters). The residence times of all of the mainstem reservoirs are below those of the CE reservoirs used in model development (minimum, .1 year). It seems unlikely that they conform to the stratification criterion of a top-to-bottom temperature difference of at least 4 degrees C. Placke and Bruggink (1980) note that none of the 4 TVA mainstem reservoirs (Chickamauga, Fort Loudoun, Nickajack, and Wilson) sampled in a 1979 eutrophication study were stably stratified. The mainstem impoundment characteristics are consistent with the fact that maximum normalized depletion rates averaged about .4 log units (or a factor of 2.5) below the other reservoirs.

146. The TVA tributary reservoirs generally show better agreement with the distribution of CE reservoirs. Normalized depletion rates are relatively high for three deep reservoirs, Watauga, Norris, and Fontana, which have maximum depths of 76, 54, and 123 meters, respectively. These deviations may reflect a morphometric dependence and/or effect of outlet level which is not accounted for by the normalization. The deepest TVA project, Fontana, has a mean depth of 31 meters. Reservoirs in the CE data set have mean depths ranging from 3.4 to 35 meters; all except one are in the 3.4- to 24- meter range. While some factor associated with depth or outlet level might contribute to the relatively high outlet oxygen depletion rate in Fontana, an alternative explanation

160

TVA M

Kentu
Pickw
Wilso
Wheel
Gunte
Nicka
Chick
Watts
Fort

TVA T

Chatu
Chero
Dougl
Fonta
Hiwas
Norri
South
Tims
Watau

o = m
x = m
* = o
f

ging
sess
ized
as a
ric,
been
x A.
for

antly
s are
.038
times
voirs
that
ottom
iggink
auga,
cation
istics
rates
other

eement
s are
ntana.
ively.
ct of
. The
ervoirs
s; all
factor
atively
anation

Figure 47

Normalized Outflow Oxygen Depletion Rates for TVA Reservoirs

```
                                               *
                                               *
                                               *
               Distribution of                 *    *
               30 CE Reservoirs  ==>       *    *    *
               mean = 3.09                 *  * * *     *
               variance = .0154            * * * * * * *
                                    *    *    * * * * * * *
               --+---+---+---+---+---+---+---+---+---+---+---+---+---+-
                2.3 2.4 2.5 2.6 2.7 2.8 2.9 3.0 3.1 3.2 3.3 3.4 3.5 3.6
 TVA Mainstem  --+---+---+---+---+---+---+---+---+---+---+---+---+---+-

   Kentucky                           o---x
   Pickwick                        o--------------------x
   Wilson                          o--------x
   Wheeler                      o-----x
   Guntersville              o-------------x
   Nickajack                    o--------x
   Chickamauga                  o------------x
   Watts Bar                 o---------------x
   Fort Loudon                  o-----x

 TVA Tributary

   Chatuge                              o---x
   Cherokee                              o-------x
   Douglas                            o-------x
   Fontana                                             o-----------x
   Hiwasse                             ox
   Norris                                      o---------x
   South Holston                     o---x
   Tims Ford                         o-------x
   Watauga                                   o-------x
               --+---+---+---+---+---+---+---+---+---+---+---+---+---+-
                2.3 2.4 2.5 2.6 2.7 2.8 2.9 3.0 3.1 3.2 3.3 3.4 3.5 3.6
```

$$\log (\text{HOD}_v\ Z_x\ /\ \sqrt{B_m})$$

o = mean oxygen depletion rate in outflow, TVA reservoir.
x = maximum oxygen depletion rate in outflow, TVA reservoir.
* = oxygen depletion rate rate at near-dam station, determined
    from vertical profile data, CE reservoir.

161

is suggested by the EPA National Eutrophication Survey report on this reservoir (EPA/NES, 1975). The Tuckasegee Arm of Fontana apparently has extensive organic sludge deposits of municipal and/or industrial origin which contribute to the development of anaerobic conditions in the hypolimnion and to mobilization of ammonia. These conditions, noted by the NES and by Louder and Baker (1966), might explain the relatively high normalized depletion rate of this reservoir.

147. The lack of oxygen depletion rates calculated in a conventional manner from vertical profile data prevents a complete understanding of the behavior of the TVA tributary reservoirs relative to model predictions, since outlet level would influence the relationship between the oxygen concentration measured in the discharge and the volume-weighted, hypolimnetic concentration estimated from vertical profiles above the dam. Maximum depletion rates from the shallower TVA tributary reservoirs (maximum depth less than 50 meters), however, agree reasonably with the distributions of CE data. Future analyses of discharge oxygen concentrations from CE reservoirs may shed additional light on these relationships but are infeasible within the scope of this project.

Metalimnetic Demands

148. The models analyzed above have focused on oxygen depletion rates below the thermocline. Estimates of average metalimnetic oxygen depletion (MOD) rates have been derived by difference from HOD rates calculated at the upper and lower boundaries of the metalimnion. Graphical and stepwise regression analyses have been applied to develop an empirical model for predicting volumetric MOD rates. The relationship between MOD and HOD rates is best summarized by Figure 48 and the following regression equation:

$$\log(MODv) = -.40 + \log(HODv) + .38 \log(Zh) \tag{60}$$
$$(R^2 = .86, \; SE^2 = .011)$$

where

$MODv$ = metalimnetic oxygen depletion rate (mg/m^3-day)

Figure 48

Volumetric MOD Rate vs. Volumetric HOD Rate and Mean Hypolimnetic Depth
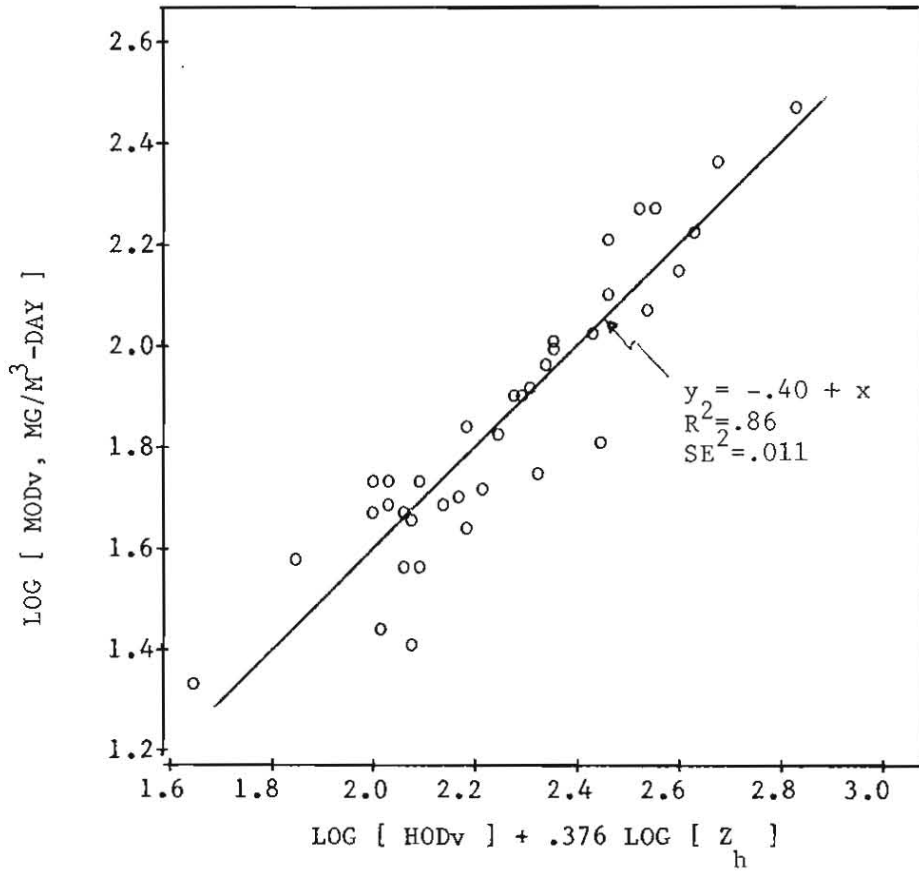
this
has
igin
the
d by
ively

in a
plete
ative
the
harge
from
m the
ters),
Future
shed
in the

letion
oxygen
rates
imnion.
develop
. The
ure 48

(60)

$$y = -.40 + x$$
$$R^2 = .86$$
$$SE^2 = .011$$

LOG [MODv , MG/M^3-DAY]

LOG [HODv] + .376 LOG [Z_h]

HODv = hypolimnetic oxygen depletion rate $(mg/m^3$-day)

Zh = mean hypolimnetic depth (m)

The model suggests that the MODv is proportional to HODv and that the proportionality constant increases with mean hypolimnetic depth, as shown in Figure 49.

149.   The significance of the above result is that the metalimnion is more likely to be the critical region from an oxygen standpoint in a deep reservoir than in a shallow reservoir. The regression suggests metalimnetic demands tend to be relatively unimportant in shallow reservoirs. The "cross-over" point where the average MODv and HODv rates are equal is a mean hypolimnetic depth of about 10 meters. The above model can be combined with any of the above HODv models to predict metalimnetic demands as a function of chlorophyll-a and mean hypolimnetic depth.

Spatial Variations in Oxygen Depletion Rate

150.   The relationships described above permit estimation of near-dam hypolimnetic and metalimnetic oxygen depletion rates as a function of surface-water trophic state indicators and hypolimnetic morphometry. In some reservoirs, volumetric HOD rates tend to increase moving upstream from the dam in the stratified portion of the pool, with the result that anoxic conditions develop earlier at upstream stations. Between-reservoir variations indicate that near-dam volumetric HOD rates increase with surface-water chlorophyll-a content and decrease with mean hypolimnetic depth. These relationships are qualitatively consistent with within-reservoir variations, since longitudinal gradients in chlorophyll and depth both generally tend to be in directions consistent with increasing volumetric HOD rates moving upstream from the dam. Longitudinal mixing within the hypolimnion would tend to offset the effects of chlorophyll-a and depth variations, however. The applicability of the between-reservoir HOD relationships to predicting spatial variations within reservoirs is examined below.

151.   A separate data set describing spatial variations in HOD rate, water quality, and morphometry in 12 reservoirs at 46 mainstem

164

Figure 49

Ratio of Volumetric MOD Rate to Volumetric HOD Rate
vs. Mean Hypolimnetic Depth

at the

h, as

imnion

in a

ggests

hallow

d HODv

. The

redict

l mean

near-

nction

ometry.

moving

th the

ations.

D rates

th mean

sistent

nts in

sistent

e dam.

set the

The

dicting

in HOD

ainstem
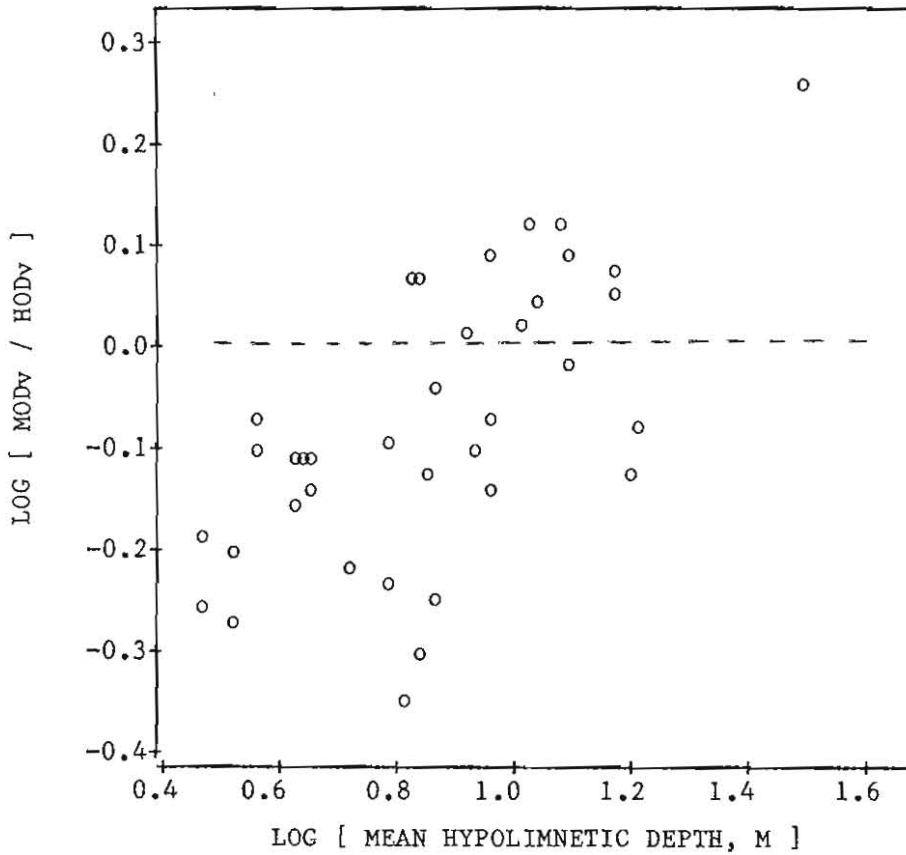
stations has been developed for model testing purposes. Mean hypolimnetic depth is a key controlling variable for between-reservoir volumetric HOD variations. One of the difficulties in treating spatial variations is the estimation of mean hypolimnetic depth at a station and subsequent expression of the HOD rate on an areal basis. The actual mean hypolimnetic depth at a station would depend upon the thermocline elevation, shape of the channel cross section, and the extent of longitudinal mixing within the hypolimnion. Because the last two are difficult to estimate without a much more exhaustive data base, a revised scheme for HOD calculation and prediction is employed below. Essentially, the scheme avoids the use of mean hypolimnetic depth by substituting maximum hypolimnetic depth as a surrogate variable, since the latter is directly obtainable from temperature profiles at a given station. HOD rates are expressed and analyzed on a volumetric, rather than areal, basis using the normalization schemes presented in Table 23.

152. Weighting of oxygen measurements within the hypolimnion at each station is done with the aid of simple geometric model which represents the channel cross-section as a single-term power function (width vs. elevation):

$$W_e = a0 \; Z_e^{a1} \tag{61}$$

where

W_e = channel width at depth Z_e (m)

Z_e = station total depth at elevation e (m)

a0,a1 = empirical parameters

Given the absence of detailed channel morphometry for each reservoir and station, an average exponent (a1) of .75 is used in the weighting calculations. Thus, the shape of an average cross section (depth vs. width) is between an inverted triangle (a1=1) and a parabola (a1=.5). The constant, "a0," factors out of the weighting calculations and does not have to be estimated. At near-dam stations, application of the above weighting scheme yields volumetric HOD rates which generally agree

to within 10% of rates calculated using detailed reservoir morphometric curves.

153. Remaining calculation procedures and screening criteria are similar to those used in estimating the near-dam depletion rates. The data set consisting of station identifiers, maximum total depth, maximum hypolimnetic depth, volumetric HOD rate, and mean chlorophyll-a is listed in upstream order within each reservoir in Appendix A.

154. Of the normalization schemes presented in Table 23, the following model has been selected for use in the spatial analysis:

$$Y_d = B_d^{.5} / Z_{xhd} \qquad (62)$$

$$\log(HOD_{vd}) = 2.94 + \log(Y_d) \qquad (R^2=.872, SE^2=.014) \qquad (63)$$

where

d = subscript denoting near-dam conditions

Y = composite variable reflecting HODv potential

Z_{xh} = maximum hypolimnetic depth (m)

This relationship is calibrated for predicting near-dam depletion rates as a function of near-dam chlorophyll-a and maximum hypolimnetic depth.

155. The station data set permits estimation of a Y value for each station. A comparison of between-reservoir vs. within-reservoir relationships is possible by applying the above equation to data from upper pool stations. In order to permit a focus on within-reservoir variations, calculated values of $\log(HODv)$ and $\log(Y)$ at each station have been subtracted from their respective near-dam values and plotted in Figure 50. A line of slope one would indicate a similarity between the within-reservoir and between-reservoir responses of HODv to changes in chlorophyll-a and maximum hypolimnetic depth.

156. Results indicate that spatial trends in volumetric HOD rates exist but are generally less dramatic than those predicted by the between-reservoir model. The lower sensitivity of the spatial variations may reflect longitudinal mixing within the hypolimnion.

167

Figure 50
Within-Reservoir Variations in Volumetric Oxygen Depletion
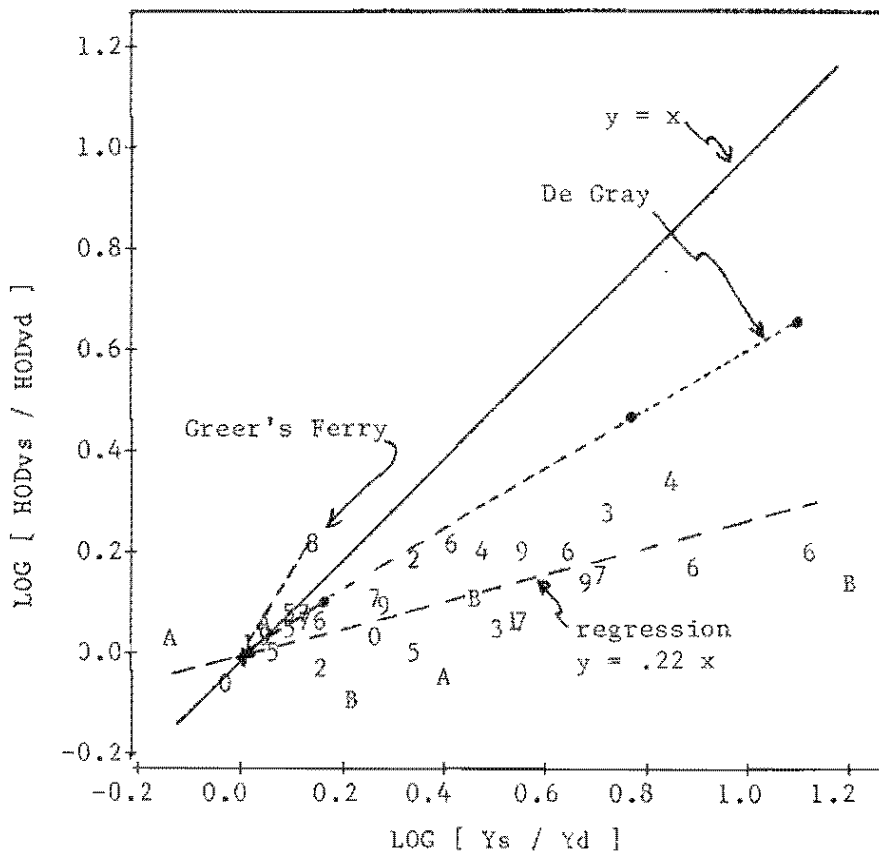
Note: Vertical Axis = log (HODv at station / HODv at dam)
Horizontal Axis = log (Y at station / Y at dam)

$Y = \sqrt{\text{Chlorophyll-a / Maximum Hypolimnetic Depth}}$

solid line = predictions of between-reservoir HODv model
dashed line = average within-reservoir response

Symbol	Reservoir		Symbol	Reservoir	
1	03307	Beltzville	7	24013	Bull Shoals
2	16393	Tygart	8	24016	Greers Ferry
3	17391	Summersville	9	24022	Norfork
4	18097	Brookville	0	24200	Table Rock
5	19122	Cumberland	A	25278	Tenkiller Ferry
6	24011	Beaver	B	30235	Sakakawea

Regression analysis of the differenced data set yields the following model:

$$\log(HOD_{vs} / HOD_{vd}) = f \log(Y_s / Y_d) \quad (R^2 = .49, \; SE^2 = .0047) \quad (64)$$

where

f = spatial response slope, averaging .22

This equation is indicated by the dashed line in Figure 50 with an average response slope of .22.

157. Analysis of residuals indicates that the above model tends to overpredict the spatial effect at stations with total hypolimnetic depths less than about 7 meters. This might be attributed to effects of incomplete organic matter oxidation in shallow hypolimnia and is qualitatively consistent with the residual patterns observed for shallow lakes (see Figure 39). The calibration and error statistics exclude data from four stations with maximum hypolimnetic depths less than 7 meters.

158. Figure 50 suggests a much higher spatial sensitivity in one reservoir (Greers Ferry, Code 24-016, symbol = 8) than in the others, since data from one upper pool station lie slightly above the prediction of the between-reservoir response model. This higher sensitivity is possibly explained by the irregular morphometry of the reservoir. The upper-pool and near-dam stations are separated by a narrow channel, which would tend to inhibit horizontal mixing within the hypolimnion, or possibly create two separate hypolimnetic basins, depending upon depth, velocity, and stratification potential within the channel. Results from Greers Ferry are consistent with the hypothesis that the lower spatial sensitivity in most reservoirs results from horizontal mixing within the hypolimnion. Data from this reservoir have been excluded from the parameter estimates and error statistics given above.

159. The combined model for predicting the volumetric oxygen depletion rate at a station is given by:

$$\log(HOD_{vs}) = \log(HOD_{vde}) + f \log(Y_s / Y_d) \quad (65)$$

where

169

$$\text{HOD}_{vde} = \text{estimated near-dam depletion rate } (mg/m^3\text{-day})$$

An advantage of this approach is that it separates the between-reservoir and within-reservoir variations. Any of the models developed in the previous section for predicting near-dam depletion rates based upon mean hypolimnetic depth, spatially weighted, or near-dam concentrations of chlorophyll-a or other trophic indicators can be used to estimate the near-dam depletion rate. The second term modifies this estimate to account for within-reservoir variations. The total variance of the predicted station $\text{HOD}v$ rate represents the sum of the variance associated with the within- and between-reservoir models.

160. Alternative models for estimating the within-reservoir variation component based upon variations in maximum depth and/or maximum hypolimnetic depth are presented in Table 25. These can be used in situations where estimates of spatial variations in chlorophyll-a are not available. Chlorophyll-a variations should be included where possible, however, particularly in reservoirs which have unusual nutrient loading and chlorophyll distributions. For example, the models based upon depth alone perform relatively poorly on Table Rock Reservoir, which is the only reservoir in the data set with significant increases in chlorophyll-a moving down the pool. These increases reflect point-source phosphorus loadings at an intermediate point along the length of the reservoir.

161. Some variations in the spatial response slope (f) would be expected from one reservoir to another, because of variations in the morphometric and hydrodynamic factors which would control longitudinal mixing within the hypolimnion. EWQOS Field Study data from De Gray reservoir (listed in Table 24) have been used for testing Equation 65. Figure 51 shows that spatial sensitivity is higher in this project than the others (averaging about .6). Thus, if data are available, recalibration of the response slope for individual reservoirs seems appropriate. Figure 51 presents a histogram of average response slopes calibrated separately for each project. The distribution suggests a median response slope of about .27, somewhat higher than the pooled

170

Table 25

Models for Within-Reservoir Variations in Volumetric HOD Rates
Based Upon Chlorophyll-a, Maximum Hypolimnetic Depth,
and Maximum Total Depth *

Symbols:

$HODv$ = volumetric oxygen depletion rate (mg/m^3-day)
B = mean chlorophyll-a (mg/m^3)
Zx = maximum depth (m)
Zxh = maximum depth of hypolimnion (m)
h = subscript denoting hypolimnetic conditions
d = subscript denoting near-dam station
s = subscript denoting upper pool station

	R^2	SE^2 **
$\log(HODvs/HODvd) = .22 \log[(Bs/Zxhs)/(Bd/Zxhd)]$	.494	.0047
$\log(HODvs/HODvd) = .29 \log[(Bs/Zxs)/(Bd/Zxd)]$	.406	.0056
$\log(HODvs/HODvd) = -.23 \log(Zxhs/Zxhd)$	.412	.0054
$\log(HODvs/HODvd) = -.40 \log(Zxs/Zxd)$	.401	.0055

* Based upon data from 11 reservoirs and 40 stations, excluding
  data from four stations with hypolimnetic depths less than
  7 meters and from Greers Ferry Reservoir, which may have two
  separate hypolimnetic basins (see text).

** Mean squared errors of within reservoir models corrected
   for degrees of freedom used in subtracting reservoir
   conditions from station conditions, i.e.:
   Error Mean Square = Residual Sum of Squares / 28

171

Figure 51
Distribution of Average Spatial Sensitivity Coefficients
Estimated for Individual Reservoirs

minimum of interval

>1.00 24016   (Greer's Ferry)

0.65|
0.60| 22014   (De Gray)
0.55|
0.50|
0.45|
0.40| 18097
0.35|
0.30| 24011 24013 24022
0.25| 16393 19122 24200
0.20| 17391
0.15| 30235
0.10| 03307
0.05| 25278
0.00|

Sensitivity Coefficient estimated from average value of:

$$\log [\ HOD_{vs} / HOD_{vd}\ ] / \log [\ (\ \sqrt{B_s}\ /\ Z_{hxs}\ )\ /\ (\ \sqrt{B_d}\ /\ Z_{hxd}\ )\ ]$$

within each reservoir

regression result (.22). The higher sensitivity of De Gray might be related to its relatively long hydraulic residence time, 2.8 years, compared with values ranging from .1 to 1.4 for the other projects tested. Development of empirical methods for predicting between-reservoir variations in spatial response slope as a function of morphometric and hydrodynamic variables may be feasible using a larger data set.

PART VI: INTERNAL RELATIONSHIPS

Introduction

162.   This   chapter   develops   models   which   relate   nutrient
concentrations and other impoundment characteristics to measures of
trophic   state,   including   chlorophyll-a,   transparency,   and   organic
nitrogen.   The chapter is organized in the following manner:

a. Data set refinements.

b. Nutrient partitioning models.

c. Chlorophyll-a models.

d. Non-algal turbidity and transparency models.

Relationships developed in this section can be linked with nutrient
retention models and used to assess the sensitivities of impoundment
water quality conditions to external nutrient loadings, as described in
Part VIII.

Data Set Refinements

163.   A data set describing water quality conditions in 67 CE
impoundments is used for model testing purposes. Summary statistics are
area-weighted, reservoir mean concentrations of surface samples (0 to
4.6 m) taken between April and October.   A total of 62 of the
impoundments were sampled at least three times between April and October
by the EPA National Eutrophication Survey. Screening criteria used to
develop the data set have been described previously (Walker, 1982a).
The data set is listed and summarized in Appendix A.

164.   To broaden regional coverage and improve the assessment of
internal relationships in small, rapidly flushed impoundments, the
EPA/NES data have been supplemented with data from five New England
Division (NED) impoundments (Parker et al., 1982).   In these cases, the
summary values are medians of 0- to 4.6-meter samples. The five NED
impoundments included in the model testing data sets were also included

in the CE reservoir data base developed at the beginning of this study (Walker, 1981).

165. Summer hydraulic residence times for each impoundment have been computed from the outflow and change in storage terms of the hydrologic balances from May through September and the mean pool volumes over that period. In cases with zero or negative net outflow (discharge + change in storage) over the summer period, summer residence times have been set equal to 3 years. Residence time enters into chlorophyll model equations as flushing rate $(1/T)$, and the flushing rate term has negligible effect on the predicted chlorophyll response at a residence time of 3 years. Thus, for the purposes of modeling chlorophyll response to pool nutrient levels, a residence time of 3 years is essentially the same as one of infinity.

Nutrient Partitioning Models

166. The partitioning of nutrients and light extinction among various dissolved and particulate components in the reservoir water column determine the amount of biomass which is produced for a given amount of total nutrient. Results of preliminary model testing indicate that the assumption that chlorophyll can be predicted directly from total phosphorus is weak in many reservoirs because of possible controlling effects of non-algal turbidity, nitrogen, depth, and/or flushing rate. An understanding of nutrient partitioning is essential to assessing the factors controlling chlorophyll-a production in a given impoundment and to the formulation, calibration, and application of empirical models.

167. Available monitoring data from CE impoundments permit estimation of the following nutrient compartments which are useful for descriptive purposes:

     a. Algae-related.

     b. Turbidity-related.

     c. Other.

In a given water sample, the sum of these compartments (or phases)

equals the total measured nutrient concentration. Since the individual phases are not directly measured, regression models have been developed to relate each phase to directly observed quantities. The algae-related phase is assumed to be proportional to mean chlorophyll-a concentration. The term "turbidity" is used loosely in this report and in the model testing report (Walker, 1982a) to mean that portion of light extinction (as measured by inverse Secchi depth) which is unrelated to chlorophyll-a, assuming that the average chlorophyll-related component is given by .025 times the chlorophyll-a concentration. The turbidity-related phase is assumed to be proportional to the non-algal turbidity level, estimated from chlorophyll-a and Secchi depth measurements. Color would also influence non-algal light extinction, but is probably relatively unimportant in most of these impoundments. The last phase includes other (primarily dissolved) inorganic and organic compounds and is assumed to be proportional to the measured ortho-phosphorus or inorganic nitrogen concentrations.

168. Using a nonlinear regression algorithm, parameters have been estimated to minimize the sums of squares of the log-transformed observed nutrient concentrations. The models are summarized by the following:

$$P = -5.7 + 1.45 \text{ Portho} + 1.72 \text{ B} + 16.8 \text{ a} \tag{66}$$

$$N = 146 + 1.09 \text{ Ninorg} + 22.2 \text{ B} + 44.2 \text{ a} \tag{67}$$

$$a = 1/S - .025 \text{ B} \tag{68}$$

where

P = total phosphorus (mg/m^3)
$Portho$ = ortho-phosphorus (mg/m^3)
N = total nitrogen (mg/m^3)
$Ninorg$ = inorganic nitrogen (mg/m^3)
B = mean chlorophyll-a (mg/m^3)
S = mean Secchi depth (m)
a = non-algal turbidity $(1/m)$

176

Details on the parameter estimates and error statistics are given in Table 26. The calibrated models (Figures 52 and 53) explain 93% and 96% of the variance in the total phosphorus and total nitrogen concentrations, respectively. Another set of models in Table 26 has been calibrated for predicting organic nitrogen and particulate phosphorus (total - ortho) based upon chlorophyll-a and non-algal turbidity levels. Observed and predicted concentrations are shown in Figures 54 and 55, respectively.

169. Residuals analysis indicates that nitrogen partitioning in the 5 New England Division (NED) impoundments studied is significantly different from that observed in the remaining 62 reservoirs. The NED impoundments are relatively unproductive and rapidly flushed, and under-prediction of nitrogen in these cases may be due to higher levels of allochthonous organic nitrogen, regional factors, and/or differences in analytical procedures between the EPA/NES and NED data. Both models have been fit to a separate data set excluding the NED impoundments (Table 26), but differences in fit are significant only in the case of nitrogen. Another reservoir (Tygart, 16-393) has also been excluded from the particulate phosphorus regressions because of the low percentage accuracy in the mean particulate phosphorus concentration (1 mg/m^3), computed from mean total and ortho-P concentrations of 5.5 mg/m^3 and 4.5, mg/m^3, respectively. Particulate phosphorus concentrations computed from total and ortho measurements would also include dissolved, non-ortho-phosphorus which may be appreciable in some cases.

170. A constant intercept term has also been included in each model. Diagnostic plots indicate that the negative intercept for phosphorus may reflect the fact that an average of about .3 l/m of non-algal turbidity is uncorrelated with phosphorus. The actual turbidity-related component of total phosphorus is more accurately given by $16.8(a-.3)$. The nitrogen models have strong positive intercepts ($146-247 \text{ mg/m}^3$), which may reflect baseline levels of dissolved organic nitrogen compounds (which would not necessarily be proportional to the dissolved inorganic fractions). Higher levels of these materials could be responsible for the NED impoundment deviations. The lower analytical

Table 26

Parameter Estimates of Nitrogen and Phosphorus Partitioning Models

	Intercept	Ortho-P or Inorg N	Chl-a	Non-Algal Turbidity	R^2	SE^2
All Data (n = 67)						
Total Phosphorus						
mean	-5.7	1.45	1.72	16.8	.934	.0099
std error	1.2	.16	.18	2.5		
Total Nitrogen						
mean	247	.98	18.1	52.9	.895	.0077
std error	28	.08	2.6	35.7		
N/P			10.5	3.2		
Minus New England Impoundments (n = 62)						
Total Phosphorus						
mean	-5.0	1.44	1.61	18.0	.929	.0096
std error	1.3	.16	.18	2.6		
Total Nitrogen						
mean	146	1.09	22.2	44.2	.960	.0030
std error	18	.05	1.7	21.3		
N/P			13.8	2.5		
Excluding Inorganic Phases **Minus New England Impoundments and Tygart (Code 16393)* (n=61)**						
Particulate Phosphorus (Total P - Ortho-P) *						
mean	-4.1	—	1.78	23.7	.843	.023
std error	1.2	—	.21	2.6		
Organic Nitrogen						
mean	157	—	22.8	75.3	.735	.012
std error	22	—	2.4	19.2		
N/P			12.8	3.2		

* Tygart excluded because of low percentage accuracy in average particulate phosphorus concentration (1 mg/m^3), computed from average total and ortho-P concentrations of 5.5 and 4.5 mg/m^3, respectively.

** "Particulate" also includes dissolved, non-ortho-phosphorus;

Figure 52

Performance of Phosphorus Partitioning Model
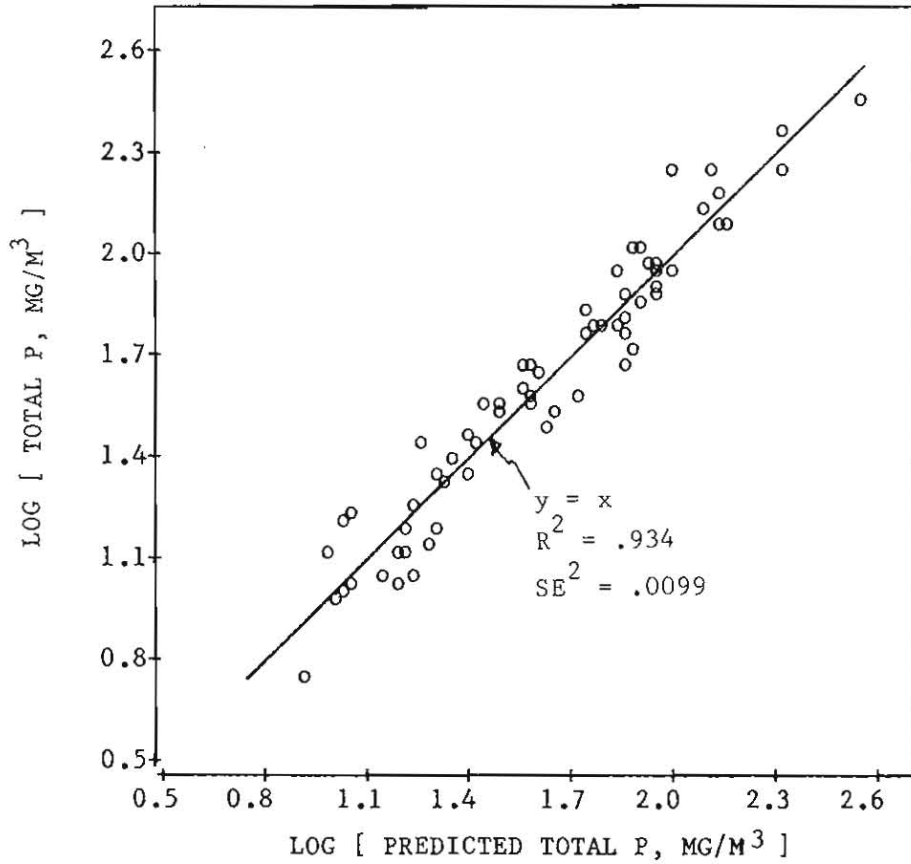
Model:

$$P = -5.7 + 1.45 \text{ P-ortho} + 1.72 \text{ B} + 16.8 \text{ a}$$

$$a = 1/S - .025 \text{ B}$$

179

Figure 53

Performance of Nitrogen Partitioning Model
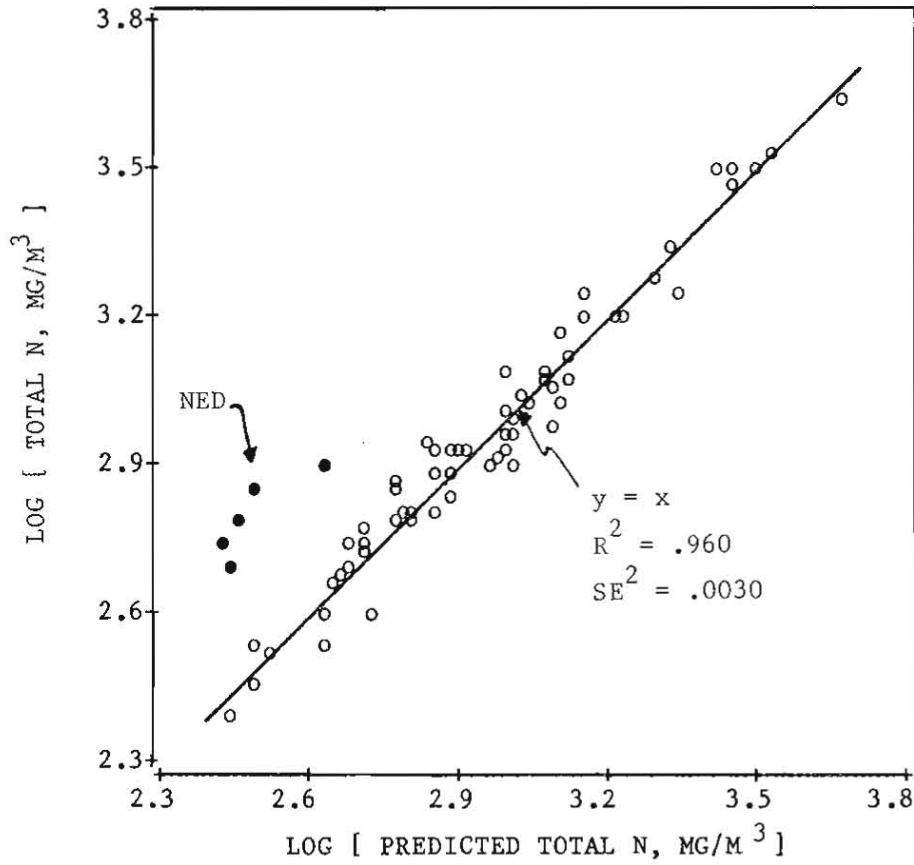
Model:

$$N = 146 + 1.09 \text{ N-inorg} + 22.2 \text{ B} + 44.2 \text{ a}$$

$$a = 1/S - .025 \text{ B}$$

180

Figure 54

Observed and Predicted Organic Nitrogen Concentrations
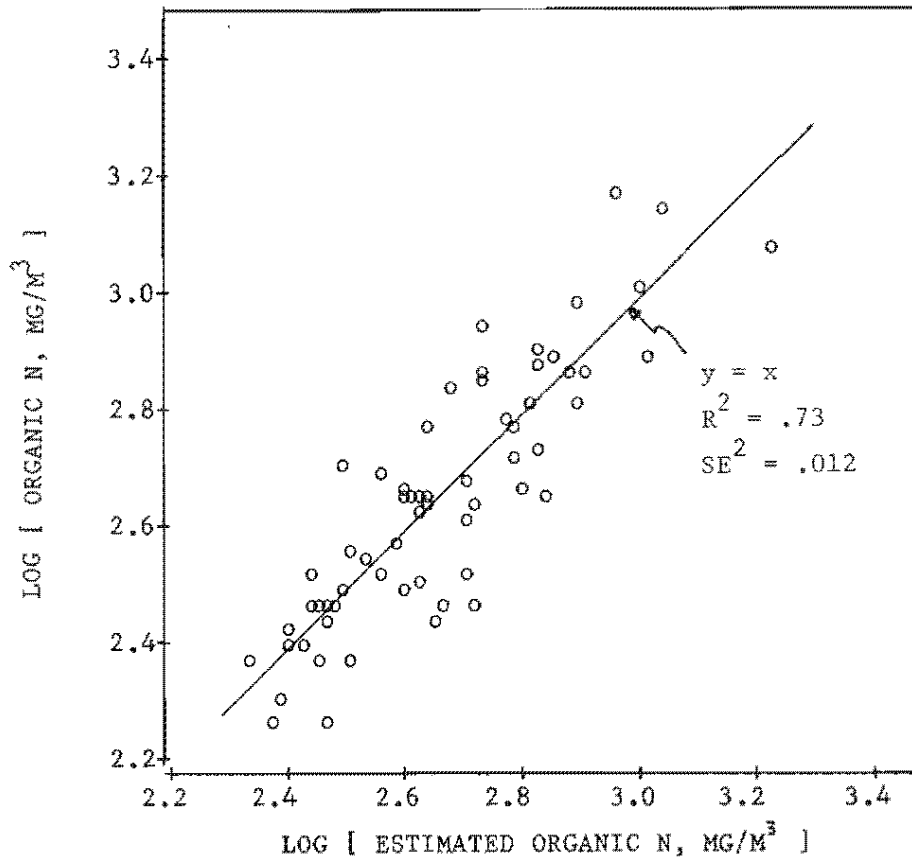
Model:

Norg = 157 + 22.8 B + 75.3 a

a = 1/S — .025 B

Figure 55

Observed and Predicted Particulate Phosphorus Concentrations
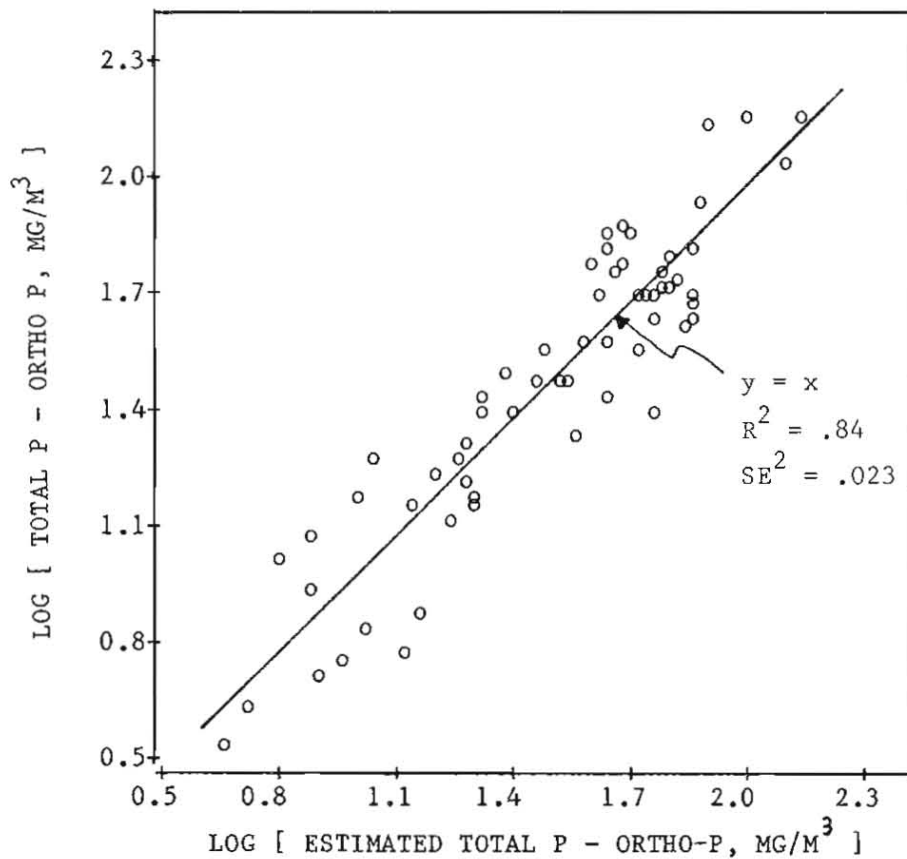
Model:

$$P - P_{ortho} = -4.1 + 1.78 \ B + 23.7 \ a$$

$$a = 1/S - .025 \ B$$

detection limit for Kjeldahl nitrogen (200 mg/m^3) provided by the EPA National Eutrophication Survey may also be a factor, although the intercept term does not vary significantly (mean = 161, standard error = 21) when impoundments with organic nitrogen concentrations less than 300 mg/m^3 are excluded, along with the NED impoundments, from the regression for total nitrogen.

171. Parameter estimates indicate that non-algal turbidity is more significant in phosphorus partitioning than in nitrogen partitioning. For the three sets of models calibrated in Table 26, the N/P ratio of the chlorophyll-related term ranges from 10 to 14, while that of the turbidity-related term ranges from 2.5 to 3.2. Some of the turbidity-associated phosphorus may be labile (readily desorbed) and should not necessarily be considered as unavailable for the purposes of predicting potential chlorophyll-a levels from total nutrient concentrations. As demonstrated in the next section, the effects of turbidity on chlorophyll-a production appear to be related primarily to a light-limitation mechanism.

172. Deviations from the relationships in Figures 52-55 reflect the combined influences of statistical errors in the dependent and independent variables and model error attributed to variations in the proportionality coefficients from one impoundment to another. The latter would, in turn, reflect variations in the nutrient requirements of algal species, environmental conditions, and physical/chemical characteristics of non-algal suspended solids and color. Despite the potential for parametric variations, the models explain high proportions of the variance in the observed data with constant coefficients and appear to be useful for descriptive purposes. Regional calibration of some coefficients (especially those representing turbidity effects) may be appropriate.

173. Figure 56 demonstrates a fundamental difference between phosphorus and nitrogen partitioning which results from the significant positive intercept in the nitrogen model. The lines in these plots represent the estimated chlorophyll-related component of non-ortho-phosphorus and organic nitrogen, respectively. Positive deviations from

183

Figure 56
Chlorophyll-Related Components of Nutrient Partitioning Models

o = chlorophyll-dominated (B*S > 8)
x = turbidity-dominated (B*S < 8)

184
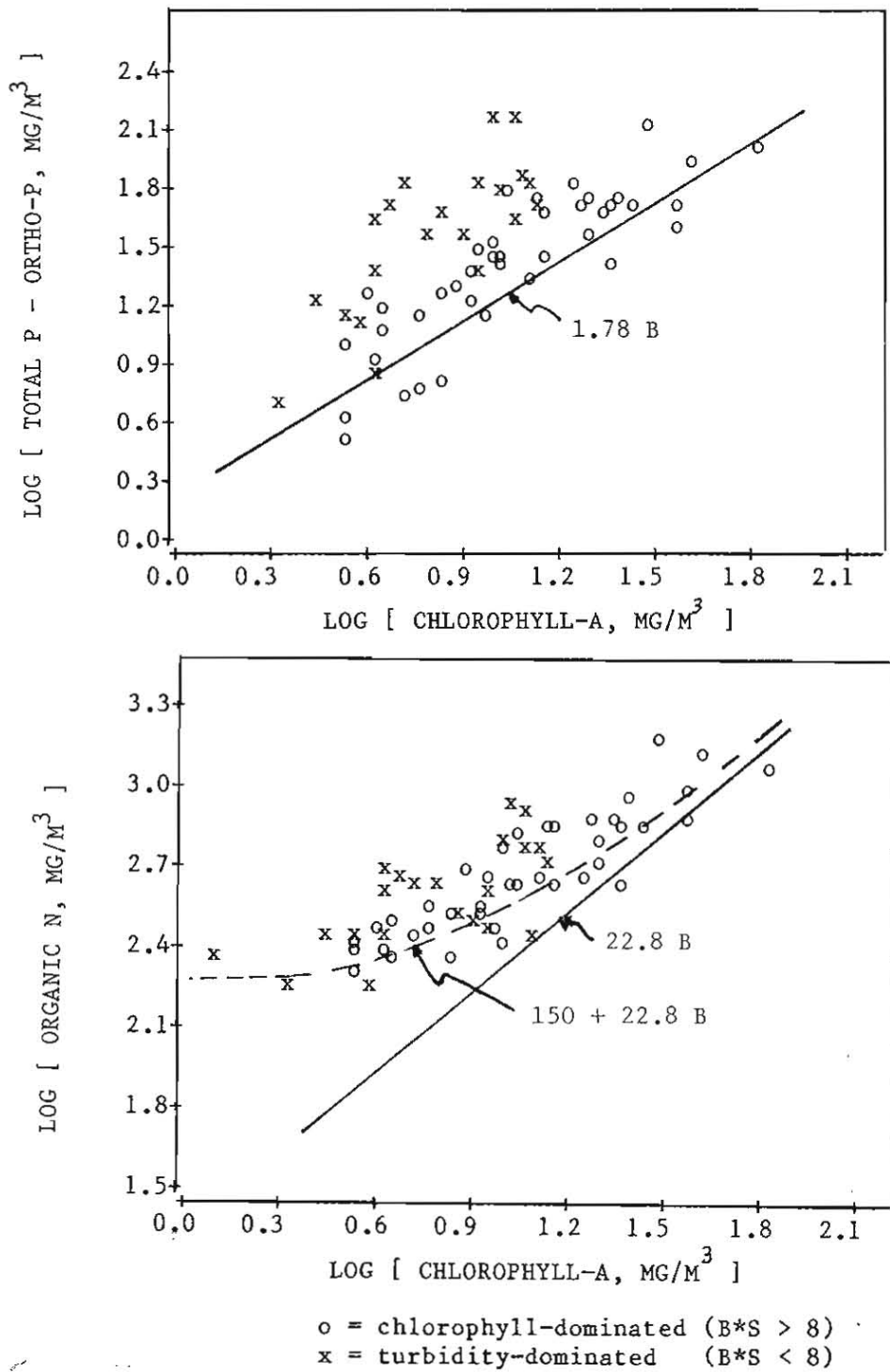
the lines reflect influences of non-algal turbidity. Based upon Equation 68, the product of chlorophyll and transparency is an indicator of the relative importance of chlorophyll vs. non-algal turbidity as factors contributing to light extinction (Walker, 1982a). Reservoirs with low chlorophyll-transparency products are dominated by non-algal turbidity and tend to show positive deviations in Figure 56, particularly in the case of phosphorus. All reservoirs show positive deviations from the chlorophyll-related component of organic nitrogen in the low-chlorophyll range. These deviations reflect the intercept of the nitrogen partitioning model, as indicated by the dashed line.

174. Figure 57 plots the ratio of organic N to non-ortho-P as a function of chlorophyll for algae-dominated systems ($B*S > 8$). Because of the nitrogen intercept term, the ratio tends to be higher at lower chlorophyll levels. Figure 57 also indicates that this behavior is not an artifact of the EPA/NES data, since basically the same relationship is found in impoundments studied under OECD Reservoir and Shallow Lakes Program (Clasen, 1980) and OECD Alpine Lakes Program (Fricker, 1980). Because of the nitrogen intercept term, the organic N/non-ortho-P ratio ranges from about 50 at low chlorophyll-a levels to about 12 at high chlorophyll-a levels. Based upon the N partitioning model, most of the organic nitrogen in relatively oligotrophic systems is unrelated to chlorophyll. Figure 58 plots organic nitrogen against non-ortho-P using different symbols to identify algae-dominated and turbidity-dominated systems. There are significant positive deviations from a constant N/P ratio of 12 at low non-ortho-phosphorus levels. Most of these deviations are corrected when an average nitrogen intercept, 150 mg/m^3, is subtracted from organic nitrogen.

175. Subtracting the nitrogen intercept term from the organic nitrogen concentration is required in order to stabilize the N/P ratio of the organic phase over the observed range of nutrient and chlorophyll-a levels. Because it represents the fraction of organic nitrogen which is uncorrelated with chlorophyll, the intercept term can be treated as "unavailable" nitrogen and probably represents relatively stable dissolved organic nitrogen compounds, possibly of allochthonous

Figure 57

Organic N/Non-Ortho-P vs. Chlorophyll-a in Algae-Dominated Systems
Derived from OECD and CE Data Sets
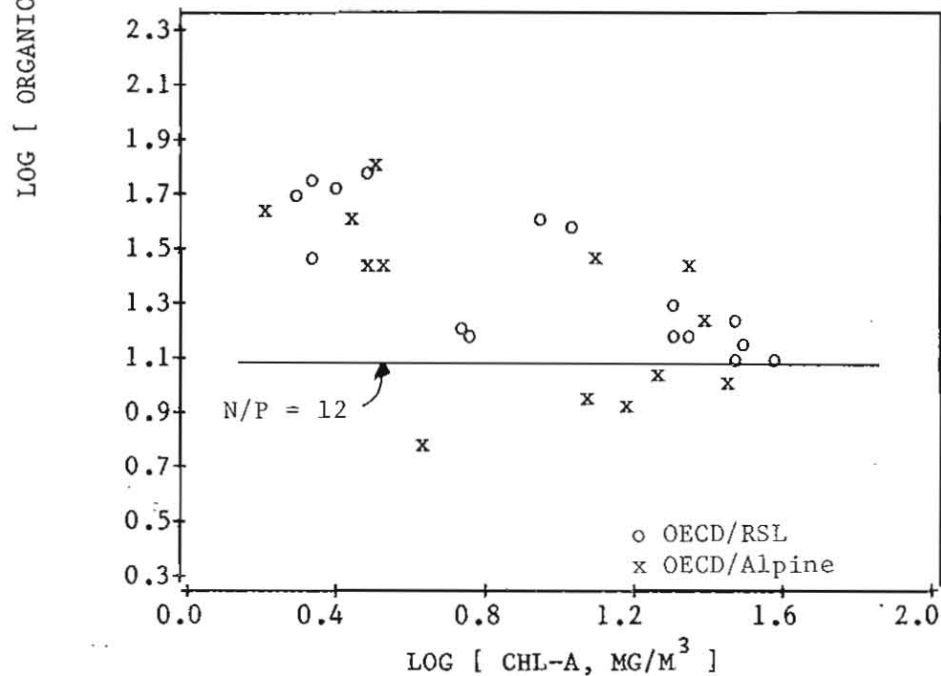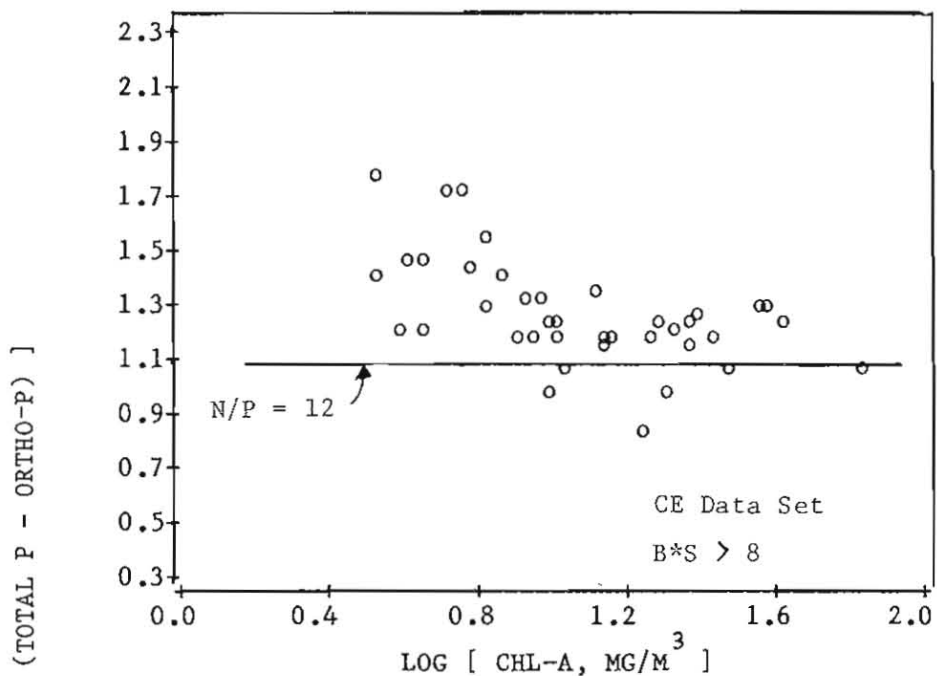
Figure 58
Organic N vs. Non-Ortho-Phosphorus
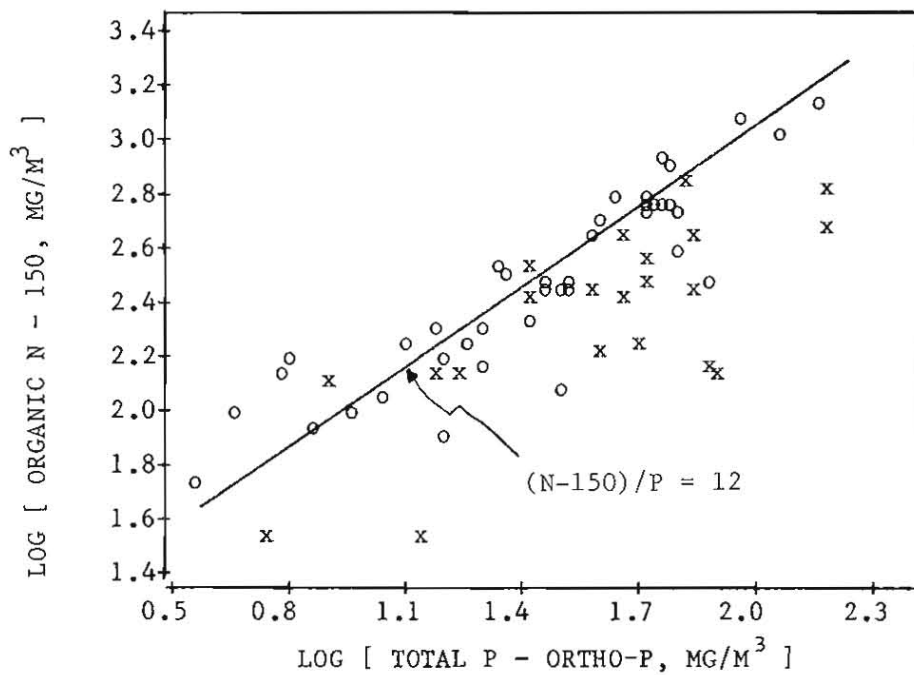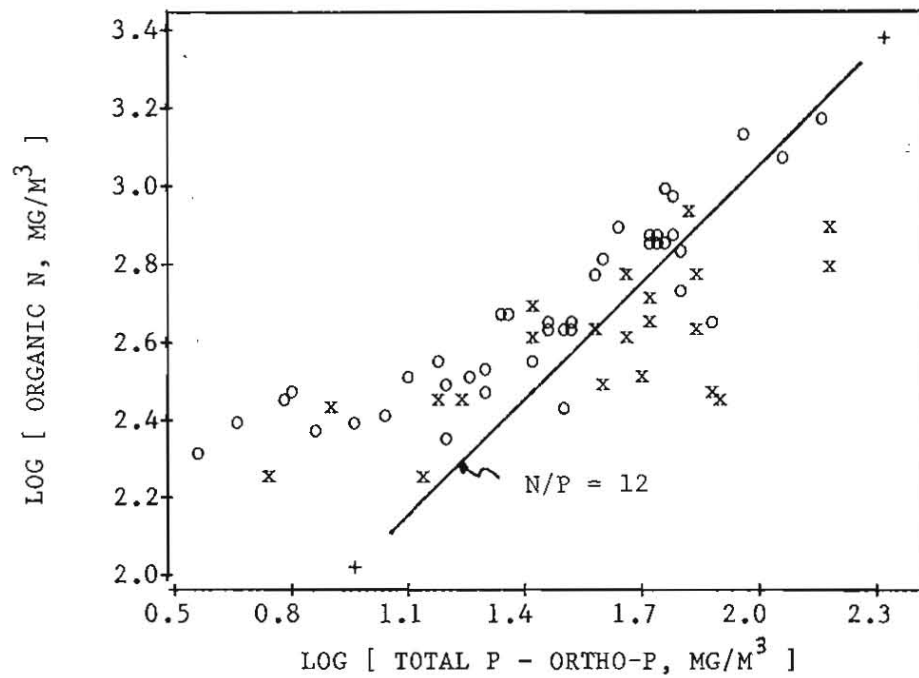
o = chlorophyll-dominated (B*S > 8)
x = turbidity-dominated   (B*S < 8)

origin. At high chlorophyll-a levels, the N/P ratio (or (N-150)/P ratio) in the organic phase approaches 12, which can be taken as an average algal nutritional requirement. These results have some important implications for prediction of chlorophyll-a concentrations from total nitrogen and total phosphorus concentrations, as developed in the next section.

Chlorophyll-a Models

Introduction

176. Preliminary testing has indicated that models relating chlorophyll-a to reservoir nutrient concentrations or normalized loadings generally have higher error variance than models for predicting other eutrophication-related variables. This reflects the inherent variability of algal populations, sparse sampling regimes, limitations in the chlorophyll-a measurement as an indicator of algal biomass, and the relatively simplistic nature of the models. Residuals analyses have indicated, however, that some of the error variance is not random, but is systematically related to certain impoundment characteristics, including nitrogen, non-algal turbidity, flushing rate, and depth. These dependencies suggest that there is room for model improvement. Most existing models assume that chlorophyll is related directly to total phosphorus concentration. Some of the variability in the slopes and intercepts of published phosphorus/chlorophyll-a regressions may be attributed to variations in other controlling factors. A more complex model is needed if it is to be generally applicable to reservoirs.

177. Development of a general model involving more than one independent variable would be preferable to calibration of simplified models separately to different data subsets (e.g., based upon N/P ratio, turbidity, flushing rate). Subsetting reduces model generality, causes parameter estimation problems because of loss of degrees of freedom, tends to create artificial classifications, and can cause difficulties in applications to reservoirs which are at or near one or more of the subset boundaries.

178. One approach to model refinement would be to expand the linear or log-linear regression model to include additional independent variables. While a multiple regression model may explain additional variance across impoundments, it may not be satisfactory for predicting the response of a given impoundment to changes in one or more of the independent variables because the linear model formulations are relatively rigid and simplistic and may not adequately reflect the dynamics and sensitivity of the system. A multivariate model which is formulated based upon theoretical considerations and calibrated to the data would have a greater chance of representing chlorophyll dynamics in a realistic manner. This approach is taken below.

Chlorophyll vs. Nitrogen and Phosphorus in Low-Turbidity Reservoirs

179. To reduce the dimensions of the problem, it is convenient to begin model development by examining simultaneous variations in chlorophyll, total phosphorus, and total nitrogen in low-turbidity reservoirs. While assessment of nitrogen vs. phosphorus limitation can be made most reliably based upon inorganic N/P ratios, prediction of chlorophyll as a function of total nutrient concentrations is required for linkage to external nutrient loading models. In order to examine the effects of nutrient limitation separately, it is necessary initially to screen the data set to eliminate impoundments in which light-limitation may be important. Based upon preliminary model testing, these conditions can be met approximately by excluding impoundments with non-algal turbidities greater than .4 1/m. When this constraint is applied, the summer hydraulic residence times of the remaining 20 impoundments exceed .04 year or 14 days and are outside of the range in which flushing is likely to be controlling. Some systematic effects of light-limitation remain in this restricted data set; these are relatively small but are considered in the more general model developed subsequently.

180. Figure 59 shows the average response of chlorophyll-a to total phosphorus and total nitrogen concentrations, based upon data from 159 station-years with non-algal turbidities less than .4 1/m and at

189

Figure 59

Response of Chlorophyll-a to Nitrogen and Phosphorus at
Low-Turbidity Stations Derived from Polynomial Regression
(Walker,1982b)
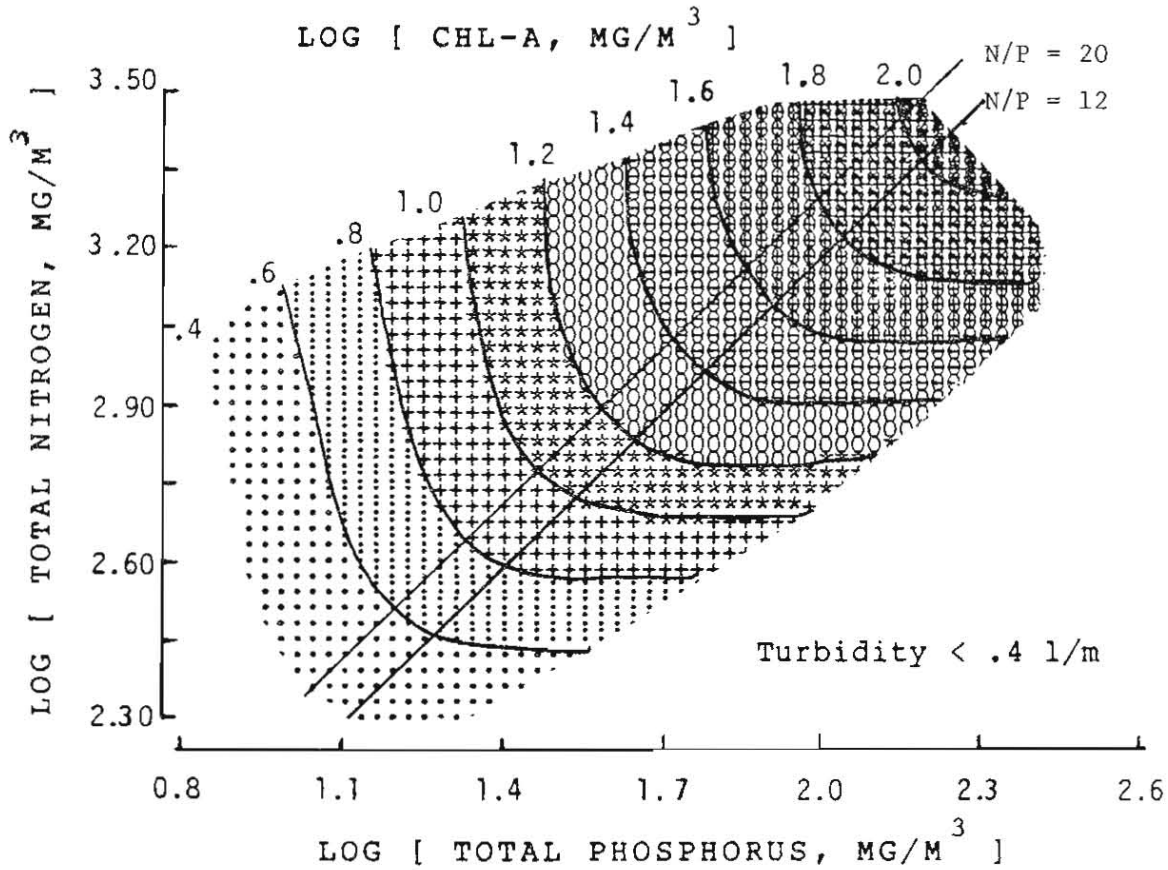
least two sampling dates per growing season (Walker, 1982b). The chlorophyll-a contours are based upon a cubic polynomial response surface with linear and quadratic interaction terms for total nitrogen and total phosphorus. This methodology provides a capability for fitting a wide variety of possible response surface shapes without having to specify model structure in great detail (Box et al., 1978). The response surface has been trimmed to reflect data regions on the N vs. P plane. The intent is to provide a data summary which reflects the basic shape of the chlorophyll response to simultaneous variations in phosphorus and nitrogen; this is used below to help formulate and test a more concise model. The polynomial response surface explains 68% of the observed variance in the station-mean concentrations; 84% of the variance is explained when estimated sampling errors in the mean chlorophyll-a and nutrient concentrations are considered (Walker,1982b).

181. Sensitivities to nitrogen and phosphorus are reflected by the contour slopes and vary with location. At high N/P ratios (upper left), the contours tend to be vertical and chlorophyll levels are more sensitive to phosphorus than to nitrogen. At low N/P ratios (lower right), the contours tend to be horizontal and chlorophyll levels are more sensitive to nitrogen. The shape of the response surface is qualitatively consistent with the limiting nutrient concept; i.e., sensitivity to a each nutrient tends to increase in regions where it is in short supply relative to algal requirements, based upon the N/P ratio. At a contour angle of 45 degrees, chlorophyll-a levels are equally sensitive to nitrogen and phosphorus. This occurs at N/P ratios ranging from about 20 at low phosphorus concentrations to 12 at high phosphorus concentrations.

182. Table 27 presents eight model formulations which have been tested against data from low-turbidity systems. Figure 60 compares the response surfaces predicted by five of these models with the polynomial response surface discussed above. The Jones and Bachman (1976) model relates chlorophyll to phosphorus and is similar to several other formulations considered in preliminary testing (Walker, 1982a). The model predicts a high sensitivity to phosphorus which is observed only

191

<div align="center">

Table 27
Models for Predicting Chlorophyll-a as a Function of
Phosphorus and Nitrogen in Low-Turbidity Reservoirs

</div>

	Reservoir-Means (n = 20)		Station-Means (n = 93)	
	R^2	SE^2	R^2	SE^2

Model 01: Bachman and Jones (1976)

$\log(B) = -1.09 + 1.46 \log(P)$

| | .45 | .095 | .34 | .114 |

Model 02: Smith (1980)

$\log(B) = -3.88 + 1.55 \log(N + 16.4\ P)$

| | .75 | .044 | .62 | .066 |

Model 03: Smith (1982)

$\log(B) = -1.52 + .653 \log(P) + .548 \log(N)$

| | .75 | .043 | .57 | .074 |

Model 04: Canfield (1983)

$\log(B) = -2.49 + .269 \log(P) + 1.06 \log(N)$

| | .72 | .048 | .59 | .071 |

Model 05: This Study - Regression vs. P

$\log(B) = -0.48 + .95 \log(P)$

| | .70 | .052 | .53 | .082 |

Model 06: This Study - Regression vs. N

$\log(B) = -3.37 + 1.50 \log(N)$

| | .58 | .073 | .46 | .094 |

Model 07: This Study - Regression vs. N and P

$\log(B) = -2.50 + .678 \log(P) + .858 \log(N)$

| | .82 | .031 | .69 | .054 |

Model 08: This Study - Regression vs. Composite Nutrient

$$Xpn = [\ P^{-2} + ((N-150)/12)^{-2}\ ]^{-.5}$$

$\log(B) = -.70 + 1.25 \log(Xpn)$

| | .84 | .028 | .71 | .051 |

NOTES: non-algal turbidity = 1/Secchi − .025* chl-a < .4 1/m
all units mg/m^3.

Figure 60

Chlorophyll-a Response to Phosphorus and Nitrogen According to Various Models
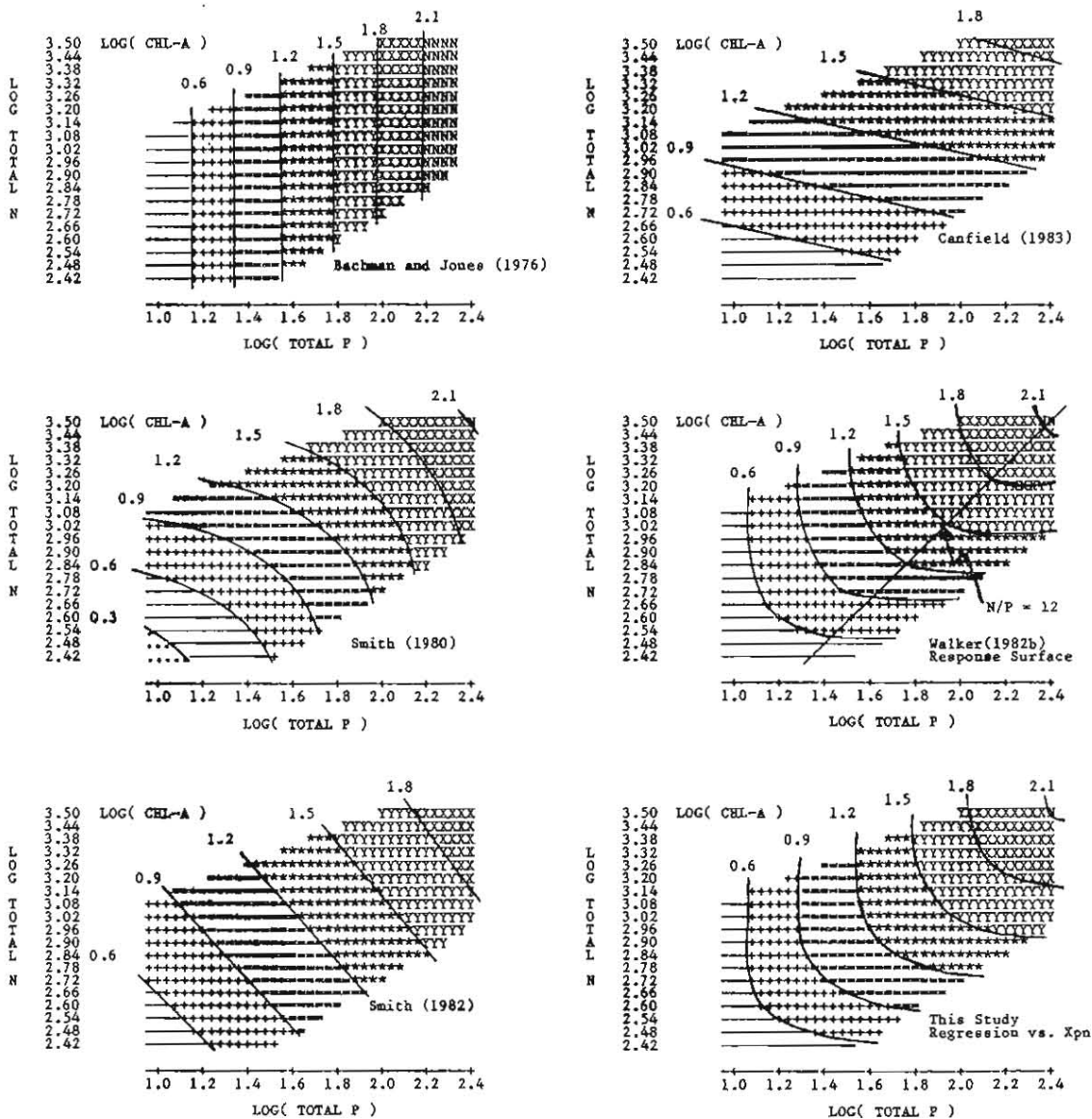
at high N/P ratios, based upon the empirical response surface, and explains only 45% of the variance in the observed reservoir-means. A multivariate model developed by Smith (1980) includes both nitrogen and phosphorus terms and explains 75% of the observed variance. The contours predicted by this model, however, are facing in the opposite direction from those in Figure 60, and suggest that chlorophyll sensitivity to phosphorus decreases with increasing N/P ratio; this result seems unrealistic.

183. Multiple regression models developed by Smith (1982) and Canfield (1983) explain 75% and 72% of the observed variance, respectively. As shown in Figure 61, the multiple regression model structure implies constant sensitivities to nitrogen and phosphorus; the chlorophyll contours are straight and parallel. Canfield's model, which is based upon data from Florida lakes, has a somewhat greater sensitivity to nitrogen. Smith found that the phosphorus slope increased from .653 to 1.173 and the nitrogen slope decreased from .548 to -.029 when his data set was restricted to lakes with total N/P ratios greater then 35. Optimization of the coefficients for the reservoir-mean data set (Model 07 in Table 27) yields slopes of .678 and .858, respectively, and increases the explained variance to 82%. While the multiple regression models explain more variance than regression on phosphorus (model 05) or nitrogen (model 06) alone, the coefficients are variable from one data set to another and the model structure requires that chlorophyll sensitivities to changes in nitrogen or phosphorus are independent of N/P ratio. The latter prediction is inconsistent with the limiting nutrient concept and the shape of the polynomial response surface.

184. Based upon error variance and response surface shape, none of the published models adequately represent the chlorophyll/nutrient relationship in low-turbidity reservoirs. A new formulation (model 08 in Table 27) has been developed which explains most of the chlorophyll variance while being consistent with the limiting nutrient concept and retaining the shape of the polynomial response surface. Chlorophyll is regressed against the following composite variable calculated from

Figure 61

Sensitivity of Composite Nutrient Concentration to
Nitrogen and Phosphorus Levels
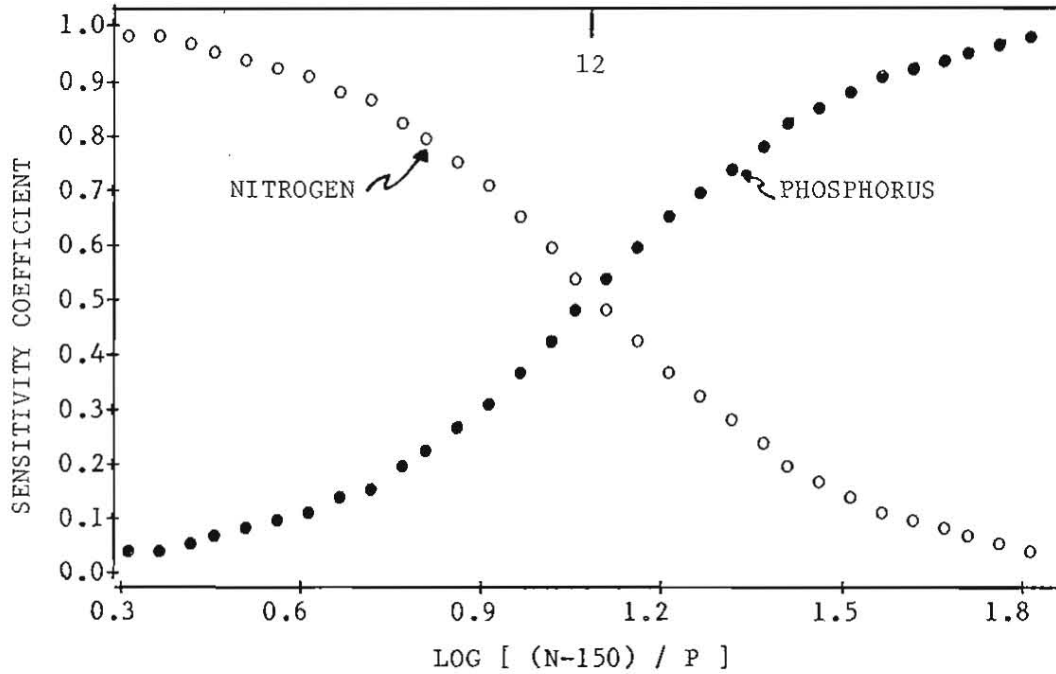
Values plotted are log-scale first derivatives:

$d \log(Xpn) / d \log(P)$ = phosphorus sensitivity

$d \log(Xpn) / d \log(N-150)$ = nitrogen sensitivity

where,

Xpn = composite nutrient concentration

$$Xpn = (P^{-2} + [(N-150)/12]^{-2})^{-.5}$$

195

phosphorus and nitrogen concentrations:

$$X_{pn} = [P^{-m} + ((N - 150)/12)^{-m}]^{-1/m} \qquad (69)$$

$$= P [1 + ((N - 150)/(12 P))^{-m}]^{-1/m} \qquad (70)$$

where

X_{pn} = composite nutrient concentration (mg/m^3)

m = nutrient exponent = 2

The composite nutrient concentration has been designed as a predictor of algal growth potential which is independent of whether phosphorus or nitrogen is limiting. As shown in Figure 61, the sensitivity of the composite nutrient concentration to changes in phosphorus (measured in terms of log derivative or percent change in Xpn for a 1 percent change in P) increases with the (N-150)/P ratio while sensitivity to nitrogen decreases. At high (N-150)/P ratios, the expression becomes equal to P and independent of N; at low ratios, it is equal to (N-150)/12 and independent of P.

185. The parameters used in the composite nutrient formulation are based upon the nutrient partitioning models developed above. The nitrogen intercept (150 mg/m^3) represents a nitrogen component which is unrelated to chlorophyll or non-algal turbidity. The nutrient ratio (N/P=12) equals the average ratio of the chlorophyll slopes in the nitrogen and phosphorus partitioning models and is thus an indicator of the average nutritional contents of algae and algae-related substances. The value of the exponent, m, partially determines the contour shape and the extent of simultaneous N and P effects. The model is relatively insensitive to this parameter; a value of 2 has been selected based upon trial and error. As shown in Figure 60, the response surface of chlorophyll predicted from regression against Xpn is reasonably similar to the polynomial response surface. The regression model explains 84% of the variance in the reservoir-mean chlorophyll measurements with a mean squared error of .028. Prediction errors are not independent of

196

mixed layer depth, however, because of the light-limitation effects described below.

General Chlorophyll-a Models

186. Preliminary model testing has indicated that variations in turbidity can have significant effects on the slopes and intercepts of chlorophyll/phosphorus regression equations in impoundments with inorganic N/P and total N/P ratios exceeding 10. The effects of non-algal turbidity on chlorophyll response to nutrients could be related to two general types of mechanisms: light-limitation and nutrient availablility. Figure 62 plots average concentrations of ortho-phosphorus and inorganic nitrogen against non-algal turbidities. In some impoundments, a portion of the total nutrient (especially phosphorus) concentration may be associated with non-algal turbidity. If this were a significant growth-limiting mechanism, one would expect lower concentrations of ortho-phosphorus in impoundments with higher turbidity. Figure 62 suggests, however, that most turbid impoundments tend to have relatively high concentrations of available nutrients. Thus, light-limitation seems more likely to be the dominant mechanism for turbidity influences on chlorophyll levels.

187. The model developed below is based upon kinetic theories of algal growth, as outlined by Lorenzen and Mitchell (1973), Meta Systems (1979), Forsberg and Shapiro (1980), and Pastorok et al. (1982). The theories attempt to consider effects of light and/or nutrient limitation on algal production in a mixed, totally absorbing surface layer. The Forsberg/Shapiro model is the only one which considers both light and nutrient limitation simultaneously. It is based upon the following differential equation for a system limited by phosphorus and/or light:

$$\frac{dB}{dt} = \frac{F\ G_{max}}{E\ Z_{mix}} \left(1 - \frac{Q_p\ B}{P} \right) B - L\ B \tag{71}$$

where

B = chlorophyll-a concentration (mg/m^3)

t = time (days)

197

Figure 62

Ortho-P and Inorganic N Concentrations Vs. Non-Algal Turbidity
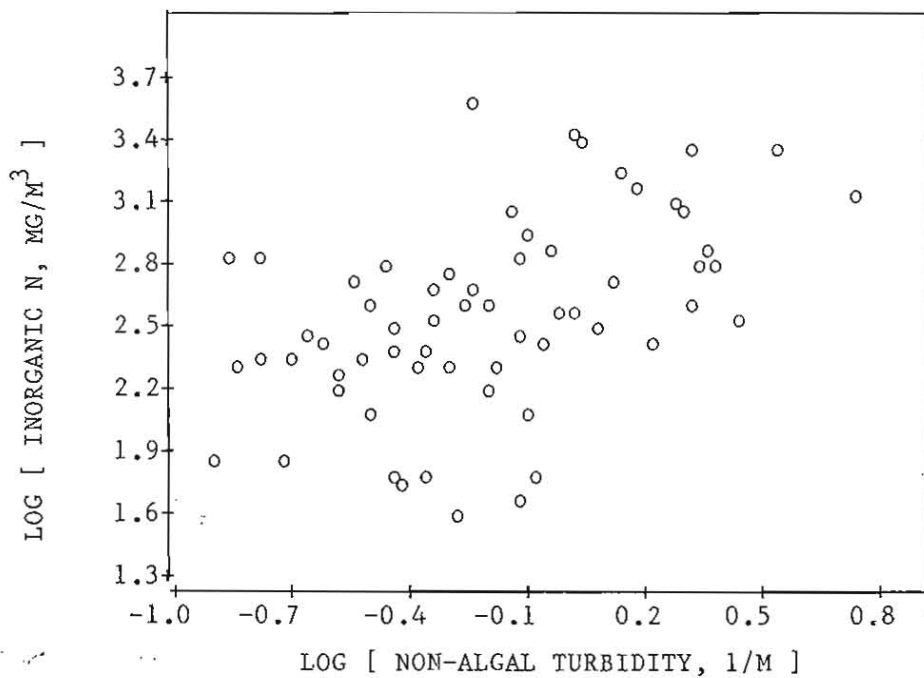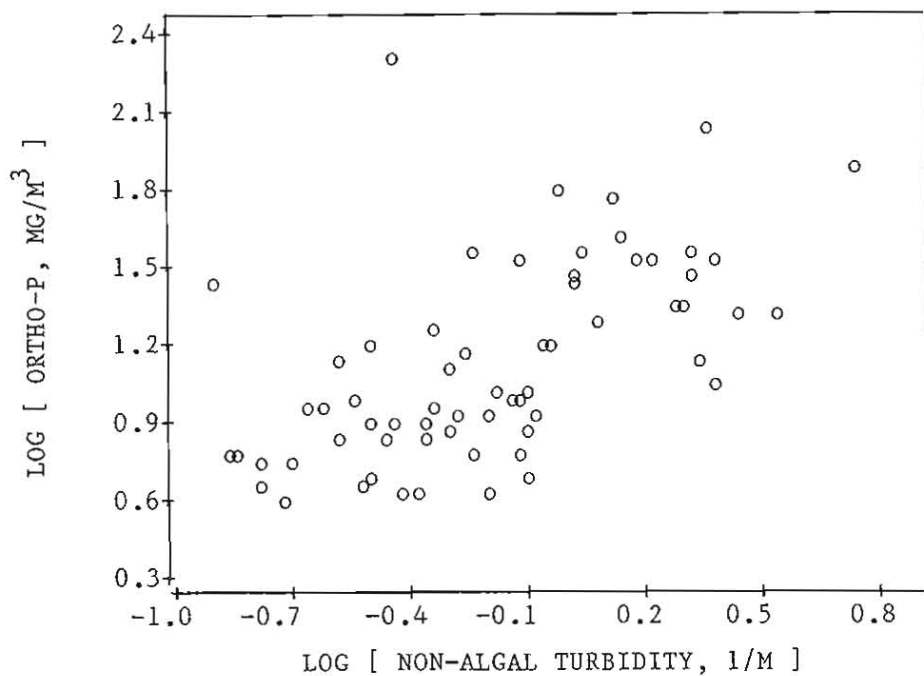
F = light integral (dimensionless)

Gmax = maximum specific algal growth rate (1/days)

E = visible light extinction coefficient (1/m)

Zmix = mean depth of mixed layer = volume / surface area (m)

Qp = algal cell quota for phosphorus (mg P / mg Chl-a)

P = total phosphorus concentration (mg/m^3)

L = total algal loss rate (1/day)

The visible light extinction coefficient, E, is related to observed Secchi depth and chlorophyll-a concentration (Meta Systems, 1979):

$$E \, S = 1.66 \qquad\qquad (72)$$

$$1/S = a + b \, B \qquad\qquad (73)$$

where

S = Secchi depth (m)

a = non-algal turbidity (1/m)

b = chlorophyll/Secchi slope (m^2/mg)

A nominal estimate of the slope parameter (b) for CE impoundments is .025 m^2/mg (Walker, 1982a). The total algal loss rate (L) can be partitioned into the following components:

$$L = D + \frac{1}{365 \, Ts} \qquad\qquad (74)$$

where

D = algal specific death rate (1/day)

Ts = summer hydraulic residence time (years)

The algal specific death rate includes limiting effects of respiration, predation and settling on the algal population. The residence time term accounts for algal removal via flushing in a mixed system.

188. By setting the time-derivative in Equation 71 equal to zero, the above equations can be solved for the maximum, steady-state

199

chlorophyll-a concentration for a given set of conditions:

$$B = \frac{P\ (\ 1 - a\ G\ )}{(\ Q_p + b\ P\ G\ )} \tag{75}$$

$$G = \frac{1.66\ Z_{mix}\ L}{G_{max}\ F} = \frac{1.66\ Z_{mix}}{G_{max}\ F}\ (\ D + \frac{1}{365\ T_s}\ ) \tag{76}$$

where

   G = dimensionless kinetic factor

The above solution follows directly from Equations 71 - 74, but differs from that presented by Forsberg and Shapiro (1980); their solution has a negative sign in the second term of the denominator, possibly attributed to a typographic error. The error was corrected in a subsequent publication by Forsberg (1980).

189. Results indicate that the chlorophyll response to phosphorus is controlled by the kinetic factor G, which is related to impoundment-specific variables Z_{mix} and T, and to algal parameters G_{max}, F, and D. The "a G" term in the numerator represents light-limitation associated with non-algal turbidity, while the "b P G" term in the denominator represents light-limitation associated with potential self-shading by phytoplankton. Both of these limiting factors vanish at low mixed depth because the light supply per unit volume is high.

190. One problem with Equation 75 is that it predicts negative algal concentrations for "a G" values exceeding 1.0. Finite algal populations would be observed, even in extremely light-limited or rapidly flushed systems, because of the potential for algal adaptation, the distribution of environmental conditions (depths, nutrient concentrations, and turbidities) within a given impoundment, and allochthonous chlorophyll-a inputs. Accordingly, the equation can been modified to reflect a decreasing response to "a G" while ensuring a positive solution. A second modification involves replacing the total phosphorus concentration with a power function of the composite nutrient concentration, developed above as a predictor of algal growth potential

which is independent of whether nitrogen or phosphorus is limiting, and dividing the numerator and denominator by the cell quota:

$$B = \frac{Bx}{(1 + b\,G\,Bx)(1 + a\,G)} \qquad (77)$$

$$Bx = \frac{Xpn^{k}}{Qx} \qquad (78)$$

where

Qx = cell quota for composite nutrient concentration

Bx = algal growth potential in absence of light and flushing controls (mg Chl-a/m^3)

k = empirical coefficient

Algal stoichiometric and kinetic parameters can be combined and estimated empirically using nonlinear regression. The unknown parameters are embedded in the following expressions:

$$G = Zmix\left(C1 + \frac{C2}{Ts}\right) \qquad (79)$$

$$Bx = Xpn^{C3} / C4 \qquad (80)$$

where

C1, C2, C3, C4 = empirical parameters

To permit calibration of the model, a Zmix value has been estimated for each impoundment as the ratio of epilimnetic volume to surface area, with thermocline depths estimated from mid-summer temperature profiles. Figure 63 shows the relationship between mean mixed-layer depth and mean total depth. The regression model explains 93 percent of the variance in Zmix and can be used in situations where estimates of thermocline depths and impoundment morphometry are not immediately available. The model should not be used outside the range of the mean depths used in

201

Figure 63

Mean Depth of Mixed Layer vs. Mean Total Depth

$$y = -.06 + 1.36 \, x - .47 \, x^2$$
$$r^2 = .932, \quad se^2 = .0026$$
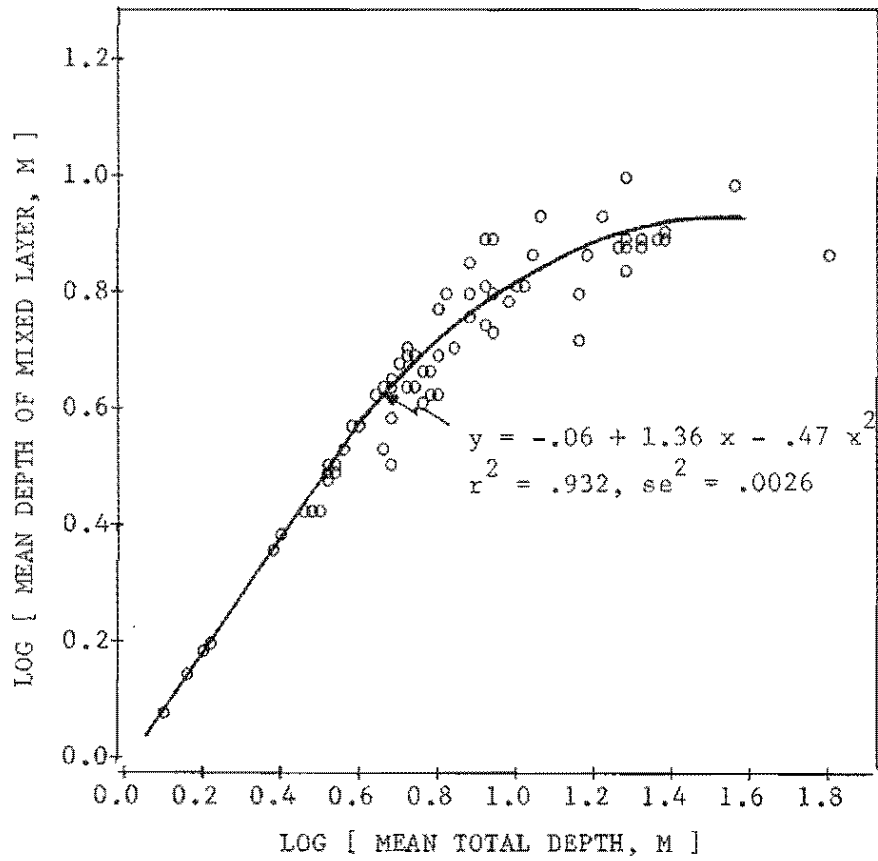
the regression. Mixed depths level off at about 10 meters for mean depths greater than about 30 meters. Refinements to mixed depth predictions should consider possible effects of surface area, flushing rate, and region on stratification potential.

191. Optimal values of the chlorophyll-a model coefficients estimated from nonlinear regression are as follows:

	Mean	Standard Error
C1	.141	.027
C2	.0039	.00087
C3	1.33	.148
C4	4.31	1.53

At a summer residence time of about 10 days, flushing and algal death rate contribute equally to kinetic limitation; i.e., C1 equals C2/Ts. In impoundments with residence times greater than 10 days, the C1 parameter controls the light-limited response. The optimal value of C1 is reasonable in relation to typical values for the corresponding algal kinetic coefficients. From the above equations:

$$C1 = 1.66 \ (\ D/Gmax \ ) \ / \ F \qquad (81)$$
$$= 1.66 \ (\quad .11 \quad) \ / \ 1.3 = .14$$

D/Gmax equals the ratio of algal death rate (due to respiration, predation, and settling) to the maximum specific growth rate. Measured respiration rates are on the order of .05 to .10 times Gmax (Zison et al. 1978; Parsons et al., 1977). A value of .11 for D/Gmax seems reasonable when other algal death mechanisms are also considered. The light factor (F) equals a dimensionless light intensity function times the day length fraction. Details on this factor and its calculation are given by Meta Systems (1979); a value of 1.3 for F corresponds to a surface light intensity of 240 cal/cm^2-day, algal saturation light intensity of 2 cal/cm^2-hr, and average day length of 13.5 hours. The surface light intensity and day length values correspond to an average summer day at 40 degrees latitude and 75% of the possible sunshine. The

saturation light intensity is reasonable for freshwater phytoplankton (Zison et al., 1978; Parsons et al., 1977). The factor is proportional to day length, but rather insensitive to the surface and saturation light intensity values. Assuming a 12-hour day, Oskam (1973) estimated a value of 1.15 for F.

192. The light-limitation kinetics employed in the model assume that the mixed layer is totally absorbing or that the photic zone does not extend below the mixed layer. This condition can be approximately met by ensuring that the ratio of mixed depth to Secchi depth exceeds 2, which corresponds roughly to less than 5% of surface light intensity remaining at the bottom of the mixed layer. In these impoundments, the above ratio ranges from .85 to 19 and is less than 2 in 7 reservoirs. In these cases, the mixed depth has been set equal to twice the Secchi depth for parameter estimation purposes, although the effects of this adjustment on the parameter estimates and error statistics are insignificant.

193. Observed and predicted concentrations are plotted in Figure 64. The model explains 80% of the variance in the chlorophyll measurements, with a mean squared error of .025. Residuals plots (Figure 65) indicate that average errors are independent of inorganic and total N/P ratios, turbidity, flushing rate, and depth. Error variance tends to be somewhat higher in turbid and/or rapidly flushed impoundments. When the data set is restricted to impoundments with non-algal turbidities less than 1 1/m, error variance is reduced to .018 and the explained variance increases to 89%.

194. The effects of various terms in the model are illustrated in Figures 66-68. Figure 66 plots observed chlorophyll-a against the maximum potential chlorophyll-a (Bx in Equation 78). Chlorophyll-a levels would be expected to approach Bx in the limit of long residence times, shallow mixed depths, and low turbidities. Figure 67 plots the B/Bx ratio vs. the numerator in Equation 77, which incorporates the effects of self-shading and non-algal turbidity on the chlorophyll response. The observed kinetic effects vary over an order of magnitude. At high values of the kinetic factor, the model indicates that

Figure 64

Observed and Predicted Reservoir Chlorophyll-a Concentrations
Using Light-Limitation Model
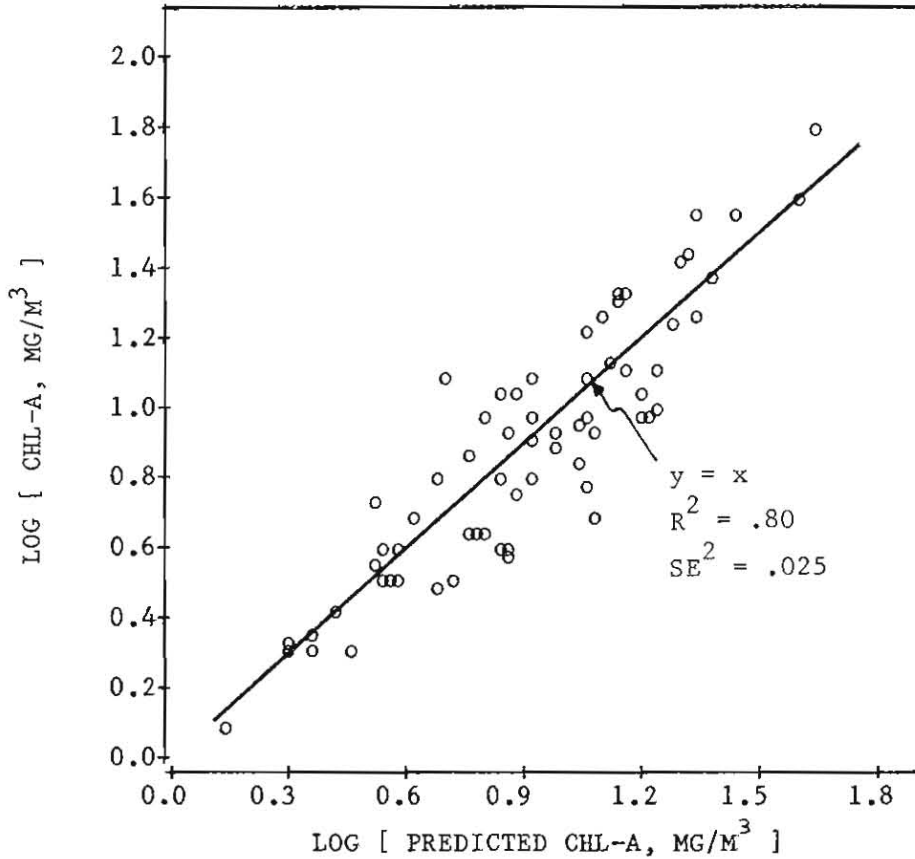
Model Equations:

$$B = Bx / [(1 + .025 \; G \; Bx) (1 + G \; a)]$$

$$G = Zmix \; (.14 + .0039/Ts)$$

$$Bx = Xpn^{1.33} / 4.31$$

Figure 65

Chlorophyll-a Residuals vs. Reservoir Characteristics
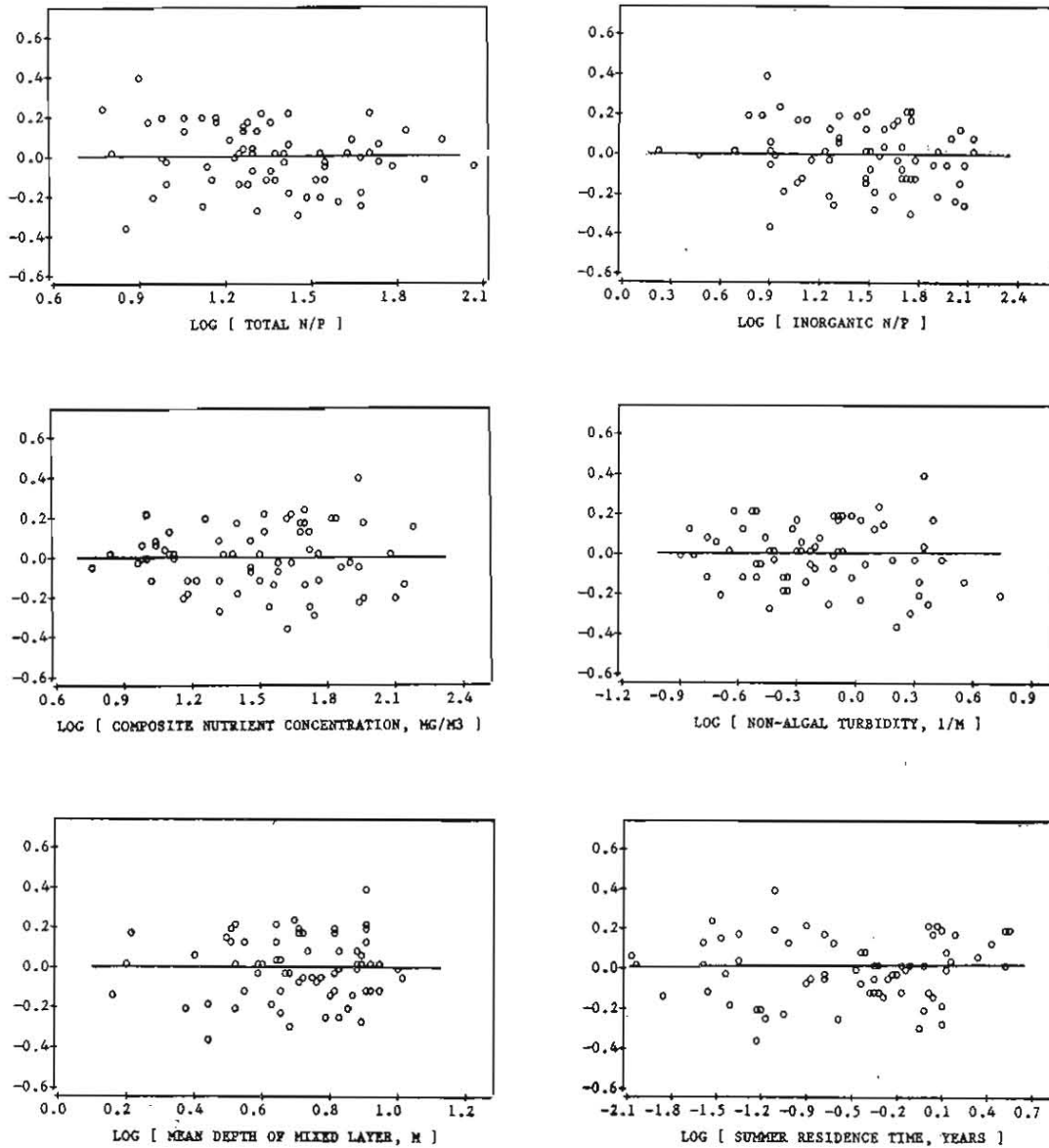
Y-Axes = Chlorophyll-a Residual = log (Observed / Predicted)

206

Figure 66

Observed vs. Potential Chlorophyll-a
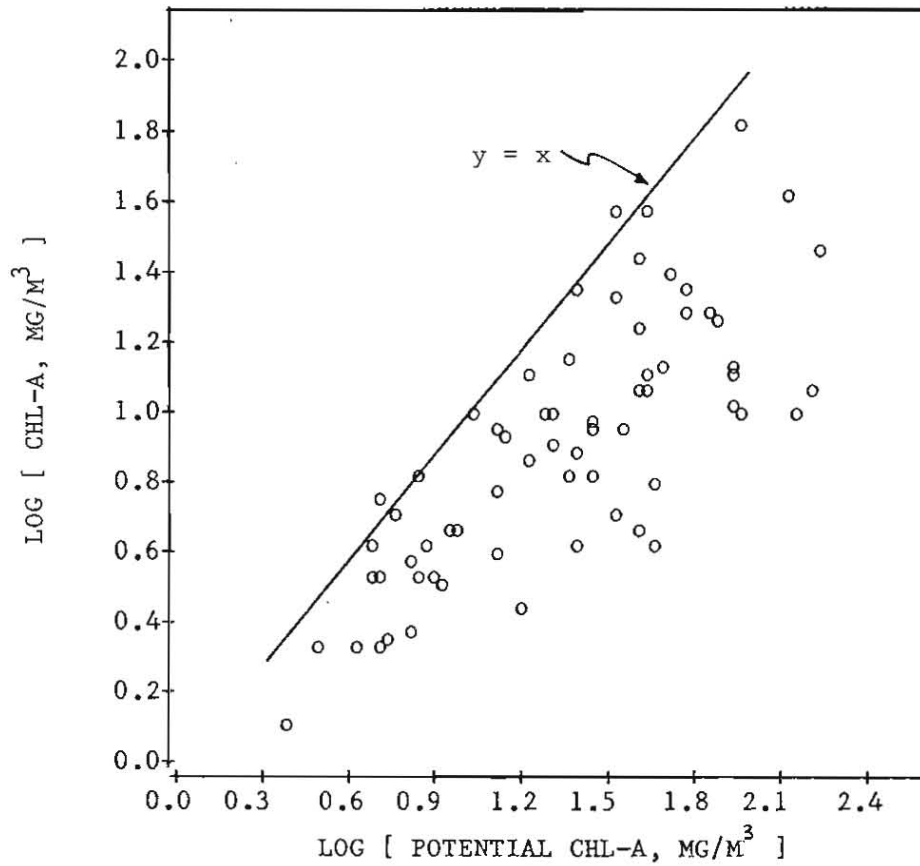
X Axis = estimated chlorophyll-a without light or flushing controls

$$= Xpn^{1.33} / 4.31$$

Figure 67

Observed/Potential Chlorophyll-a vs. Light-Limitation Factor

Y Axis = log [B / Bx]
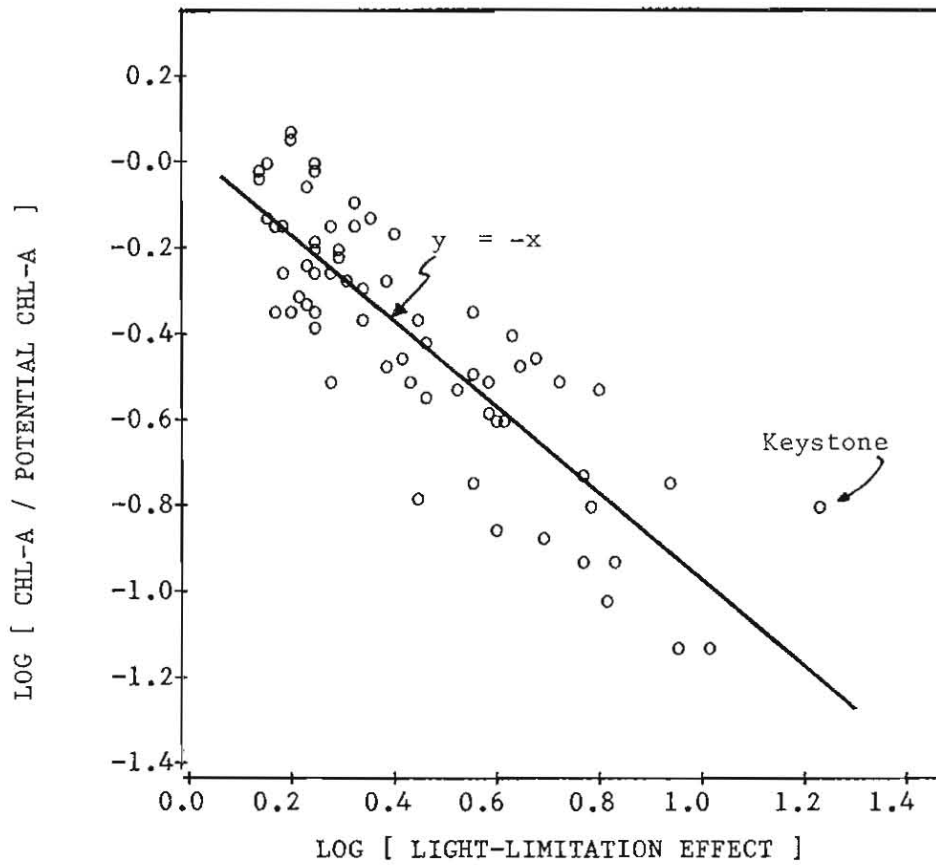
X Axis = log [(1 + .025 G Bx) (1 + G a)]

where,

$$Bx = Xpn^{1.33} / 4.31$$

$$G = Zmix (.14 + .0039/Ts)$$

a = non-algal turbidity (1/m)

Figure 68

Comparison of Self-Shading and Non-Algal Turbidity Components
of Light-Limitation

X Axis = log [1 + .025 G Bx]
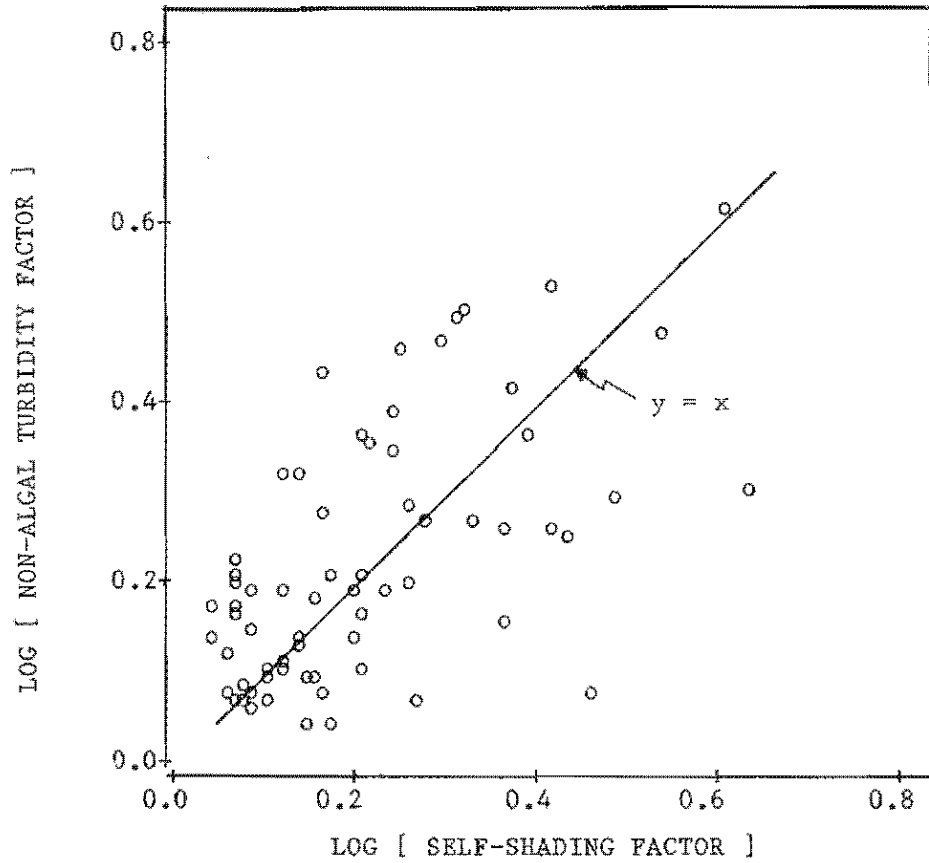
Y Axis = log [1 + G a]

chlorophyll response to nutrients is reduced by about a factor of 10. Figure 68 shows that potential self-shading and non-algal turbidity contribute about equally, on the average, to the total light-limitation effect. Since the self-shading term is calculated from the maximum potential chlorophyll-a (Bx), the actual self-shading is considerably less for most impoundments. Thus, light-limitation effects are controlled primarily by non-algal turbidity in most impoundments.

195. The controlling effects of flushing are reduced in situations where one reservoir is located immediately downstream of another. The model assumes that the input term of the algal mass balance equation is controlled by growth within the impoundment and not by external inflows. Because of this, the model will underpredict chlorophyll levels in rapidly flushed impoundments which have significant upstream algal sources. For example, when applied to Cheatham Reservoir on the Cumberland River in Tennessee, a run-of-the-river system with a summer residence time of 1.8 days, the model predicts an average chlorophyll level of 1.4 mg/m^3, compared with an observed mean chlorophyll-a level of 8.3 mg/m^3. This reservoir is located immediately below Old Hickory Reservoir, however, which has a longer residence time (9 days) and observed and predicted chlorophyll levels of 7.4 and 5.4 mg/m^3, respectively. Most of the chlorophyll measured in Cheatham probably originated in or above Old Hickory. Model error statistics and parameter estimates exclude Cheatham. In this type of system, there is little opportunity for changes in algal populations moving through the downstream impoundment and predictions would be based more reliably upon the inflow conditions than upon the above kinetic model. Future refinements to the model might consider including external chlorophyll-a inflows as a specific algal source term in the mass balance equation (Equation 71).

196. The residual histogram in Figure 69 shows that chlorophyll-a predictions are accurate to within a factor of two for most projects. Exceptions are Wister Reservoir (Code 25-281, residual = -.36, observed = 5.0, predicted = 11.5) and Keystone (Code 25-273, residual = .40, observed = 12.2, predicted = 4.9). These projects are located in

Figure 69

Histogram of Chlorophyll-a Model Residuals

```
minimum of interval

.45|
.40| 25273                        (Keystone)
.35|
.30|
.25|                                                                              |
.20| 17256 17258 17373 19119 29207                                                |
.15| 17245 17249 21196 25370 26355 29106 29108 30064                             |
.10| 16254 16317 17391 19342                                                      |
.05| 01174 03307 06372 24016 29195                                               |
.00| 01173 10003 15237 17241 19122 20088 24193 24200 25107 31077                 |
-.05| 01170 16393 18092 19340 19343 20081 20087 26354 28219 29111 32204|
-.10| 10072 18120                                                                 |
-.15| 01172 16243 16328 17242 24013 25267 25278 29194 30235                      |
-.20| 01165 17248 18093                                                           |
-.25| 10411 17247 24022 25105 25275                                              |
-.30| 24011 29110                                                                 |
-.35|
-.40| 25281                        (Wister)                2-Fold Accuracy Limit
-.45|
```

Symbol = DDRRR, DD = CE District Code, RRR = CE Reservoir Code

eastern Oklahoma and have relatively high non-algal turbidities. While the behavior of Wister is unexplained, the apparent prediction error in the case of Keystone is partially related to high spatial and temporal variability in chlorophyll and transparency and to overestimation of the mean mixed-layer depth, as described below.

197.   Temperature profiles indicate that Keystone was thermally unstratified during the periods of sampling by the EPA/NES. Accordingly, the mean depth of the mixed layer has been set equal to the mean total depth (7.8 meters). Density stratification may have existed, however, because of differences in salinity between the two major tributary arms (Arkansas and Cimarron). Based upon summer conductivity profiles, density stratification occurred at depths ranging from 7 to 15 m for various stations and sampling dates. In some instances, conductivity increased more than two-fold with depth and was accompanied by decreases in dissolved oxygen. For mixed layer total depths ranging from 7 to 15 m, mixed layer mean depths would range from 4.6 to 6 m and chlorophyll model predictions would range from 10.3 to 7.2 mg/m^3, compared with the 4.9 mg/m^3 prediction for a mean mixed layer depth of 7.8 meters and the observed chlorophyll-a mean of 12.2 mg/m^3. Thus, part of the prediction error for this reservoir could be attributed to overestimation of mixed layer depth.

198.   As shown in Figure 67, the model predicts that Keystone is the most light-limited of the impoundments in the data set. The estimated light-limitation factor is 16.6, compared with a maximum of 10.2 for the other reservoirs. The EPA/NES working paper on this reservoir discusses the importance of light limitation: "Comparisons of light penetration values and corresponding chlorophyll-a levels (positive relationship) strongly suggest that the latter are controlled by, rather than control, the high turbidity in this lake." The reservoir was sampled four times at nine locations in 1974. Station-mean transparencies and chlorophyll-a concentrations ranged from 0.1 to 0.6 m and 3 to 72 mg/m^3, respectively. Inorganic nutrient concentrations were generally high and above growth-limiting levels. On one sampling round (June), transparencies were extremely low (median, 0.1

212

vs. 0.5 to 0.6 m on other rounds) and chlorophyll concentrations were also low (median, 1.6 vs. 3.9 to 22 mg/m^3 on other rounds). Chlorophyll-a concentrations were generally highest at the shallow inflow stations, where depth-averaged light intensity would tend to be greatest at a given turbidity.

199. The high level of spatial and temporal variability within the reservoir imposes limitations on the accuracies of the reservoir-mean concentration estimates for Keystone and may also cause problems with model implementation because of the nonlinear nature of the equation. Additional insights are derived from applying the chlorophyll model to individual stations and sampling rounds (Figures 70 and 71). To apply the model in this manner, estimates of the mean depth of the mixed layer and effective hydraulic residence time are required for each station and sampling round. Mean mixed-layer depths have been estimated at one-half the station total depths; this corresponds to a triangular channel cross section. Variations in hydrologic conditions from one sampling round to another have been considered by applying the corresponding monthly-mean reservoir hydraulic residence times, which range from .04 to .17 year. While a more complex hydrodynamic model would be required to account for spatial variations in flushing rate, model predictions are generally insensitive to flushing rates in this range.

200. Applied to the individual Keystone samples, the model explains 66% of the observed variance with a mean squared error of .16 (Figure 70). The range of chlorophyll-a measurements (.2 to 181 mg/m^3) made within this reservoir is wider than the range of reservoir-mean concentrations in the model development data set (1 to 64 mg/m^3). Figure 71 plots the ratio of observed/potential chlorophyll-a ratio against the estimated light-limitation factor. The latter ranges from about 1.7 to 210, compared with a range of 1.3 to 10.2 in the reservoir-mean data set (see Figure 67).

201. Despite the extrapolations beyond the ranges of the development data set, the model does a reasonable job of predicting the chlorophyll-a response and effects of light-limitation within Keystone. The error variance for predicting the individual measurements is about

213

Figure 70

Observed and Predicted Instantaneous Chlorophyll-a
Concentrations at Various Locations in Keystone Reservoir
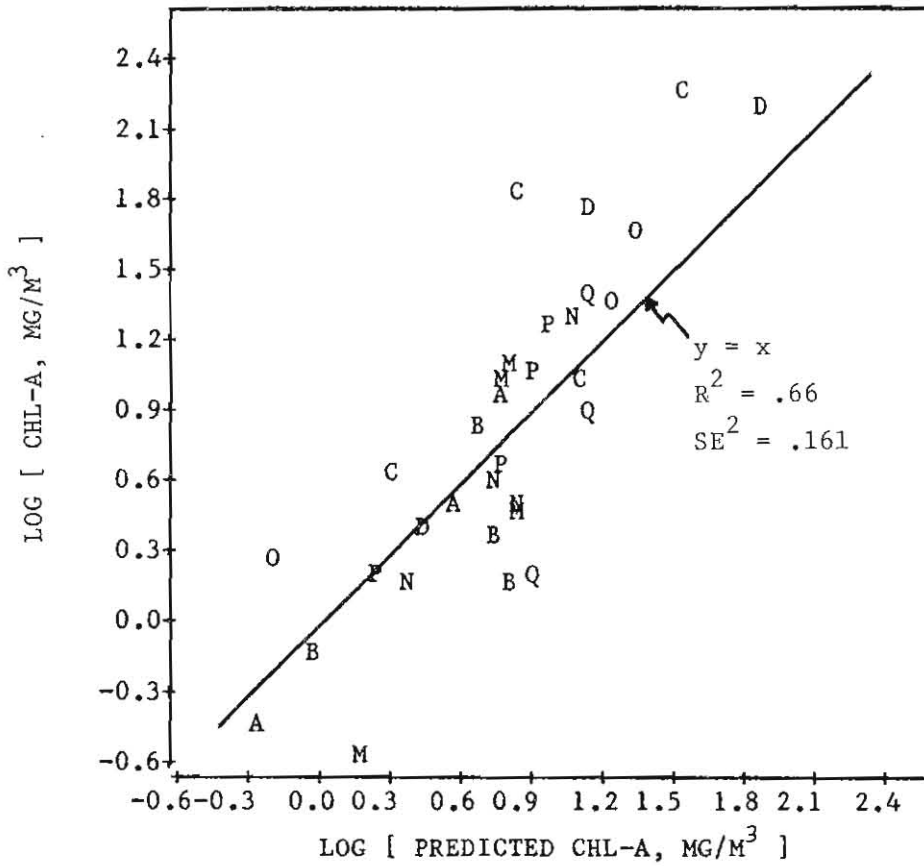
Symbol = Station
See Figure 64 for Model Formulation

Figure 71

Observed and Predicted Light-Limitation Effects Based Upon
Instantaneous Measurements in Keystone Reservoir
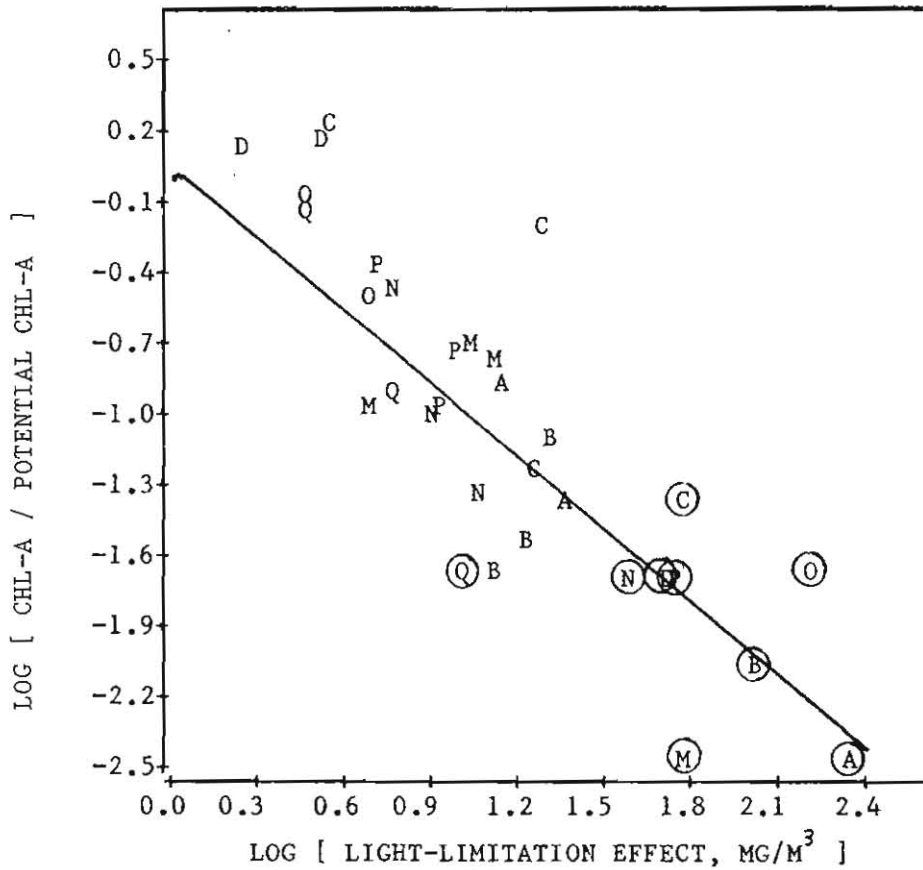
Stations Identified in Figure 70
See Figure 64 for Model Formulation
Circled Symbols = June Sampling Round (high-turbidity)

six times that for predicting the reservoir-mean values, partially because of reduced data accuracy and possible effects of non-steady-state conditions when the model is applied to instantaneous measurements. Some positive bias may be present at low values of the light-limitation factor (Figure 71) and at high predicted chlorophyll-a concentrations (Figure 70), although the slope and intercept of the observed vs. predicted regression are not significantly different from 1.0 and 0.0, respectively, at $p<.05$. The underpredictions generally occur at stations near the reservoir inflow and may reflect problems with the estimates of effective mixed layer depth at these locations, where velocities and gradients in depth tend to be relatively high and measured chlorophyll concentrations may be influenced by algae grown in shallower (less light-limited) areas further upstream. 'The under-prediction of reservoir-mean chlorophyll-a partially results from inclusion of two extremely high chlorophyll-a measurements (155 and 181 mg/m^3) on the computed reservoir-average concentration, averaging of model input variables over a wide range of conditions, and possible overestimation of mixed layer depth because salinity-induced density stratification was not considered.

202. The model developed above considers the controlling effects of phosphorus, nitrogen, light, and flushing rate on chlorophyll production. When linked with nutrient retention models (as developed in Parts II and III), uncertainty remains with respect to the possible effects of nitrogen fixation on the nitrogen budget and resulting chlorophyll production, particularly in impoundments with low N/P ratios, since a predictive model for nitrogen fixation has not been developed. Reliable nitrogen loading and/or pool concentration data may not be available for some impoundments. For economic reasons, it may be desirable in planning a reservoir study to forgo the intensive sampling and laboratory analyses required for development of a detailed nitrogen budget if preliminary surveys indicate that a reservoir is clearly not nitrogen-limited (based upon inorganic N/P ratios). A model which considers phosphorus, light, and flushing rate alone would be desirable for these situations. This can be achieved by using total phosphorus in

place of composite nutrient concentration and recalibrating the model to impoundments with inorganic N/P ratios exceeding 10. The revised model uses Bp (phosphorus-limited chlorophyll-a) in place of Bx in Equation 80 with the following optimal parameter estimates:

$$G = Zmix (.19 + \frac{.0042}{Ts}) \tag{82}$$

$$Bp = P^{1.37} / 4.88 \tag{83}$$

where

Bp = phosphorus-limited chlorophyll-a (mg/m^3)

For 53 reservoirs with inorganic N/P ratios greater than 10, the model explains 82% of the chlorophyll variance with a mean squared error of .022 log units. In situations where nitrogen limitation is judged unimportant and/or unpredictable, this version is simpler than Equation 80 and has reduced data requirements. The model would tend to overpredict chlorophyll in reservoirs which are nitrogen-limited, however.

203. Effects of light limitation on algal growth would be complicated in situations where the algae are not uniformly distributed within the mixed layer. The relative buoyancy of some blue-green algal types may result in surface algal densities which are considerably higher than the mixed layer-mean concentration. Surface algal concentrations would be exposed to light intensities which are considerably higher than the mixed layer-mean intensity and this would tend to offset the potential effects of light-limitation. The existing data set does not permit assessment of these effects, however, because it is based upon depth-integrated (photic zone) chlorophyll-a samples. In situations where potential light-limitation and nitrogen-limitation effects are offset by bouyant, nitrogen-fixing algae, it seems reasonable that the mean chlorophyll-a concentration would approach the phosphorus-limited chlorophyll-a level, as estimated from Equation 83. The prediction of blue-green algal abundance in reservoirs is an area suggested for future research.

217

204.   Figure 72 shows that Bp defines the upper limits of the chlorophyll/phosphorus distribution in four different data sets: CE reservoirs, OECD reservoirs, EPA/NES lakes, and Minnesota lakes. Data sources are described below. Deviations from Bp reflect influences of nitrogen, light, and flushing rate.   The plots suggest that Bp can provide a conservative (upper-bound) estimate of mean chlorophyll in situations   where   the   controlling   effects   of factors other than phosphorus are either insignificant or are offset by algal adaptive mechanisms.

Independent Testing

205.   Table 28 summarizes error statistics and parameter estimates for ten chlorophyll-a models applied to the reservoir-mean values.   The first five were previously developed from other lake and/or reservoir data sets and include terms for phosphorus and/or nitrogen. Models 06-09 are derived from regression analyses of this data set, using phosphorus (Model 06), phosphorus and nitrogen (Model 07), composite nutrient concentration (Model 08), and composite nutrient concentration, turbidity, mean depth, and residence time (Model 09) as independent variables.   Model 10 is the theoretical formulation incorporating phosphorus, nitrogen, light, and flushing effects, as developed above.

206.   Model 09 is based upon a step-wise regression in which linear and logarithmic terms were allowed to enter into the equation. The resulting equation suggests that chlorophyll-a is proportional to composite nutrient concentration and that the proportionality constant decreases with turbidity, depth, and flushing rate.   The inclusion of flushing rate (1/Ts) as a linear term provides low sensitivity at high residence times and becomes important (has at least a factor of two effect on the predicted chlorophyll-a) in impoundments with residence times less than 5 days.   While the multivariate regression model explains slightly more variance than the theoretical model (Model 10), the former has less generality, as demonstrated below.

207. Table 29 describes eleven data sets which have been used to test each of the models in Table 28.   The compilation of these

Figure 72

Chlorophyll-a vs. Total Phosphorus for Various Data Sets
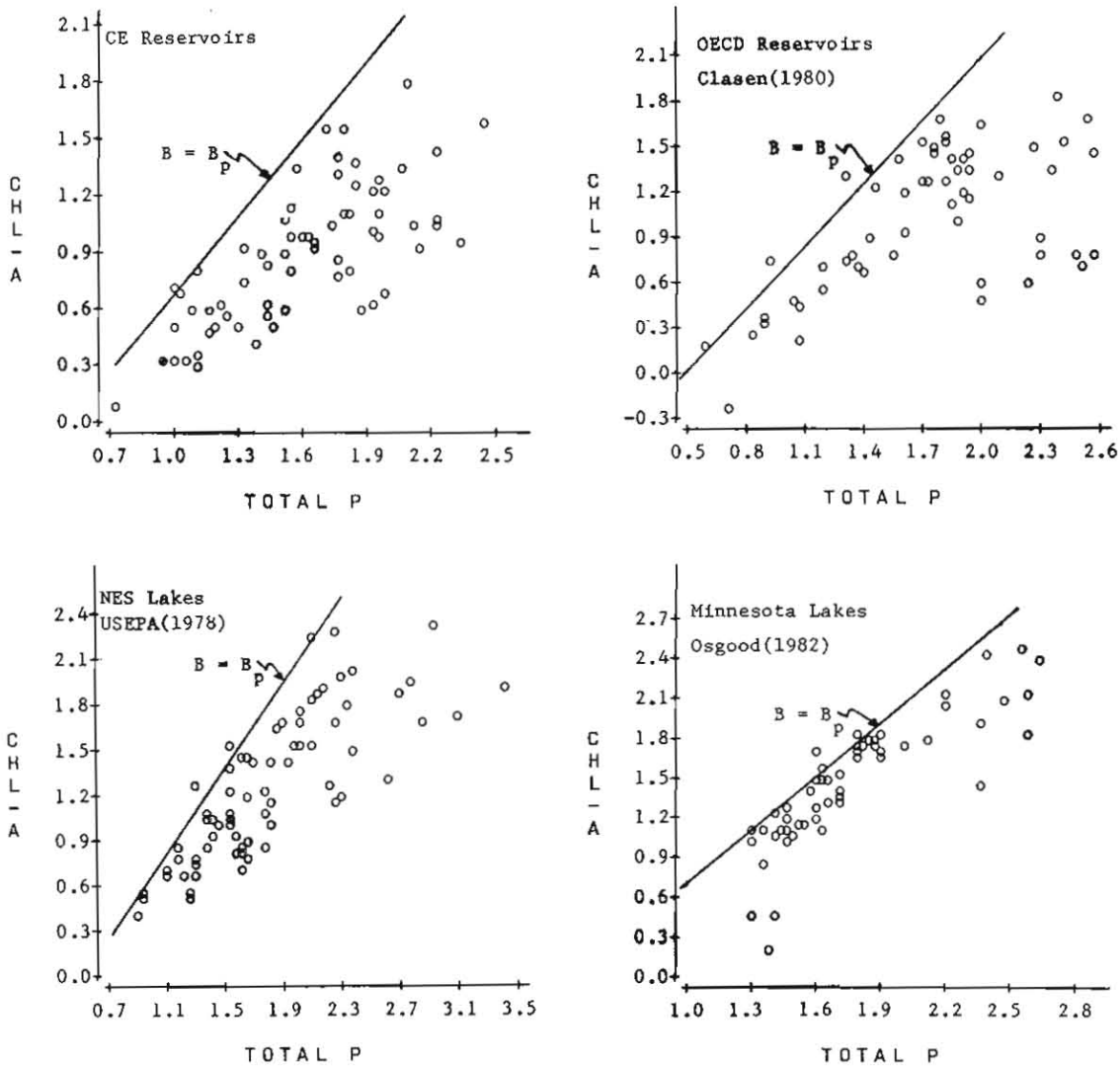
Units: mg/m^3, log10 scales
Bp = phosphorus-potential chlorophyll-a = $P^{1.37}/4.88$

Table 28
Error Statistics for General Chlorophyll-a Models Applied to
Reservoir-Mean Data

	R^2	SE^2
Model 01: Jones and Bachman (1976)		
$\log(B) = -1.09 + 1.46 \log(P)$	-1.05	.268
Model 02: Kerekes (1981) *		
$\log(B) = -.6 + \log(P)$	.36	.084
Model 03: Smith (1980)		
$\log(B) = -3.88 + 1.55 \log(N + 16.4\ P)$	-.09	.143
Model 04: Smith (1982)		
$\log(B) = -1.56 + .65 \log(P) + .55 \log(N)$	.01	.130
Model 05: Canfield (1983)		
$\log(B) = -2.49 + .27 \log(P) + 1.06 \log(N)$	.13	.114
Model 06: Regression vs. P		
$\log(B) = -.22 + .70 \log(P)$	.55	.059
Model 07: Regression vs. N and P		
$\log(B) = -.69 + .60 \log(P) + .21 \log(N)$	.56	.057
Model 08: Regression vs. Xpn		
$\log(B) = -.29 + .80 \log(Xpn)$	.60	.053
Model 09: Multivariate Regression		
$\log(B) = \log(Xpn) - .33 - .57 \log(a)$ $- .39 \log(Z) - .0041/Ts$	.82	.024
Model 10: Theoretical, Modified from Forsberg and Shapiro (1980)		
$Bx = Xpn^{1.33} / 4.31,\quad G = Zmix\ (\ .14 + .0039/Ts\ )$		
$B = Bx / [\ (1 + .025\ G\ Bx)\ (1 + G\ a)\ ]$	.80	.025

NOTE: statistics based upon data from 66 CE reservoirs

* Model 02 similar to that derived for P-limited, low-turbidity
  CE impoundments in preliminary studies (Walker, 1982a)

Table 29
Key to Data Sets Used in Testing Chlorophyll-a Models

Code	Source	N	Notes
A	This Study	66	(Excluding Cheatham)
B	EPA/NES	102	NES Compendium, CE Reservoirs
C	"	241	NES Compendium, non-CE Reservoirs
D		73	NES Compendium, Natural Lakes
E	Higgins & Kim (1981)	9	TVA Tributary Reservoirs
F	"	7	TVA Mainstem Reservoirs
G	Clasen (1980) *	39	OECD/RSL - All
H	"	12	OECD/RSL - Natural Lakes
I	"	15	OECD/RSL - Pumped Storage Reservoirs
J	"	12	OECD/RSL - Other Reservoirs
K	Combined	368	Sets C-G Combined

Screening Criteria Applied to Independent Data Sets:
    (1) non-missing values for N, P, T, Z, B, S.
    (2) $N > 250$ mg/m^3.

* Chl-a estimates for OECD/RSL data sets are annual-means.

independent data sets has been described previously (Walker, 1982a).
Two of the data sets (D and H) consist exclusively of data from natural
lakes. Constraints applied in compiling the independent data sets
include complete nutrient budget information and total nitrogen
concentrations exceeding 250 mg/m^3. The lower detection limit for
Kjeldahl nitrogen measurements in the EPA/NES program was 200 mg/m^3, and
impoundments with median total nitrogen levels less than about 250 mg/m^3
tended to have a high percentage of TKN measurements less than the
detection limit. Based upon seasonal variations in residence time which
are typical of impoundments in the model development data set, summer
residence times are assumed to equal twice the average annual values in
the impoundments used for model testing. In most cases, mixed layer
depths have been estimated from the regression equation in Figure 63 and
constrained to a maximum of 10 meters in impoundments with mean depths
exceeding 40 meters. Exceptions are the TVA Mainstem and OECD/RSL
Pumped Storage impoundments which are unstratified because of rapid
flushing rates (Placke and Bruggink, 1980) and artificial mixing
(Clasen, 1980), respectively.

208. Complete error statistics are listed by model and data set in
Table 30 and mean squared errors are summarized in Table 31. Results
indicate that Model 10 is the most general of those tested on the
independent data sets. When all non-CE lakes and reservoirs are
combined (Data Set K), the model explains 68% of the observed variance
with a mean squared error of .055, compared with .024 for the model
development data set. The increase in error partially reflects
differences in data reduction procedures and lack of data screening for
adequacy of sampling regime and accuracy of summary values. Based upon
the F statistics listed in Table 30, the parameters (slopes and
intercepts) of Model 10 are generally more stable than those of the
other models when applied to independent data sets.

209. The phosphorus gradient model developed in Part IV employs a
simple chlorophyll/phosphorus regression model to predict algal
profiles. Excluding reservoirs with inorganic N/P ratios less than 10
and non-algal turbidities greater than 1 1/m, the relationship between

222

Table 30
Summary of Chlorophyll-a Model Error Statistics

MODEL	MEAN	MSE	MABS	R2	INT	SLOPE	MSE*	F
A - COE all (n=66, Obs. Chl-a Variance = .133)								
01	-.350	.268	.401	-1.046	.299	.477	.061	113.0**
02	-.106	.084	.224	.359	.197	.696	.061	13.4**
03	-.194	.143	.287	-.090	.281	.563	.068	37.4**
04	-.246	.130	.290	.013	.060	.731	.061	38.3**
05	-.164	.114	.261	.129	.189	.665	.075	18.5**
06	.000	.059	.194	.548	.000	1.000	.061	0.0
07	.000	.057	.192	.563	.000	1.000	.059	0.0
08	.000	.053	.178	.598	.000	1.000	.054	0.0
09	.000	.022	.127	.830	.000	1.000	.023	0.0
10	.002	.024	.125	.818	-.005	1.008	.025	0.0
B - EPA/NES/CE Reservoirs (n=102, Obs. Chl-a Variance = .103)								
01	-.300	.241	.377	-1.370	.447	.404	.061	150.2**
02	-.052	.083	.226	.183	.361	.589	.061	19.0**
03	-.100	.125	.280	-.230	.466	.462	.065	48.2**
04	-.168	.103	.253	-.016	.260	.618	.060	37.9**
05	-.062	.095	.246	.066	.400	.545	.068	21.2**
06	.057	.065	.205	.363	.194	.846	.061	3.8
07	.068	.064	.205	.270	.199	.852	.059	5.1**
08	.071	.059	.199	.416	.184	.871	.054	5.7**
09	.071	.039	.165	.618	.205	.848	.032	11.5**
10	.041	.037	.159	.633	.145	.886	.035	4.0
C - EPA/NES Non-CE Reservoirs (n=241, Obs. Chl-a Variance = .134)								
01	-.380	.360	.461	-1.687	.492	.360	.097	327.3**
02	-.097	.136	.279	-.018	.415	.526	.097	49.8**
03	-.154	.169	.307	-.266	.446	.473	.085	119.4**
04	-.200	.141	.281	-.052	.239	.628	.084	83.2**
05	-.077	.112	.254	.164	.349	.598	.084	41.9**
06	-.034	.101	.251	.243	.266	.756	.097	6.4**
07	.048	.092	.243	.310	.214	.822	.089	6.0**
08	.064	.086	.238	.357	.170	.885	.082	7.4**
09	-.007	.072	.200	.460	.311	.679	.055	39.4**
10	.006	.057	.184	.572	.166	.836	.045	6.9**
D - EPA/NES Natural Lakes (n=73, Obs. Chl-a Variance = .257)								
01	-.272	.307	.382	-.211	.458	.516	.091	87.3**
02	.057	.110	.266	.568	.347	.754	.091	8.3**
03	-.162	.158	.295	.378	.313	.661	.090	28.3**
04	-.121	.090	.239	.644	.028	.890	.075	8.5**
05	-.063	.087	.238	.656	-.023	.969	.086	1.7
06	.219	.138	.295	.457	.134	1.083	.091	19.5**
07	.199	.121	.269	.525	.052	1.142	.080	19.3**
08	.207	.117	.274	.538	-.111	1.309	.066	29.6**
09	-.103	.074	.212	.709	.037	.895	.062	7.8**
10	-.013	.050	.175	.802	-.058	1.036	.051	.3

(continued)

Table 30 (Continued)

MODEL	MEAN	MSE	MABS	R2	INT	SLOPE	MSE*	F
E − TVA Tributary Reservoirs (n=7, Obs. Chl-a Variance = .017)								
01	.006	.041	.177	−1.734	.502	.362	.004	37.0**
02	.105	.023	.129	−.568	.424	.529	.004	20.2**
03	.017	.036	.145	−1.409	.513	.353	.009	12.1**
04	−.083	.021	.122	−.426	.345	.506	.005	12.4**
05	−.063	.031	.162	−1.109	.461	.382	.010	8.4
06	.115	.017	.115	−.141	.275	.760	.004	14.0**
07	.109	.016	.109	−.077	.287	.736	.004	12.8**
08	.092	.015	.092	−.007	.337	.646	.004	10.4**
09	.087	.019	.107	−.262	.403	.546	.004	13.3**
10	.057	.010	.085	.313	.325	.631	.004	6.6
F − TVA Mainstem Reservoirs (n=8, Obs. Chl-a Variance = .030)								
01	−.680	.495	.680	−17.853	.120	.414	.027	70.1**
02	−.396	.180	.396	−5.853	.031	.605	.027	23.6**
03	−.363	.151	.363	−4.768	−.067	.719	.025	21.3**
04	−.458	.230	.458	−7.762	−.284	.848	.027	31.7**
05	−.297	.111	.297	−3.221	−.121	.821	.030	11.9**
06	−.264	.090	.264	−2.431	−.140	.869	.027	10.3**
07	−.235	.075	.235	−1.859	−.242	1.008	.027	8.3
08	−.240	.080	.240	−2.047	−.234	.994	.030	7.6
09	−.087	.022	.123	.152	−.060	.965	.020	1.5
10	−.083	.024	.129	.100	.124	.731	.020	1.6
G − OECD/RSL − All (n=39, Obs. Chl-a Variance = .189)								
01	−.507	.674	.578	−2.652	.676	.255	.162	62.8**
02	−.153	.265	.371	−.434	.622	.373	.162	13.4**
03	−.485	.598	.589	−2.239	.701	.243	.173	48.9**
04	−.401	.421	.481	−1.278	.587	.334	.168	30.3**
05	−.405	.473	.549	−1.561	.706	.253	.178	33.4**
06	.026	.178	.335	.038	.516	.535	.162	2.9
07	−.023	.186	.339	−.009	.535	.495	.164	3.6
08	−.035	.201	.349	−.089	.587	.443	.167	5.0
09	−.475	.386	.480	−1.092	.214	.558	.127	40.7**
10	−.071	.065	.209	.646	−.113	1.054	.063	1.6
H − OECD/RSL − Natural Lakes (n=12, Obs. Chl-a Variance = .252)								
01	−.061	.042	.127	.818	.153	.818	.034	2.5
02	.163	.060	.195	.740	−.022	1.194	.034	5.6
03	.118	.029	.132	.875	−.018	1.137	.014	7.5**
04	.043	.026	.143	.887	−.369	1.385	.008	13.6**
05	.143	.066	.217	.716	−.254	1.408	.034	6.6
06	.255	.129	.296	.443	−.359	1.715	.034	17.9**
07	.267	.127	.301	.448	−.414	1.802	.016	43.8**
08	.268	.130	.307	.438	−.377	1.761	.022	30.3**
09	−.219	.090	.232	.608	−.552	1.249	.041	8.1**
10	.068	.022	.116	.906	−.104	1.164	.015	3.5

(continued)

224

Table 30 (Concluded)

MODEL	MEAN	MSE	MABS	R2	INT	SLOPE	MSE*	F

I -- OECD/RSL - Pumped Storage Only (n=15, Obs. Chl-a Variance = .156)

MODEL	MEAN	MSE	MABS	R2	INT	SLOPE	MSE*	F
01	-.872	1.286	.959	-7.813	1.472	-.153	.161	53.6**
02	-.378	.486	.546	-2.330	1.505	-.223	.161	16.2**
03	-.936	1.151	.941	-6.886	1.917	-.360	.157	48.4**
04	-.718	.795	.728	-4.449	1.857	-.370	.156	31.7**
05	-.790	.870	.809	-4.962	2.108	-.485	.155	35.7**
06	-.107	.226	.446	-.820	1.568	-.320	.161	5.9
07	-.202	.283	.424	-.937	1.712	-.404	.158	6.9**
08	-.221	.319	.454	1.187	1.651	-.355	.158	8.8**
09	-.703	.719	.707	-3.925	.931	.124	.167	25.9**
10	-.098	.083	.260	.432	-.696	1.474	.075	1.8

J -- OECD/RSL - Reservoirs Only (n=12, Obs. Chl-a Variance = .175)

MODEL	MEAN	MSE	MABS	R2	INT	SLOPE	MSE*	F
01	-.496	.542	.553	-2.371	.449	.346	.129	20.1**
02	-.187	.193	.327	-0.202	.375	.506	.129	4.0
03	-.526	.476	.606	-1.964	.373	.391	.160	12.8**
04	-.448	.347	.511	-1.159	.183	.549	.138	10.0**
05	-.470	.383	.556	-1.386	.248	.494	.160	9.4**
06	-.038	.117	.235	.273	.232	.727	.129	0.4
07	-.088	.125	.272	.223	.185	.737	.133	0.6
08	-.105	.125	.261	.222	.203	.708	.126	1.0
09	-.444	.266	.444	-.658	-.041	.711	.061	21.2**
10	-.175	.087	.237	.458	-.060	.898	.066	2.9

K - All Non-CE Combined (C-G) (n=368, Obs. Chl-a Variance = .173)

MODEL	MEAN	MSE	MABS	R2	INT	SLOPE	MSE*	F
01	-.371	.379	.457	-1.202	.459	.409	.109	455.3**
02	-.075	.143	.286	.168	.372	.597	.109	58.3**
03	-.192	.210	.332	-.216	.422	.499	.102	196.3**
04	-.209	.160	.294	.071	.206	.666	.098	117.3**
05	-.114	.144	.281	.166	.328	.614	.104	70.2**
06	.065	.115	.266	.334	.203	.858	.109	10.1**
07	.065	.106	.255	.385	.168	.894	.101	9.6**
08	.076	.103	.254	.402	.142	.931	.097	11.7**
09	-.078	.104	.229	.395	.300	.660	.072	84.4**
10	-.011	.055	.182	.681	.083	.910	.054	4.4

Residual Statistics (Observed - Predicted):
  MEAN = mean residual   MSE = mean square
  R2 = fraction of variance explained   MABS = mean absolute value

Observed vs. Predicted Regression:
  INT = regression intercept   SLOPE = regression slope
  MSE* = regression mean squared error with N-2 degrees of freedom
  F = F statistic for HO: INT=0 and SLOPE=1 (2,N-2 degrees of freedom)
  ** indicates HO that is rejected at p<.01

225

Table 31

Summary of Mean Squared Errors by Data Set and Model

D a t a   S e t

Model	A CE	B CE	C Res.	D Lakes	E Tribs.	F Mains.	G All	H Lakes	I Pumped	J Res.	K Combined C-G
		----EPA/NES-----			--- TVA ---		---- OECD/RSL -------				
01	268	241	360	307	41	495	674	42	1286	542	379
02	84	83	136	110	23	180	265	60	486	193	143
03	143	125	169	158	36	151	598	29	1151	476	210
04	130	103	141	90	21	230	421	26	795	347	160
05	114	95	112	87	31	111	473	66	870	383	144
06	59	65	101	138	17	90	178	129	226	117	115
07	57	64	92	121	16	75	186	127	283	125	106
08	53	59	86	117	15	80	201	130	319	125	103
09	22	39	72	74	19	22	386	90	719	266	104
10	24	37	57	50	10	24	65	22	83	87	55
N	66	102	241	73	7	8	39	12	15	12	368
Var.	133	103	134	257	17	30	189	252	156	175	173

Model Codes identified in Table 28, Data Set Codes in Table 29.
Complete Error Statistics given in Table 30.
Entries = Mean Squared Error for log10(Chlorophyll-a) x 1000.
N = number of impoundments.
Var. = variance of observed log10(chlorophyll-a) x 1000.

chlorophyll and phosphorus across reservoirs is roughly linear with an average intercept of -.6 on log scales. This result was obtained in preliminary testing of CE reservoir data (Walker, 1982a) and in the OECD synthesis report (OECD, 1982). Figure 73 compares the distributions of the chlorophyll/phosphorus ratio with residuals from the more complex model developed above, using observed and estimated turbidities (see Non-Algal Turbidity and Transparency). When all reservoirs are considered, the variance of the chlorophyll/phosphorus ratio is between 2.1 and 3.1 times the model residual variance. For reservoirs with inorganic N/P ratios less than 10 and turbidities < 1 1/m, the variances differ by a factor of 1.6 to 2.1.

210. Thus, there is still some benefit to using the more complex model under low-turbidity, phosphorus-limited conditions. In modeling gradients or reservoir-mean conditions, the chlorophyll/phosphorus ratio could be viewed essentially as a calibration factor to be be estimated based upon observed data. Predictions of the light-limitation model can be used to obtain prior estimates of the chlorophyll/phosphorus ratio, based upon reservoir-mean conditions. The B/P ratio varies, however, with phosphorus concentration, nitrogen concentration, turbidity level, mixed depth, and flushing rate, so that problems may arise in assuming a fixed ratio when applying the simpler model in a predictive mode.

211. While the Keystone data discussed above demonstrate the applicability of the model for predicting within-reservoir variations in an unstratified reservoir, additional development would be required to adapt the light-limitation model for use in gradient simulations. This would require a definition for the mean depth of the mixed layer at a station and a method for simulating longitudinal variations in non-algal turbidity. When viewed longitudinally, reservoir profiles often show descreasing nutrient and turbidity levels and increasing depth and residence time. Qualitatively, the model structure indicates that longitudinal increases in depth would tend to offset decreases in turbidity and nutrients in terms of the influence on the computed light-limitation factor. This covariance would tend favor relatively constant B/Bx or B/P ratios moving down the pool at stations where flushing and

Figure 73

Comparison of Residual Distributions with Chlorophyll/Total P Ratios

log10(Chlorophyll-a / Total P)

```
                                                 Mean    Variance
-0.10
-0.20 o                              all data   -.706      .074
-0.30 o o o o                          o only   -.556      .041
-0.40 o o o o
-0.50 o o o o x
-0.60 o o o o o o
-0.70 o o o o o o o o o x x x x x x
-0.80 o o o x x x x x x
-0.90 o o x x x x
-1.00 o o x x x x
-1.10 x x
-1.20 x x
-1.30 x x x
-1.40 x
```
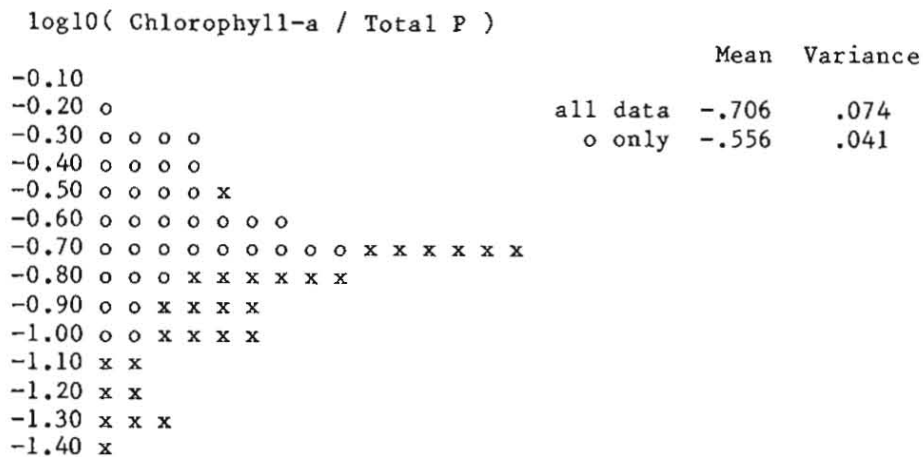
Chlorophyll Residual = log10(Observed/ Predicted)
Observed Turbidities

```
 0.40 x
 0.30                                all data    .002      .024
 0.20 o o o x x                        o only    .014      .022
 0.10 o o o o o o o o o x x x x
 0.00 o o o o o o o o o o x x x x x x
-0.10 o o o o o x x x x x x x x x
-0.20 o o o o o o o o x x x x x
-0.30 o o o o x x x
-0.40 x
```
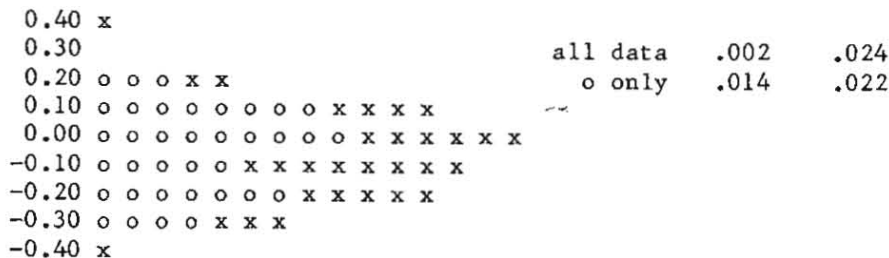
Chlorophyll Residual = log10(Observed/ Predicted)
Estimated Turbidities

```
 0.40 x
 0.30                                all data   -.015      .035
 0.20 o o o o o o o x x                 o only    .024      .028
 0.10 o o o o o o o x x x
 0.00 o o o o o o x x x x x x
-0.10 o o o o o o o o o x x x x
-0.20 o o o o o o o x x x x x x x
-0.30 o o o x x x
-0.40 x x x
-0.50 x
```
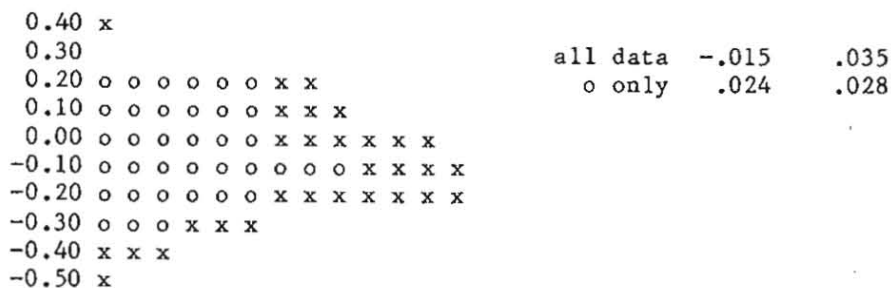
Symbol

```
    ⎧ Inorganic N/P < 10,
x   ⎨ Non-Algal Turbidity > 1 1/m, or        (n = 30)
    ⎩ Summer Residence Time < .04 years
```

o   other reservoirs   (n = 36)

228

nitrogen are not limiting.

Non-Algal Turbidity and Transparency

212. Estimates of non-algal turbidity levels are required in order to predict chlorophyll according to the above scheme. In applying the model to an existing impoundment, average non-algal turbidity levels can be calculated from chlorophyll and Secchi depth measurements using Equation 73. Non-algal turbidity is attributed to inorganic suspended solids, color, and non-chlorophyll-related biological materials. Regional watershed characteristics relating to geology and land use are probably significant controlling factors. Generally, color tends to be important in the Southeast, while inorganic suspended solids are more important in portions of the Great Plains, Lower Mississippi, and Southwest. In this data set, reservoirs with the highest nonalgal turbidities are located in eastern Kansas and Oklahoma. In particular, all six CE impoundments sampled by the EPA/NES and located in the Neosho and Verdigris River Basins in Southeastern Kansas had non-algal turbidities ranging from 2 to 6 1/m. Regional data can aid in estimating turbidity levels in the absence of direct measurements.

213. The following regression equation has been developed from the data set to provide approximate independent estimates of non-algal turbidity levels:

$$\log(a) = .23 - .28 \log(Z) - .21 \log(Tsu) + .36 \log(P)$$
$$- .027 \, LAT + .35 \, d \tag{84}$$

$$(R^2 = .75, \; SE^2 = .037)$$

where

   a = non-algal turbidity (1/m) = 1/S − .025 B

   Z = mean depth (m)

   Ts = summer hydraulic residence time (years)

   P = pool total phosphorus concentration (mg/m^3)

   LAT = latitude (degrees N)

   d = regional dummy = 1, for CE District codes greater than 24
                    = 0, elsewhere

All coefficients in the above equation are significant at p<.01. Observed and predicted values are shown in Figure 74. The District codes required for estimation of the regional factor are given in Appendix A; codes greater than 24 correspond to Western states, including CE Divisions in the Southwest (exclusive of Little Rock District), Missouri River, North Pacific, and South Pacific. While not reflected in the above equation, additional data from the EPA National Eutrophication Survey indicate that impoundments in Mississippi (Vicksburg District) should also be included in the high-turbidity group. A general increasing north-to-south trend is incorporated in the latitude term; the 14-degree range corresponds to factor of 2.4. The equation incorporates only gross regional differences and does not account for relatively high-frequency spatial variations attributed to geologic and land use differences within a given region.

214. The negative depth and residence time terms indicate that turbidity levels tend to be higher in shallow and/or rapidly flushed impoundments. This suggests that sedimentation and resuspension are important controlling factors. Association of phosphorus with inorganic and organic sediments is also reflected by the phosphorus term in the equation. This term does not necessarily mean, however, that a change in phosphorus concentration within a given impoundment will result in a change in non-algal turbidity because phosphorus is probably acting as a surrogate for the actual determining variables, especially inorganic suspended solids. The data base does not permit inclusion of certain factors, such as inflow sediment and color levels, which are direct determinants for non-algal turbidity. The above equation should only be used for preliminary estimation purposes and not outside of the regional distribution of impoundments in the data set (see Part I). Better estimates should be based upon direct measurement and analysis of regional data bases.

215. Additional perspectives on regional variations in non-algal turbidity can be derived from Figure 75, which is based upon data from EPA/NES compendium (USEPA, 1978). Log-mean non-algal turbidities are

230

Figure 74

Observed and Predicted Non-Algal Turbidity
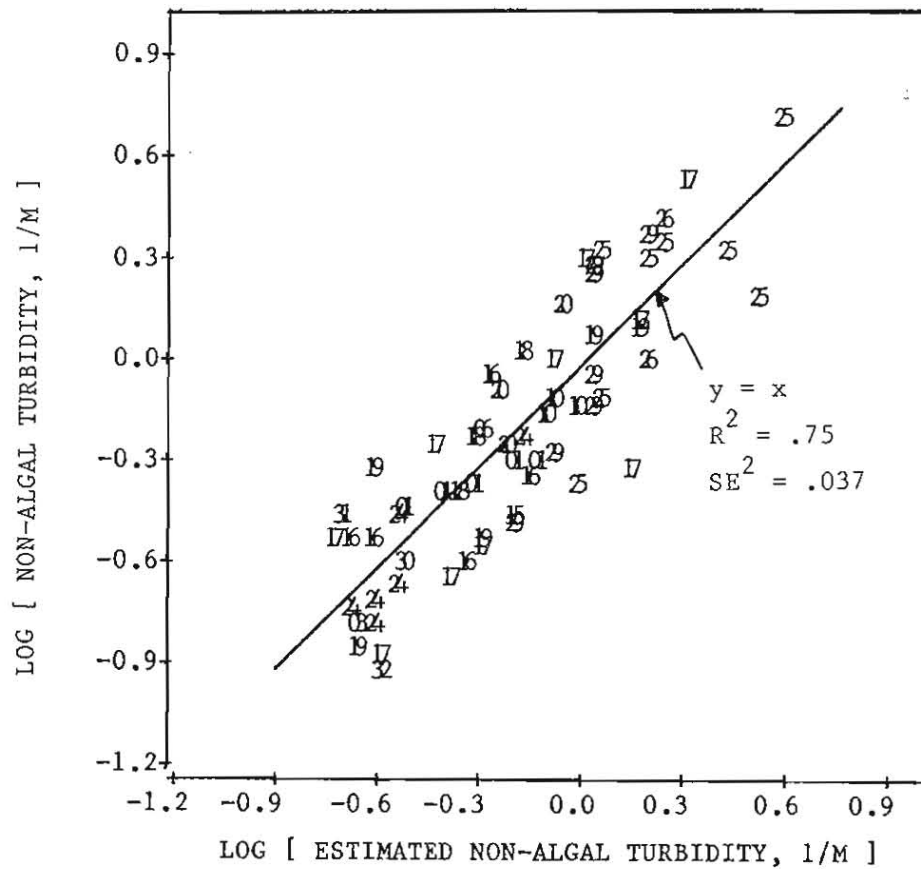
Symbol = CE District Code

X-Axis = .23 − .28 log(Z) −.20 log(Ts) + .36 log(P) −.027 LAT + .35 d

Y-Axis = log(a) = log(1/S − .025 B)

where

Z = mean total depth (m) Ts = summer residence time(yrs)

P = mean total p (mg/m^3)   LAT = latitude (deg N)

d = regional dummy = 1 for CE District Codes > 24
                                = 0 otherwise

a = non-algal turbidity (1/m)   B = mean chlorophyll-a (mg/m^3)

S = mean Secchi depth (m)

231

Figure 75

DISTRIBUTION OF NON-ALGAL TURBIDITY
BY STATE AND IMPOUNDMENT TYPE

EPA/NES Data, >= 2 Lakes and 2 Reservoirs Per State

+ = Lake Mean   ● = Reservoir Mean

LOG (Non-Algal Turbidity, 1/M)

232
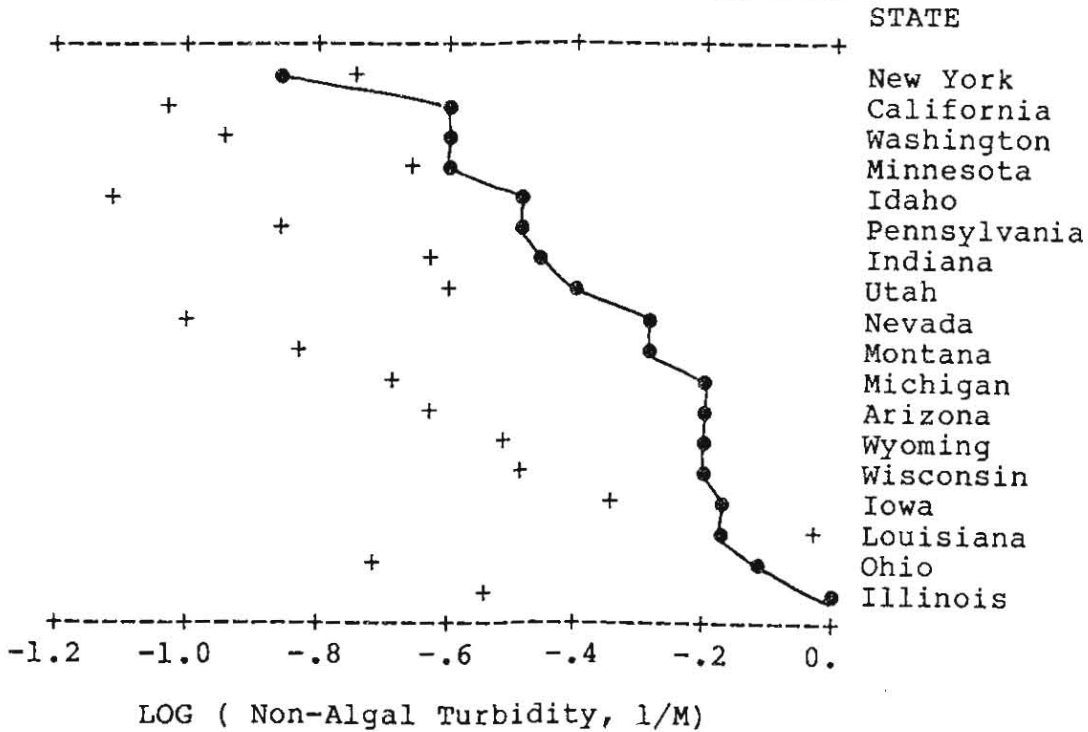
shown by state and impoundment type (natural lake vs. reservoir) for each state with data for at least two lakes and two reservoirs. The states are sorted in order of increasing turbidities for reservoirs. The reservoir-means exceed the lake-means in 16 out of 18 states. This suggests that lake/reservoir differences in turbidity exist within regions; these differences are probably attributed to differences in watershed characteristics and allochothonous sediment loadings.

216. To provide some perspective on time-series behavior within a given system, Figure 76 plots transparency against chlorophyll-a for various years in Lake Washington. Despite a phosphorus concentration range of 14 - 70 mg/m^3 attributed to control of point-source loadings, estimated non-algal turbidity remained relatively constant in the .1 to .2 1/m range. Responses to control of non-point loadings, especially particulate phosphorus, may be qualitatively different, however, and need additional investigation.

217. Table 32 summarizes error statistics for linkage of the chlorophyll-a and turbidity models to predict transparency. Chlorophyll and transparency error variances are given for each of four scenarios involving combinations of observed and estimated non-algal turbidity levels (Figure 74) and observed and estimated mixed depths (Figure 63). Results indicate that uncertainty in the estimation of mean mixed layer depth from mean total depth does not contribute to chlorophyll or transparency error variance. The error variance of the mixed depth model (.0026) is small relative to that of the chlorophyll model (.024) and does not propagate through the model.

218. Because non-algal turbidity accounts for a significant porportion of the total light extinction in many impoundments, the error variance for the transparency prediction depends strongly upon whether observed (.002) or estimated (.013) turbidities are used. Essentially, using observed turbidities puts transparency on both sides of the equation and artificially reduces prediction error. Observed and predicted transparencies using estimated turbidities in both the chlorophyll and transparency models are shown in Figure 77 (R^2 = .87, SE^2 = .013).

233

Figure 76

Chlorophyll-a and Transparency Variations in Lake Washington
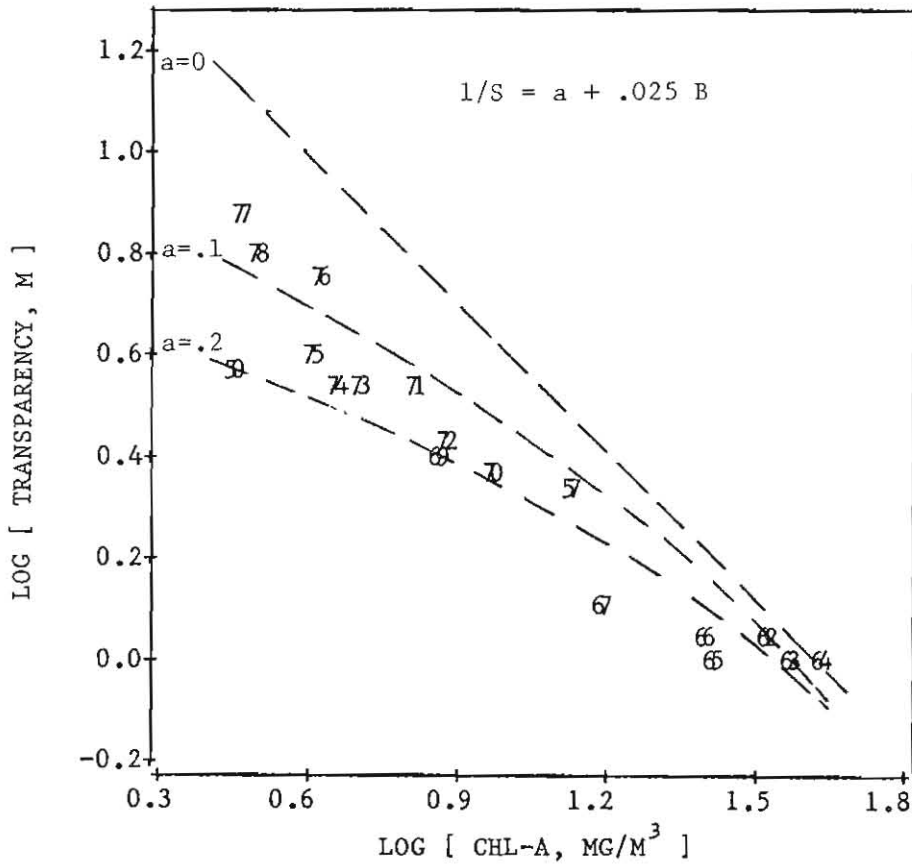
Table 32

Chlorophyll and Transparency Model Error Statistics

| Input Variables | | Chlorophyll-a | | Transparency | |
Mixed Depth	Non-Algal Turbidity	R^2	SE^2	R^2	SE^2
Observed	Observed	.808	.025	.978	.002
Estimated*	Observed	.821	.024	.977	.002
Observed	Estimated**	.734	.035	.871	.013
Estimated*	Estimated**	.750	.033	.869	.014

* Mixed Depth Estimated from Mean Depth (Figure 63)
** Turbidity Estimated from Multiple Regression Model (Figure 74)

Chlorophyll-a Predicted from Model 10, Table 28

Transparency Predicted from :

$$1/S = a + .025 \ B$$

Error statistics based upon data from 66 CE Reservoirs.

Figure 77

Observed and Predicted Transparency
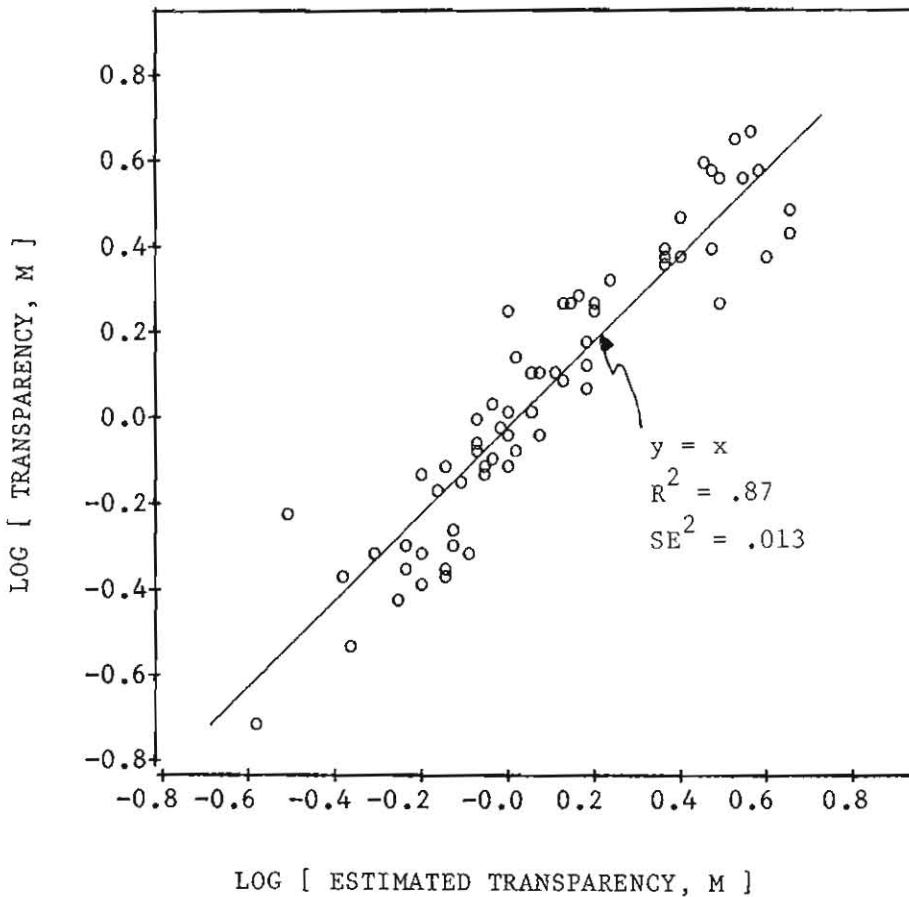
Model: $1/S = a + .025 B$

a = non-algal turbidity (1/m), estimated from Figure 74

B = chlorophyll-a, (mg/m³) estimated from Model 10 in Table 28
    using estimated turbidities

219. When estimated turbidities are used in the chlorophyll-a model, error variance increases from .025 to .035. Regression analysis indicates that the average sensitivity (log/log slope) of predicted chlorophyll-a concentrations to turbidity is -.57 (see model 09 in Table 28). Most of the error variance for the turbidity model (.037) propagates directly through the chlorophyll model (.57 x .57 x .037 = .012) to cause the observed variance increase of .010. Using observed turbidities, chlorophyll-a error variance is also artificially reduced because measured chlorophyll-a values occur on both sides of the equation, although this effect is much less significant than that observed for transparency because turbidity is more strongly correlated with transparency (r=-.91) than with chlorophyll-a (r =.22). The accuracy of chlorophyll-a predictions is partially limited by ability to predict turbidity, although the error variance using estimated turbidity levels is still significantly lower than the error variance of other models which do not include turbidity as an independent variable (see Table 28).

PART VII: MULTIVARIATE CLASSIFICATION SYSTEM

220. In the model testing report (Walker, 1982a), the use of multivariate statistical methods to summarize relationships among impoundment eutrophication response variables was demonstrated. The covariance matrix of average total phosphorus, chlorophyll-a, transparency, and organic nitrogen measurements from 26 phosphorus-limited, low-turbidity reservoirs was subjected to a principal components analysis. The first two principal components were found to explain 96% of the variance in the individual response measurements. Potential uses of the principal components in ranking and classifying impoundments were demonstrated. Classification schemes of this type are useful primarily for the interpretation and summary of data from existing impoundments. Models developed in Part VI of this report can be used for predictive purposes.

221. This chapter presents a revised multivariate analysis based upon data from 66 impoundments. A more general classification scheme is developed by employing a larger data base and including data from nitrogen-limited and turbid impoundments. In order to consider nitrogen-limited systems, the composite nutrient concentration is used in place of total phosphorus; this provides a measure of algal growth potential which is independent of whether the limiting nutrient is phosphorus or nitrogen. As described in Part VI, organic nitrogen concentrations in the five New England impoundments included in the data set are higher than those predicted based upon other measures of trophic state. To permit inclusion of NED impoundments in the classification scheme, the reported organic nitrogen levels have been reduced by 300 mg/m^3 prior to calculation of principal components. This bias may represent an allochthonous organic nitrogen component which is less important in the other impoundments.

222. The correlation matrix of response measurements is summarized in Table 33, along with the mean and standard deviation of each variable. Multiple regression equations (Table 34) provide additional perspectives on relationships among the variables. Table 34 indicates

Table 33

Correlation Matrix of Response Measurements

	Chl-a	Org-N	Xpn	Secchi	Mean	Std. Dev.
Chl-a	1.000	.845	.774	-.560	.89	.365
Org-N	.845	1.000	.878	-.671	2.63	.228
Xpn	.774	.878	1.000	-.853	1.47	.351
Secchi	-.560	-.671	-.853	1.000	.05	.324

NOTES:

All variables transformed to log10 scales
Based upon data from 66 CE reservoirs
Units mg/m^3, except Secchi (meters)
Xpn = composite nutrient concentration

$$Xpn = [\, P^{-2} + ((\, N - 150\,)/12\,)^{-2}\,]^{-.5}$$

P = total phosphorus concentration (mg/m^3)
N = total nitrogen concentration   (mg/m^3)

Organic nitrogen values adjusted downward by 300 mg/m^3
for 5 New England Division impoundments.

239

Table 34

Multiple Regression Equations Relating Water Quality Measurements

Independent Variable	Intercept	Dependent Variable				R^2	SE^2
		Chl-a	Org-N	Xpn	Secchi		
Chl-a	.922	–	–	–	-.631	.314	.0929
Chl-a	-2.672	–	1.354	–	–	.715	.0386
Chl-a	-.292	–	–	.804	–	.598	.0543
Chl-a	-2.444	–	1.067	.351	.197	.727	.0382
Org-N	2.160	.528	–	–	–	.715	.0150
Org-N	1.793	–	–	.570	–	.771	.0120
Org-N	2.655	–	–	–	-.472	.450	.0290
Org-N	1.734	.235	–	.464	.105	.846	.0084
Xpn	.807	.744	–	–	–	.598	.0503
Xpn	-2.091	–	1.353	–	–	.771	.0286
Xpn	1.517	–	–	–	-.924	.728	.0340
Xpn	-.443	.116	.698	–	-.522	.902	.0126
Secchi	.494	-.498	–	–	–	.314	.0733
Secchi	2.563	–	-.955	–	–	.450	.0586
Secchi	1.209	–	–	-.788	–	.728	.0290
Secchi	.658	.136	.329	-1.085	–	.762	.0263

All variables log10-transformed.

that significant reductions in regression mean squared errors are achieved when more than one independent variable is used as a predictor, particularly in the case of composite nutrient concentration. As found in preliminary studies, chlorophyll-a is most strongly correlated with organic nitrogen concentration, which appears to be a relatively good indicator of trophic status because it is less influenced by non-algal turbidity than are transparency, phosphorus, or composite nutrient concentration in most of the impoundments studied. The relatively strong correlation between transparency and composite nutrient concentration reflects covariance with chlorophyll-related materials and association of phosphorus with non-algal turbidity.

223. Results of a principal components analysis of the response covariance matrix are summarized in Table 35. The first two principal components explain 82.2% and 13.3% of the source variance, respectively. Coefficients of the principal components are qualitatively similar to those found in preliminary studies, except that the signs in the second component have been arbitrarily reversed. The higher percentage explained by the second component (13.3% vs. 7.9% in the preliminary study) and slight modifications of coefficient values result from inclusion of turbid and nitrogen-limited impoundments in the revised classification system. While the second component accounts for a relatively small portion of the total variance, it explains 75% of that remaining after consideration of the first component. The high percentage of variance explained by two principal components indicates that differences in these measurements from one impoundment to another can be effectively summarized along two dimensions which can serve as a useful classification system.

224. Correlations and regression equations relating response measurements and composite variables to the principal components are summarized in Table 36. These statistics help to provide some physical interpretations. The first principal component is strongly correlated with each of the individual measurements; correlation coefficients range from .89 for chlorophyll-a to .97 for composite nutrient concentration. The second component is strongly correlated with composite variables,

241

Table 35

Principal Components Analysis of Water Quality Covariance Matrix

	Component			
	1	2	3	4
Eigenvalue	.340	.055	.013	.006
Cumulative R-Squared	.822	.955	.986	1.000
Coefficients				
Chl-a	.554	.689	-.456	-.104
Org-N	.359	.162	.506	.768
Xpn	.583	-.205	.531	-.580
Secchi	-.474	.676	.504	-.253
Mean	2.270	.772	-	-
Standard Deviation	.583	.235	.114	.084

All variables log10-transformed.

Table 36

Impoundment Characteristics vs. Principal Components

Product-Moment Correlation Coefficients:

Variable	PC-1	PC-2
Chlorophyll-a	.885	.443
Organic Nitrogen	.919	.167
Secchi Depth	-.852	.490
Composite Nutrient	.968	-.137
Non-Algal Turbidity	.610	-.756
Chl-a * Secchi	.144	.986
Chl-a / Xpn	-.070	.870

Multiple Regression Equations:

Variable	Intercept	Coefficient PC1	Coefficient PC2	R^2	SE^2
Chl-a	-.899	.554	.688	.979	.0028
Org-N	1.691	.359	.162	.872	.0069
Xpn	.304	.583	-.204	.955	.0057
Secchi	.605	-.474	.676	.965	.0038
Turbidity	-.176	.393	-1.208	.944	.0081
Chl-a * Secchi	-.295	.080	1.365	.993	.0008
Chl-a / Xpn	-1.203	-.028	.894	.761	.0144

All statistics computed on log scales.

such as the product of chlorophyll and transparency (r=.99) and the ratio of chlorophyll-a to limiting nutrient concentration (r=.87). The product of chlorophyll-a and transparency is proportional to the fraction of light extinction attributed to chlorophyll and, based upon the kinetic theory of algal growth described in Part VI, is also proportional to the light-limited, areal photosynthetic rate under nutrient-saturated conditions.

225. Results indicate that the first is a quantitative factor which reflects total concentrations, while the second is a qualitative factor which reflects the partitioning of light extinction and nutrients between algal and non-algal components. The addition of the qualitative dimension permits a more accurate and complete summary of relationships among these measurements than is possible by considering only one dimension or by relating each pair of measurements separately. In one sense, the classification system can be viewed as a two-dimensional version of a Carlson-type trophic state index system (Carlson, 1977). The latter is one-dimensional because it is defined based upon one type of measurement (transparency) and assumes that there are one-to-one relationships between transparency and chlorophyll-a and between transparency and total phosphorus. The applicability of this type of index system to CE reservoirs is limited, primarily because non-algal turbidity causes variability in transparency and phosphorus measurements which is unrelated to chlorophyll-a or "trophic state."

226. Simultaneous variations in PC-1 and PC-2 are shown in Figure 78. The arrows depict directions of increasing chlorophyll-a, transparency, organic nitrogen, and composite nutrient concentration, based upon the definitions of the principal components and the multiple regression equations in Table 36. Projects with the highest chlorophyll-a concentrations tend to be located in the upper right-hand corner of the plot, where the quantities of material in the water column are high and strongly associated with chlorophyll. Of the other three measurements, the organic nitrogen vector is most similar to the chlorophyll-a vector. This reflects that fact that organic nitrogen is a good trophic state indicator because it is only weakly related to non-

Figure 78

Distribution of CE Reservoirs on PC-2 vs. PC-1 Axes
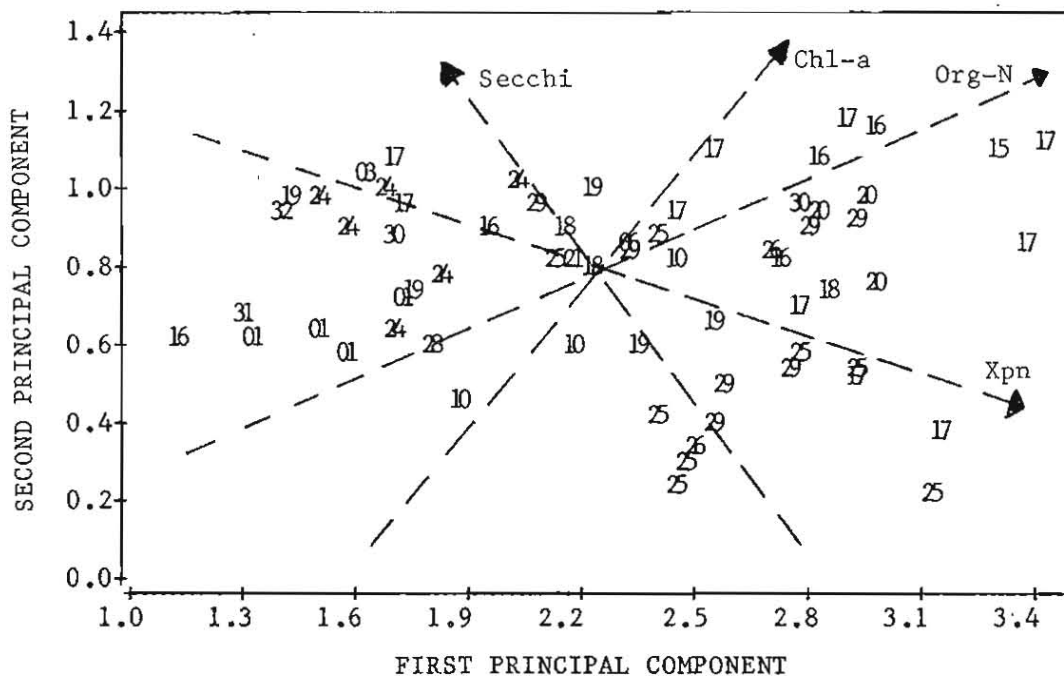
X-Axis:

$$PC-1 = .554 \log(B) + .359 \log(Org-N) + .583 \log(Xpn) - .474 \log(S)$$

Y-Axis:

$$PC-2 = .689 \log(B) + .162 \log(Org-N) - .205 \log(Xpn) + .676 \log(S)$$

Symbols:

CE District Code   see Appendix A)

Arrows:

Gradient Vectors Showing Directions of Increasing Chlorophyll-a,
Secchi, Organic Nitrogen, and Composite Nutrient Concentration,
Based upon Multiple Regression Equations

245

algal turbidity. Figure 79 verifies the chlorophyll distribution by using different symbols to depict variations in chlorophyll concentration. Observed chlorophyll-a contours are shown in relation to those predicted by the multiple regression equation in Table 36. The intent of Figure 79 is to demonstrate the general directions of increasing chlorophyll-a concentrations. The light-limitation model developed in Part VI should be used for predictive purposes.

227. All of the measurements needed to compute PC-1 and PC-2 values may not be available in some applications. Table 37 presents regression equations which can be used to estimate the principal components from each of the 1-, 2-, and 3- variable combinations of response measurements. Generally, missing data would be of less consequence in estimating PC-1 than in estimating PC-2. Since the second is a qualitative factor, at least two types of measurements are required, preferably chlorophyll-a and transparency. The classification system can be used in the absence of organic nitrogen measurements without sacrificing accuracy, since more than 99% of the variance in both PC-1 and PC-2 can be explained using the other three response variables.

228. Since PC-1 is strongly correlated with composite nutrient concentration (r=.97) and PC-2 is strongly correlated with the chlorophyll-transparency product (r=.99), it is possible to simplify the classification system by considering only these two composite variables. Regressions presented in Table 38 indicate that using Xpn and B*S as predictors, a total of 91.3% of the variance in the original four variables can be captured (vs. 95.5% for PC-1 and PC-2). The distribution of reservoirs on the B*S vs. Xpn axes (Figure 80) is qualitatively similar to that shown in Figure 78. Use of this revised classification system facilitates computation and interpretation of the components. Observed and predicted chlorophyll-a contours are shown in Figure 81.

229. In applying the system in a predictive mode, the X-axis or composite nutrient concentration can be estimated from external nutrient loadings using the phosphorus and nitrogen retention models developed in

246

Figure 79

Distribution of Chlorophyll-a Values on PC-2 vs. PC-1 Axes
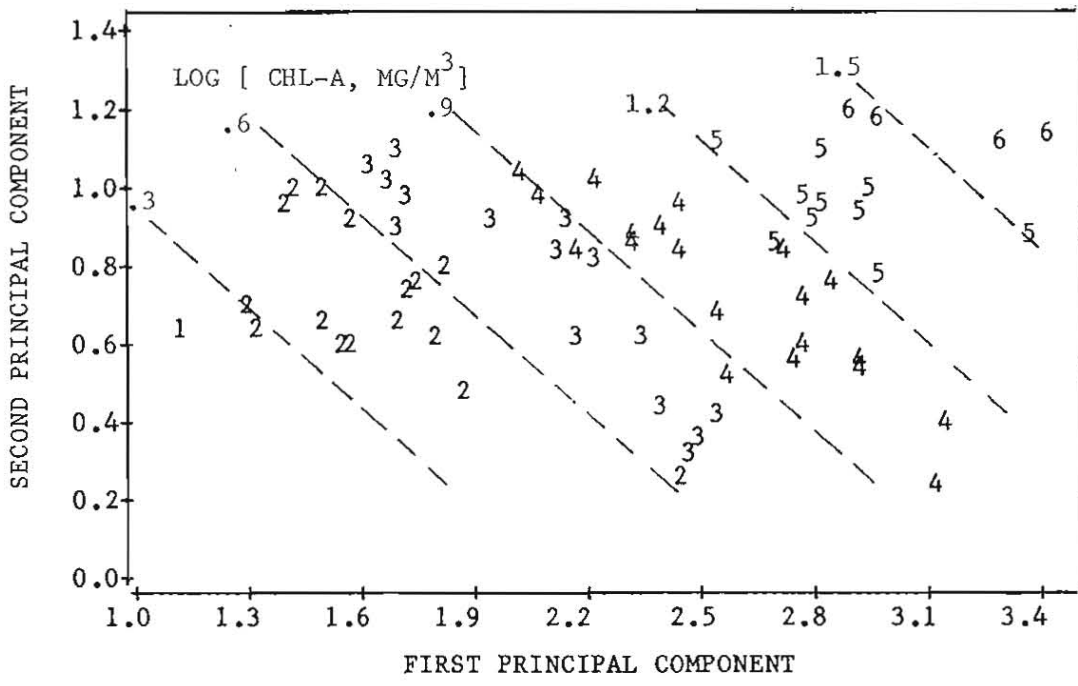
on by
ohyll
on to
The
of
model

PC-2
ents
ipal
s of
less
the
are
tion
ents
in
onse

ient
the
the
es.
as
our
The
is
sed
the
in

or
ent
in

Symbol   Max log(Chl-a,mg/m3)

Symbol	Max log(Chl-a,mg/m3)
1	.3
2	.6
3	.9
4	1.2
5	1.5
6	1.8

Predicted Contours from Multiple Regression Equation:

$$\log(B) = -.858 + .554 \, (PC\text{-}1) + .688 \, (PC\text{-}2)$$

Table 37

Equations for Estimating Principal Components
From Water Quality Measurements

| Dependent Variable | Intercept | Independent Variable Coefficient | | | | R^2 | SE^2 |
		Chl-a	Org-N	Xpn	Secchi		
PC1- 1 Var	2.349	--	-	-	-1.531	.725	.0948
	1.013	1.413	--	-	--	.783	.0750
	-3.913	-	2.350	--	~	.844	.0538
	-.090	--	--	1.606	-	.936	.0220
PC1 - 2 Var	-2.298	.604	1.532	--	-	.885	.0403
	.118	-	-	1.470	-.172	.939	.0215
	-1.942	-	1.616	-	-.769	.945	.0194
	-1.478	-	.773	1.165	--	.957	.0151
	1.474	.949	--	-	-.932	.967	.0114
	.068	.542	--	1.170	-	.982	.0062
PC1 - 3 Var	-1.354	-	.950	.777	-.364	.967	.0117
	-.312	.490	.203	1.097	-	.983	.0059
	-.258	.622	.765	-	-.778	.988	.0043
	.623	.638	-	.750	-.436	.997	.0011
PC1-Definition	0.000	.554	.359	.583	-.474	1.000	.0000
PC2 - 1 Var	.906	--	-	-.092	-	.019	.0550
	.320	-	.172	--	-	.028	.0545
	.518	.285	--	--	--	.197	.0450
	.754	--	-	-	.355	.240	.0425
PC2 - 2 Var	2.144	.683	-.753	-	--	.348	.0371
	-1.411	--	1.293	-.828	-	.379	.0354
	-.294	--	-	.692	.994	.530	.0267
	-1.712	--	.928	-	.793	.686	.0178
	1.163	.880	-	-.799	-	.767	.0131
	.133	.673	-	-	.779	.990	.0005
PC2 - 3 Var	-1.684	-	.897	.037	.812	.687	.0181
	.445	.781	.384	-.938	-	.792	.0120
	.280	.726	-	-.130	.727	.996	.0022
	.091	.665	.019	-	.783	.991	.0005
PC2-Definition	0.000	.689	.162	-.205	.676	1.000	.0000

Independent variables log10-transformed.

Table 38

Impoundment Characteristics vs. Revised Principal Components

Product-Moment Correlation Coefficients:

Variable	Xpn	B*S
Chlorophyll-a	.774	.564
Organic Nitrogen	.878	.280
Secchi Depth	-.853	.368
Composite Nutrient	1.000	.017
Non-Algal Turbidity	.670	-.662
Chl-a * Secchi	.017	1.000
Chl-a / Xpn	-.285	.827

Multiple Regression Equations:

Measurement	Intercept	Xpn	B*S	R^2	SE^2
Chl-a	-.858	.794	.617	.901	.0136
Org-N	1.623	.567	.185	.841	.0085
Xpn	.000	1.000	.000	1.000	.0000
Secchi	.858	-.794	.382	.875	.0136
Turbidity	-.556	.729	-.777	.903	.0141
Chl-a * Secchi	.000	.000	1.000	1.000	.0000
Chl-a / Xpn	-.859	-.206	.618	.774	.0136

All statistics computed on log scales.

Figure 80

Distribution of CE Reservoirs on B*S vs. Xpn Axes

Symbols:

    CE District Code (see Appendix A)

Arrows:

    Gradient Vectors Showing Directions of Increasing Chlorophyll-a,
    Secchi, Organic Nitrogen, and Composite Nutrient Concentration,
    Based upon Multiple Regression Equations

250

Figure 81

Distribution of Chlorophyll-a Values on B*S vs. Xpn Axes
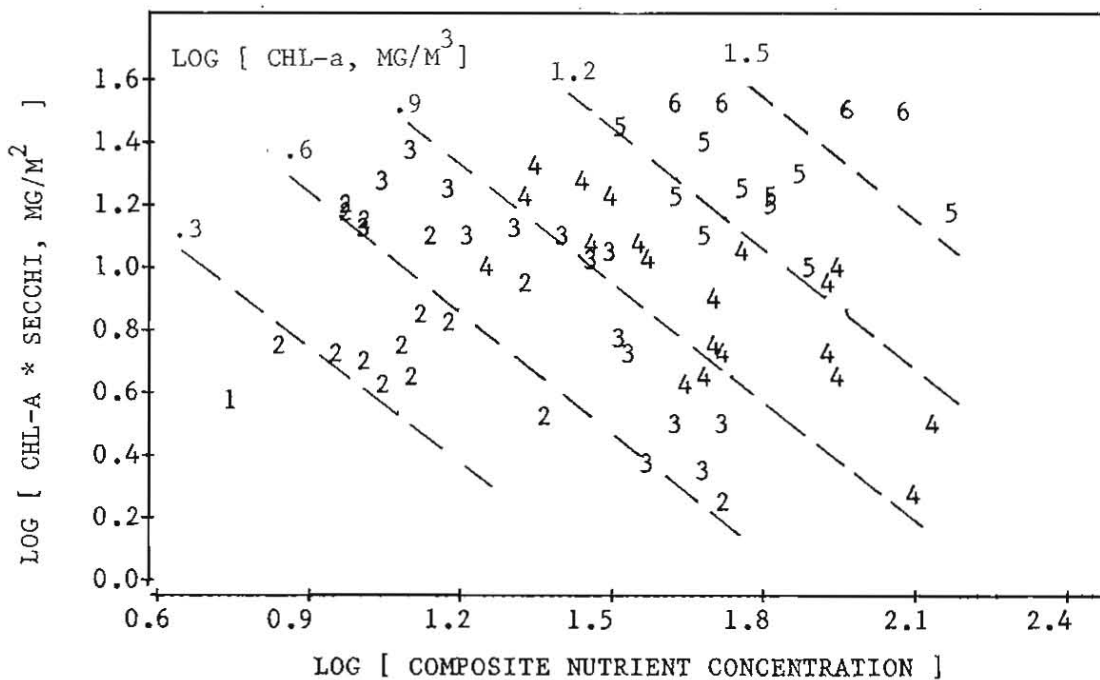
Symbol Max log(Chl-a, mg/m^3)

1	.3
2	.6
3	.9
4	1.2
5	1.5
6	1.8

Predicted Contours from Multiple Regression Equation:

$$\log(B) = -.858 + .794 \log(Xpn) + .617 \log(B*S)$$

previous chapters (see Part VIII). The Y-Axis or chlorophyll-transparency product can be estimated from models developed in Part VI. Observed and predicted B*S values are shown in Figures 82 and 83 using each of two predictive scenarios. In Figure 82, observed non-algal turbidity is treated as an input variable to the chlorophyll and transparency submodels, and a total of 86% of the variance in B*S is explained. In Figure 83, non-algal turbidity is estimated independently using the relationship developed in Figure 74 (Part VI) and a total of 50% of the variance in B*S is explained. In both cases, prediction variance is greater at low B*S values because the calculations are more sensitive to non-algal turbidity in this range. It is apparent that variance in predicting turbidity contributes to variance in predicted B*S values. Improvements in the turbidity submodel would be needed to reduce error variance when the classification system is used in a predictive mode. This is not a problem, however, when the system is used to assist in data interpretation and classification of existing impoundments because measured turbidities and chlorophyll-transparency products can be employed.

230. Despite the fact that PC-1 explains a large portion of the variance in trophic state indicators, it is risky to define it as a "trophic state index" because two reservoirs can have similar PC-1 levels or nutrient concentrations but very different chlorophyll-a and transparency levels. This point is illustrated by a comparison of data from two Ohio reservoirs (Table 39). These reservoirs have similar PC-1 values (2.95 and 2.90, respectively) and average Carlson trophic state indices (Carlson, 1977) (64 and 65, respectively), but chlorophll-a concentrations differ by a factor of 3.5. Mosquito Creek has a relatively high chlorophyll-Secchi product (31 mg/m^2), would be classified as "algae-dominated," and conforms reasonably well to Carlson's index system (index range 62 to 66). Delaware has a relatively low chlorophyll-Secchi product (4.4 mg/m^2), would be classified as "turbidity-dominated," and does not conform to Carlson's index system (index range 53 to 72). This type of comparison is not unusual in the CE data set; there are several examples of this type of

252

phyll-
t VI.
using
algal
and
*S is
ently
l of
ction
more
that
cted
d to
n a
m is
ting
ency

the
as a
PC-1
and
lata
C-1
ate
l-a
s a
be
to
a
be
's
lot
of

Figure 82

Observed vs. Estimated Chlorophyll-Transparency Products
Using Measured Turbidity Values
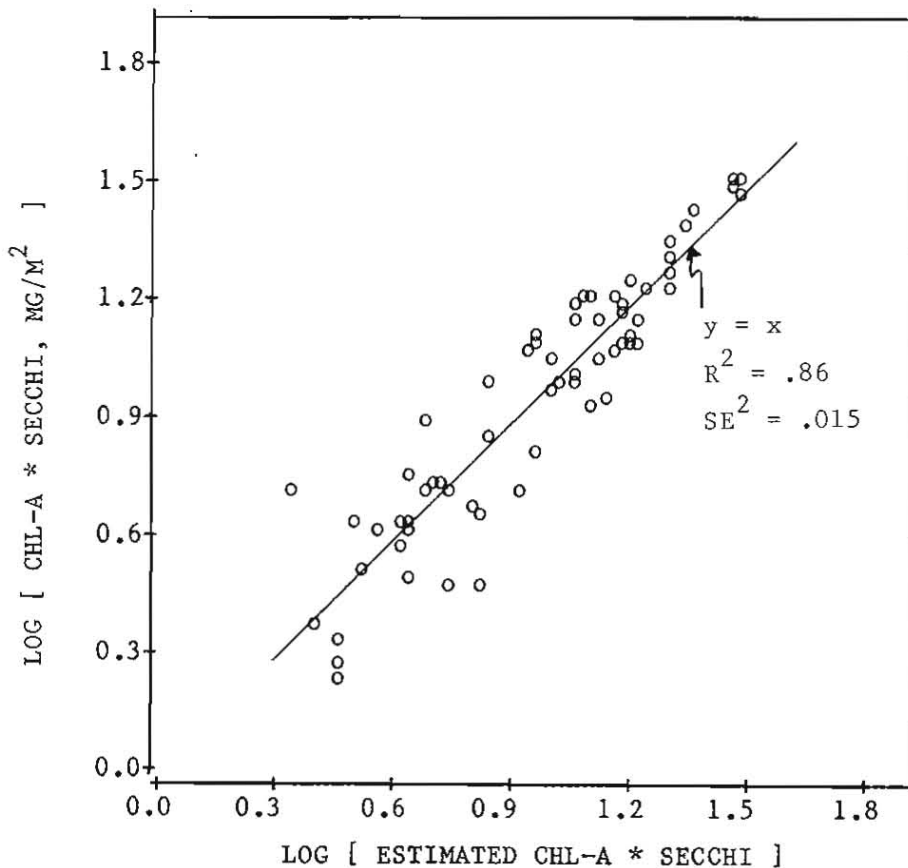
$$X\text{-Axis} = B*S = B / (a + .025\ B)$$

where

   B = chlorophyll-a estimated from model in Figure 64 (mg/m^3)

   a = observed non-algal turbidity $(1/m)$

253

Figure 83

Observed vs. Estimated Chlorophyll-Transparency Products
Using Estimated Turbidity Values
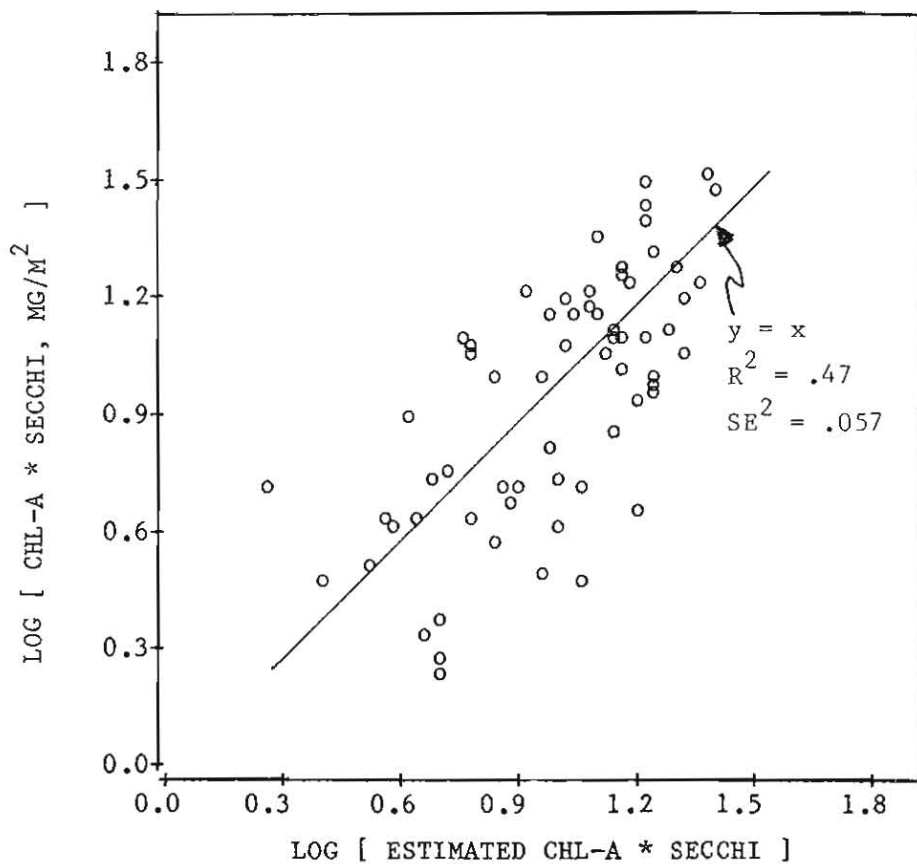
X-Axis = B*S = B / (a + .025 B)

where .

    B = chlorophyll-a estimated from model in Figure 64
       using estimated turbidities (mg/m^3)

    a = non-algal turbidity estimated from Figure 74 (1/m)

Table 39

Comparisons of Water Quality Data from Two Reservoirs

Variable	Units	Mosquito Creek	Delaware	Difference* or Ratio
Chlorophyll-a	mg/m^3	35	10	3.50
Secchi	m	.89	.44	2.02
Organic N	mg/m^3	1019	890	1.15
Composite Nutrient	mg/m^3	50	85	.59
Total P	mg/m^3	62	91	.68
Total N	mg/m^3	1200	3020	.40
Non-Algal Turbidity	1/m	.25	2.02	.12
Carlson Indices				
Chlorophyll-a	–	66	53	13*
Secchi	–	62	72	–10*
Total P	–	64	69	–5*
Mean	–	64	65	–1*
Principal Components				
PC-1	–	2.95	2.90	–.05*
PC-2	–	1.17	.52	.65*
Chl-a * Secchi	mg/m^2	31	4.4	7.05

* Difference used for logarithmic variables.

behavior. If one were to rank or compare these two reservoirs based upon PC-1 (or average Carlson index) alone, a lot of information would be lost and results would be misleading. Principal components and related variables are listed in Tables 40 and 41, sorted by PC-1 and PC-2, respectively.

231. Figure 84 compares the distributions of CE reservoirs, TVA reservoirs (Higgins and Kim, 1981), and 73 natural lakes sampled by the EPA National Eutrophication Survey on B*S vs. Xpn axes. The source and screening criteria for the lake and reservoir data are described in Table 29, Part VI. There is a clear distinction between TVA mainstem and tributary reservoirs along the second dimension because of the relative importance of non-algal turbidity and flushing rate as factors controlling productivity in the former (Placke and Bruggink, 1980). While there is considerable overlap between the lake and reservoir distributions, the lakes, on the average, tend to have higher B*S values (geometric mean = 19) than the CE reservoirs (geometric mean = 8.7). The difference in means is statistically significant at p<.01. The lake with lowest B*S product (Blackfish Lake, Arkansas) is relatively shallow (mean depth 1.8 meters) and rapidly flushed (residence time .021 year). Lake/reservoir differences in the chlorophyll-transparency product reflect a greater importance of turbidity and light-limitation as factors controlling the productivity of some reservoirs. Variations in the B*S product as a function of region and impoundment type are shown in Figure 85, based upon EPA/NES data (USEPA,1978).

Table 40

Table 40
CE Reservoirs Sorted by First Principal Component

Code	Reservoir	State	PC-1	PC-2	Xpn	B*S	B
16393	TYGART	WV	1.10	0.61	0.74	0.56	0.08
31077	DWORSHAK	ID	1.26	0.69	0.82	0.71	0.30
01170	BALL MOUNTAIN	VT	1.29	0.63	0.93	0.70	0.32
19343	DALE HOLLOW	TN	1.39	0.98	0.96	1.16	0.51
32204	KOOKANUSA (LIBBY)	MT	1.39	0.95	0.99	1.13	0.51
01172	NORTH HARTLAND	VT	1.47	0.65	0.99	0.66	0.32
24016	GREERS FERRY	AR	1.49	0.97	0.97	1.15	0.59
01174	TOWNSEND	VT	1.51	0.58	1.02	0.60	0.34
24022	NORFOLK	AR	1.54	0.89	1.13	1.07	0.51
01173	NORTH SPRINGFIELD	VT	1.54	0.57	1.08	0.62	0.36
03307	BELTZVILLE	PA	1.61	1.04	1.03	1.25	0.70
24013	BULL SHOALS	AR	1.66	1.00	1.17	1.21	0.63
24193	CLEARWATER	MO	1.67	0.64	1.06	0.71	0.56
17391	SUMMERSVILLE	WV	1.67	1.08	1.09	1.35	0.80
30235	SAKAKAWEA (GARRISON)	ND	1.69	0.88	1.20	1.08	0.63
17373	JOHN W FLANNAGAN	VA	1.70	0.95	0.99	1.10	0.73
01165	EVERETT	NH	1.71	0.71	1.15	0.79	0.49
19122	CUMBERLAND (WOLF CREEK)	KY	1.73	0.74	1.11	0.84	0.59
28219	CONCHAS	NM	1.76	0.60	1.09	0.62	0.52
24011	BEAVER	AR	1.79	0.77	1.31	0.93	0.57
10003	HOLT	AL	1.86	0.47	1.35	0.50	0.41
16328	ALLEGHENY (KINZUA)	PA	1.92	0.91	1.30	1.11	0.75
24200	TABLE ROCK	MO	2.00	1.02	1.33	1.29	0.91
29195	STOCKTON	MO	2.06	0.96	1.31	1.21	0.94
25278	TENKILLER FERRY	OK	2.11	0.82	1.48	1.03	0.80
18093	MONROE	IN	2.13	0.89	1.38	1.08	0.84
21196	WAPPAPELLO	MO	2.14	0.81	1.24	0.97	0.98
10411	BANKHEAD	AL	2.14	0.61	1.51	0.70	0.60
18120	BARREN RIVER	KY	2.21	0.80	1.44	0.99	0.89
19340	J PERCY PRIEST	TN	2.21	1.00	1.43	1.25	0.99
06372	JOHN H KERR	VA	2.30	0.85	1.44	1.05	0.99
29194	POMME DE TERRE	MO	2.31	0.84	1.55	1.05	0.92
19342	OLD HICKORY	TN	2.32	0.61	1.51	0.74	0.87
25281	WISTER	OK	2.38	0.43	1.61	0.47	0.70
25370	KEMP	TX	2.38	0.88	1.39	1.06	1.09
17241	ATWOOD	OH	2.42	0.94	1.49	1.19	1.14
10072	WALTER F GEORGE (EUFAULA)	GA	2.43	0.81	1.55	0.99	0.96
25267	EUFAULA	OK	2.44	0.31	1.67	0.32	0.64
25275	OOLOGAH	OK	2.44	0.23	1.71	0.22	0.59
26354	LAVON	TX	2.47	0.35	1.55	0.36	0.81
29110	PERRY	KS	2.52	0.40	1.71	0.47	0.77
19119	BARKLEY	KY	2.53	0.66	1.68	0.87	1.05
17256	PLEASANT HILL	OH	2.54	1.10	1.51	1.42	1.34
29111	POMONA	KS	2.55	0.51	1.62	0.60	0.92
26355	LEWISVILLE	TX	2.68	0.83	1.67	1.08	1.22
16243	BERLIN	OH	2.70	0.82	1.74	1.03	1.12
17247	DEER CREEK	OH	2.74	0.70	1.91	0.92	1.01
29106	KANOPOLIS	KS	2.74	0.55	1.66	0.63	1.04
30064	CHERRY CREEK	CO	2.75	0.97	1.60	1.20	1.31
25107	MARION	KS	2.76	0.59	1.70	0.71	1.10
29108	MILFORD	KS	2.77	0.90	1.79	1.20	1.28
20087	SHELBYVILLE	IL	2.80	0.95	1.85	1.26	1.27
16317	SHENANGO RIVER	PA	2.80	1.07	1.66	1.38	1.41
18092	MISSISSINEWA	IN	2.83	0.75	1.93	0.98	1.11
17258	TAPPAN	OH	2.87	1.17	1.62	1.50	1.55
25273	KEYSTONE	OK	2.90	0.54	1.91	0.70	1.09
29207	HARLAN COUNTY	NE	2.90	0.91	1.80	1.18	1.34
17248	DELAWARE	OH	2.90	0.52	1.93	0.63	0.99
20088	REND	IL	2.92	0.97	1.74	1.22	1.37
20081	CARLYLE	IL	2.94	0.75	1.88	0.97	1.24
16254	MOSQUITO CREEK	OH	2.95	1.17	1.70	1.49	1.55
25105	JOHN REDMOND	KS	3.10	0.21	2.08	0.25	0.97
17242	BEACH CITY	OH	3.12	0.38	2.13	0.48	1.04
15237	ASHTABULA (BALDHILL)	ND	3.27	1.10	2.07	1.47	1.59
17249	DILLON	OH	3.34	0.87	2.15	1.15	1.45
17245	CHARLES MILL	OH	3.39	1.13	1.95	1.48	1.80

PC-1 = first principal component
PC-2 = second principal component
Xpn = log10(composite nutrient concentration, mg/m^3)
B*S = log10(chlorophyll-a x Secchi, mg/m^2)
B = log10(chlorophyll-a, mg/m^3)

Table 41
CE Reservoirs Sorted by Second Principal Component

Code	Reservoir	State	PC-1	PC-2	Xpn	B*S	B
25105	JOHN REDMOND	KS	3.10	0.21	2.08	0.25	0.97
25275	OOLOGAH	OK	2.44	0.23	1.71	0.22	0.59
25267	EUFAULA	OK	2.44	0.31	1.67	0.32	0.64
26354	LAVON	TX	2.47	0.35	1.55	0.36	0.81
17242	BEACH CITY	OH	3.12	0.38	2.13	0.48	1.04
29110	PERRY	KS	2.52	0.40	1.71	0.47	0.77
25281	WISTER	OK	2.38	0.43	1.61	0.47	0.70
10003	HOLT	AL	1.86	0.47	1.35	0.50	0.41
29111	POMONA	KS	2.55	0.51	1.62	0.60	0.92
17248	DELAWARE	OH	2.90	0.52	1.93	0.63	0.99
25273	KEYSTONE	OK	2.90	0.54	1.91	0.70	1.09
29106	KANOPOLIS	KS	2.74	0.55	1.66	0.63	1.04
01173	NORTH SPRINGFIELD	VT	1.54	0.57	1.08	0.62	0.36
01174	TOWNSEND	VT	1.51	0.58	1.02	0.60	0.34
25107	MARION	KS	2.76	0.59	1.70	0.71	1.10
28219	CONCHAS	NM	1.76	0.60	1.09	0.62	0.52
16393	TYGART	WV	1.10	0.61	0.74	0.56	0.08
19342	OLD HICKORY	TN	2.32	0.61	1.51	0.74	0.87
10411	BANKHEAD	AL	2.14	0.61	1.51	0.70	0.60
01170	BALL MOUNTAIN	VT	1.29	0.63	0.93	0.70	0.32
24193	CLEARWATER	MO	1.67	0.64	1.06	0.71	0.56
01172	NORTH HARTLAND	VT	1.47	0.65	0.99	0.66	0.32
19119	BARKLEY	KY	2.53	0.66	1.68	0.87	1.05
31077	DWORSHAK	ID	1.26	0.69	0.82	0.71	0.30
17247	DEER CREEK	OH	2.74	0.70	1.91	0.92	1.01
01165	EVERETT	NH	1.71	0.71	1.15	0.79	0.49
19122	CUMBERLAND (WOLF CREEK)	KY	1.73	0.74	1.11	0.84	0.59
20081	CARLYLE	IL	2.94	0.75	1.88	0.97	1.24
18092	MISSISSINEWA	IN	2.83	0.75	1.93	0.98	1.11
24011	BEAVER	AR	1.79	0.77	1.31	0.93	0.57
18120	BARREN RIVER	KY	2.21	0.80	1.44	0.99	0.89
21196	WAPPAPELLO	MO	2.14	0.81	1.24	0.97	0.98
10072	WALTER F GEORGE (EUFAULA)	GA	2.43	0.81	1.55	0.99	0.96
25278	TENKILLER FERRY	OK	2.11	0.82	1.48	1.03	0.80
16243	BERLIN	OH	2.70	0.82	1.74	1.03	1.12
26355	LEWISVILLE	TX	2.68	0.83	1.67	1.08	1.22
29194	POMME DE TERRE	MO	2.31	0.84	1.55	1.05	0.92
06372	JOHN H KERR	VA	2.30	0.85	1.44	1.05	0.99
17249	DILLON	OH	3.34	0.87	2.15	1.15	1.45
30235	SAKAKAWEA (GARRISON)	ND	1.69	0.88	1.20	1.08	0.63
25370	KEMP	TX	2.38	0.88	1.39	1.06	1.09
18093	MONROE	IN	2.13	0.89	1.38	1.08	0.84
24022	NORFOLK	AR	1.54	0.89	1.13	1.07	0.51
29108	MILFORD	KS	2.77	0.90	1.79	1.20	1.28
29207	HARLAN COUNTY	NE	2.90	0.91	1.80	1.18	1.34
16328	ALLEGHENY (KINZUA)	PA	1.92	0.91	1.30	1.11	0.75
17241	ATWOOD	OH	2.42	0.94	1.49	1.19	1.14
17373	JOHN W FLANNAGAN	VA	1.70	0.95	0.99	1.10	0.73
20087	SHELBYVILLE	IL	2.80	0.95	1.85	1.26	1.27
32204	KOOKANUSA (LIBBY)	MT	1.39	0.95	0.99	1.13	0.51
29195	STOCKTON	MO	2.06	0.96	1.31	1.21	0.94
20088	REND	IL	2.92	0.97	1.74	1.22	1.37
30064	CHERRY CREEK	CO	2.75	0.97	1.60	1.20	1.31
24016	GREERS FERRY	AR	1.49	0.97	0.97	1.15	0.59
19343	DALE HOLLOW	TN	1.39	0.98	0.96	1.16	0.51
19340	J PERCY PRIEST	TN	2.21	1.00	1.43	1.25	0.99
24013	BULL SHOALS	AR	1.66	1.00	1.17	1.21	0.63
24200	TABLE ROCK	MO	2.00	1.02	1.33	1.29	0.91
03307	BELTZVILLE	PA	1.61	1.04	1.03	1.25	0.70
16317	SHENANGO RIVER	PA	2.80	1.07	1.66	1.38	1.41
17391	SUMMERSVILLE	WV	1.67	1.08	1.09	1.35	0.80
17256	PLEASANT HILL	OH	2.54	1.10	1.51	1.42	1.34
15237	ASHTABULA (BALDHILL)	ND	3.27	1.10	2.07	1.47	1.59
17245	CHARLES MILL	OH	3.39	1.13	1.95	1.48	1.80
17258	TAPPAN	OH	2.87	1.17	1.62	1.50	1.55
16254	MOSQUITO CREEK	OH	2.95	1.17	1.70	1.49	1.55

PC-1 = first principal component
PC-2 = second principal component
Xpn = log10(composite nutrient concentration, mg/m^3)
B*S = log10(chlorophyll-a x Secchi, mg/m^2)
B   = log10(chlorophyll-a, mg/m^3)

Figure 84
Distribution of CE Reservoirs, TVA Reservoirs, and
EPA/NES Natural Lakes on B*S vs. Xpn Axes
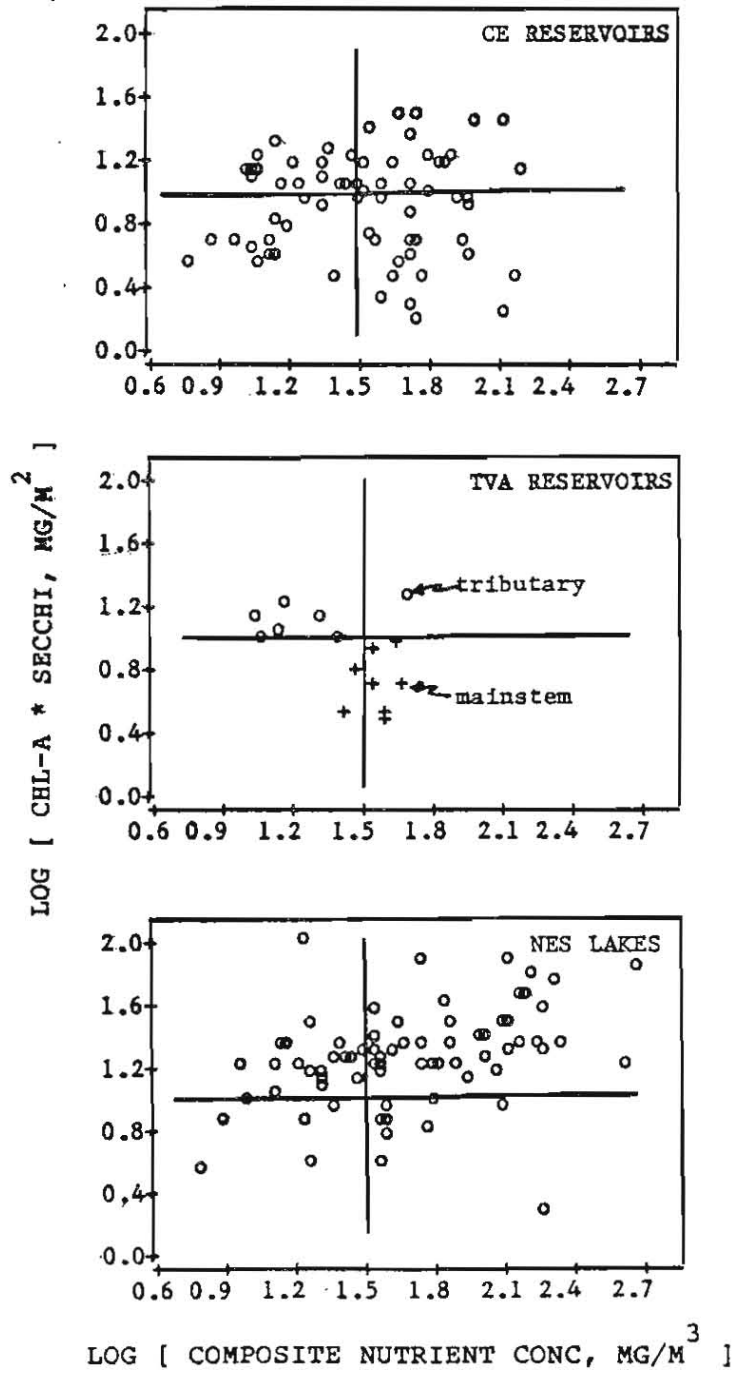
NOTE: Lines indicate mean values for CE Reservoirs.

Figure 85

DISTRIBUTION OF CHLOROPHYLL-SECCHI PRODUCTS
BY STATE AND IMPOUNDMENT TYPE

EPA/NES Data, >= 2 Lakes and 2 Reservoirs Per State

+ = Lake Mean   ● = Reservoir Mean

STATE

New York
Indiana
Wisconsin
Pennsylvania
Michigan
Minnesota
Utah
Louisiana
Ohio
Iowa
Washington
California
Idaho
Illinois
Montana
Wyoming
Arizona
Nevada

0.8 0.9 1.0 1.1 1.2 1.3 1.4 1.5 1.6

LOG (Chl-a * Secchi , mg/m^2)

260
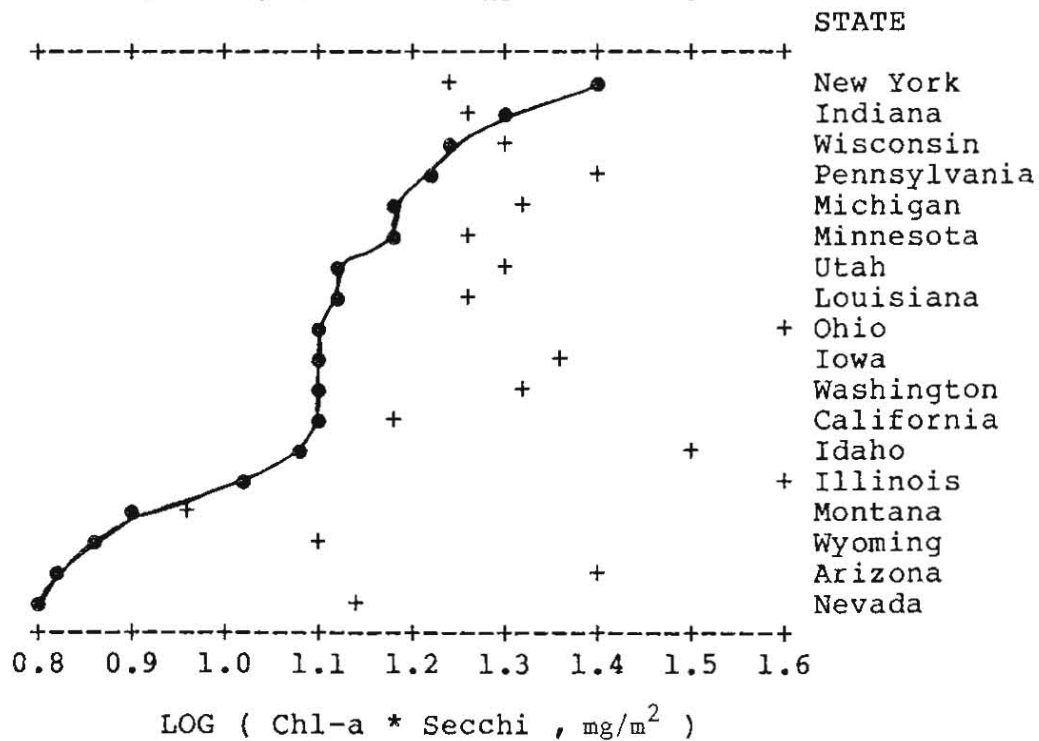
PART VIII: MODEL NETWORK

Introduction

232. Models developed in previous chapters can be linked to provide a basis for predicting eutrophication-related water quality conditions as a function of external nutrient loadings. This chapter summarizes the control pathways, equations, and error statistics for the model network. The objective is to provide a concise summary of the research results and to assess the propagation of errors through the various submodels. Details on model development, independent testing, limitations, and calculation of model input variables are described in previous chapters; these should be studied prior to using the relationships summarized below. Variable ranges and region (see Part I) should be reviewed to assess applicability to a particular reservoir. Simplified procedures which predict reservoir response, measured in terms of hypolimnetic oxygen status and the first principal component of eutrophication-related surface water quality measurements, as direct functions of inflow phosphorus concentration and mean depth are also presented and suggested for use in preliminary assessments. A manual detailing data reduction and model application procedures is under development (Walker, in preparation).

233. Merging of data sets used in developing the nutrient retention models and internal relationships provides data from 40 reservoirs for evaluating the performance of the model network. Both nutrient loading and oxygen depletion rate information are available for 16 reservoirs.

Network Structure and Error Propagation

234. The model network is formed by linking nutrient retention models described in Chapters II and III with internal relationships described in Chapters V, VI, and VII. Figure 86 summarizes control pathways in the network. Symbol definitions, variable ranges, and model equations are summarized in Tables 42, 43, and 44, respectively.

261

Figure 86

M O D E L   N E T W O R K

Inflow Total P
Inflow Ortho-P
Mean Depth
Hyd. Res. Time

Reservoir
Total P

Inflow Total N
Inflow Inorg N
Mean Depth
Hyd. Res. Time

Reservoir
Total N

Mixed Layer Depth
Summer Res. Time

Composite Nutrient
Concentration

Hypol. Oxygen
Depletion Rate

Chlorophyll-a

Transparency

Organic N

Particulate P

Region
Latitude
Total P
Summer Res. Time
Mean Depth

Non-Algal
Turbidity

PC-1

PC-2

Table 42

Definitions of Variables in Model Network

P	= Total Phosphorus (mg/m^3)
Pi	= Inflow Total P (mg/m^3)
Pio	= Inflow Ortho-P (mg/m^3)
Pia	= Inflow Available P (mg/m^3)
K2	= Effective Second-Order Decay Rate for N or P $(m^3/mg-yr)$
Fot	= Tributary Ortho-P/Total P
T	= Hydraulic Residence Yime (years)
Qs	= Surface Overflow Rate (m/yr)
N	= Total Nitrogen (mg/m^3)
Ni	= Inflow Total N (mg/m^3)
Nin	= Inflow Inorganic N (mg/m^3)
Nia	= Inflow Available N (mg/m^3)
Fin	= Tributary Inorganic N/Total N
Xpn	= Composite Nutrient Concentration (mg/m^3)
B	= Chlorophyll-a (mg/m^3)
a	= Non-Algal Turbidity (1/m)
S	= Secchi Depth (m)
Zmix	= Mean Depth of Mixed Layer (m)
G	= Kinetic Factor Used in Chlorophyll-a Model
Ts	= Summer Hydraulic Residence Time (years)
Norg	= Organic Nitrogen (mg/m^3)
Portho	= Ortho-P (mg/m^3)
HODa	= Areal Hypolimnetic Oxygen Depletion Rate (near dam) (mg/m^2-day)
HODv	= Volumetric Hypol. Oxygen Depletion Rate (mg/m^3-day)
Zh	= Mean Hypolimnetic Depth (m)
PC-1	= First Principal Component of Response Measurements
PC-2	= Second Principal Component of Response Measurements
Z	= Mean Total Depth (m)
d	= Regional Dummy (=1 for CE District Codes > 24, =0 Otherwise)
LAT	= Latitude (deg-N)
LONG	= Longitude (deg-W)

Table 43

Statistical Summary of Model Input and Output Variables

Variable	Mean	Standard Deviation	Minimum	Maximum
----------- Input Variables -----------------				
Pi	2.04	.440	1.13	2.65
Pio	1.57	.474	.82	2.55
Fot	-.49	.220	-1.22	-.07
Ni	3.27	.277	2.82	3.92
Nin	2.92	.407	1.54	3.87
Fin	-.38	.269	-1.37	-.04
Ts	-.60	.580	-1.88	.52
T	-.79	.603	-2.09	.24
Qs	1.67	.518	.62	2.86
Zmix	.71	.194	.15	.94
Zh	.91	.233	.46	1.20
Z	.88	.346	.15	1.78
LAT	38.72	3.305	33.07	47.51
LONG	88.74	7.970	75.64	116.3
----------- Output Variables -----------------				
P	1.68	.392	1.00	2.44
N	3.00	.279	2.39	3.63
Xpn	1.55	.347	.82	2.15
B	.97	.335	.30	1.80
S	.03	.331	-.72	.66
a	-.22	.382	-.91	.70
Norg	2.68	.221	2.27	2.18
P-Portho	1.48	.412	.63	2.17
HODa	2.80	.153	2.55	3.10
HODv	1.89	.323	1.56	2.65
PC-1	2.39	.569	1.26	3.39
PC-2	.81	.228	.21	1.13

All variables except LAT, LONG on log scales
symbols defined in Table 42.

Table 44

Summary of Equations in Model Network

Model 1: Phosphorus Retention

$$P = (-1 + (1 + 4\ K2\ \text{Pia}\ T)^{.5})/\ 2\ K2\ T$$

Method A: Inflow Available Phosphorus

$$\text{Pia} = 2.26\ \text{Pio} + .33\ (\ \text{Pi} - \text{Pio})$$

$$K2 = .17\ \text{Qs}\ /\ (\text{Qs} + 13.3)$$

Method B: Decay Rate Formulation

$$\text{Pia} = \text{Pi}$$

$$K2 = .056\ \text{Qs}\ \text{Fot}^{-1}\ /\ (\ \text{Qs} + 13.3\ )$$

Model 2: Nitrogen Retention

$$N = (-1 + (1 + 4\ K2\ \text{Nia}\ T)^{.5})/\ 2\ K2\ T$$

Method A: Inflow Available Nitrogen

$$\text{Nia} = 1.05\ \text{Nin} + .43\ (\ \text{Ni} - \dot{\text{Nin}}\ )$$

$$K2 = .00157\ \text{Qs}\ /\ (\ \text{Qs} + 2.8\ )$$

Method B: Decay Rate Formulation

$$\text{Nia} = \text{Ni}$$

$$K2 = .0035\ \text{Qs}\ \text{Fin}^{-.59}\ /\ (\ \text{Qs} + 17.3))$$

(continued)

Table 44 (Concluded)

Model 3: Chlorophyll-a

$$Xpn = (P^{-2} + ((N-150)/12)^{-2})^{-.5}$$

$$Bx = Xpn^{1.33} / 4.31$$

$$G = Zmix (.14 + .0039 / Ts)$$

$$B = Bx / [(1 + .025\ Bx\ G) (1 + G\ a)]$$

Model 4: Secchi Depth

$$S = 1 / (a + .025\ B)$$

Model 5: Organic Nitrogen

$$Norg = 157 + 22.8\ B + 75.3\ a$$

Model 6: Particulate Phosphorus (Total P - Ortho-P)

$$P - Portho = -4.1 + 1.78\ B + 23.7\ a$$

Model 7: Hypolimnetic Oxygen Depletion Rates

$$HODa = 240\ B^{.5}$$

$$HODv = HODa / Zh$$

Model 8: Principal Components

$$PC-1 = .554\ \log(B) + .359\ \log(Norg) + .583\ \log(Xpn) -.474\ \log(S)$$

$$PC-2 = .689\ \log(B) + .162\ \log(Norg) - .205\ \log(Xpn) +.676\ \log(S)$$

Model 9: Non-Algal Turbidity

$$a = 1/S - .025\ B$$

$$\log(a) = .23 - .28\ \log(Z) - .20\ \log(Ts)$$

$$+.36\ \log(P) -.027\ LAT + .35\ d$$

Chlorophyll-a and non-algal turbidity are key variables used to predict other responses, including transparency, organic nitrogen, particulate (non-ortho) phosphorus, and hypolimnetic oxygen depletion rate. Error statistics for each variable are summarized in Table 45 using different combinations of observed and estimated chlorophyll-a and turbidity concentrations. Error statistics for chlorophyll-a are presented for four cases, involving different combinations of observed and predicted non-algal turbidities and nutrient concentrations.

235. The low error variance for the nutrient retention model (.008 for composite nutrient concentration) partially reflects the relatively low hydraulic residence times of reservoirs in the data set. As demonstrated in Part II, phosphorus retention error variance increases with hydraulic residence time and would tend to become more important to chlorophyll-a predictions in reservoirs with lower flushing rates. In the limit of low residence times, outflow and reservoir nutrient concentrations approach the average inflow concentrations and reservoir water quality predictions become insensitive to the choice of nutrient retention model and its parameter estimates. While the establishment of nutrient balances and predictions of pool and outflow nutrient concentrations become "easier" in rapidly flushed reservoirs, the predictions of biological response to nutrients become more difficult because non-algal turbidity, flushing rate, allochthonous sources of chlorophyll, and unsteady-state conditions tend to become more important as factors regulating algal populations.

236. Two alternative formulations for nutrient retention are summarized in Table 44. These differ with respect to the treatment of the effects of inflow nutrient partitioning (ortho vs. non-ortho-phosphorus and inorganic vs. organic nitrogen). One method (A) employs the nutrient availability concept by using a weighted sum of the two components as the effective inflow concentration. The other method (B) uses total inflow concentrations and computes the effective second-order decay rate as a function of tributary ortho-P/total P and inorganic N/total N ratios. The data do not permit discrimination between these two approaches either for predicting nutrient concentrations or for

267

Table 45
Model Network Error Summary

Variable	Mean Square	Standard Error	F90	Mean Absolute Value	R^2
Total P	.014	.118	1.724	.091	.907
Total N	.009	.095	1.548	.077	.882
Xpn	.008	.089	1.510	.068	.935
Turbidity	.037	.192	2.425	.162	.742
Turbidity **	.037	.192	2.425	.164	.742
Chlorophyll-a					
Case a *	.023	.152	2.011	.122	.793
Case b *	.036	.190	2.396	.155	.671
Case c *	.023	.152	2.011	.126	.792
Case d *	.036	.190	2.396	.158	.671

Response Variables using Estimated Turbidities:

———————————— Observed Chl-a ————————————					
Secchi	.017	.130	1.823	.108	.839
Org-n	.014	.120	1.737	.092	.716
TP-Ortho-P	.026	.162	2.109	.130	.847
HODa	.006	.077	1.429	.062	.733
HODv	.006	.077	1.429	.062	.940
——————————— Estimated Chl-a (Case c) ———————————					
Secchi	.015	.122	1.758	.097	.860
Org-n	.012	.110	1.656	.088	.743
TP-Ortho-P	.023	.152	2.011	.126	.861
HODa	.008	.089	1.510	.080	.624
HODv	.008	.089	1.510	.080	.916
PC-1	.022	.148	1.980	.116	.930
PC-2	.018	.134	1.855	.113	.642
——————————— Estimated Chl-a (Case d) ———————————					
Secchi	.011	.105	1.621	.083	.894
Org-n	.012	.110	1.656	.082	.754
TP-Ortho-P	.021	.145	1.949	.119	.870
HODa	.010	.100	1.585	.084	.551
HODv	.010	.100	1.585	.084	.899
PC-1	.024	.155	2.041	.118	.925
PC-2	.029	.170	2.191	.143	.426

```
*   Case      Turbidity    Nutrients
    a         observed     observed
    b         estimated    observed
    c         observed     estimated from loadings
    d         estimated    estimated from loadings
** Turbidity estimated using estimated phosphorus.
F90 = approximate 90% confidence factor for predicted value:
```

$$Y/F90 < Y < F90 \cdot Y$$

Based upon data from 40 CE reservoirs (16 for HODa, HODv).

predicting other response measurements. In most cases, they yield essentially the same results. The error statistics listed in Table 45 are based upon method A and are essentially equivalent to those for method B.

237. Chlorophyll error mean squares are independent of whether observed or estimated nutrient concentrations are used as inputs. This indicates that the error variances of the nutrient retention models do not propagate through the chlorophyll-a submodel. The lack of propagation reflects: (1) the low error variance of the nutrient retention submodels (.008 for composite nutrient concentration) relative to that of the chlorophyll-a submodel (.023 - .036); (2) the relative importance of the uncertainty associated with predicting the biological response to nutrient levels vs. that associated with establishing the nutrient balance; and (3) the effects of data errors in the estimates of reservoir nutrient and chlorophyll-a levels. Data errors result from estimation of reservoir-mean values based upon the limited sampling regimes employed by the EPA/NES; if all of the error variance were associated with the data, then no error propagation would be expected.

238. Chlorophyll error variance increases from .023 to .036 when estimated non-algal turbidities are used in place of observed values. Thus, ability to predict chlorophyll-a is partially limited by errors in the turbidity submodel. As discussed in Chapter VI, the latter suffers from lack of direct measurements of the determining variables (e.g., inorganic suspended solids and color loadings) and is intended only to provide gross perspective. Observed non-algal turbidities (calculated from chlorophyll and Secchi depth measurements) should be used when available for model applications to existing impoundments. Predictions of the turbidity submodel should be refined based upon regional data bases.

239. A residual correlation matrix and multiple regression equations are presented in Tables 46 and 47, respectively, to further illustrate error propagation through the network when estimated turbidities are used in all submodels. When the error terms are regressed against each other, 45% of the chlorophyll-a prediction errors

269

Table 46

Correlation Matrix of Error Terms in Model Network

Variable	01	02	03	04	05	06	07	08	09	10	11
01 Turbidity	1.00	-.18	-.05	-.14	-.64	-.82	-.16	-.05	-.51	-.27	-.84
02 Total P	-.18	1.00	.28	.86	.38	-.11	.40	.63	.03	.68	.20
03 Total N	-.05	.28	1.00	.62	.06	-.01	.57	.18	.05	.39	.04
04 Xpn	-.14	.86	.62	1.00	.28	-.10	.62	.62	.05	.72	.14
05 Chl-a	-.64	.38	.06	.28	1.00	.31	.36	.28	.66	.78	.92
06 Secchi	-.82	-.10	-.01	-.10	.31	1.00	-.03	-.14	.28	-.14	.66
07 Organic N	-.16	.40	.57	.62	.36	-.03	1.00	.43	.33	.72	.31
08 TP-Ortho-P	.05	.63	.18	.62	.28	-.14	.43	1.00	.00	.55	.14
09 HODv	-.51	.03	.05	.05	.66	.28	.33	.00	1.00	.33	.64
10 PC-1	-.27	.68	.39	.71	.78	-.14	.72	.55	.33	1.0	.55
11 PC-2	-.84	.20	.04	.14	.92	.66	.31	.14	.64	.55	1.00

NOTES: Based upon data from 40 CE reservoirs (16 for HODv)
using estimated turbidities in all submodels.
All values expressed on log scale.

Table 47

Multiple Regression Equations Relating Error Terms

Error		Intercept	Xpn	Submodel Chl-a	Turbidity	R^2
Chl-a	**	.00	.42	–	−.62*	.45
	***		.19		−.61	
Secchi		−.02	−.19	−.17*	−.56*	.77
			.16	−.31	−1.04	
Org-N		.02	.68*	.14	.05	.43
			.56	.26	.08	
TP-Portho		.03	.93*	.17	.14*	.41
			.58	.24	.19	
PC-1		.02	.92*	.69*	.28*	.94
			.52	.86	.35	
PC-2		.00	−.22*	.60*	−.37*	.96
			−.11	.68	.42	

* Regression coefficient significant at $p < .05$.

** First line gives coefficients of multiple regression
   equation relating prediction errors to submodel errors.

*** Second line gives standardized regression coefficients
   which reflect relative influence of each term on
   prediction variance.

Based upon correlation matrix in Table 46.

are explained by errors in turbidity and composite nutrient concentration, although the latter term is significant only at $p < .11$. Much of the transparency prediction error variance (77%) is explained by errors in turbidity and chlorophyll-a; the strength of the turbidity term reflects the fact that non-algal turbidity accounts for a major fraction of the total light extinction in many reservoirs. Errors in organic nitrogen and particulate phosphorus are most strongly related to errors in composite nutrient concentration, but only 41-43% of the variance is explained. Errors in the principal components are related to all three submodels (composite nutrient, chlorophyll-a, and turbidity).

240. Results indicate that errors in predicting chlorophyll-a, the most direct measure of algal growth, are limited more by the performances of the turbidity and chlorophyll-a submodels than by the those of the nutrient retention models. The conclusion that chlorophyll-a prediction errors are controlled more by errors in the phosphorus/chlorophyll relationship than by errors in the phosphorus retention model was reached in a previous analysis of data from northern lakes (Walker, 1977). Future refinements to the model network should focus more on the turbidity and chlorophyll-a submodels, if the objective is to reduce chlorophyll prediction error. Additional insights into error propagation could be derived from estimating and tracking the model and data error components of each submodel. Ability to improve the chlorophyll submodel through further analysis of this data set is limited by data errors in the mean chlorophyll-a estimates; these errors, in turn, reflect the EPA/NES sampling regime, particularly with respect to temporal freqency (3-4 per growing season for the reservoirs studied here). Larger data sets developed from more intensive sampling regimes would be needed to provide a basis for further model improvements.

241. Figure 87 presents observations and predictions for 11 elements of the model network. Different symbols are used to identify nitrogen-limited and high-turbidity impoundments. Chlorophyll-a plots are given using observed and estimated turbidities. For other components, predictions are based upon estimated turbidities exclusively

272

Figure 87
Observed and Predicted Reservoir Water Quality Conditions
Derived from Model Network

LOG [TOTAL P, MG/M3]

$R^2 = .91$
$SE^2 = .014$

LOG [ESTIMATED TOTAL P, MG/M3]

LOG [TOTAL N, MG/M3]

$R^2 = .88$
$SE^2 = .009$
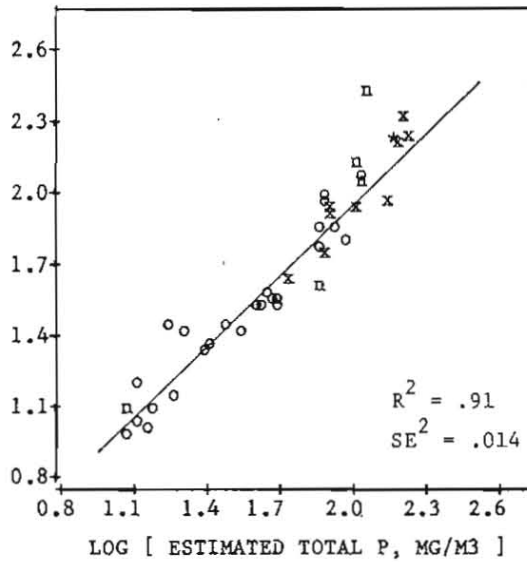
LOG [ESTIMATED TOTAL N, MG/M3]

LOG [COMPOSITE NUTRIENT, MG/M3]

$R^2 = .94$
$SE^2 = .008$
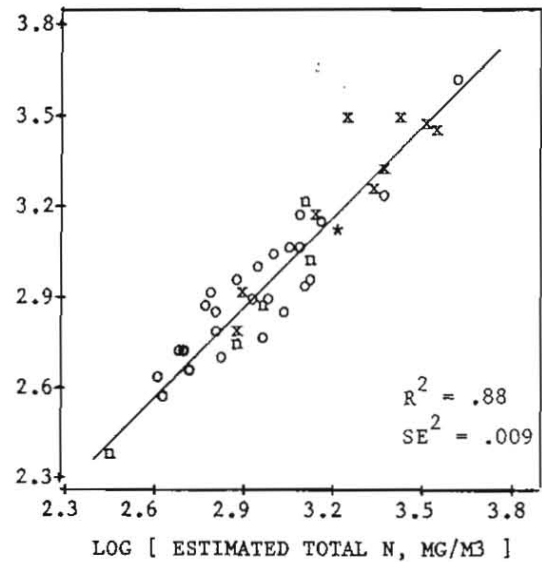
LOC [EST. COMPOSITE NUTRIENT, MG/M3]

LOG [NON-ALGAL TURBIDITY, 1/M]

$R^2 = .74$
$SE^2 = .037$

LOG [ESTIMATED TURBIDITY, 1/M]

Symbol	Inorganic N/P	Non-Algal Turbidity
o	> 10	< 1 (1/m)
n	< 10	< 1
x	> 10	> 1
*	< 10	> 1

273

Figure 87 (Continued)
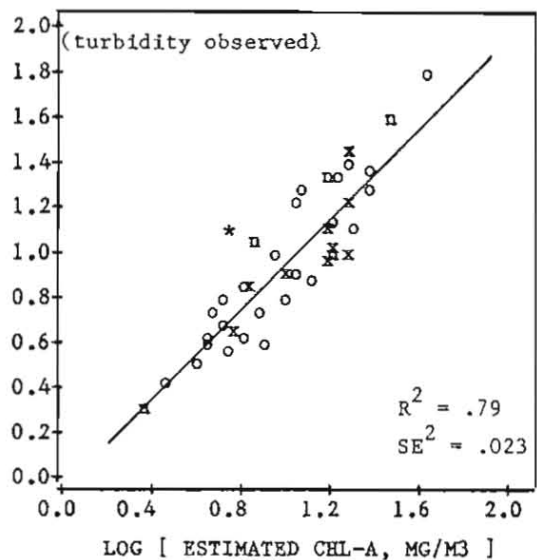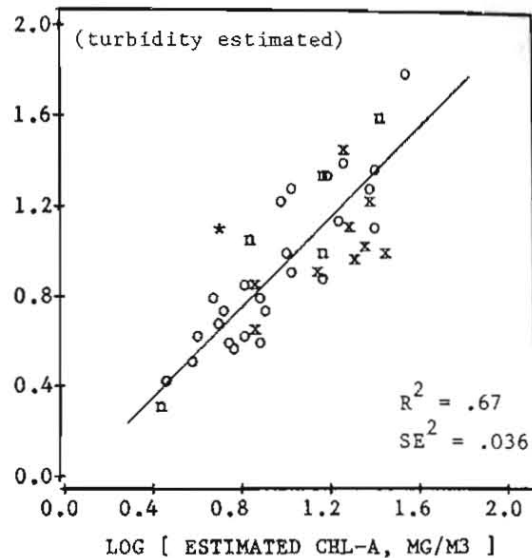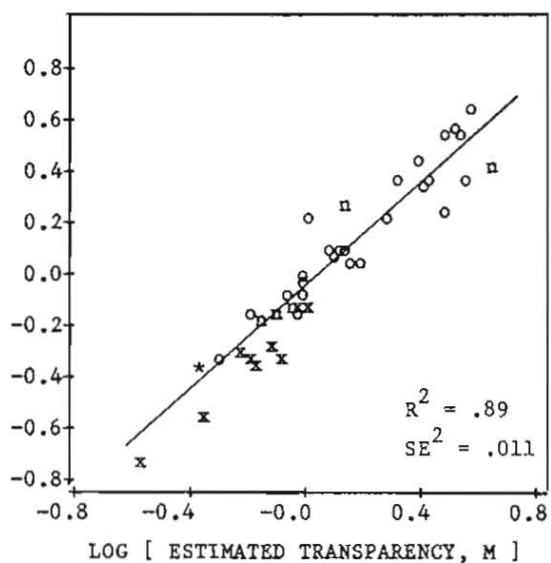
Symbol	Inorganic N/P	Non-Algal Turbidity
o	> 10	< 1 (1/m)
n	< 10	< 1
x	> 10	> 1
*	< 10	> 1

274
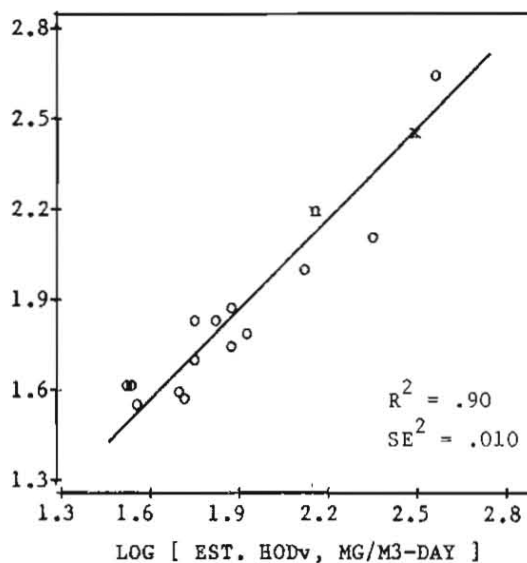
Figure 87 (Concluded)

LOG [ORGANIC NITROGEN, MG/M3]
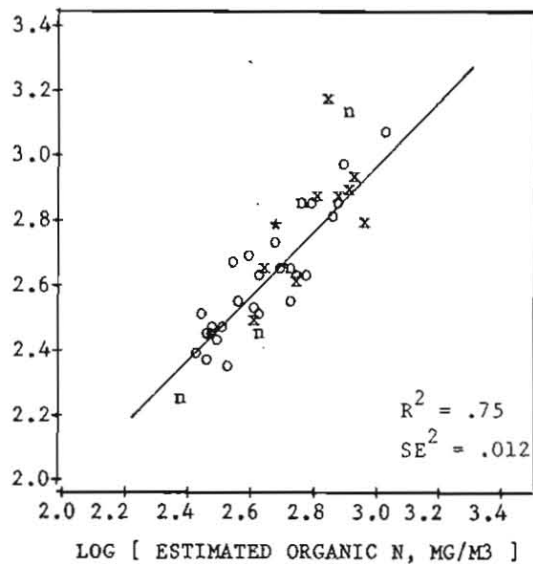
LOG [ESTIMATED ORGANIC N, MG/M3]

$R^2 = .75$
$SE^2 = .012$

LOG [TOTAL P - ORTHO P, MG/M3]

LOG [ESTIMATED TOTAL P - ORTHO-P, MG/M3]

$R^2 = .87$
$SE^2 = .021$

PC-1

ESTIMATED PC-1

$R^2 = .93$
$SE^2 = .024$

PC-2

ESTIMATED PC-2

$R^2 = .43$
$SE^2 = .029$

Symbol	Inorganic N/P	Non-Algal Turbidity
o	> 10	< 1 (1/m)
n	< 10	< 1
x	> 10	> 1
*	< 10	> 1

275
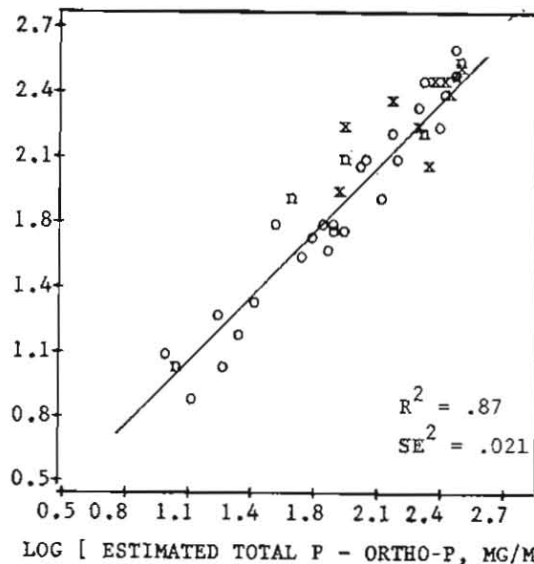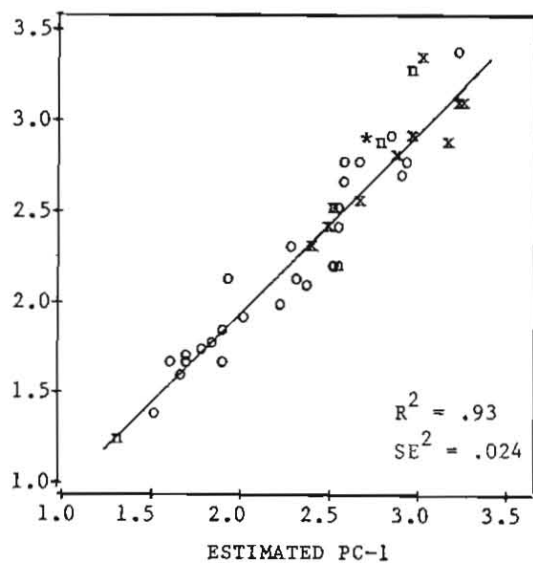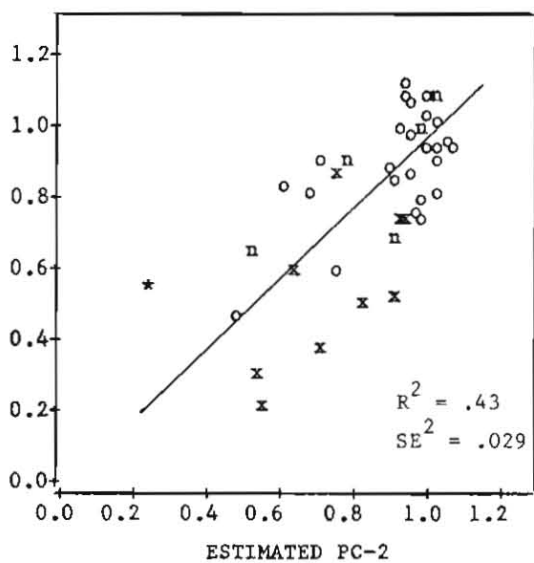
(i.e. Case d in Table 45).

242. Only one impoundment (Keystone) is classified in both the high-turbidity and nitrogen-limited group (symbol=*). This appears as an outlier in the chlorophyll-a plots because of the high spatial and temporal variability of chlorophyll and turbidity, low accuracy of the observed mean chlorophyll-a concentration, and possible effects of salinity-induced density stratification, as detailed in Part VI. Station-mean chlorophyll-a concentrations range from 2.8 to 93 mg/m^3 (3.8 mg/m^3 at dam), in comparison with predicted mean values of 4.6 and 4.7 mg/m^3, using observed and estimated turbidities, respectively. The reservoir is light-limited and the validity of the chlorophyll-a model for predicting within-reservoir variations has been demonstrated in Part VI. Keystone illustrates the need for considering spatial and temporal variations in some reservoirs, as illustrated in Part V.

Comparison with OECD Chlorophyll-a Models

243. Table 48 and Figure 88 present perspectives on the performance of the model network for predicting chlorophyll-a in relation to alternative models developed under the OECD eutrophication program (Rast and Lee, 1978; OECD, 1982). Figure 88 shows observations and predictions in relation to 2-fold error margins. The OECD models relate chlorophyll-a levels to the normalized phosphorus loading expression developed by Vollenweider (1976) and Larsen and Mercier (1976). These relationships assume that algal production is limited by phosphorus supply and that the determining variables are inflow total phosphorus concentration and hydraulic residence time. Computed error statistics for the OECD models refer to seasonal inflow concentration and residence times (based upon nutrient residence time criteria described in Parts II and III), which yield lower chlorophyll-a prediction variance than annual values using both the OECD models and those developed here.

244. When all reservoirs are included, the OECD models have mean squared errors ranging from .086 to .109, compared with .023 to .036 for the network. As shown in Figure 88, the OECD North American model tends

276

Table 48

Error Statistics for Chlorophyll-a Predictions
Based upon Nutrient Loadings for Various Reservoir
Groups and Models

Model	Mean	Standard Deviation	Mean Square	t-Test (mean=0)
--------------- all data (n=40) ---------------				
OECD	-0.059	0.288	0.086	-1.296
OECD-NA	-0.173	0.282	0.109	-3.880*
Network-1	0.004	0.153	0.023	0.165
Network-2	-0.009	0.194	0.037	-0.290
Network-3	0.014	0.151	0.023	0.586
Network-4	0.001	0.192	0.036	0.033
--- inorg N/P > 10, Ts > .04 yrs (n=30) ----				
OECD	-0.031	0.308	0.096	-0.551
OECD-NA	-0.147	0.301	0.112	-2.675*
Network-1	-0.024	0.136	0.019	-0.967
Network-2	-0.040	0.181	0.034	-1.210
Network-3	-0.014	0.133	0.018	-0.577
Network-4	-0.030	0.180	0.033	-0.913
------ inorg N/P > 10, Ts > .04 yrs --------				
----------- a < 1 1/m (n=24) ------------------				
OECD	0.053	0.258	0.069	1.006
OECD-NA	-0.066	0.254	0.069	-1.273
Network-1	-0.003	0.138	0.019	-0.106
Network-2	0.005	0.166	0.028	0.148
Network-3	0.009	0.132	0.018	0.334
Network-4	0.019	0.160	0.026	0.582
------ inorg N/P > 10, Ts > .04 yrs --------				
----------- a < .4 1/m (n=10) ---------------				
OECD	0.098	0.297	0.098	1.043
OECD-NA	-0.030	0.290	0.085	-0.327
Network-1	-0.014	0.107	0.012	-0.414
Network-2	-0.004	0.123	0.015	-0.103
Network-3	0.022	0.103	0.011	0.675
Network-4	0.032	0.118	0.015	0.858

OECD: Synthesis Report $B = .37 \ Pv^{.79}$
           (OECD, 1982)

OECD-NA: North American Project $B = .55 \ Pv^{.76}$
           (Rast and Lee, 1978)

$$Pv = Pi \ / \ (1 + T^{.5})$$

CE Network	Non-Algal Turbidities	Nutrient Submodels
1	observed	inflow available nutrients
2	estimated	" " "
3	observed	decay rate formulations
4	estimated	" " "

Figure 88
Chlorophyll-a Predicted from Network and OECD Models

LOG [CHLOROPHYLL-A, MG/M3]

(turbidity observed)

R^2 = .79
SE^2 = .023

LOG [ESTIMATED CHL-A, MG/M3]

LOG [CHLOROPHYLL-A, MG/M3]

(turbidity estimated)

R^2 = .67
SE^2 = .036

LOG [ESTIMATED CHL-A, MG/M3]

LOG [CHLOROPHYLL-A, MG/M3]

OECD-NA: B = .55 $Pv^{.76}$
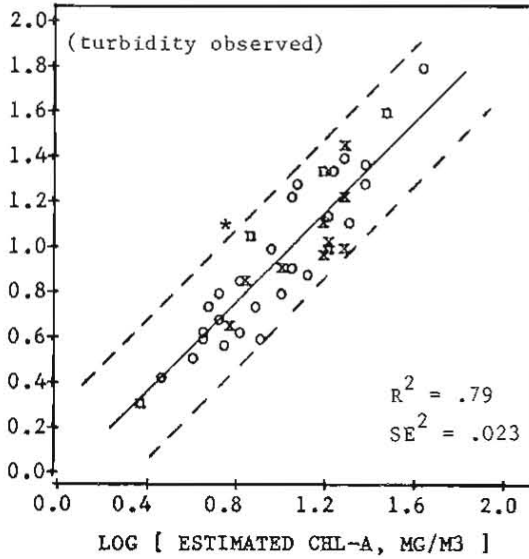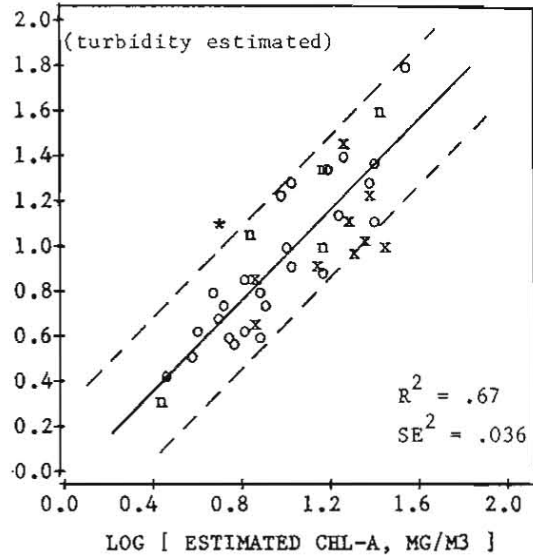
LOG [NORMALIZED P LOADING, MG/M3]
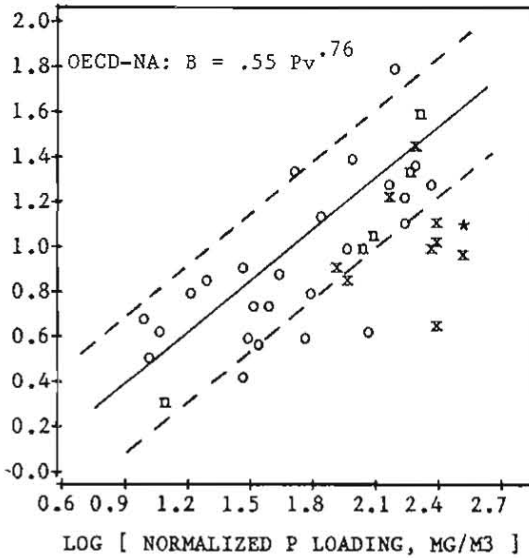
Symbol	Inorganic N/P	Non-Algal Turbidity
o	> 10	< 1 (1/m)
n	< 10	< 1
x	> 10	> 1
*	< 10	> 1

NOTE: dashed lines indicate 2-fold confidence limits.

to underpredict chlorophyll-a levels in nitrogen-limited and/or turbid impoundments. For 24 reservoirs with inorganic N/P ratios greater than 10, non-algal turbidities less than 1 l/m, and summer hydraulic residence times greater than .04 year (2 weeks), predictions of both OECD models are unbiased (mean error not significantly different from zero) and have mean squared errors of .069, compared .018-.028 for the model network. The calculated error variance of the OECD models is similar to that reported in the OECD (1982) synthesis report (.066), based upon data from 67 P-limited lakes and reservoirs. Further reductions in turbidity (< .4 l/m) have little influence on the error statistics.

245. Results indicate that the OECD models are unbiased in P-limited, low-turbidity CE reservoirs, but have substantially higher (2.5 to 4-fold) error variance than the models developed here when applied to CE reservoir data. The difference in variance reflects construction of the nutrient retention formulations to account for second-order decay kinetics and nutrient availability and construction of the chlorophyll-a submodel to account for effects of nitrogen, light, depth, and flushing rate on algal production. In previous chapters, these formulations have been shown to have reasonable generality when applied to independent data sets.

Simplified Screening Models

246. Preliminary studies (Walker, 1982a) have indicated that reservoir eutrophication responses can be predicted from inflow total phosphorus concentration and mean depth. Despite the fact that hydrologic factors (residence time or overflow rate) are important components in the network described above, they are secondary to depth and inflow concentration as controlling factors in this group of reservoirs when the entire model linkage is considered (inflow conditions, morphometry, and hydrology to reservoir trophic state response). This reflects the relatively low hydraulic residence times of these reservoirs (median .22 year) and possible offsetting effects of hydrologic variations in the model network. For example, as

279

hydraulic residence time increases, pool nutrient concentrations decrease because of additional nutrient retention, but the opportunity for biological expression of nutrients increases because flushing rate and non-algal turbidity become less important as growth-regulating factors. The increase in nutrient retention with residence time is also dampened by the apparent second-order decay kinetics, which cause residence time sensitivities ranging from 0 to $-.5$, and by decreases in the effective decay coefficients at low overflow rates (Equation 19).

247. Depth is an important factor because it partially regulates nutrient retention (Equation 9), chlorophyll production from nutrients (light-limitation mechanism), and oxygen depletion (supply of hypolimnetic oxygen per unit area at onset of stratification). All of the depth mechanisms are in the same direction, i.e., favoring less productivity and less oxygen depletion in deeper reservoirs.

248. Based upon the importance of mean depth and inflow phosphorus concentration, preliminary assessments of reservoir trophic status and oxygen depletion can be derived from the simplified models presented below. These models require minimal data, can be implemented graphically, and are useful as preliminary screening tools. Both models employ inflow available phosphorus concentration as a predictor in place of inflow total phosphorus because the former provides more accurate predictions and the resulting model residuals are independent of inflow phosphorus partitioning (ortho-P/total P ratio). In each model, inflow total phosphorus can be used in the absence of inflow available phosphorus estimates, but with loss of accuracy. The model network described above provides more predictive detail, accounts for additional controlling factors, and should be used in final analyses.

249. Figure 89 presents an empirical relationship for predicting the first principal component of reservoir response measurements as a function of inflow available phosphorus concentration and mean depth. The equation has been derived from a step-wise regression analysis and explains 93% of the variance in PC-1 with a mean squared error of .024. Hydrologic factors (residence time or overflow rate) did not enter significantly into the regression. As described in Part VII, PC-1 is a

Figure 89
Simplified Procedure for Predicting First Principal Component of
Reservoir Response Measurements

PREDICTED PC-1
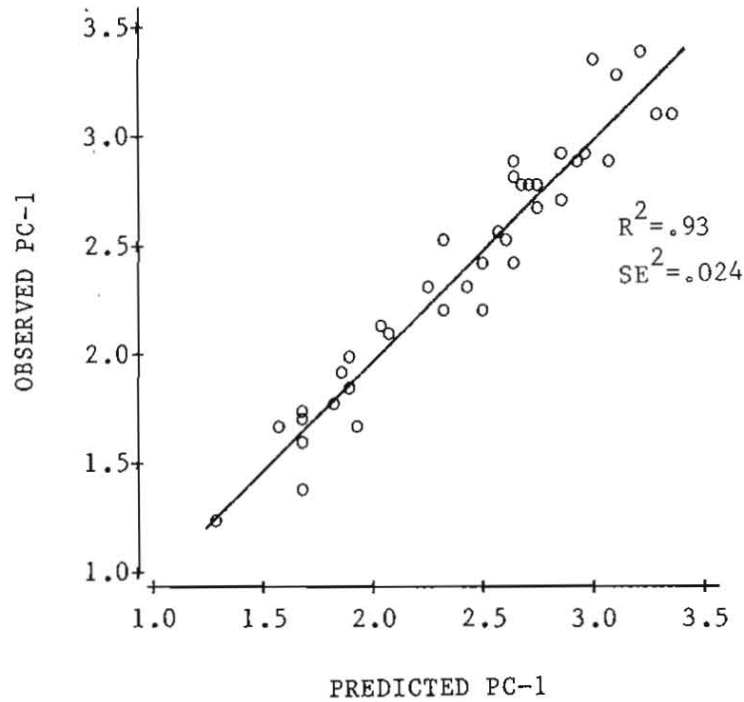
Calculation of PC-1 from Observed Response Data (see Table 37):

$$Xpn = [P^{-2} + ((N-150)/12)^{-2}]^{-.5}$$

$$PC-1 = .554 \log(B) + .359 \log(Norg) + .750 \log(Xpn) - .474 \log(S)$$

Estimation of PC-1 from inflow phosphorus concentration and mean depth:

$$PC-1 = 1.07 + \log(Pia) [1.08 - .52 \log(Z)], \quad (R^2=.93, SE^2=.024)$$

$$Pia = 2.26 \, Pio + .33 \, (Pi - Pio)$$

where

    PC-1 = first principal component of pool water quality data
    Xpn = composite nutrient concentration (mg/m^3)
    P   = mean total phosphorus (mg/m^3)
    N   = mean total nitrogen (mg/m^3)
    B   = mean chlorophyll-a (mg/m^3)
    Norg = mean organic nitrogen (mg/m^3)
    S   = mean Secchi depth (m)
    Pia = inflow available phosphorus (mg/m^3)
    Z   = reservoir mean depth (m)
    Pi   = inflow total phosphorus (mg/m^3)
    Pio = inflow ortho phosphorus (mg/m^3)

quantitative measure of eutrophication which is strongly correlated with nutrients, chlorophyll-a, organic nitrogen, and inverse transparency. It does not distinguish between "algae-dominated" and "turbidity-dominated" reservoirs, however.

250. The graphical version of the model (Figure 90) provides a rapid means for predicting reservoir water quality conditions in relation to the distribution of PC-1 values in CE reservoirs, expressed in percentiles (see Table 40). The model should not be used outside of the ranges of inflow phosphorus concentration and mean depths shown in Figure 90, or in reservoirs with overflow rates less than 5 m/yr (minimum in data set). Inflow total phosphorus concentration can be used in place of inflow available phosphorus without modifying the equation, but the mean squared error increases from .023 to .031.

251. Figure 91 displays hypolimnetic oxygen status as a function of inflow available phosphorus concentration and mean depth in stratified reservoirs. The data set was developed and used in preliminary testing of oxygen depletion models (Walker, 1982a). Different symbols indicate "oxic," "intermediate," and "anoxic" reservoirs, as defined in Figure 91, based upon oxygen profile data from mid-pool and near-dam stations. The clustering of symbols on the Pia vs. Z plot suggests a linear discriminant function for predicting oxygen status, similar in general form to that developed by Reckhow (1978) for northern lakes, but with modified coefficients. The steepness of the discriminant lines reflects the relative importance of mean depth as a factor controlling oxygen depletion.

252. One project (Sakakawea, "oxic") is misclassified as "anoxic" by the discriminant function. Longitudinal gradients and plug-flow behavior are very important in this reservoir (see Figure 32, Part IV). The classification error may be related to differences in inflow phosphorus concentration and mean depth between the upper pool areas (shallow, unstratified, eutrophic) and the lower pool areas (deep, stratified, oligotrophic). Based upon EPA/NES pool water quality measurements, the average available phosphorus concentration at the first stratified station is 21 mg/m^3 and the mean depth of the

282

Figure 90

PC-1 vs. Inflow Available Phosphorus Concentration and Mean Depth

LOG [MEAN DEPTH, M]
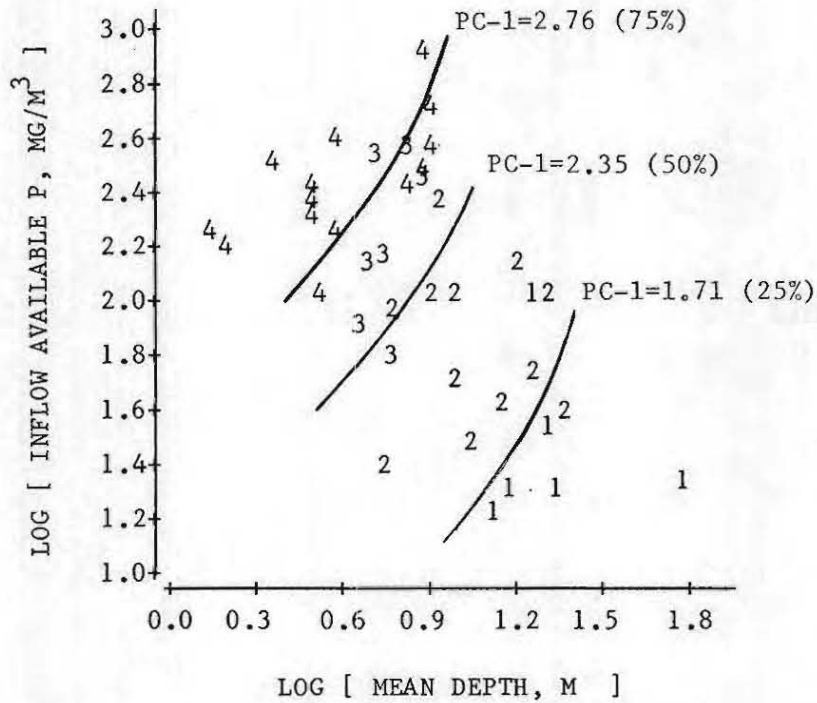
Symbol	Maximum PC-1	Percentile *
1	1.71	25%
2	2.35	50%
3	2.76	75%
4	> 2.76	

* based upon data from 66 CE reservoirs (see Figure 78)

Lines correspond to solution of the following equation:

$$PC-1 = 1.07 + \log(Pia) [1.08 - .52 \log(Z)]$$

at 25%, 50%, and 75% percentiles of PC-1 distribution.

Figure 91
Simplified Procedure for Predicting Oxygen Status as
a Function of Inflow Available Phosphorus and Mean Depth

LOG [MEAN DEPTH, M]
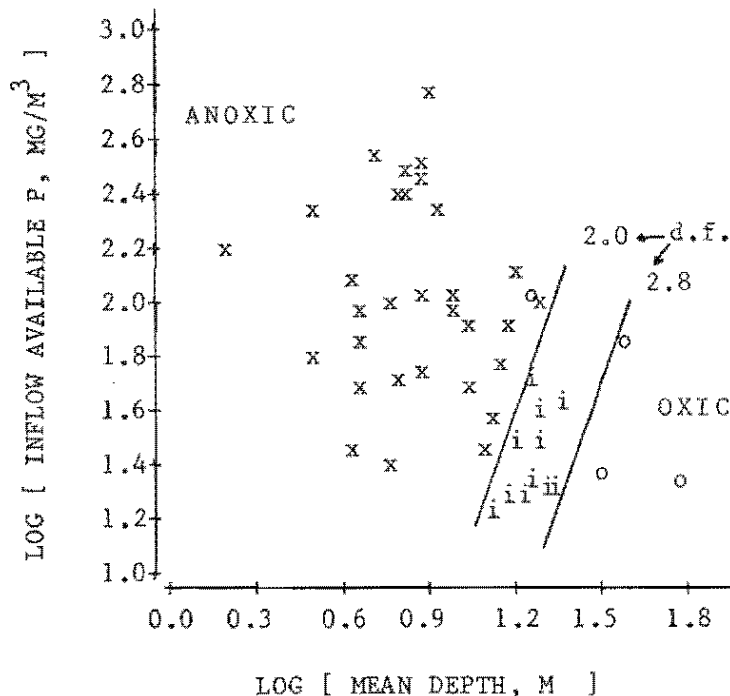
		Percent of Hypolimnetic Depth Reaching a Dissolved Oxygen	
Symbol	Oxygen Status	Concentration < 2 g/m^3	d.f.
x	anoxic	> 80%	< 2.0
i	intermediate	20 - 80 %	2.0 to 2.8
o	oxic	< 20 %	> 2.8

Applicable to thermally stratified reservoirs only with mid-summer
top-to-bottom temperature differences of at least 6 degrees C.
Details on data set development given in Walker(1982a).

Groups discriminated by following function:

$$d.f. = 3 \log(Z) - \log(Pia)$$

$$Pia = 2.26 \ Pio + .33 \ (Pi - Pio)$$

where

d.f. = discriminant function
Z = mean depth (m)
Pia = inflow available phosphorus concentration (mg/m^3)
Pi = inflow total phosphorus concentration (mg/m^3)
Pio = inflow ortho phosphorus concentration (mg/m^3)

284

stratified portion of the pool is about 28 meters. Using these values in place of the total reservoir values (110 mg/m^3 and 18 meters, respectively), the discriminant function increases from 1.7 to 3.0 and the predicted classification changes from "anoxic" to "oxic."

253. Most of the reservoirs are classified as "anoxic." One would expect significant variations in hypolimnetic water quality within the anoxic group, however. Reduction of nitrates, sulfates, iron, and manganese and generation of ammonia and sulfides are expected to be more severe in reservoirs which become anoxic in June, as compared with September, for example. Since these processes all depend upon the input of reducing power, they would be expected to be more important in reservoirs in the upper left corner of Figure 91, furthest from the oxic/intermediate discriminant line. With additional data reduction and analysis, it may be possible to enhance this model to permit further discrimination within the anoxic group, based upon observed nitrate depletion and/or the timing of the onset of anaerobic conditions. Since the model applies only to stratified reservoirs, a means for predicting stratification potential is also needed for applications to proposed reservoirs or to existing reservoirs without thermal profile data.

PART IX: CONCLUSIONS

a. Reductions in error variance and improvements in model generality have been achieved by modifying empirical model structures to account for effects of nonlinear nutrient retention kinetics, inflow nutrient partitioning, seasonal variations in nutrient and water loadings, and algal growth limitation by nitrogen, light, and flushing rate.

b. By superimposing second-order phosphorus retention model kinetics inferred from cross-sectional data sets on a hydraulic network which accounts for advection and dispersion, it is possible to simulate longitudinal variations in phosphorus in reservoir arms dominated by one major tributary. Because of hydrologic variations, low residence times, and other factors, observed phosphorus, chlorophyll, and transparency levels tend to be more variable at or near inflow stations and gradient model prediction errors tend to be greater.

c. Areal hypolimnetic oxygen depletion rate is correlated with surface chlorophyll-a and other measures of trophic state, but independent of temperature and morphometric chracteristics within the limits of the data base. An analysis of covariance indicates that, at a given chlorophyll-a level, oxygen depletion rates in reservoirs average 41% higher than depletion rates in natural lakes. This difference may be attributed to effects of spatial variations, outlet levels, higher allochthonous demands, and/or higher benthic oxygen demands in reservoirs. Metalimnetic oxygen demands tend to become more important than hypolimnetic demands in deeper reservoirs.

d. A principal components analysis of surface water quality data suggests a two-dimensional framework for classifying reservoirs with respect to eutrophication-related conditions. The first two principal components explain 95.5% of the variance in the data. The first dimension is quantitative and reflects the total nutrient

286

supply. The second dimension is qualitative and reflects the partitioning of nutrients and light extinction between organic and inorganic forms. Based upon kinetic theories of algal growth, the second dimension is also related to light-limited productivity. Information on both dimensions provides a more complete description of reservoir water quality than any single measurement, composite variable, or index.

e. Simplified models employing mean depth and inflow available phosphorus concentration as independent variables provide preliminary indications of reservoir surface water quality (measured in terms of the first principal component of eutrophication-related measurements) and hypolimnetic oxygen status.

f. Error analyses indicate that predictions of chlorophyll-a, the most direct measure of eutrophication response, are limited more by uncertainties in estimating the biological response to nutrients than by uncertainties in estimating nutrient retention. This partially reflects variabilities in the chlorophyll-a data, influences of light and kinetic factors on algal production, and the relatively low hydraulic residence times of reservoirs in the model development data set.

g. Additional research in the following areas may lead to a better understanding of reservoir eutrophication dynamics and further model refinements:

   (1) Discrimination among methods of accounting for inflow nutrient availability (inflow fraction weighting schemes vs. modified decay rates).

   (2) Development and testing of a-priori methods for estimating longitudinal dispersion rates used in gradient simulations.

   (3) Modification of the gradient model to permit simulation of more complex morphometries and inflow distributions and to permit consideration of the effects of limitation by light, nitrogen, and flushing on chlorophyll profiles.

(4) Discrimination between linear and log-linear methods for estimating near-dam areal oxygen depletion rates from chlorophyll-a.

(5) Further assessment of possible differences between reservoirs with surface outlets and those with hypolimnetic or mixed release schemes on near-dam oxygen depletion rates.

(6) Development of methods for predicting longitudinal variations in oxygen depletion rate.

(7) Development of methods for predicting non-algal turbidity levels as a function of direct determining factors.

(8) Extension of hypolimnetic oxygen depletion models to permit estimation of nitrate and sulfate reduction.

(9) Analysis of possible effects of region and other factors on nitrogen retention and nitrogen partitioning, particularly with respect to the nitrogen intercept, which is interpreted as organic nitrogen unrelated to chlorophyll-a or turbidity; TKN analytical methods more accurate than those used by the EPA National Eutrophication Survey (detection limit 200 mg/m^3) may be required to support further analysis.

(10) Development of methods for predicting qualitative aspects of algal populations (in particular, blue-green dominance) as a function of nutrient inflows, hydrology, morphometry, and/or other related factors.

h. While second-order decay kinetics appear to have reasonable generality for predicting between-reservoir variations in average phosphorus levels and within-reservoir, spatial variations, available data do not permit testing of the approach for predicting temporal variations within a given reservoir in response to changes in inflow conditions. Since this would probably represent the most common type of application, future development of data sets to support time-series testing of the nutrient retention and other submodels is recommended.

288

i. Because of model structural improvements and calibration to CE reservoir data, the relationships developed in this report would be expected to have less error variance than other published approaches when applied to CE reservoirs within the regional, morphometric, hydrologic, nutrient loading, and water quality limits of the model development data sets. Considerable error variance remains, however, and additional analysis is required to provide a basis for interpreting the sources of this error (e.g., model vs. parameteric vs. data) and to develop guidelines for model use, including possible reservoir-specific calibration of some coefficients. These areas will be considered in the future development of an applications manual.

REFERENCES

Armstrong, D. E., Anderson, M. A., Perry, J. R., and Flatness, D. 1977. "Availability of Pollutants Associated with Access to the Great Lakes," unpublished EPA Progress Report, Wisconsin.

Bachman, R. W. 1980. "Prediction of Total Nitrogen in Lakes and Reservoirs," Restoration of Lakes and Inland Waters, Proceedings of an International Symposium on Inland Waters and Lake Restoration, Portland, Maine, U. S. Environmental Protection Agency, Office of Water Regulations and Standards, Washington, EPA-440/5-81-010, pp 320-324.

Box, G. E. P., Hunter, W. G., and Hunter, J. S. 1978. Statistics for Experimenters, Wiley and Sons, New York.

Canfield, D. E. 1983. "Prediction of Chlorophyll-a Concentrations in Florida Lakes: The Importance of Phosphorus and Nitrogen," Water Resources Bulletin, Vol 19, No. 2, pp 255-262.

Canfield, D. E., and Bachman, R. W. 1981. "Prediction of Total Phosphorus Concentrations, Chlorophyll-a, and Secchi Depths in Natural and Artificial Lakes," Canadian Journal of Fisheries and Aquatic Sciences, Vol 38, No. 4, pp 414-423.

Carlson, R. E. 1977. "A Trophic State Index for Lakes," Limnology and Oceanography, Vol 22, No. 2, pp 361-369.

Carlson, R. E., Kalff, J., and Leggett, W. C. 1979. "The Phosphorus and Nitrogen Budgets of Lake Memphremagog (Quebec-Vermont) with a Predictive Model of Its Nutrient Concentration Following Sewage Removal," Final Report, Contract OSU5-0157, Inland Waters Directorate, Fisheries and Environment Canada, Publication No. 24, Lake Memphremagog Project Limnology Research Group, Department of Biology, McGill University, Quebec, Canada.

Chapra, S. C. 1975. "Comment on 'An Empirical Method of Estimating the Retention of Phosphorus in Lakes' by W. B. Kirchner and P. J. Dillon," Water Resources Research, Vol 11, No. 6, pp 1033-1034.

Chapra, S. C. 1982. "A Budget Model Accounting for the Positional Availability of Phosphorus in Lakes," Water Research, Vol 16, pp 205-209.

Chapra, S. C., and Reckhow, K. H. 1983. Engineering Approaches for Lake Management; Volume 2: Mechanistic Modeling, Butterworth Publishers, Boston, Mass.

Charlton, M. N. 1980. "Hypolimnion Oxygen Consumption in Lakes: Discussion of Productivity and Morphometry Effects," Canadian Journal of Fisheries and Aquatic Sciences, Vol 37, pp 1531-1539.

Clasen, J. 1980. "OECD Cooperative Programme for Monitoring of Inland Waters - Regional Project - Shallow Lakes and Reservoirs," Organization for Economic Cooperation and Development.

Cornett, R. J., and Rigler, F. H. 1979. "Hypolimnetic Oxygen Deficits: Their Prediction and Interpretation," Science, Vol 205, pp 580-581.

Cowen, W. F., and Lee, G. F. 1976a. "Algal Nutrient Availability and Limitation in Lake Ontario Tributary Waters," Ecological Research Series, EPA-600/3-76-094a.

Cowen, W. F., and Lee, G. F. 1976b. "Phosphorus Availability in Particulate Materials Transported by Urban Runoff," J. Water Pollution Control Federation, Vol 48, pp 580-591.

Dorich, R. A., and Nelson, D. W. 1978. "Algal Availability of Soluble and Sediment Phosphorus in Drainage of the Black Creek Watershed," Unpublished Report, Purdue Agricultural Experiment Station.

Edmundson, W. T., and Lehman, J. T. 1981. "The Effect of Changes in Nutrient Income on the Condition of Lake Washington," Limnology and Oceanography, Vol 26, No. 1, pp 1-29.

Fischer, H. B. 1973. "Longitudinal Dispersion and Turbulent Mixing in Open-Channel Flow," Annual Reviews of Fluid Mechanics, pp 59-78.

Fischer, H. B., List, E. J., Koh, R. C. Y, Imberger, J., and Brooks, N. H. 1979. Mixing in Inland and Coastal Waters, Academic Press, New York.

Forsberg, B. R. 1980. "Predicting Algal Response to Destratification," Restoration of Lakes and Inland Waters, Proceedings of an International Symposium on Inland Waters and Lake Restoration, Portland, Maine, U. S. Environmental Protection Agency, Office of Water Regulations and Standards, Washington, EPA-440/5-81-010, pp 134-139.

Forsberg, B. R., and Shapiro, J. 1980. "The Effects of Artificial Destratification on Algal Populations," Surface Water Impoundments, H. G. Stefan, ed., Proceedings of ASCE Conference, Minneapolis, Minnesota, pp 851-864.

Fricker, H. J. 1980. "OECD Eutrophication Programme - Alpine Lakes Project," Organization for Economic Cooperation and Development, Swiss Federal Board of Environmental Protection, Bern.

Frisk, T. 1981. "New Modifications of Phosphorus Models," Acta Fennica, Vol 11, pp 7-17.

Frisk, T., Niemi, J. S., and Kinnunen, K. A. I. 1981. "Comparison of Statistical Phosphorus-Retention Models," Ecological Modelling, Vol 12, pp 11-27.

291

Harris, G. P. 1980. "Temporal and Spatial Scales in Phytoplankton Ecology," Canadian Journal of Fisheries and Aquatic Sciences, Vol 37, pp 877-900.

Higgins, J. M. 1982. Personal communication, oxygen depletion data for TVA reservoirs, Division of Water Resources, Tennessee Valley Authority, Chattanooga, Tennessee.

Higgins, J. M.,and Kim, B. R. 1981. "Phosphorus Retention Models for Tennessee Valley Authority Reservoirs," Water Resources Research, Vol 17, No. 3, pp 571-576.

Higgins, J. M., Poppe, W. L., and Iwanski, M. L. 1980. "Eutrophication Analysis of TVA Reservoirs," Surface Water Impoundments, H. G. Stefan, ed., Proceedings of ASCE Conference, Minneapolis, Minnesota.

Hutchinson, G. E. 1938. "On the Relation Between the Oxygen Deficit and the Productivity and Typology of Lakes," Int. Rev. Gesamten Hydrobiol., Vol 36, pp 336-355.

Hydroscience, Inc. 1971. "Simplified Mathematical Modeling of Water Quality," prepared for U. S. Environmental Protection Agency.

Jones, J. R.,and Bachman, R. W. 1976. "Prediction of Phosphorus and Chlorophyll Levels in Lakes," J. Water Pollution Control Federation, Vol 48, pp 2176-2182.

Katelle, M. J.,and Uttormark, P. D. 1971. "Problem Lakes in the United States," prepared for U. S. Environmental Protection Agency, Office of Research and Monitoring, University of Wisconsin, Water Resources Center, Madison, W72-8987.

Kerekes, J. J. 1981. Miscellaneous figures from the OECD Summary Analysis, unpublished.

Kirchner, W. B.,and Dillon, P. J. 1975. "An Empirical Method of Estimating the Retention of Phosphorus in Lakes," Water Resources Research, Vol 11, No. 1, pp 182-183.

Lam, D. C. L. and Jacquet, J. M. 1976. "Computations of Physical Transport and Regeneration of Phosphorus in Lake Erie," J. Fish. Res. Bd. Canada, Vol 33, No. 2, pp 550-563.

Lappalainen, K. M. 1975. "Phosphorus Loading Capacity of Lakes and a Mathematical Model for Water Quality Prognosis," NORDFORSK, Helsinki, Finland, Publication No. 1, pp 425-441.

Larsen, D. P., and Mercier, H. T. 1976. "Phosphorus Retention Capacity of Lakes," J. Fish. Res. Bd. Can., Vol 33, pp 1742-1750.

Lasenby, D. C. 1975. "Development of Oxygen Deficits in Southern Ontario Lakes," <u>Limnology and Oceanography,</u> Vol 20, No. 6, pp 993-999.

Lee, G. F., Jones, R. A., and Rast, W. 1980. "Availability of Phosphorus to Phytoplankton and Its Implications for Phosphorus Management Strategies," <u>Phosphorus Management Strategies for Lakes,</u> R. C. Loehr, C. S. Martin, and W. Rast, eds., Ann Arbor Science, Michigan.

Levenspiel, O. 1972. <u>Chemical Reaction Engineering,</u> John Wiley and Sons, New York.

Li, W. C., Armstrong, D. E., and Harris, R. F. 1974. "Biological Availability of Sediment Phosphorus to Macrophytes," Technical Report WIS WRC 74-09, Water Resources Center, University of Wisconsin, Madison.

Logan, T. J. 1978. "Chemical Extraction as an Index of Bioavailability of Phosphate in Lake Erie Basin Suspended Sediments," Final Report, Lake Erie Wastewater Management Study, Corps of Engineers, Buffalo, New York.

Logan, T. J., Verhoff, F. H., and DePinto, J. V. 1979. "Biological Availability of Total Phosphorus," Lake Erie Wastewater Management Study, U. S. Army Corps of Engineers, Buffalo.

Lorenzen, M. W., and Mitchell, R. 1973. "Theoretical Effects of Artificial Destratification on Algal Production in Impoundments," <u>Environmental Science and Technology,</u> Vol 7, pp 939-944.

Louder, D. E., and Baker, W. D. 1966. "Some Interesting Limnological Aspects of Fontana Reservoir," <u>Proc. 20th Ann. Conf.,</u> SE Assoc. Game & Fish Comm., Asheville, N. C., pp 380-390.

Mathias, J. A., and Barica, J. 1980. "Factors Controlling Oxygen Depletion in Ice-Covered Lakes," <u>Canadian Journal of Fisheries and Aquatic Sciences,</u> Vol 37, pp 185-194.

Meta Systems. 1979. "Costs and Water Quality Impacts of Reducing Agricultural Nonpoint Source Pollution - An Analysis Methodology," prepared for U. S. Environmental Protection Agency, Athens Environmental Research Laboratory, EPA-600/5-79-009.

Norvell, W. A., and Frink, C. R. 1975. "Water Chemistry and Fertility of Twenty-Three Connecticut Lakes," Bulletin No. 759, Connecticut Agricultural Experiment Station, New Haven.

Omelia, C. R. 1972. "An Approach to the Modeling of Lakes," <u>Schweitz Zeitschrift fur Hydrologie,</u> Vol 34, pp 1-33.

293

Omernik, J. M. 1977. "Nonpoint Source - Stream Nutrient Level Relationships: A Nationwide Study," Corvallis Environmental Research Laboratory, U. S. Environmental Protection Agency, EPA-600/3-77-105.

Organization for Economic Cooperation and Development. 1982. Eutrophication of Waters - Monitoring, Assessment, and Control, Synthesis Report of the OECD Cooperative Programme on Eutrophication, Paris, OECD Publications, Washington.

Osgood, R. A. 1982. "Using Differences Among Carlson's Trophic State Index Values in Regional Water Quality Assessment," Water Resources Bulletin, Vol 18, No. 1, pp 67-74.

Oskam, G. 1973. "A Kinetic Model of Phytoplankton Growth and Its Use in Algal Control by Reservoir Mixing," Geophysical Monograph Series, Vol 17, pp 629-631.

Papst, M. H., Mathias, J. A., and Barica, J. 1980. "Relationship Between Thermal Stability and Summer Oxygen Depletion in a Prairie Pothole Lake," Canadian Journal of Fisheries and Aquatic Sciences, Vol 37, pp 1433-1438.

Parker, L. V., Brockett, B. E., Butler, P. L., Cragin, J. H., Govoni, J. W., Jenkins, T. F., and Keller, D. B. 1982. "Baseline Water Quality Measurements at Six Corps Reservoirs - Summer 1981," U. S. Army Cold Regions Research and Engineering Laboratory, Hanover, N. H.

Parsons, T. R., Takahashi, M., and Hargrave, B. 1977. Biological Oceanographic Processes, 2d ed., Permagon Press, N. Y.

Pastorok, R. A., Lorenzen, M. W., and Ginn, T. C. 1982. "Environmental Aspects of Artificial Aeration and Oxygenation on Reservoirs: A Review of Theory, Techniques, and Experiences," Technical Report E-82-3, U. S. Army Engineer Waterways Experiment Station, CE, Vicksburg, Miss.

Peters, R. H. 1979. "Concentration and Kinetics of Phosphorus Fractions Along the Trophic Gradient of Lake Mempremagog," J. Fish. Res. Bd. Canada, Vol 36, pp 970-979.

Placke, J. F., and Bruggink, D. J. 1980. "Trophic Status of Selected TVA Reservoirs," draft report, Division of Water Resources, Office of Natural Resources, Tennessee Valley Authority.

Porter, K. S. 1975. Nitrogen and Phosphorus, Food Production, Waste, and the Environment, Ann Arbor Science, Mich.

Rast, W. 1978. Personal communication, oxygen depletion data from OECD North American Lakes Project.

Rast, W., and Lee, G. F. 1978. "Summary Analysis of the North American (U. S. Portion) O.E.C.D. Eutrophication Project: Nutrient Loading - Lake Response Relationships and Trophic State Indices," Corvallis Environmental Research Laboratory, U. S. Environmental Protection Agency, EPA-600-3-78-008.

Reckhow, K. H. 1977. "Phosphorus Models for Lake Management," Ph.D. Thesis, Harvard University.

Reckhow, K. H. 1978. "Lake Quality Discriminant Analysis," Water Resources Bulletin, Vol 14, No. 4, pp 856-867.

Reckhow, K. H., and Chapra, S. C. 1983. Engineering Approaches for Lake Management; Volume 1: Data Analysis and Empirical Modeling, Butterworth Publishers, Boston, Mass.

Roesner, L. A., Gigure, P. R., and Evenson, D. E. 1977. "Computer Program Documentation for Stream Quality Model (QUAL-II)," prepared for Southeast Michigan Council of Governments, published by Center for Water Quality Modeling, U. S. Environmental Protection Agency, Athens Research Laboratory.

Smith, V. H. 1980. "A Retrospective Look at the Effects of Phosphorus Removal in Lakes," Restoration of Lakes and Inland Waters, Proceedings of an International Symposium on Inland Waters and Lake Restoration, Portland, Maine, U. S. Environmental Protection Agency, Office of Water Regulations and Standards, Washington, EPA-440/5-81-010, pp 73-77.

Smith, V. H. 1982. "The Nitrogen and Phosphorus Dependence of Algal Biomass in Lakes: An Empirical and Theoretical Analysis," Limnology and Oceanography, Vol 27, No. 6, pp 1101-1111.

Snedecor, G. W., and Cochran, W. G. 1972. Statistical Methods, Iowa State University Press, Ames, Iowa.

Snow, P. D., and DiGiano, F. A. 1976. "Mathematical Modeling of Phosphorus Exchange Between Sediments and Overlying Water in Shallow Eutrophic Lakes," report to the Division of Water Pollution Control, Massachusetts Department of Environmental Quality Engineering, Department of Civil Engineering, University of Massachusetts, Amherst, Report No. Env. E. 54-76-3.

Sonzogni, W. C., Chapra, S. C., Armstrong, D. E., and Logan, T. J. 1982. "Bioavailability of Phosphorus Inputs to Lakes," Journal of Environmental Quality, Vol 11, No. 4, pp 555-562.

Taylor, A. W., and Kunishi, H. M. 1971. "Phosphate Equilibria on Stream Sediment in a Watershed Draining an Agricultural Region," Journal of Agricultural and Food Chemistry, Vol 19, pp 827-831.

U. S. Environmental Protection Agency, National Eutrophication Survey. 1975. "Report on Fontana Lake, Swain and Graham Counties, North Carolina," Working Paper No. 379, Pacific Northwest Environmental Research Laboratory.

U. S. Environmental Protection Agency, National Eutrophication Compendium. 1978. Working Papers 474-477, Corvallis Environmental Research Laboratory and Las Vegas Environmental Monitoring and Support Laboratory.

Vollenweider, R. A. 1969. "Possibilities and Limits of Elementary Models Concerning the Budget of Substances in Lakes," Arch. Hydrobiol., Vol 66, No. 1, pp 1-36.

Vollenweider, R. A. 1975. "Input-Output Models with Special Reference to the Phosphorus Loading Concept in Limnology," Schweitz. Z. Hydrol., Vol 37, pp 53-84.

Vollenweider, R. A. 1976. "Advances in Defining Critical Loading Levels for Phosphorus in Lake Eutrophication," Mem. Ist. Ital. Idrobiol., Vol 33, pp 53-83.

Vollenweider, R. A., and Kerekes, J. 1979. "Co-operative Programme on Monitoring of Inland Waters (Eutrophication Control) Condensed Synthesis Report," Draft, Organization for Economic Cooperation and Development, Paris.

Walker, W. W. 1977. "Some Analytical Methods Applied to Lake Water Quality Problems," Ph.D. Thesis, Harvard University.

Walker, W. W. 1979. "Use of Hypolimentic Oxygen Depletion Rate as a Trophic State Index for Lakes," Water Resources Research, Vol 15, No. 6, pp 1463-1470.

Walker, W. W. 1980. "Analysis of Water Quality Variations in Reservoirs: Implications for Monitoring and Modelling Efforts," Surface Water Impoundments, Proceedings of a conference held in Minneapolis, Minnesota, H. G. Stefan, ed., American Society of Civil Engineers, pp 482-496.

Walker, W. W. 1981. "Empirical Methods for Predicting Eutrophication in Impoundments; Report 1, Phase I: Data Base Development," Technical Report E-81-9, U. S. Army Engineer Waterways Experiment Station, CE, Vicksburg, Miss.

Walker, W. W. 1982a. "Empirical Methods for Predicting Eutrophication in Impoundments; Report 2, Phase II: Model Testing," Technical Report E-81-9, U. S. Army Engineer Waterways Experiment Station, CE, Vicksburg, Miss.

Walker, W. W. 1982b. "An Empirical Analysis of Phosphorus, Nitrogen, and Turbidity Effects on Reservoir Chlorophyll-a Levels," presented at the International Symposium on Reservoir Ecology and Management; sponsored by UNESCO, Universite' Laval, Quebec, Canada, 1981, published in Canadian Water Resources Journal, Vol 7, No. 1, pp 88-107.

Walker, W. W. 1982c. "Calibration and Testing of a Eutrophication Analysis Procedure for Vermont Lakes," prepared for Vermont Agency of Environmental Protection, Water Quality Division, Lakes Program.

Walker, W. W. 1984. "Empirical Methods for Predicting Eutrophication in Impoundments; Phase III: Guidelines for Model Application," Technical Report E-81-9, in preparation, U. S. Army Engineer Waterways Experiment Station, CE, Vicksburg, Miss.

Walker, W. W., and Kuhner, J. 1979. "An Empirical Analysis of Factors Controlling Eutrophication in Midwestern Impoundments," Environmental Effects of Hydraulic Engineering Works, E. E. Driver and W. O. Winderlich, eds., Tennessee Valley Authority.

Zison, S. W., Mills, W. B., Deimer, D., and Chen, C. W. 1978. "Rates, Constants, and Kinetics Formulations in Surface Water Modeling," U. S. Environmental Protection Agency, Athens Environmental Research Laboratory, Georgia, EPA-600/3-78-105.

APPENDIX A

Data Listings

Table A1

CE District Codes

ID	District	Division
01	NEW ENGLAND	NEW ENGLAND
02	NEW YORK	NORTH ATLANTIC
03	PHILADELPHIA	"
04	BALTIMORE	"
05	NORFOLK	"
06	WILMINGTON	SOUTH ATLANTIC
07	CHARLESTON	"
08	SAVANNAH	"
09	JACKSONVILLE	"
10	MOBILE	"
11	BUFFALO	NORTH CENTRAL
12	DETROIT	"
13	CHICAGO	"
14	ROCK ISLAND	"
15	ST PAUL	"
16	PITTSBURGH	OHIO RIVER
17	HUNTINGTON	"
18	LOUISVILLE	"
19	NASHVILLE	"
20	ST LOUIS	LOWER MISSISSIPPI
21	MEMPHIS	"
22	VICKSBURG	"
23	NEW ORLEANS	"
24	LITTLE ROCK	SOUTHWEST
25	TULSA	"
26	FORT WORTH	"
27	GALVESTON	"
28	ALBUQUERQUE	"
29	KANSAS CITY	MISSOURI RIVER
30	OMAHA	"
31	WALLA WALLA	NORTH PACIFIC
32	SEATTLE	"
33	PORTLAND	"
34	SACRAMENTO	SOUTH PACIFIC
35	SAN FRANCISCO	"
36	LOS ANGELES	"

Table A2

Reservoir Codes and Locations

Code	Reservoir	Major Trib.	State	Lat	Long	Outlet
01165	EVERETT	PISCATAQUOG	NH	43.092	71.660	
01170	BALL MOUNTAIN	WEST	VT	43.127	72.776	
01172	NORTH HARTLAND	OTTAQUECHEE	VT	43.601	72.353	
01173	NORTH SPRINGFIELD	BLACK	VT	43.336	72.509	
01174	TOWNSHEND	WEST	VT	43.083	72.699	
02176	WATERBURY	LITTLE	VT	44.381	72.770	
03307	BELTZVILLE	POHOPOCO	PA	40.848	75.638	H/M/E
04312	F J SAYERS (BLANCHARD)	BALD EAGLE	PA	41.048	77.604	H/E
06372	JOHN H KERR	ROANOKE	VA	36.598	78.301	H
08074	CLARK HILL	SAVANNAH	SC	33.661	82.199	H
08330	HARTWELL	SAVANNAH	GA	34.356	82.822	H
10003	HOLT	BLACK WARRIOR	AL	33.252	87.450	H
10069	ALLATOONA	ETOWAH	GA	34.163	84.727	H
10071	SEMINOLE (WOODRUFF)	APALACHICOLA	GA	30.708	84.865	H
10072	WALTER F GEORGE (EUFAULA)	CHATTAHOOCHEE	GA	31.600	85.050	H
10076	SIDNEY LANIER	CHATTAHOOCHEE	GA	34.158	84.072	H
10411	BANKHEAD	BLACK WARRIOR	AL	33.449	87.349	H
14099	RED ROCK	DES MOINES	IA	41.369	92.979	
15237	ASHTABULA (BALDHILL)	SHEYENNE	ND	47.033	98.083	H
15399	EAU GALLE	EAU GALLE	WI	44.856	92.244	
16243	BERLIN	MAHONING	OH	41.045	81.002	H
16254	MOSQUITO CREEK	MOSQUITO	OH	41.299	80.758	H
16317	SHENANGO RIVER	SHENANGO	PA	41.264	80.463	H
16328	ALLEGHENY (KINZUA)	ALLEGHENY	PA	41.841	79.003	H/E
16393	TYGART	TYGART VALLEY	WV	39.313	80.033	H
17241	ATWOOD	INDIAN	OH	40.526	81.285	
17242	BEACH CITY	SUGAR	OH	40.634	81.558	
17245	CHARLES MILL	MOHICAN/BLACK F	OH	40.740	82.363	
17247	DEER CREEK	SCIOTO/DEER	OH	39.622	83.216	
17248	DELAWARE	OLETANGY	OH	40.358	83.069	
17249	DILLON	LICKING	OH	39.992	82.082	
17256	PLEASANT HILL	MOHICAN/CLEAR F	OH	40.623	82.325	
17258	TAPPAN	LITTLE STILLWTR	OH	40.356	81.227	
17373	JOHN W FLANNAGAN	POUND	VA	37.233	82.348	
17389	BLUESTONE	NEW	WV	37.640	80.887	
17391	SUMMERSVILLE	GAULEY	WV	38.217	80.891	
18092	MISSISSINEWA	MISSISSINEWA	IN	40.716	85.956	H
18093	MONROE	SALT	IN	39.007	86.512	H/M
18094	SALAMONIE	SALAMONIE	IN	40.807	85.679	H
18095	C M HARDEN (MANSFIELD)	BIG RACOON	IN	39.717	87.072	H/M
18097	BROOKVILLE	WHITEWATER	IN	39.439	85.003	H/M
18120	BARREN RIVER	BARREN	KY	36.891	86.124	H/M
18121	BUCKHORN	KENTUCKY	KY	37.339	83.470	H
18126	GREEN RIVER	GREEN	KY	37.247	85.339	H/M
18128	NOLIN RIVER	NOLIN	KY	37.278	86.247	H/M
18129	ROUGH RIVER	ROUGH	KY	37.619	86.499	H
18134	CAVE RUN	LICKING	KY	38.119	83.533	H/E
19119	BARKLEY	CUMBERLAND	KY	37.021	88.221	H
19122	CUMBERLAND (WOLF CREEK)	CUMBERLAND	KY	36.869	85.145	H

Code	Reservoir	Major Trib.	State	Lat	Long	Outlet
19338	CHEATHAM	CUMBERLAND	TN	36.324	87.226	M
19340	J PERCY PRIEST	STONES	TN	36.151	86.617	H
19342	OLD HICKORY	CUMBERLAND	TN	36.297	86.655	H
19343	DALE HOLLOW	OBEY	TN	36.538	85.441	H
20081	CARLYLE	KASKASKIA	IL	38.618	89.351	
20087	SHELBYVILLE	KASKASKIA	IL	39.406	88.783	
20088	REND	BIG MUDDY	IL	38.037	88.956	
21196	WAPPAPELLO	ST FRANCIS	MO	36.928	90.284	
22014	DE GRAY	CADDO	AR	34.214	93.113	H/M/E
22189	ENID	YOCONA	MS	34.158	89.903	H/M/E
24011	BEAVER	WHITE	AR	36.420	93.847	H
24012	BLUE MOUNTAIN	PETIT JEAN	AR	35.101	93.650	H
24013	BULL SHOALS	WHITE	AR	36.367	92.572	H
24016	GREERS FERRY	LITTLE RED	AR	35.517	91.997	H
24022	NORFOLK	WHITE/N FK	AR	36.249	92.237	H
24193	CLEARWATER	BLACK	MO	37.133	90.775	H
24200	TABLE ROCK	WHITE	MO	36.595	93.311	H
25020	MILLWOOD	LITTLE SALINE	AR	33.691	93.965	
25105	JOHN REDMOND	NEOSHO	KS	38.237	95.768	
25107	MARION	COTTONWOOD	KS	38.372	97.081	
25267	EUFAULA	CANADIAN/S	OK	35.306	95.362	
25269	FORT SUPPLY	WOLF	OK	36.553	99.571	
25273	KEYSTONE	ARKANSAS	OK	36.151	96.251	
25275	OOLOGAH	VERDIGRIS	OK	36.421	95.678	
25278	TENKILLER FERRY	ILLINOIS	OK	35.596	95.049	
25281	WISTER	POTEAU	OK	34.936	94.719	
25348	TEXONA (DENNISON)	RED	TX	33.818	96.572	
25370	KEMP	WICHITA	TX	33.758	99.150	
26345	BELTON (BELL)	LEON	TX	31.106	97.474	H/M
26347	CANYON	GUADALUPE	TX	29.868	98.198	H
26354	LAVON	TRINITY/E FK	TX	33.031	96.482	E
26355	LEWISVILLE	TRINITY	TX	33.069	96.964	H/E
26361	SOMERVILLE	YEGUA	TX	30.322	96.525	H
26362	STILLHOUSE HOLLOW (LAPASAS)	LAMPASAS	TX	31.022	97.532	H
26364	WHITNEY	BRAZOS	TX	31.865	97.371	H
28219	CONCHAS	CANADIAN/S	NM	35.402	104.190	E
29106	KANOPOLIS	SMOKY HILL	KS	38.606	97.967	H/E
29108	MILFORD	REPUBLICAN	KS	39.077	96.891	H
29110	PERRY	DELAWARE	KS	39.114	95.425	H
29111	POMONA	110-MILE CK	KS	38.647	95.563	H
29113	TUTTLE CREEK	BIG BLUE	KS	39.254	96.602	H
29194	POMME DE TERRE	POMME DE TERRE	MO	37.901	93.318	H/E
29195	STOCKTON	SAC	MO	37.695	93.765	E
29207	HARLAN COUNTY	REPUBLICAN	NE	40.069	99.208	H
30064	CHERRY CREEK	CHERRY	CO	39.655	104.854	E
30235	SAKAKAWEA (GARRISON)	MISSOURI	ND	47.503	101.431	H
31077	DWORSHAK	CLEARWATER/N FK	ID	46.516	116.299	M
32204	KOOKANUSA (LIBBY)	KOOTENAI	MT	48.410	115.313	H/M/E
33300	HILLS CREEK	WILLAMETTE/MID	OR	43.708	122.423	
35029	MENDOCINO	RUSSIAN	CA	39.198	123.181	H

Code = DDRRR, where DD = District (Table A-1), RRR = Reservoir
Outlet = growing season discharge mode
    (E = epilimnetic, M = metalimnetic, H = hypolimnetic)

Table A3

Phosphorus Balances - Tributary Monitoring Year

Code	Inflow P Components				Fot	Po	Z	T
	a	b	c	d				
03307	13.5	6.6	0.0	0.5	0.49	11.0	13.5	0.245
04312	169.8	107.2	57.0	0.3	0.63	83.2	4.6	0.047
06372	131.8	36.3	2.6	0.8	0.28	25.7	9.3	0.245
08074	56.2	15.8	0.0	0.7	0.28	24.5	10.7	0.263
08330	53.7	20.9	9.6	1.2	0.39	9.1	13.8	0.537
10003	38.9	11.2	0.0	0.0	0.29	33.9	11.0	0.014
10069	75.9	16.6	0.0	0.5	0.22	25.7	9.1	0.158
10071	95.5	30.9	0.2	0.2	0.32	75.9	3.0	0.017
10072	95.5	33.1	0.6	0.4	0.35	91.2	5.9	0.083
10076	79.4	32.4	6.4	1.8	0.41	18.6	15.1	0.891
10411	64.6	15.1	0.0	0.1	0.23	52.5	9.3	0.038
14099	616.6	182.0	1.2	0.3	0.30	218.8	3.5	0.036
15237	295.1	154.9	8.9	3.9	0.52	223.9	3.8	0.490
16243	263.0	151.4	110.5	1.3	0.58	57.5	5.1	0.224
16317	97.7	35.5	0.0	0.5	0.36	70.8	3.2	0.051
16328	45.7	12.3	0.0	0.4	0.27	30.9	13.2	0.166
17241	89.1	21.4	0.0	2.1	0.24	27.5	4.4	0.302
17242	257.0	53.7	10.3	0.3	0.21	208.9	1.5	0.013
17245	173.8	51.3	0.0	0.6	0.30	154.9	1.7	0.035
17248	269.2	95.5	0.0	0.3	0.35	173.8	3.1	0.035
17249	169.8	91.2	0.0	0.2	0.54	128.8	3.5	0.025
17256	56.2	24.5	0.0	0.4	0.44	55.0	5.8	0.083
17373	77.6	7.4	0.0	0.5	0.10	12.3	19.5	0.316
17389	45.7	18.2	0.6	0.1	0.40	45.7	9.8	0.021
17391	24.0	6.8	0.0	0.1	0.28	15.1	20.0	0.060
18092	338.8	107.2	0.0	0.4	0.32	131.8	7.4	0.091
18093	30.2	8.9	1.2	2.6	0.30	12.9	5.2	0.457
18120	55.0	45.7	12.1	0.6	0.83	46.8	7.9	0.158
19119	131.8	47.9	1.3	0.1	0.36	123.0	5.0	0.023
19122	57.5	12.6	0.0	0.4	0.22	33.9	22.4	0.288
19340	141.3	93.3	8.5	0.8	0.66	102.3	8.3	0.209
19342	107.2	32.4	0.3	0.1	0.30	93.3	5.8	0.018
19343	17.4	7.6	0.0	1.4	0.44	8.3	14.5	0.676
20081	199.5	61.7	0.0	1.0	0.31	120.2	3.6	0.123
20087	173.8	97.7	0.0	1.0	0.56	104.7	6.0	0.200
20088	309.0	55.0	0.0	5.3	0.18	87.1	3.2	0.575
22189	288.4	83.2	0.0	1.6	0.29	64.6	5.6	0.309
24011	61.7	17.0	0.0	1.6	0.28	16.2	17.8	0.955
24013	18.2	7.6	0.0	0.6	0.42	12.3	20.9	0.437
24200	49.0	43.6	38.1	0.9	0.95	18.2	19.5	0.589
25020	61.7	17.0	0.7	0.3	0.28	47.9	2.3	0.025
25105	380.2	104.7	0.0	0.7	0.28	177.8	2.5	0.055
25269	74.1	20.4	0.0	9.3	0.28	51.3	2.3	0.708
25273	389.0	123.0	1.6	0.2	0.32	109.6	8.1	0.066
25278	93.3	55.0	6.5	0.6	0.59	47.9	15.8	0.339
25348	398.1	85.1	5.2	1.3	0.21	91.2	9.8	0.407
26347	18.6	8.3	0.0	1.3	0.45	11.2	13.5	0.575

(continued)

A5

Inflow P Components

Code	a	b	c	d	Fot	Po	Z	T
26354	229.1	75.9	6.2	1.7	0.33	49.0	5.0	0.288
26355	257.0	91.2	23.1	2.0	0.35	77.6	6.6	0.437
26361	120.2	49.0	3.2	2.0	0.41	66.1	4.6	0.309
26362	49.0	14.5	1.0	1.1	0.30	17.0	12.0	0.457
29106	588.8	138.0	3.5	2.0	0.23	89.1	4.8	0.316
29108	524.8	208.9	2.1	4.2	0.40	60.3	7.8	1.096
29111	138.0	53.7	2.8	2.0	0.39	58.9	5.5	0.372
29113	1047.1	269.2	5.2	1.4	0.26	134.9	7.8	0.355
29207	436.5	371.5	13.1	8.3	0.85	123.0	6.9	1.905
30235	354.8	22.4	0.4	1.5	0.06	26.9	18.2	0.891
31077	19.5	7.9	0.0	0.3	0.41	16.6	57.5	0.603
33300	39.8	30.9	0.0	0.2	0.78	35.5	37.2	0.288
35029	128.8	26.3	0.0	0.5	0.20	63.1	13.5	0.245
N	60	60	60	60	60	60	60	60
Mean	178.0	62.1	5.7	1.3	0.38	70.1	10.0	0.321
Stdev	186.8	68.3	16.7	1.7	0.18	55.3	9.1	0.335
Min	13.5	6.6	0.0	0.0	0.06	8.3	1.5	0.013
Max	1047.1	371.5	110.5	9.3	0.95	223.9	57.5	1.905

Inflow Phosphorus Concentration Components (mg/m^3)

a = total
b = ortho
c = point-source
d = atmospheric

Fot = tributary ortho-P/total-P ratio
Po = outflow total P (mg/m^3)
Z   = annual mean depth (m)
T   = annual mean hydraulic residence time (years)

Table A4

Nitrogen Balances - Tributary Monitoring Year

| Code | Inflow N Components | | | | Fin | No | Z | T |
	a	b	c	d				
03307	1148	708	0	18	0.62	1148	13.5	0.245
04312	2692	1820	108	10	0.68	2042	4.6	0.047
06372	1349	363	18	26	0.25	1230	9.3	0.245
08074	692	275	0	25	0.39	891	10.7	0.263
08330	692	257	15	39	0.35	1000	13.8	0.537
10003	1288	617	0	1	0.48	1660	11.0	0.014
10069	741	302	4	17	0.40	562	9.1	0.158
10071	1413	447	0	6	0.32	1349	3.0	0.017
10072	1023	427	2	14	0.41	1148	5.9	0.083
10076	1047	479	23	59	0.44	794	15.1	0.891
10411	1698	912	0	4	0.54	1549	9.3	0.038
14099	9550	7079	2	10	0.74	7244	3.5	0.036
15237	2884	776	37	129	0.25	2188	3.8	0.490
16243	2884	1778	278	44	0.58	2089	5.1	0.224
16317	1514	708	0	16	0.47	1479	3.2	0.051
16328	692	372	0	13	0.54	1288	13.2	0.166
17241	2399	1549	67	69	0.64	955	4.4	0.302
17242	4074	3020	111	9	0.73	3802	1.5	0.013
17245	3311	1905	7	21	0.57	2951	1.7	0.035
17248	4467	3236	12	11	0.72	3981	3.1	0.035
17249	2570	1660	1	7	0.65	2570	3.5	0.025
17256	2042	1413	7	14	0.69	1549	5.8	0.083
17373	1318	437	0	16	0.33	1349	19.5	0.316
17389	1380	1023	4	2	0.74	1413	9.8	0.021
17391	912	708	0	3	0.78	851	20.0	0.060
18092	5754	3467	5	12	0.60	3981	7.4	0.091
18093	933	603	10	87	0.66	708	5.2	0.457
18120	2042	1096	38	20	0.53	1230	7.9	0.158
19119	1175	631	2	5	0.54	1148	5.0	0.023
19122	1047	380	0	13	0.36	912	22.4	0.288
19340	871	692	369	25	0.65	891	8.3	0.209
19342	1000	457	1	3	0.46	933	5.8	0.018
19343	661	380	0	47	0.58	1479	14.5	0.676
20081	4169	2951	1	34	0.71	3631	3.6	0.123
20087	8318	7586	2	33	0.91	6166	6.0	0.200
20088	2692	933	0	178	0.34	1413	3.2	0.575
22189	1660	479	0	55	0.28	871	5.6	0.309
24011	1023	479	0	54	0.47	776	17.8	0.955
24013	759	479	0	21	0.63	776	20.9	0.437
24200	2089	933	188	30	0.45	1413	19.5	0.589
25020	724	200	2	11	0.27	457	2.3	0.025
25105	3467	1380	3	22	0.40	1995	2.5	0.055
25269	1479	447	4	309	0.25	891	2.3	0.708
25273	3162	871	4	8	0.27	1479	8.1	0.066
25278	1950	776	13	21	0.39	1862	15.8	0.339
25348	2692	447	4	42	0.16	1175	9.8	0.407
26347	1413	955	1	43	0.68	724	13.5	0.575

(continued)

A7

Table A4 (Concluded)

Code	Inflow N Components				Fin	No	Z	T
	a	b	c	d				
26354	2138	676	17	58	0.31	891	5.0	0.288
26355	1995	562	122	66	0.23	955	6.6	0.437
26361	1820	275	9	68	0.13	1230	4.6	0.309
26362	1380	447	3	38	0.32	646	12.0	0.457
29106	2692	617	6	66	0.22	1585	4.8	0.316
29108	2754	977	5	141	0.35	1479	7.8	1.096
29111	3236	1072	8	68	0.33	2291	5.5	0.372
29113	4898	1862	16	46	0.38	2291	7.8	0.355
29207	7413	1000	37	275	0.12	1230	6.9	1.905
30235	1445	178	2	49	0.11	550	18.2	0.891
31077	692	35	0	10	0.04	389	57.5	0.603
33300	191	32	0	8	0.15	245	37.2	0.288
35029	955	151	0	18	0.15	759	13.5	0.245
N	60	60	60	60	60	60	60	60
Mean	2241	1113	26	43	0.44	1609	10.0	0.321
Stdev	1855	1394	66	58	0.20	1280	9.1	0.335
Min	191	32	0	1	0.04	245	1.5	0.013
Max	9550	7586	369	309	0.91	7244	57.5	1.905

Inflow Nitrogen Components (mg/m^3)
a   total
b   inorganic
c   point-source
d   atmospheric

Fin = tributary inorganic N / total N ratio
No   = outflow nitrogen concentration (mg/m^3)
Z   = annual mean depth (m)
T   = annual mean hydraulic residence time (years)

Table A5
Phosphorus Balance Data — Pool Monitoring Period

Code	Inflow Phosphorus a	b	c	Fot	P	T	Ts	Zs
03307	13.5	6.6	13.5	0.49	10.8	0.246	0.298	13.5
04312	165.6	104.8	182.0	0.44	95.5	0.048	0.095	5.4
06372	134.9	33.9	128.8	0.26	39.4	0.174	0.309	9.3
10003	38.0	11.0	30.2	0.29	23.5	0.015	0.025	11.0
10411	64.6	15.1	66.1	0.23	34.0	0.042	0.068	9.3
15237	302.0	154.9	302.0	0.51	274.1	0.347	0.390	3.8
16243	251.2	138.0	—	0.27	65.0	0.191	0.399	5.2
16317	95.5	35.5	117.5	0.36	59.2	0.051	0.100	3.4
16328	45.7	12.3	57.5	0.27	21.7	0.174	0.391	13.8
17241	93.3	22.9	123.0	0.23	35.4	0.380	0.821	4.5
17242	257.0	50.1	251.2	0.18	167.3	0.008	0.013	1.4
17245	177.8	51.3	169.8	0.29	120.3	0.028	0.044	1.6
17248	269.2	91.2	263.0	0.36	92.2	0.027	0.059	3.2
17249	166.0	87.1	208.9	0.54	174.2	0.017	0.034	3.2
17256	51.3	21.9	64.6	0.44	36.9	0.053	0.129	5.8
17373	72.4	7.8	57.5	0.09	10.3	0.389	0.897	20.0
17391	24.0	6.8	21.9	0.28	12.6	0.055	0.200	22.4
18092	338.8	107.2	309.0	0.32	89.8	0.078	0.170	7.2
18093	28.8	8.1	33.1	0.24	28.0	0.407	1.116	5.4
18120	56.2	45.7	61.7	0.79	33.6	0.145	0.316	7.9
19119	131.8	47.9	134.9	0.36	132.8	0.022	0.029	4.8
19122	57.5	12.6	50.1	0.22	14.6	0.372	0.570	23.4
19340	141.3	93.3	173.8	0.64	42.8	0.219	0.482	8.3
19342	102.3	31.6	100.0	0.30	56.7	0.021	0.024	5.8
19343	17.4	7.6	—	0.43	9.9	0.741	1.206	14.5
20081	199.5	61.7	195.0	0.31	84.8	0.120	0.178	3.7
20087	177.8	100.0	208.9	0.56	72.2	0.209	0.369	6.5
20088	309.0	56.2	—	0.17	71.4	0.617	3.000	3.2
24011	63.1	17.0	—	0.27	26.7	1.000	1.153	17.8
24013	18.2	7.6	25.1	0.41	16.6	0.468	0.565	21.9
24200	47.9	45.7	—	0.50	26.0	0.589	0.651	20.0
25105	380.2	102.3	363.1	0.28	219.1	0.041	0.061	2.3
25267	363.1	89.1	363.1	0.22	85.8	0.468	0.433	7.2
25273	389.0	123.0	380.2	0.31	167.0	0.065	0.080	7.8
25278	93.3	55.0	91.2	0.56	35.7	0.331	0.342	15.5
26355	316.2	134.9	—	0.29	98.3	1.097	1.425	6.5
29108	660.7	195.0	446.7	0.40	92.2	0.417	1.113	7.8
29111	138.0	53.7	131.8	0.38	45.3	0.331	0.518	5.4
29207	398.1	354.8	—	0.85	114.4	1.738	3.310	7.2
30235	218.8	19.1	—	0.06	28.0	1.148	0.887	18.2
31077	19.5	7.9	—	0.41	12.8	0.589	0.398	60.3
N	41	41	32	41	41	41	41	41
Mean	168.0	64.1	160.2	0.36	70.2	0.329	0.564	10.4
Stdev	142.9	66.7	120.1	0.17	61.0	0.374	0.713	10.1
Min	13.5	6.6	13.5	0.06	9.9	0.008	0.013	1.4
Max	660.7	354.8	446.7	0.85	274.1	1.738	3.310	60.3

Inflow Phosphorus (mg/m^3) P = reservoir total P (mg/m^3)
a = annual, total   T = annual residence time (years)
b = annual, ortho   Ts = summer residence time (years)
c = summer, total   Zs = summer mean depth (m)
Fot = tributary ortho P/Total P ratio

A9

Table A6
Nitrogen Balance Data - Pool Monitoring Year

Code	Inflow Nitrogen a	b	c	Fin	N	T	Ts	Zs
03307	1175	704	1158	0.62	942	0.246	0.298	13.5
04312	2692	1788	2806	0.66	1698	0.048	0.095	5.4
06372	1413	378	1296	0.25	617	0.174	0.309	9.3
10003	1288	631	1334	0.48	1131	0.015	0.025	11.0
10411	1698	914	1706	0.54	1536	0.042	0.068	9.3
15237	2951	832	2951	0.25	1692	0.347	0.390	3.8
16243	2884	1833	--	0.58	1404	0.191	0.399	5.2
16317	1514	709	1298	0.47	1040	0.051	0.100	3.4
16328	692	370	932	0.54	739	0.174	0.391	13.8
17241	2399	1451	2223	0.64	882	0.380	0.821	4.5
17242	4266	3261	3817	0.73	2854	0.008	0.013	1.4
17245	3388	1970	3118	0.57	1722	0.028	0.044	1.6
17248	4786	3533	4289	0.72	3019	0.027	0.059	3.2
17249	2570	1650	2177	0.65	3102	0.017	0.034	3.2
17256	2138	1509	1739	0.69	929	0.053	0.129	5.8
17373	1318	430	1296	0.33	509	0.389	0.897	20.0
17391	912	709	732	0.78	839	0.055	0.200	22.4
18092	5754	3459	5077	0.60	3092	0.078	0.170	7.2
18093	912	633	912	0.66	721	0.407	1.116	5.4
18120	1995	1073	1933	0.53	734	0.145	0.316	7.9
19119	1175	637	1152	0.54	771	0.022	0.029	4.8
19122	1047	373	1075	0.36	473	0.372	0.570	23.4
19340	891	699	1118	0.65	567	0.219	0.482	8.3
19342	1023	444	1040	0.46	617	0.021	0.024	5.8
19343	661	379	-	0.58	445	0.741	1.206	14.5
20081	4266	2972	3853	0.71	2087	0.120	0.178	3.7
20087	8318	7460	7162	0.91	4306	0.209	0.369	6.5
20088	2754	929	-	0.34	1204	0.617	3.000	3.2
24011	1023	482	-	0.47	525	1.000	1.153	17.8
24013	759	473	759	0.63	529	0.468	0.565	21.9
24200	2089	927	-	0.45	598	0.589	0.651	20.0
25105	3467	1475	3382	0.40	1851	0.041	0.061	2.3
25267	1995	285	1998	0.15	830	0.468	0.433	7.2
25273	3162	873	2985	0.27	1275	0.065	0.080	7.8
25278	1950	785	1945	0.39	810	0.331	0.342	15.5
26355	2399	821	-	0.23	796	1.097	1.425	6.5
29108	2399	1308	2496	0.35	1162	0.417	1.113	7.8
29111	3236	1070	3097	0.33	1520	0.331	0.518	5.4
29207	7413	999	-	0.12	1060	1.738	3.310	7.2
30235	1288	140	-	0.11	381	1.148	0.887	18.2
31077	708	35	-	0.04	243	0.589	0.398	60.3
N	41	41	32	41	41	41	41	41
Mean	2409	1254	2290	0.48	1250	0.329	0.564	10.4
Stdev	1744	1321	1572	0.20	898	0.374	0.713	10.1
Min	661	35	732	0.04	243	0.008	0.013	1.4
Max	8318	7460	7162	0.91	4306	1.738	3.310	60.3

Inflow Nitrogen Conc. (mg/m^3) N = reservoir total N (mg/m^3)
a = annual, total   T = annual residence time (years)
b = annual, inorganic   Ts = summer residence time (years)
c = summer, total   Zs = summer mean depth (m)
Fin = tributary inorganic N / total N

A10

Table A7

Reservoir Water Quality - Pool Monitoring Period

Code	P	Portho	N	Ninorg	B	S	Z	Zmix	Ts
01165	15.0	6.3	693	56	3.1	2.00	2.7	2.7	0.038
01172	10.0	4.0	767	190	2.1	2.20	4.3	3.4	0.027
01173	13.0	8.0	540	36	2.3	1.80	1.5	1.5	0.008
01170	9.0	4.0	476	51	2.1	2.40	8.2	6.3	0.036
01174	11.0	7.0	585	52	2.2	1.80	2.4	2.4	0.008
03307	10.8	5.1	942	651	5.0	3.53	13.5	5.2	0.298
06372	39.4	9.5	617	186	9.7	1.15	9.4	6.4	0.309
10003	23.5	6.8	1131	839	2.6	1.23	10.9	8.7	0.025
10072	45.0	9.1	864	262	9.2	1.06	5.9	5.0	0.125
10411	34.0	9.2	1536	1026	4.0	1.25	9.4	6.6	0.068
15237	274.1	187.1	1692	299	39.1	0.75	3.8	3.8	0.390
16243	65.0	14.9	1404	684	13.2	0.82	5.3	4.4	0.399
16254	61.1	6.4	1198	179	35.1	0.89	3.1	3.1	2.504
16317	59.2	8.3	1040	306	25.9	0.92	3.4	3.4	0.100
16328	21.7	7.4	739	377	5.6	2.29	14.0	6.3	0.391
16393	5.5	4.5	624	390	1.2	3.02	18.4	9.9	0.140
17241	35.4	5.7	882	441	13.8	1.12	4.5	3.8	0.821
17242	167.3	19.8	2854	2042	10.9	0.28	1.4	1.4	0.013
17245	120.3	12.0	1722	521	63.6	0.48	1.6	1.6	0.044
17247	86.4	25.7	3288	2594	10.2	0.81	4.9	4.4	0.089
17248	92.2	28.5	3019	2130	9.7	0.44	3.2	3.2	0.059
17249	174.2	39.0	3102	1592	28.2	0.50	3.2	3.0	0.034
17256	36.9	9.1	929	483	22.0	1.20	5.7	4.3	0.129
17258	50.3	8.6	1035	245	35.7	0.89	4.5	3.2	1.028
17373	10.3	4.2	509	200	5.4	2.34	19.9	7.7	0.897
17391	12.6	5.7	839	605	6.3	3.55	22.4	7.8	0.200
18092	89.8	33.3	3092	2349	12.9	0.74	7.3	5.8	0.170
18093	28.0	7.5	721	233	7.0	1.72	5.4	4.1	1.116
18120	33.6	8.1	734	363	7.8	1.26	8.0	5.5	0.316
19119	132.8	56.2	771	482	11.3	0.66	4.8	4.8	0.029
19122	14.6	7.0	473	196	3.9	1.76	23.3	8.1	0.570
19338	142.5	71.0	759	463	8.3	0.65	4.3	4.3	0.005
19340	42.8	15.2	567	112	9.7	1.84	8.4	5.5	0.482
19342	56.7	17.9	617	299	7.4	0.74	5.8	4.2	0.024
19343	9.9	5.6	445	193	3.2	4.55	14.6	7.4	1.206
20081	84.8	31.6	2087	1330	17.2	0.54	3.7	3.7	0.178
20087	72.2	33.7	4306	3652	18.7	0.98	6.5	5.0	0.369
20088	71.4	14.9	1204	237	23.6	0.71	3.2	3.2	3.000
21196	34.7	4.6	388	113	9.5	0.99	3.2	3.1	0.077
24011	26.7	7.3	525	228	3.7	2.32	17.7	7.5	1.153
24013	16.6	4.3	529	198	4.3	3.80	21.7	7.9	0.565
24016	12.4	3.6	316	69	3.9	3.61	18.5	7.7	2.045
24022	15.8	5.1	467	201	3.2	3.70	18.0	7.0	0.844
24193	17.5	4.1	336	150	3.6	1.44	4.4	4.4	0.044
24200	26.0	8.8	598	262	8.1	2.42	19.7	7.7	0.651
25105	219.1	73.9	1851	1209	9.4	0.19	2.3	2.3	0.061
25107	63.7	12.7	1117	594	12.5	0.41	4.2	4.2	1.273
25267	85.8	34.5	830	374	4.4	0.47	7.3	7.2	0.433
25273	167.0	100.0	1275	682	12.2	0.41	7.8	7.8	0.080

(continued)

A11

Table A7 (Concluded)

Code	P	Portho	N	Ninorg	B	S	Z	Zmix	Ts
25275	75.4	30.8	976	557	3.9	0.43	6.0	6.0	0.209
25278	35.7	16.8	810	461	6.3	1.71	15.8	8.5	0.342
25281	98.6	31.2	680	234	5.0	0.59	2.8	2.7	0.059
25370	32.2	10.1	595	112	12.2	0.95	5.1	5.1	0.962
26354	67.9	19.4	655	319	6.4	0.36	4.5	4.5	0.542
26355	98.3	27.0	796	337	16.6	0.72	6.4	6.3	1.425
28219	20.2	5.7	338	45	3.3	1.25	8.1	6.6	0.640
29106	54.5	10.8	1186	581	10.9	0.39	5.0	5.0	0.173
29108	92.2	32.7	1162	614	18.9	0.84	7.9	7.8	1.113
29110	57.6	20.9	1554	1109	5.9	0.50	5.7	4.6	0.771
29111	45.3	20.3	1520	1105	8.4	0.47	5.4	4.7	0.518
29194	44.9	13.4	827	364	8.4	1.35	9.3	6.0	0.963
29195	21.6	6.5	902	591	8.8	1.83	10.5	7.5	1.232
29207	114.4	60.7	1060	334	22.1	0.69	7.2	6.4	3.310
30064	57.4	8.1	825	54	20.5	0.77	4.9	4.9	3.000
30235	28.0	12.7	381	148	4.3	2.82	18.2	7.7	0.887
31077	12.8	7.6	243	58	2.0	2.59	60.0	7.3	0.398
32204	29.5	26.0	273	69	3.2	4.26	35.0	9.7	0.295
N	67	67	67	67	67	67	67	67	67
Mean	58.7	20.6	1072	560	11.1	1.45	9.3	5.4	0.593
Stdev	53.4	27.8	813	676	10.7	1.08	9.2	2.1	0.746
Min	5.5	3.6	243	36	1.2	0.19	1.4	1.4	0.005
Max	274.1	187.1	4306	3652	63.6	4.55	60.0	9.9	3.310

P   = total P (mg/m^3)   S   = Secchi depth (m)
Portho = ortho-P (mg/m^3)   Z   = mean depth (m)
N   = total N (mg/m^3)   Zmix = mean depth of mixed layer (m)
Ninorg = inorganic N (mg/m^3)   Ts   = summer residence time (yrs)
B   = chlorophyll-a (mg/m^3)

Table A8
Phosphorus Gradient Data

Code	Ratio	A	L	Pi	T	Z	Fot
03307	1.07	3.8	7.9	13.5	0.295	13.5	0.49
10003	1.20	13.2	29.5	30.2	0.025	11.0	0.29
10411	1.51	38.9	123.0	66.1	0.068	9.3	0.23
15237	1.20	21.4	41.7	302.0*	0.347	3.8	0.51
16243	5.37	12.3	26.9	251.2	0.398	5.2	0.27
17241	3.16	6.5	13.8	123.0	0.813	4.5	0.23
17245	1.51	5.5	15.5	169.8	0.044	1.6	0.29
17248	1.66	5.3	13.8	263.0	0.059	3.2	0.36
17249	1.78	6.5	19.1	208.9	0.034	3.2	0.54
17256	1.35	3.0	8.3	64.6	0.129	5.8	0.44
18092	2.75	12.9	30.9	309.0	0.170	7.2	0.32
18120	2.29	40.7	49.0	61.7	0.316	7.9	0.79
19119	1.74	223.9	190.5	134.9	0.030	4.8	0.36
19122	2.63	204.2	154.9	50.1	0.575	23.4	0.22
19340	2.95	60.3	70.8	173.8	0.479	8.3	0.64
20081	1.38	125.9	44.7	195.0	0.178	3.7	0.31
20087	2.75	60.3	37.2	208.9	0.372	6.5	0.56
24011	5.25	117.5	120.2	63.1*	1.000	17.8	0.27
24013	1.86	218.8	147.9	18.2*	0.468	21.9	0.41
25105	2.57	37.2	26.9	363.1	0.062	2.3	0.28
25278	1.86	51.3	49.0	91.2	0.339	15.5	0.56
29108	2.75	66.1	20.4	446.7	1.122	7.8	0.40
30235	25.12	1380.4	269.2	218.8*	1.148	18.2	0.06
31077	1.29	64.6	83.2	19.5*	0.589	60.3	0.41
N	24	24	24	24	24	24	24
Mean	3.21	115.8	66.4	160.3	0.377	11.1	0.38
Stdev	4.80	277.9	67.6	119.5	0.346	12.2	0.16
Min	1.07	3.0	7.9	13.5	0.025	1.6	0.06
Max	25.12	1380.4	269.2	446.7	1.148	60.3	0.79

Ratio = maximum/minimum station-mean total P
A   = surface area (km^2)
L   = pool length (km)
Pi *   = inflow total P (mg/m^3)
T *   = residence time (years)
Z   = mean depth (m)
Fot   = tributary ortho-P / total P ratio

* annual values (summer otherwise), according to P residence
  time criteria (see text)

A13

Table A9
Oxygen Depletion Rate Data

| Code | Hypolimnion | | | | Hypol. + Metalimnion | | | | |
	Zx	Z	A	HODa	Zx	Z	A	HODa	MODv
02176	14.9	7.1	1.8	708	22.6	11.4	2.6	1076	90.2
03307	21.0	8.1	1.2	548	33.2	12.2	2.6	835	68.9
06372	18.9	5.9	49.9	593	26.5	8.1	108.7	702	80.0
16317	5.5	2.9	11.3	1267	8.5	4.0	19.8	1397	285.8
16328	22.9	8.3	16.6	505	35.1	12.1	38.5	623	47.6
16393	21.3	8.8	3.6	435	30.5	13.4	5.5	560	·35.8
17373	45.7	15.4	2.7	559	54.9	17.6	4.0	570	27.1
17391	51.8	15.7	2.7	670	65.5	18.7	5.1	721	35.2
18092	9.1	3.5	2.5	1026	15.2	5.7	5.9	1373	225.2
18094	10.7	3.2	1.5	861	15.2	4.2	3.9	815	165.1
18095	8.5	2.9	2.0	738	11.6	4.1	3.5	760	139.6
18097	23.5	6.6	7.2	916	31.1	8.9	16.2	1354	158.8
18120	11.0	4.1	14.2	525	15.5	5.8	25.1	650	99.6
18121	10.7	5.9	1.6	439	13.7	6.4	2.3	399	43.3
18126	15.2	4.3	12.9	467	19.8	6.3	21.2	569	78.0
18128	22.9	6.6	11.7	866	25.9	9.4	16.0	928	64.1
18129	13.4	3.5	6.5	756	16.5	4.5	10.9	897	181.9
18134	11.9	3.2	11.0	693	19.5	6.6	27.2	897	115.5
19122	29.0	10.1	105.6	508	38.1	14.6	155.3	748	52.1
19340	19.8	6.6	26.4	1052	24.4	7.7	42.7	1321	184.1
19343	22.0	6.2	28.6	356	34.1	10.4	78.5	334	25.1
22014	42.7	11.9	17.4	548	51.8	13.5	31.6	606	43.8
24011	38.4	11.8	30.2	476	53.7	15.6	69.4	762	53.0
24013	40.5	14.5	74.4	592	55.8	19.2	139.5	840	45.7
24016	37.5	10.7	50.3	462	46.6	13.8	82.6	626	47.3
24022	34.1	10.3	26.1	419	52.3	15.9	69.4	801	53.5
24200	47.3	14.3	74.9	964	59.5	17.5	132.6	1287	78.8
25278	24.7	8.8	17.2	671	36.9	12.9	36.6	880	64.4
26345	18.3	5.1	11.7	432	27.4	7.9	31.8	466	50.8
26347	27.4	7.0	7.5	472	39.6	10.5	20.9	568	49.9
26362	23.5	7.1	8.3	687	31.1	9.3	16.1	660	54.1
26364	12.5	4.4	7.2	550	21.6	6.2	29.0	629	96.0
29194	12.2	4.1	6.9	628	21.3	7.3	20.3	834	105.1
29195	16.8	4.2	26.3	673	22.9	6.8	50.8	911	122.4
30235	34.1	12.1	553.0	450	46.3	16.4	964.0	688	45.4
32204	82.3	30.4	111.7	357	94.5	34.8	141.8	510	21.0
35029	21.3	8.8	4.3	265	27.4	11.9	5.8	393	36.6
N	37	37	37	37	37	37	37	37	37
Mean	25.0	8.2	36.5	625	33.7	11.1	65.9	784	85.7
Stdev	15.4	5.3	91.6	219	18.1	6.0	158.0	278	60.7
Min	5.5	2.9	1.2	265	8.5	4.0	2.3	334	21.0
Max	82.3	30.4	553.0	1267	94.5	34.8	964.0	1397	285.8

Zx = maximum depth (m)
Z = mean depth (m)
A = surface area (km^2)
HODa = areal oxygen depletion rate (mg/m^2-day)
MODv = volumetric oxygen depletion rate in metalimnion (mg/m^3-day)

Table A10
Stratification Characteristics of Reservoirs Used
in Oxygen Depletion Analysis

Code	Zx	Z	Ts	DTx	TGx	Th
02176	26.8	12.7	0.37	13	0.9	12.0
03307	38.7	13.5	0.29	17	1.1	10.1
06372	32.6	9.4	0.26	10	0.7	15.0
16317	10.7	3.4	0.10	9	1.9	14.0
16328	40.9	14.0	0.35	10	0.4	10.0
16393	41.2	18.4	0.11	14	0.6	13.4
17373	66.2	20.0	0.87	17	0.8	12.0
17391	84.8	22.4	0.18	18	1.1	14.0
18092	22.3	7.3	0.13	8	1.0	12.0
18094	22.9	6.3	−	10	1.6	13.0
18095	19.5	7.3	−	5	1.8	11.0
18097	36.6	10.7	−	14	2.0	9.0
18120	20.7	8.0	0.26	16	1.1	9.0
18121	20.7	7.7	−	16	1.8	14.0
18126	26.5	9.1	−	15	2.2	11.0
18128	30.8	9.0	−	12	1.6	13.0
18129	22.6	7.0	−	12	2.0	15.0
18134	22.6	8.2	−	16	2.0	11.0
19122	53.1	23.2	0.41	17	0.7	13.0
19340	27.4	8.4	0.42	8	2.0	14.0
19343	43.0	14.6	0.77	18	1.2	12.0
22014	59.8	14.5	2.50	17	1.5	9.0
24011	62.8	17.7	0.95	17	1.1	11.0
24013	68.3	22.0	0.61	15	1.6	12.0
24016	57.6	18.4	1.38	16	1.8	9.3
24022	60.6	18.0	0.73	15	0.7	11.0
24200	68.6	19.7	0.65	16	0.8	11.0
25278	43.9	15.7	0.35	12	0.4	14.0
26345	33.5	10.7	3.80	11	0.8	14.0
26347	47.3	13.3	1.35	13	0.7	14.0
26362	37.2	11.6	1.32	14	0.8	14.0
26364	28.7	7.9	0.99	8	0.3	15.0
29194	27.1	9.3	−	17	2.3	9.0
29195	32.0	10.0	−	12	2.1	12.0
30235	55.2	18.2	1.19	17	0.8	7.0
32204	101.2	35.0	0.90	11	0.4	12.0
35029	30.8	13.6	0.35	12	1.1	9.0
N	37	37	27	37	37	37
Mean	41.2	13.4	0.80	13	1.2	11.9
Stdev	20.1	6.3	0.80	3	0.6	2.1
Min	10.7	3.4	0.10	5	0.3	7.0
Max	101.2	35.0	3.80	18	2.3	15.0

Zx = maximum total depth (m)
Z = mean total depth (m)
Ts = summer residence time (yrs)
DTx = max. top-to-bottom temperature dif. (deg-C)
TGx = max. vertical temperature gradient (deg-C/m)
Th = mean hypolimnetic temperature (deg-C)

Table A11
Surface Water Quality Data Used in Oxygen Depletion Studies

Code	Near-Dam Station Means				Area-Weighted Res. Means			
	B	P	S	Norg	B	P	S	Norg
02176	3.3	7.0	2.34	–	5.0	7.0	2.34	–
03307	5.4	12.0	3.56	291	5.0	10.8	3.53	291
06372	7.6	26.0	1.83	284	9.7	39.4	1.15	431
16317	15.3	45.0	1.02	614	25.9	59.2	0.92	734
16328	2.7	18.0	2.69	493	5.6	21.7	2.29	362
16393	1.4	6.0	2.79	255	1.2	5.5	3.02	234
17373	4.8	10.0	2.84	276	5.4	10.3	2.34	309
17391	5.6	11.0	4.37	159	6.3	12.6	3.55	234
18092	10.3	64.0	0.94	674	12.9	89.8	0.74	743
18094	6.0	38.0	1.07	643	–	–	–	–
18095	9.4	27.0	1.04	665	–	–	–	–
18097	8.0	16.0	1.17	639	12.0	30.0	1.07	588
18120	4.9	19.0	1.83	375	7.8	33.6	1.26	371
18121	2.8	19.0	1.45	231	–	–	–	–
18126	2.7	25.0	1.65	213	–	–	–	–
18128	5.6	18.0	1.68	198	–	–	–	–
18129	3.7	17.0	1.73	194	–	–	–	–
18134	4.0	18.0	1.30	275	–	–	–	–
19122	4.2	11.0	2.34	229	3.9	14.6	1.76	277
19340	6.8	26.0	2.31	334	9.7	42.8	1.84	455
19343	1.8	10.0	6.40	260	3.2	9.9	4.55	252
22014	5.0	15.0	2.36	383	6.2	18.0	2.36	330
24011	2.7	11.0	4.19	214	3.7	26.7	2.32	297
24013	2.3	13.0	4.78	362	4.3	16.6	3.80	331
24016	3.4	11.0	3.86	375	3.9	12.4	3.61	247
24022	2.2	15.0	4.65	292	3.2	15.8	3.70	266
24200	12.3	18.0	2.31	464	8.1	26.0	2.42	336
25278	3.9	35.0	2.08	454	6.3	35.7	1.71	349
26345	4.0	16.0	3.96	480	5.7	16.0	3.55	350
26347	2.6	8.0	4.24	270	2.6	16.0	2.92	260
26362	3.7	15.0	3.51	300	3.9	20.0	2.39	250
26364	4.0	20.0	2.34	450	6.9	22.0	2.16	550
29194	8.9	35.0	1.93	437	8.4	44.9	1.35	463
29195	5.5	17.0	2.11	330	8.8	21.6	1.83	311
30235	1.4	15.0	4.32	302	4.3	28.0	2.82	233
32204	1.4	24.0	7.50	201	3.2	29.5	4.26	204
35029	2.0	14.0	2.44	250	3.0	15.0	3.00	275
N	37	37	37	36	30	30	30	29
Mean	4.9	19.6	2.78	357	6.5	25.0	2.49	356
Stdev	3.1	11.6	1.52	147	4.6	17.4	1.02	141
Min	1.4	6.0	0.94	159	1.2	5.5	0.74	204
Max	15.3	64.0	7.50	674	25.9	89.8	4.55	743

B = chlorophyll-a (mg/m^3) S = Secchi depth (m)
P = total P (mg/m^3) Norg = organic N (mg/m^3)

Table A12
Data Used in Analysis of Spatial HOD Variations

Code	Project	HODv	Zx	Zxh	B
03307305	Beltzville	70	38.1	20.3	5.4
03307306		79	23.6	5.8	5.0
16393312	Tygart	57	40.6	20.7	1.4
16393313		51	32.6	12.8	1.0
16393314		84	25.2	8.6	1.1
17391310	Summersville	36	71.8	39.0	5.6
17391312		39	41.7	8.8	2.7
17391313		65	25.6	6.5	4.0
18097502	Brookville	130	35.2	22.7	8.0
18097503		201	22.2	10.7	15.0
18097504		270	11.6	4.5	15.0
19122325	Cumberland	56	54.8	27.1	4.2
19122327		54	31.7	13.1	4.3
19122328		60	40.6	21.9	3.9
19122329		64	41.5	22.7	4.2
19122330		55	39.9	21.4	3.3
24011312	Beaver	41	61.3	35.4	2.7
24011313		46	51.5	25.6	2.6
24011314		64	39.2	16.4	3.6
24011315		62	31.0	9.8	3.7
24011316		58	20.3	6.8	5.5
24011317		63	15.9	3.9	5.3
24013321	Bull Shoals	39	67.2	41.3	2.3
24013322		43	61.8	36.1	2.8
24013323		45	57.9	32.0	2.3
24013325		49	51.8	27.5	3.2
24013326		43	36.6	18.6	5.4
24013327		53	28.7	13.7	6.3
24016311	Greer's Ferry	47	54.1	33.4	3.4
24016312		75	49.9	29.1	4.5
24022318	Norfork	44	58.8	31.2	2.2
24022320		45	53.2	28.7	2.1
24022321		53	42.4	19.3	2.7
24022322		59	34.5	11.4	6.3
24022323		68	32.9	11.4	3.5
24200317	Table Rock	65	64.2	42.7	12.3
24200319		55	56.4	34.8	6.5
24200320		73	41.5	19.8	4.4
24200321		68	34.1	14.0	4.0
25278306	Tenkiller Ferry	79	45.7	24.9	3.9
25278307		82	38.1	17.2	4.5
25278308		66	27.5	9.6	7.1
30235320	Sakakawea	33	57.4	38.1	1.4
30235322		26	42.2	22.9	1.3
30235324		41	35.4	16.1	2.0
30235325		44	25.0	5.8	7.6

Code = station identifier (DDRRRSSS), DD=district,
       RRR=reservoir, SSS=station (upstream order)
HODv = station volumetric HOD rate (mg/m^3-day)
Zx   = station maximum depth (m)
Zxh = station maximum hypolimnetic depth (m)
B   = station mean chlorophyll-a (mg/m^3)

A17

Table A13
Lake Oxygen Depletion Rate Data

Lake	Source	Z	Zx	Zh	Th	B	HODa
Bomoseen	1	8.2	19.8	3.6	12.0	5.4	380
Fairfield	1	7.2	12.8	2.8	11.0	10.5	450
Harveys	1	20.0	44.2	16.4	6.0	3.6	430
Hortonia	1	5.6	18.3	3.6	9.0	3.7	410
Iroquois	1	5.8	11.3	2.3	12.0	10.5	590
Morey	1	8.3	13.1	2.0	10.0	9.5	510
Parker	1	7.6	14.7	3.1	11.0	6.2	400
St Catherines	1	10.7	19.5	5.4	10.0	3.2	400
Shadow	1	20.9	42.4	15.7	5.0	3.8	430
Sunset	1	18.6	36.0	14.5	8.0	1.4	170
Alexander	2	7.4	16.2	3.3	10.0	0.8	170
East Twin	2	9.9	24.4	6.8	6.0	2.3	560
Long	2	4.6	22.0	5.6	6.0	2.8	220
Quassapaug	2	8.7	19.8	4.8	7.0	2.9	450
Shenipsit	2	9.2	20.7	6.6	9.0	5.3	530
Waramaug	2	6.7	12.2	4.3	12.0	9.0	420
West Hill	2	9.7	18.0	4.4	8.0	1.8	250
Beech	3	9.8	32.0	--	-	1.0	360
Bob	3	18.0	65.0	--	-	1.2	230
Boshkung	3	23.4	75.0	--	--	1.1	190
Eagle	3	7.9	26.0	-	-	1.8	180
Four-Mile	3	9.3	22.0	--	-	1.4	300
Haliburton	3	19.6	55.0	--	-	1.0	310
Halls	3	27.2	76.0	-	-	0.8	130
Maple	3	11.6	40.0	-	-	1.1	380
Moose	3	16.6	40.0	-	--	1.8	270
Pine	3	7.4	20.0	-	--	1.5	270
Twelve-Mile	3	11.5	26.0	-	--	1.3	170
Calhoun	4	10.6	27.0	-	7.0	8.0	1090
Canadarago	4	7.7	12.8	--	12.0	7.0	1010
Harriet	4	8.8	26.0	--	7.0	3.4	450
Sammamish	4	18.0	32.0	--	7.0	6.0	530
Shagawa	4	5.7	13.7	-	8.0	31.0	1280
Washington-64	4	33.0	65.2	28.5	4.0	29.0	840
N	34	34	34	18	23	34	34
Mean	2	12.2	30.0	7.4	8.6	5.3	434
Stdev	1	6.8	18.3	6.9	2.4	6.9	267
Min	1	4.6	11.3	2.0	4.0	0.8	130
Max	4	33.0	76.0	28.5	12.0	31.0	1280

Source Codes:
    1 = Vermont Lakes (Walker, 1982)
    2 = Connecticuit Lakes (Norvell and Frink, 1973)
    3 = Ontario Lakes (Lasenby, 1973)
    4 = OECD North American Project Lakes (Rast, 1978)
Z   = mean depth (m)
Zx   = maximum depth (m)
Th   = mean hypolimnetic temperature (deg-C)
B   = mean chlorophyll-a (mg/m^3)
HODa = areal hypolimnetic oxygen depletion rate (mg/m^2-day)

Table A14
Outflow Oxygen Depletion Data from TVA Reservoirs (Higgins, 1982)

Reservoir	Zx	Z	Zi	B	OODx	OODm
------------------- Tennessee River Mainstem Reservoirs -------------------						
Kentucky	32.5	5.0	17.3	9.1	42.8	32.8
Pickwick	23.4	6.5	16.2	3.9	90.0	25.7
Wilson	29.5	12.3	6.9	5.9	42.8	28.5
Wheeler	19.3	5.3	8.9	4.4	41.4	28.5
Guntersvil	17.6	4.2	10.9	4.8	50.0	24.2
Nickajack	17.7	6.8	12.2	2.8	44.2	28.5
ChickamaugA	24.2	5.0	14.5	3.0	47.1	24.2
Watts Bar	22.5	7.3	19.2	6.2	60.0	22.8
Fort Loudon	26.1	7.3	23.0	5.9	50.0	35.7
----------------------- Tributary Reservoirs -----------------------						
Chatuge	33.0	9.5	24.6	5.5	61.4	48.5
Cherokee	38.8	13.9	26.4	10.9	111.4	70.0
Douglas	28.9	10.7	26.2	6.3	85.7	55.7
Fontana	123.3	37.8	60.5	4.1	65.7	31.4
Hiwasse	65.4	20.2	34.9	5.0	37.1	31.4
Norris	54.2	16.3	39.9	2.1	71.4	40.0
So Holston	67.8	23.4	32.8	6.5	47.1	32.8
Tims Ford	41.9	14.9	36.7	6.1	68.5	40.0
Watauga	76.0	24.5	45.5	2.9	50.0	30.0

Zx = maximum depth (m)
Z = mean depth (m)
Zi = average intake depth (m)
B = mean chlorophyll-a (mg/m^3)
$OODx$ = maximum outflow oxygen depletion rate $(mg/m^3\text{-day})$
$OODm$ = mean outflow oxygen depletion rate $(mg/m^3\text{-day})$

A19

APPENDIX B: NOTATION

a	=	non-algal turbidity (1/m)
a0 - a2	=	empirical parameters
A1,A2	=	model parameters
AS	=	surface area (km^2)
Ac	=	hydraulic cross section (m^2 x 10^3)
Ah	=	hypolimnetic surface area (km^2)
Ar	=	calculated total surface area of reservoir (km^2)
Ar*	=	input total surface area of reservoir (km^2)
At	=	surface area below elevation Et (km^2)
b	=	chlorophyll/Secchi slope (m^2/mg)
b	=	reservoir-specific morphometric factor (Part IV)
B	=	area-weighted, reservoir-mean chlorophyll-a (mg/m^3)
Bd	=	near-dam, station-mean chlorophyll-a (mg/m^3)
Bm	=	area-weighted, reservoir-mean chlorophyll-a (mg/m^3)
Bp	=	phosphorus-limited chlorophyll potential (mg/m^3)
Bs	=	station-mean chlorophyll-a (mg/m^3)
Bx	=	nutrient-limited chlorophyll potential (mg/m^3)
B*S	=	product of chlorophyll-a and transparency (mg/m^2)
B1 - B3	=	empirical parameters
C	=	total phosphorus concentration in model segment (mg/m^3)
C1 - C4	=	empirical parameters
Cbod	=	BOD concentration in hypolimnion (mg/m^3)
Cs	=	suspended sediment concentration (mg/m^3)
d	=	subscript denoting near-dam conditions (Part IV)
d	=	regional dummy variable
d.f.	=	discriminant function (dimensionless)
dP	=	point-source inflow phosphorus addition (mg/m^3)
D	=	longitudinal dispersion coefficient (Part IV) (km^2/yr)
D	=	algal specific death rate (Part VI) (1/day)
DF	=	Fischer longitudinal dispersion coefficient (km^2/yr)
DN	=	numerical dispersion coefficient (km^2/yr)

e	=	subscript denoting estimated value
E	=	eddy diffusive flow (Part IV) (hm^3/yr)
E	=	visible light extinction coefficient (Part VI) (1/m)
Eh	=	elevation at upper boundary of hypolimnion (m)
Et	=	elevation at upper boundary of metalimnion (m)
f	=	spatial response slope
fs	=	fraction of incoming phosphorus load immediately settled
F	=	light integral (dimensionless)
F(B)	=	chlorophyll productivity function (dimensionless)
F(Th)	=	termperature effect term (dimensionless)
F(Z)	=	mean depth morphometric term (dimensionless)
F(Zh)	=	mean hypolimnetic depth morphometric term (dimensionless)
Fin	=	tributary inorganic N / total N ratio
Fot	=	tributary ortho-P / total-P ratio
Fw	=	width scaling factor
Fz	=	depth scaling factor
G	=	dimensionless kinetic factor
GQ	=	fraction of inflow volume input at upper end of pool
GW	=	fraction of phosphorus loading input at upper end of pool
Gmax	=	maximum specific growth rate (1/day)
H	=	station maximum depth (m)
HODa	=	areal hypolimnetic oxygen depletion rate (mg/m^2-day)
HODv	=	volumetric hypolimnetic oxygen depletion rate (mg/m^3-day)
HODvde	=	estimated near-dam oxygen depletion rate (mg/m^3-day)
i	=	subscript denoting model segment
I	=	trophic state index (dimensionless)
k	=	exchangeable phosphorus partition coefficient $(mg/kg)/(mg/m^3)$
K1	=	effective first-order decay rate (1/yr)
K2	=	effective second-order decay rate (m^3/mg-yr)
Ka	=	BOD accumulation rate (1/day)
Kd	=	BOD oxidation rate (1/day)
L	=	reservoir length (Part IV) (km)
L	=	total algal loss rate (Part VI) (1/day)
LAT	=	latitude (degrees N)

LONG	=	longitude (degrees W)
LS	=	segment length (km)
m	=	nutrient exponent (dimensionless)
MODv	=	volumetric metalimnetic oxygen depletion rate (mg/m^3-day)
n	=	total number of segments
N	=	reservoir total nitrogen concentration (mg/m^3)
Ni	=	inflow total nitrogen concentration (mg/m^3)
Nia	=	inflow available nitrogen concentration (mg/m^3)
Niin	=	inflow inorganic nitrogen (mg/m^3)
Ninorg	=	inorganic nitrogen concentration (mg/m^3)
Niorg	=	inflow organic nitrogen (mg/m^3)
No	=	outflow total nitrogen concentration (mg/m^3)
Norg	=	organic nitrogen concentration (mg/m^3)
Nd	=	dimensionless dispersion rate group
Nr	=	dimensionless reaction rate group
Oi	=	average oxygen concentration (mg/m^3) on day i
P	=	reservoir total phosphorus concentration (mg/m^3)
PC-1	=	first principal component of reservoir water quality data
PC-2	=	second principal component of reservoir water quality data
Pe	=	estimated reservoir or outlet total phosphorus (mg/m^3)
Pex	=	exchangeable phosphorus in solution (mg/m^3)
Pi	=	inflow total phosphorus concentration (mg/m^3)
Pia	=	inflow available phosphorus concentration (mg/m^3)
Pino	=	inflow non-ortho-phosphorus concentration (mg/m^3)
Pio	=	inflow ortho-phosphorus concentration (mg/m^3)
Pmax	=	maximum, station-mean total P (mg/m^3)
Pmin	=	minimum, station-mean total P (mg/m^3)
Po	=	outflow total phosphorus concentration (mg/m^3)
Portho	=	mean ortho-phosphorus concentration (mg/m^3)
Ps	=	segment outflow phosphorus (mg/m^3)
Psi	=	segment inflow phosphorus (mg/m^3)
Pt	=	total phosphorus concentration at time of travel t (mg/m^3)
Ptex	=	total exchangeable phosphorus in suspension (mg/m^3)
Pv	=	Vollenweider/Larsen-Mercier normalized P loading (mg/m^3)

QL   = local inflow (hm^3/yr)

QT   = total outflow (hm^3/yr)

Qp   = algal cell quota for phosphorus (mg P/mg Chl-a)

Qs   = surface overflow rate (m/yr)

Qx   = cell quota for composite nutrient concentration

Rp   = total phosphorus retention coefficient (dimensionless)

s   = subscript denoting conditions at station s

S   = mean Secchi depth (m)

SK2   = first derivative of log(Pe) with respect to log (K2)

SPi   = first derivative of log(Pe) with respect to log (Pi)

Se   = slope of energy gradeline (m/km)

t   = time (Part VI) (days)

t   = time of travel from upper end of pool (Part IV) (years)

type   = dummy variable = 0 for lakes, 1 for reservoirs

T   = hydraulic residence time (years)

TODa   = areal depletion rate below elevation Et $(\text{mg/m}^2\text{-day})$

Th   = mean hypolimnetic temperature   (deg-C)

Tp   = phosphorus residence time (years)

Ts   = summer hydraulic residence time (years)

Tss   = segment hydraulic residence time (years)

U   = nominal advective velocity (km/yr)

U1   = effective first-order settling velocity (m/yr)

U2   = effective second-order settling velocity $(\text{m}^4/\text{mg-yr})$

Umax   = maximum settling velocity (m/yr)

Us   = shear velocity (km/yr)

V   = volume $(\text{hm}^3 = 10^6 \text{ m}^3)$

Var   = variance operator

Vh   = hypolimnetic volume (hm^3)

Vm   = metalimnetic volume (hm^3)

Vm   = metalimnetic volume (hm^3)

Vr   = calculated total volume of reservoir (hm^3)

Vr*   = input total volume of reservoir (hm^3)

Vt   = volume below elevation Et (hm^3)

W   = reservoir mean width (km)

WL   = local phosphorus loading (kg/yr)

Wbod   = organic matter (BOD) input to hypolimnion (mg/m^3-day)

We   = channel width at depth Ze (m)

Win   = inflow inorganic nitrogen weight

Worg   = inflow organic nitrogen weight

Ws   = station top width (m)

X   = dummy variable

Xpn   = composite nutrient concentration (mg/m^3)

Y   = exchangeable phosphorus adsorbed to solid phase (Part II)(mg/kg)

Y   = predicted chl-a, organic n, or 1/Secchi in model segment (Part IV)

Yd   = composite variable reflecting HODv potential

Z   = mean depth (m)

Zc   = depth at which U = .5 Umax (m)

Ze   = station total depth at elevation e (m)

Zh   = mean hypolimnetic depth (m)

Zmix   = mean depth of mixed layer = volume / surface area (m)

Zt   = mean depth below elevation Et (m)

Zx   = maximum lake depth (m)

Zxh   = maximum hypolimnetic depth (m)

         = superscript denoting conditions after equilibration